

2015

Assessing the effects of long-term ocean acidification on benthic communities at CO₂ seeps

Baggini, Cecilia

<http://hdl.handle.net/10026.1/3321>

<http://dx.doi.org/10.24382/3890>

Plymouth University

All content in PEARL is protected by copyright law. Author manuscripts are made available in accordance with publisher policies. Please cite only the published version using the details provided on the item record or document. In the absence of an open licence (e.g. Creative Commons), permissions for further reuse of content should be sought from the publisher or author.

ASSESSING THE EFFECTS OF LONG-TERM OCEAN
ACIDIFICATION ON BENTHIC COMMUNITIES AT CO₂ SEEPS

by

CECILIA BAGGINI

A thesis submitted to Plymouth University and Bremen University in
partial fulfilment for the degree of

DOCTOR OF PHILOSOPHY

and

DOCTOR OF SCIENCE (DR. RER. NAT.)

School of Marine Science and Engineering
Marine Biology & Ecology Research Centre (MBERC)

In collaboration with
Hellenic Centre for Marine Research
University of Palermo

November 2014

This copy of the thesis has been supplied on condition that anyone who consults it is understood to recognise that its copyright rests with its author and that no quotation from the thesis and no information derived from it may be published without the author's prior consent.

Assessing the effects of long-term ocean acidification on benthic communities at CO₂ seeps

Cecilia Baggini

Abstract

Ocean acidification has the potential to profoundly affect marine ecosystems before the end of this century, but there are large uncertainties on its effects on temperate benthic communities. Volcanic CO₂ seeps provide an opportunity to examine and improve our understanding of community responses to ocean acidification. In this thesis, two Mediterranean CO₂ seeps (Methana in Greece and Vulcano in Italy) were used to investigate the responses of macroalgae and their epifaunal communities to increased CO₂. Changes in plant-herbivore interactions at elevated CO₂, as well as adaptation potential of dominant macroalgae and responses of macroalgae and epifauna to concurrent exposure to elevated CO₂ and copper pollution, were also examined. Firstly, I determined that volcanic seeps off Methana (Greece) are suitable for ocean acidification studies as they do not have confounding gradients in temperature, salinity, total alkalinity, nutrients, hydrogen sulphide, heavy metals or wave exposure. Calcifying macroalgae abundance decreased as CO₂ increased both at Methana and at Vulcano, while furoid algae seemed to benefit from elevated pCO₂ levels. Seasonality greatly affected macroalgal responses to increasing CO₂, according to the annual cycles of dominant species. Epifaunal communities of dominant furoid algae changed at elevated pCO₂ as well, with calcifying invertebrates decreasing and polychaetes increasing near the seeps. Herbivore control of macroalgal biomass did not greatly change at elevated pCO₂ levels, as limpets had a minor role in controlling macroalgal biomass off

Vulcano (Italy) and sea urchins were replaced by herbivorous fish near seeps off Methana. The two macroalgal species examined for signs of long-term acclimatisation (*Cystoseira corniculata* (Turner) Zanardini and *Jania rubens* (Linnaeus) J.V.Lamouroux) to ocean acidification using reciprocal transplants did not appear to have permanently acclimatised to elevated pCO₂ levels, but changed their physiology in four to nine months depending on the local environment. Furthermore, when exposed to a 36-hour copper pulse at elevated pCO₂ levels both seaweed species accumulated more copper in their tissues compared to those exposed to copper in reference pCO₂ conditions, and this resulted in altered epifaunal assemblages on *C. corniculata*. These observations suggest that benthic communities will significantly change as CO₂ levels increase, and that long-term acclimatisation is not likely to play a significant role; this would have profound consequences for benthic ecosystems and the services they provide.

Untersuchungen zu den Langzeiteffekten der Ozeanversauerung auf benthische Lebensgemeinschaften an natürlichen CO₂-Quellen

Cecilia Baggini

Zusammenfassung

Ozeanversauerung hat das Potenzial, Meeresökosysteme noch vor dem Ende dieses Jahrhunderts nachhaltig zu verändern. Große Unsicherheiten gibt es allerdings bislang über die Auswirkungen auf Benthosgemeinschaften der gemäßigten Breiten. Natürliche vulkanische CO₂-Quellen bieten die Möglichkeit, unser Verständnis der Reaktionen natürlicher Lebensgemeinschaften auf die Versauerung der Ozeane zu erweitern. In dieser Arbeit wurden zwei Standorte natürlicher CO₂-Quellen im Mittelmeer CO₂ untersucht (Methana in Griechenland und Vulcano in Italien), um die Reaktionen von Makroalgen und deren Aufwuchsgemeinschaften auf erhöhte CO₂-Konzentrationen zu untersuchen. Veränderungen von Pflanze/Herbivor-Wechselwirkungen bei erhöhtem CO₂, sowie das Anpassungspotential von dominanten Makroalgen und die Reaktionen von Makroalgen und Epifauna auf die gleichzeitige Exposition unter erhöhtem CO₂ und Kupferverschmutzung wurden erfasst. Zunächst stellte ich fest, dass die natürlichen CO₂-Quellen vor Methana (Griechenland) gut für Versauerungsstudien geeignet sind, da sie nicht wesentlich durch zusätzliche Schwankungen in der Temperatur, im Salz- und Gesamtalkaligehalt, in der Nährstoffverfügbarkeit, im Gehalt von Schwefelwasserstoff und Schwermetallen oder der Wellenexposition beeinflusst sind. An beiden Standorten verringerte sich die Abundanz kalkbildender Makroalgen mit zunehmender CO₂-Konzentration, während fucoide Algen von

einem erhöhten $p\text{CO}_2$ profitierten. Abhängig von den spezifischen Jahreszyklen der jeweils dominanten Arten wurde ein starker saisonaler Einfluss auf die Reaktionen von Makroalgen auf steigende CO_2 -Konzentrationen ermittelt. Die Epifauna-Gemeinschaften auf dominanten fucoiden Algen veränderten sich ebenfalls mit steigendem $p\text{CO}_2$, indem die Abundanz kalkbildender Wirbelloser abnahm und Polychaeten in der Nähe der Quellen zunahm. Die Kontrolle der Großalgen-Biomasse durch Herbivore veränderte sich bei erhöhtem $p\text{CO}_2$ nur unwesentlich: Napfschnecken spielten eine untergeordnete Rolle bei der Kontrolle der Makroalgenbiomasse vor Vulcano (Italien) und am Standort Methana wurden in der Nähe der CO_2 -Quellen Seeigel durch herbivore Fische ersetzt. Die beiden Makroalgen-Arten (*Cystoseira corniculata* (Turner) Zanardini und *Jania rubens* (Linnaeus) J.V.Lamouroux), welche mittels reziproker Transplantationen auf Anzeichen langfristiger Anpassungen an Ozeanversauerung untersucht wurden, scheinen sich nicht genetisch an den erhöhten $p\text{CO}_2$ angepasst zu haben, aber änderten ihre Physiologie innerhalb weniger Monate in Abhängigkeit von der lokalen Umgebung. Eine zusätzliche 36-stündige Kupferexposition bei erhöhtem $p\text{CO}_2$ führte in beiden Algenarten zur verstärkten Akkumulation von Kupfer im Gewebe im Vergleich zu den Kontrollbedingungen unter normalem $p\text{CO}_2$. Dieser zusätzliche Faktor führte zu einer Veränderung der Epifauna-Gemeinschaft von *C. corniculata*. Diese Beobachtungen legen nahe, dass sich benthische Lebensgemeinschaften bei einem Anstieg des CO_2 -Niveaus deutlich verändern, und dass eine genetische Anpassung vermutlich nicht erfolgt. Daraus könnten sich weitreichende Folgen für benthische Ökosysteme und ihre Dienstleistungen ergeben.

Contents:

List of figures.	14
List of tables .	18
Acknowledgements .	23
Author's declaration .	24
1. Community responses to ocean acidification at temperate rocky reefs: possible causes and adaptation potential .	29
1.1 Introduction .	30
1.2 Community effects of ocean acidification at temperate rocky reefs .	35
1.2.1 Laboratory and mesocosm experiments .	36
1.2.2 Field pCO ₂ manipulation .	37
1.2.3 Areas with naturally elevated pCO ₂ .	38
1.2.4 Modelling approach .	43
1.3 Mechanisms driving community changes .	45
1.3.1 Changes in organism physiology .	45
1.3.2 Changes in biological interactions .	52
1.4 Adaptation potential .	54
1.5 Interaction with other anthropogenic stressors .	56
1.6 Thesis aims and objectives .	58

2. Assessing the suitability of a volcanic seep area off Methana (Greece) for ocean acidification studies	66
2.1 Introduction	68
2.2 Methods	70
2.2.1 Study area.	70
2.2.2 Site descriptions	71
2.2.3 Seawater physicochemical parameters	73
2.2.4 Seawater nutrient concentration	74
2.2.5 Free sulphides in seawater	75
2.2.6 Heavy metals in sediment	76
2.2.7 Heavy metals in macroalgae	79
2.2.8 Wave exposure	80
2.2.9 Statistical analyses	82
2.3 Results	83
2.3.1 Seawater physicochemical parameters	83
2.3.2 Seawater nutrient concentration	85
2.3.3 Free sulphides in seawater	86
2.3.4 Heavy metals in sediment	86
2.3.5 Heavy metals in macroalgae	87
2.3.6 Wave exposure	89
2.4 Discussion	89

3. Changes in subtidal macroalgal communities along pCO₂ gradients at Mediterranean volcanic seeps	93
3.1 Introduction	95
3.2 Methods	97
3.2.1 Methana experimental design and data analysis	97
3.2.2 Vulcano study site	99
3.2.3 Vulcano experimental design, methods and data analysis	103
3.3 Results	104
3.3.1 Methana benthic community	104
3.3.2 Vulcano macroalgal communities	113
3.4 Discussion	119
4. Canopy algal epifauna changes at elevated pCO₂ at two Mediterranean volcanic seeps	125
4.1 Introduction	127
4.2 Methods	130
4.2.1 Methana	130
4.2.2 Vulcano	131
4.2.3 Statistical analyses	133
4.3 Results	135
4.3.1 Methana	135
4.3.2 Vulcano	141

4.4 Discussion	. 148
5. Effect of herbivores on benthic communities at different pCO₂ levels	. 153
5.1 Introduction	. 155
5.2 Methods	. 160
5.2.1 Vulcano	. 160
5.2.1.1 Study site	. 160
5.2.1.2 Limpet exclusion	. 161
5.2.1.3 Limpet abundances and feeding rates	. 163
5.2.1.4 Statistical analyses	. 163
5.2.2 Methana	. 165
5.2.2.1 Herbivore survey	. 165
5.2.2.2 Herbivore exclusion	. 165
5.2.2.3 Statistical analyses	. 167
5.3 Results	. 168
5.3.1 Vulcano	. 168
5.3.1.1 Environmental parameters	. 168
5.3.1.2 Limpet exclusion, abundance and feeding rates	. 168
5.3.2 Methana	. 175
5.3.2.1 Environmental parameters	. 175
5.3.2.2 Herbivore surveys	. 176

5.3.2.3 Herbivore exclusion 178
5.4 Discussion 183
6. Seaweed acclimatisation to high pCO₂ at volcanic seeps 190
6.1 Introduction 192
6.2 Methods 195
6.2.1 Experimental design and field sampling 195
6.2.2 Laboratory analyses 197
6.2.3 Statistical analyses 199
6.3 Results 199
6.3.1 Growth and epiphyte cover 199
6.3.2 Photosynthetic parameters 202
6.3.3 Pigments content. 204
6.3.4 Carbon, nitrogen and phosphorous content 208
6.3.5 Total phenolic compounds 212
6.4 Discussion 213
7. A short-term copper pulse affects macroalgal copper accumulation and indirectly alters epifaunal colonisation at elevated pCO₂ 220
7.1 Introduction 222
7.2 Methods. 226
7.2.1 Study area. 226
7.2.2 Experimental design. 226

7.2.3 Environmental parameters monitoring. 228
7.2.4 Sampling and laboratory analyses. 229
7.2.5 Statistical analyses. 231
7.3 Results 232
7.3.1 Environmental parameters. 232
7.3.2 Copper exposure and accumulation. 233
7.3.3 Maximum quantum yield (F_v/F_m). 236
7.3.4 Pigments content. 241
7.3.5 Invertebrate re-colonisation. 246
7.4 Discussion 250
8. General discussion 257
8.1 Main findings and implications for marine systems 258
8.1.1 Benthic community responses to ocean acidification 260
8.1.2 Changes in biological interactions at elevated pCO ₂ 262
8.1.3 Adaptation potential to ocean acidification 264
8.1.4 Interaction with other stressors 269
8.2 Summary and direction for future research 270
References 274
Appendices 333
Appendix A: Benthic percent cover at Methana and biomass at Vulcano (Chapter 3) 333

Appendix B: Epifaunal abundance at Methana and Vulcano (Chapter 4)	336
Appendix C: Benthic functional groups cover at Vulcano and Methana (Chapter 5)	. 342
Appendix D: Epifaunal abundance at Methana (Chapter 7)	. 347
Appendix E: Publications	. 349

List of Figures

1.1	Projected seawater inorganic carbon chemistry until 2300	33
1.2	Changes in seagrass epiphytes at elevated CO ₂	40
1.3	Taxonomic variation in effects of ocean acidification	47
1.4	Visual abstract of thesis aims	60
2.1	Map of Methana study sites	72
2.2	Photos of Methana benthic communities at different pCO ₂ levels	73
2.3	Variability in pH at the study sites off Methana	83
2.4	Mean Sediment Quality Guidelines-quotient (SQG-Q) calculated with PEL and ERM at Methana	87
3.1	Map of Vulcano study sites	100
3.2	Map of iron concentrations at Vulcano	102
3.3	Map of Marine Sediment Pollution Index (MSPI) at Vulcano	103
3.4	Shannon diversity (H') and Pielou's evenness (J') at high, intermediate and reference CO ₂ at Methana	106
3.5	Percentage cover of canopy-forming algae and calcifying algae off Methana	111
3.6	Photo of macroalgal communities off Methana in autumn	112
3.7	Percentage cover of dominant macroalgal species off Methana	113
3.8	Mean Shannon diversity (H') and Pielou's evenness (J') at Vulcano	115

3.9 Biomass of canopy-forming algae, calcifying algae, non-calcifying green algae and turf algae at Vulcano	118
3.10 Biomass of <i>Sargassum vulgare</i> , <i>Dictyopteris membranacea</i> , <i>Flabellia petiolata</i> and <i>Caulerpa prolifera</i> at Vulcano	119
4.1 Study sites at Vulcano	132
4.2 Macroalgal species sampled for epifauna at Methana and Vulcano .	132
4.3 Dry mass of <i>C. corniculata</i> off Methana	136
4.4 MDS plot of invertebrate assemblages on <i>C. corniculata</i> thalli at Methana	139
4.5 Abundances of broad taxonomic groups of epifaunal invertebrates of <i>C. corniculata</i> at Methana.	140
4.6 MDS plot of morphology of <i>Cystoseira</i> spp. and <i>S. vulgare</i> thalli collected at Vulcano	142
4.7 Axis length, order of branching and frond density of <i>Cystoseira</i> spp. and <i>S. vulgare</i> thalli collected at Vulcano	143
4.8 Diversity of epifaunal communities on <i>Cystoseira</i> spp. and <i>S. vulgare</i> thalli collected at Vulcano	146
4.9 Abundances of broad taxonomic groups of invertebrates found on thalli of <i>Cystoseira</i> spp. and <i>S. vulgare</i> collected at Vulcano	147
5.1 Main grazers on Mediterranean intertidal and subtidal shores .	158
5.2 Vulcano study sites	161
5.3 Rocky shore on Vulcano with experimental units	162

5.4	Pictures of the three herbivore exclusion treatments at Methana	. 166
5.5	Percent cover of species significantly affected by experimental treatments at Vulcano	. 172
5.6	Limpet abundance at Vulcano during the exclusion experiment	. 173
5.7	Limpet length at Vulcano during the exclusion experiment	. 174
5.8	Percentage of wax disc grazed by limpets at Vulcano.	. 175
5.9	Sea urchin abundances at Methana study sites	. 177
5.10	Biomass of herbivorous fish at Methana	. 178
5.11	MDS plot for the herbivore exclusion experiment performed at Methana	. 180
5.12	Biomass of fleshy and erect algae of the herbivore exclusion experiment conducted at Methana	. 181
5.13	Biomass and percent cover of functional groups at Methana at the end of the exclusion experiment	. 182
6.1	Scheme of the experimental design for reciprocal transplantations at Methana	. 195
6.2	Relative growth of <i>C. corniculata</i> thalli transplanted at Methana	. 200
6.3	Relative growth of <i>J. rubens</i> thalli transplanted at Methana	. 201
6.4	Epiphyte cover of <i>C. corniculata</i> thalli transplanted at Methana	. 202
6.5	Pigments content of <i>C. corniculata</i> thalli transplanted at Methana	. 205
6.6	Pigments content of <i>J. rubens</i> thalli transplanted at Methana	. 207

6.7 Phycobilins content of <i>J. rubens</i> thalli transplanted at Methana	. 208
6.8 C:N and N:P ratios of <i>C. corniculata</i> thalli transplanted at Methana	. 209
6.9 C and N percent content of <i>J. rubens</i> thalli transplanted at Methana	210
6.10 Inorganic carbon percent content of <i>J. rubens</i> thalli transplanted at Methana 211
6.11 Phenols concentration of <i>C. corniculata</i> thalli transplanted at Methana 213
6.12 Typical macroalgal assemblage off Methana in September 2013	. 219
7.1 World map of copper production in 2005 225
7.2 Scheme of the experimental design for copper exposure experiment at Methana 227
7.3 <i>Jania rubens</i> transplanted near seeps off Methana 227
7.4 Copper concentration of <i>C. corniculata</i> thalli transplanted at Methana 234
7.5 Copper concentration of <i>J. rubens</i> thalli transplanted at Methana	. 236
7.6 Changes in maximum quantum yield (F_v/F_m) following <i>C. corniculata</i> thalli transplant and copper exposure 238
7.7 Changes in maximum quantum yield (F_v/F_m) following <i>J. rubens</i> thalli transplant and copper exposure 240
7.8 Pigment concentrations of <i>C. corniculata</i> thalli transplanted at Methana 242

7.9 Pigment concentrations of <i>J. rubens</i> thalli transplanted at Methana .	244
7.10 Phycobilin concentrations of <i>J.rubens</i> thalli transplanted at Methana 246
7.11 MDS plot of invertebrate assemblages on <i>C. corniculata</i> thalli from the copper exposure experiment 248
7.12 Abundances of broad taxonomic groups of <i>C. corniculata</i> epifauna from the copper exposure experiment 250
8.1 Visual abstract of thesis results 259
8.2 Typical seascape near seeps off Methana and at reference sites .	263
8.3 Photo of <i>J. rubens</i> thalli transplanted near seeps off Methana .	268

List of Tables

1.1 Summary of thesis sampling trips, measured parameters and sample sizes 61
2.1 Composition of Methana gas emissions. 71
2.2 PEL and ERM threshold values 79
2.3 Classification of a shore point wave exposure 82
2.4 Measured and calculated carbonate system parameters at Methana	84
2.5 Seawater nutrient concentrations at Methana in June 2013 85
2.6 Concentrations of sediment heavy metal at Methana 86

2.7 <i>Dictyota</i> sp. metal content at Methana	88
2.8 Comparison of metal concentration in <i>Dictyota</i> spp. at Methana with values found in the literature for unpolluted sites	88
2.9 Modified effective fetch and maximum fetch at Methana	89
3.1 Temperature, salinity, total alkalinity and dissolved nutrient concentrations at Vulcano	101
3.2 PERMANOVA on percentage cover of Methana benthic communities	105
3.3 ANOVA results for Shannon diversity (H') and Pielou's evenness (J') of Methana benthic communities	106
3.4 SIMPER analysis of Methana benthic communities	107
3.5 PERMANOVA analysis on biomass of Vulcano benthic communities	114
3.6 ANOVA for Shannon diversity (H') and Pielou's evenness (J') of Vulcano macroalgal communities	115
3.7 SIMPER analysis of Vulcano benthic communities	116
4.1 ANOVA on biomass of <i>C. corniculata</i> at Methana	135
4.2 PERMANOVA on epiphyte communities of <i>C. corniculata</i> at Methana	136
4.3 PERMANOVA on epifaunal communities of <i>C. corniculata</i> at Methana	137
4.4 PERMANOVA on invertebrate communities of <i>C. corniculata</i> at Methana grouping taxa into broad taxonomic groups	138

4.5 PERMANOVA on morphology of <i>Cystoseira</i> spp. and <i>S. vulgare</i> thalli collected at Vulcano 141
4.6 PERMANOVA on epifauna of <i>Cystoseira</i> spp. and <i>S. vulgare</i> thalli collected at Vulcano 144
4.7 ANOVA on epifaunal diversity of <i>Cystoseira</i> spp. and <i>S. vulgare</i> thalli collected at Vulcano 145
4.8 Response to increasing CO ₂ of the main epifaunal taxa at Methana and Vulcano 150
5.1 pH, temperature and salinity measured during the experiment at Vulcano 168
5.2 PERMANOVA analyses of percentage benthic cover in the experimental plots at Vulcano. 169
5.3 SIMPER analysis showing the average dissimilarities between sites and treatments at Vulcano 170
5.4 pH, temperature and salinity measured at Methana 175
5.5 ANOVA on sea urchin densities measured at Methana 176
5.6 ANOVA on log-transformed herbivorous fish biomass at Methana 177
5.7 PERMANOVA on percentage cover of the tiles deployed at Methana for the herbivore exclusion experiment 179
5.8 PERMANOVA on biomass of macroalgae growing on tiles deployed at Methana for the herbivore exclusion experiment 181
6.1 ANOVA results for transplanted <i>C. corniculata</i> thalli growth 200

6.2 ANOVA results for transplanted <i>J. rubens</i> thalli growth	. 201
6.3 MANOVA on photosynthetic parameters in <i>C. corniculata</i> thalli transplanted at Methana	. 203
6.4 Photosynthetic parameters of <i>C. corniculata</i> thalli transplanted at Methana	. 203
6.5 MANOVA on photosynthetic parameters in <i>J. rubens</i> thalli transplanted at Methana	. 204
6.6 Photosynthetic parameters of <i>J. rubens</i> thalli transplanted at Methana	. 204
6.7 MANOVA on pigments content in <i>C. corniculata</i> thalli transplanted at Methana	. 205
6.8 MANOVA on pigments content in <i>J. rubens</i> thalli transplanted at Methana	. 206
6.9 MANOVA on phycobilins content in <i>J. rubens</i> thalli transplanted at Methana	. 208
6.10 MANOVA on C:N and N:P ratios in <i>C. corniculata</i> thalli transplanted at Methana	. 209
6.11 MANOVA on C and N content in <i>J. rubens</i> thalli transplanted at Methana	. 210
6.12 ANOVA on transplanted <i>J. rubens</i> thalli inorganic carbon content	. 211
6.13 ANOVA on phenols content of <i>C. corniculata</i> thalli transplanted at Methana	. 212

7.1 pH, total alkalinity, temperature and salinity measured during the experiments 233
7.2 ANOVA on copper concentration in <i>C. corniculata</i> thalli 234
7.3 ANOVA on copper concentration in <i>J. rubens</i> thalli 235
7.4 ANOVA on change in maximum quantum yield (F_v/F_m) after transplant and after copper exposure for <i>C. corniculata</i> thalli 237
7.5 ANOVA on change in maximum quantum yield (F_v/F_m) after transplant and after copper exposure for <i>J. rubens</i> thalli 239
7.6 MANOVA on pigment concentrations in <i>C. corniculata</i> thalli 241
7.7 MANOVA on pigment concentrations in <i>J. rubens</i> thalli 243
7.8 MANOVA on phycobilins concentrations in <i>J. rubens</i> thalli 245
7.9 PERMANOVA analyses of invertebrate abundances in <i>C. corniculata</i> thalli from copper exposure experiment 247
7.10 SIMPER analysis showing the average dissimilarities between sites and copper treatments 249
8.1 Summary of short- and long-term effects of transplant to elevated CO ₂ in <i>C. corniculata</i> and <i>J. rubens</i> 266

Acknowledgements

I would like to thank my supervisory team, Prof. Jason Hall-Spencer, Prof. Kai Bischof, Dr Marco Milazzo, Dr Antonella Pancucci-Papadopoulou and Dr Eva Krasakopoulou, who all helped with this thesis according to their expertise.

I am immensely grateful for all the help I have received during fieldwork, especially from Alessio Deidda, who travelled to Italy and Greece to help me in most of my sampling trip. I also received great help from Maria Salomidi, Laura Bray, Emanuela Voutsinas, Yiannis Issaris and Eva Krasakopoulou from the Hellenic Centre for Marine Research during fieldwork at Methana and from Mariagrazia Graziano, Marco Milazzo, Giuseppe Bruno and Laura Ciriminna at Vulcano. I would also like to thank Kai Bischof for generously loaning me his Diving PAM.

I am extremely grateful to the staff from Bremen University and the Leibniz Center for Tropical Marine Ecology, especially Laurie Hofmann and Mirta Teichberg, for the very enjoyable collaboration and the training during my visit in Bremen. Many people at the Hellenic Centre for Marine Research have helped me in the laboratory analysis, and I especially want to thank Louisa Giannoudi, Alexandra Pavlidou and Eleni Rouselaki. Antonella Pancucci-Papadopoulou from HCMR and Renato Chemello and Annamaria Mannino from University of Palermo greatly helped me to identify invertebrates and macroalgae.

I would also like to thank everyone at the Marine Biology and Ecology Research Centre at Plymouth University for their help during the last three years, especially Balbina Ramsay and Laura Pettit for the precious company during countless hours of microscopy work, and Andy Foggo and Richard Billington for their help with phenols analysis.

AUTHOR'S DECLARATION

At no time during the registration for the degree of Doctor of Philosophy has the author been registered for any other University award without prior agreement of the Graduate Committee. Work submitted for this research degree at the Plymouth University has not formed part of any other degree either at Plymouth University or at another establishment.

This study was financed with the aid of a studentship from the Joint Doctorate programme MARES selected under Erasmus Mundus coordinated by Ghent University (FPA 2011-0016) and carried out in collaboration with Bremen University, University of Palermo and the Hellenic Centre for Marine Research. Additional funding was granted by the EU FP7 project 'Mediterranean Sea Acidification under a changing climate' (grant agreement no. 265103) to fund part of the fieldwork, the EU FP7 European Project on Ocean Acidification (EPOCA) funded a research training visit to Bremen University and the British Ecological Society, Plymouth Marine Science and Education Foundation and Plymouth Marine Institute granted me travel bursaries to attend international conferences.

Relevant scientific seminars and conferences were regularly attended at which work was often presented; work from this project and collaborations established during this period lead to a number of publications:

- **C. Baggini**, Y. Issaris, M. Salomidi, J.M. Hall-Spencer (2014). Herbivore diversity improves benthic community resilience to ocean acidification. *Journal of Experimental Marine Biology and Ecology* (accepted pending revisions).

- **C. Baggini**, M. Salomidi, E. Voutsinas, L. Bray, E. Krasakopoulou, J.M. Hall-Spencer (2014). Seasonality affects macroalgal community response to increases in pCO₂. *PLoS ONE*, 9: e106520.
- L.C. Hofmann, K. Bischof, **C. Baggini**, A. Johnson, K. Koop-Jakobsen, M. Teichberg (2014). CO₂ and inorganic nutrient enrichment affect the performance and competitive strength of a calcifying green alga and its non-calcifying epiphyte. *Oecologia* (accepted pending revisions).
- G. Langer., G. Nehrke, **C. Baggini**, R. Rodolfo-Metalpa, J.M. Hall-Spencer, J. Bijma (2014). Limpets counteract ocean acidification induced shell corrosion by thickening of aragonitic shell layers. *Biogeosciences Discussions*, 11: 12571-12590.
- P. Calosi, S.P.S. Rastrick, M. Graziano, S.C. Thomas, **C. Baggini**, H.A. Carter, J. Hall-Spencer, M. Milazzo, J.I. Spicer (2012). Ecophysiology of sea urchins living near shallow water CO₂ vents: Investigations of acid-base balance and ionic regulation using *in-situ* transplantation. *Marine Pollution Bulletin*, 73: 470-484.
- S. Hahn, R. Rodolfo-Metalpa, E. Griesshaber, W.W. Schmahl, D. Buhl, J.M. Hall-Spencer, **C. Baggini**, K.T. Fehr, A. Immenhauser (2012). Marine bivalve shell geochemistry and ultrastructure from modern low pH environments: environmental effect versus experimental bias. *Biogeosciences*, 9: 1897-1914.

Presentations at conferences:

- Using CO₂ vents as a natural analogue for ocean acidification (2011). Oral presentation, 4th Annual Plymouth Marine Science Conference, Plymouth, UK.

- Effects of ocean acidification on *Mytilus galloprovincialis* and *Patella caerulea* at natural CO₂ vents (2012). Poster presentation, Third Symposium on the ocean in a high CO₂ world, Monterey, California.
- Effects of short-term copper exposure on seaweeds acclimatised to high CO₂ (2013). Pollution Responses in Marine Organisms symposium, Faro, Portugal.
- Greek CO₂ vents show community effects of ocean acidification in the oligotrophic Aegean Sea (2013). INTECOL, London, UK.

List of research chapters and declaration of own contribution

Chapters 2 and 3: the same contributions apply to both chapters

Chapter 2: Assessing the suitability of a volcanic seep area off Methana (Greece) for ocean acidification studies

Chapter 3: Changes in subtidal macroalgal communities along pCO₂ gradients at Mediterranean volcanic seeps

Contributors: Cecilia Baggini, Maria Salomidi, Emanuela Voutsinas, Laura Bray, Eva Krasakopoulou, Jason M. Hall-Spencer

Contributions: I designed and performed the sampling with help from MS, EV, LB and EK; I analysed all samples with help from EK, performed statistical analyses and wrote the manuscript with help from all authors; JMH-S supervised the thesis.

Chapter 4: Canopy algal epifauna changes at elevated pCO₂ at two Mediterranean volcanic seeps

Contributors: Cecilia Baggini, Renato Chemello, Marco Milazzo, Mariagrazia Graziano, Antonella Pancucci-Papadopoulou, Laura Ciriminna, Jason Hall-Spencer

Contributions: I designed the experiment with help from MG, RC and MM, and performed the sampling with help from LC, who also helped processing the samples; I identified all invertebrates with help from RC and AP, performed statistical analyses and wrote the manuscript; JMH-S supervised the thesis.

Chapter 5: Effect of herbivores on benthic communities at different pCO₂ levels

Contributors: Cecilia Baggini, Mariagrazia Graziano, Marco Milazzo, Maria Salomidi, Yiannis Issaris, Marco Franzitta, Giuseppe Bruno, Jason Hall-Spencer

Contributions: I designed the experiment with help from MG and MM, and performed the sampling with help from MM, GB, MS and YI; I processed all samples with help from MF, performed statistical analyses and wrote the manuscript with help from all co-authors; JMH-S supervised the thesis.

Chapters 6 and 7: the same contributions apply to both chapters

Chapter 6: Seaweed acclimatisation to high pCO₂ at volcanic seeps

Chapter 7: A short-term copper pulse affects macroalgal copper accumulation and indirectly alters epifaunal colonisation at elevated pCO₂

Contributors: Cecilia Baggini, Kai Bischof, Murray Brown, Jason Hall-Spencer

Contributions: I designed the experiment with feedback from MB during the transfer process, performed the sampling, processed all samples, performed

statistical analyses and wrote the manuscript; JMH-S and KB supervised the thesis and provided useful feedback on the manuscript.

DECLARATION/ ERKLÄRUNG

Ich erkläre

1. die Arbeit ohne unerlaubte fremde Hilfe angefertigt,
2. keine anderen als die von mir angegebenen Quellen und Hilfsmittel benutzt und
3. die den benutzten Werken wörtlich oder inhaltlich entnommenen Stellen als solche kenntlich gemacht zu haben.

Word count of main body of thesis: 53,331

Signed

Date.....

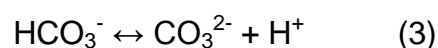
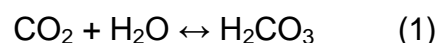
Chapter 1

Community responses to ocean acidification on temperate rocky reefs: possible causes and adaptation potential

1.1 Introduction

Since the beginning of industrial revolution, man has released huge quantities of carbon dioxide to the atmosphere. Atmospheric CO₂ concentrations reached 400 ppmv in April 2014 (NOAA, 2014) and are rising more rapidly than previously thought (Intergovernmental Panel on Climate Change, 2014). This increase is a concern, as atmospheric CO₂ was relatively constant over the last 800.000 years, with values ranging between 172 and 300 ppmv (Lüthi *et al.*, 2008). About one fourth of anthropogenic CO₂ emissions has been absorbed by the oceans, thereby reducing their effects in the atmosphere (Le Quéré *et al.*, 2009), but at the same time increasing the carbon dioxide concentration in seawater. A trend in increasing surface ocean pCO₂ parallel to the increase in atmospheric carbon dioxide is clearly detectable using long-term monitoring stations (Brewer *et al.*, 1997; Hofmann *et al.*, 2011).

Increased seawater pCO₂ causes changes in the ocean carbonate system, a process referred to as 'ocean acidification' (Caldeira and Wickett, 2003). When carbon dioxide dissolves in water it forms carbonic acid (H₂CO₃), a weak acid that is highly unstable in seawater (1). H₂CO₃ readily dissociates to form bicarbonate ions (HCO₃⁻) and hydrogen ions (2). Bicarbonate ions can in turn dissociate to produce carbonate ions (CO₃²⁻) and hydrogen ions. However, increased [H⁺] causes reaction (3) to reverse and bicarbonate ions to become more stable in seawater.



Overall, ocean acidification causes a decrease in seawater pH (i.e. an increase in $[H^+]$) and carbonate ion concentration and an increase in aqueous CO_2 ($CO_{2(aq)}$), dissolved inorganic carbon and $[HCO_3^-]$, with total alkalinity remaining constant. Decreased carbonate ion concentrations are leading to lower calcium carbonate saturation state (Ω_{CaCO_3}) in the world oceans, meaning that $CaCO_3$ is becoming more likely to dissolve. This happens because $[CO_3^{2-}]$ is one of the determinants of calcium carbonate saturation, as shown in equation (4).

$$\Omega_{CaCO_3} = [Ca^{2+}] [CO_3^{2-}] / K_{sp}^* \quad (4)$$

There are two forms of calcium carbonate: aragonite and calcite. These have different solubility product constants (K_{sp}^*) and thus different solubility, with aragonite being less stable than calcite in seawater (Tyrrell, 2008). A third form of calcium carbonate, high-magnesium calcite, forms the carbonic skeleton of some organisms and is even more soluble than aragonite. K_{sp}^* varies with pressure and temperature, making calcium carbonate more likely to dissolve at low temperatures and high pressure. Deep polar waters are already undersaturated (i.e. $\Omega_{CaCO_3} < 1$) with respect to aragonite, whereas superficial waters are predicted to become undersaturated in the next decades (Orr *et al.*, 2005; Steinacher *et al.*, 2009; Tittensor *et al.*, 2010).

With regards to the global ocean, mean pH has already decreased from ~ 8.2 to ~ 8.1 compared to pre-industrial times (Key *et al.*, 2004), probably the lowest value in the last two million years (Hönisch *et al.*, 2009). A further decrease of approximately 0.4 units is projected for the end of this century according to the “business as usual” scenario (Caldeira and Wickett, 2003), which underestimates the present rate of anthropogenic CO_2 release into the atmosphere (IPCC, 2014). For the year 2300, different emission scenarios

depend on improvements in fossil fuel extraction techniques. In the “business as usual” scenario, the mean ocean pH is predicted to reach a value of 7.4, but if mining techniques improve the subsequent increase in anthropogenic emissions could lead to a mean ocean pH of 7.1. Moreover, methane hydrate exploitation could cause ocean pH to reach a minimum of 6.8 (Caldeira and Wickett, 2005). The predicted changes in seawater carbonate chemistry are illustrated in Figure 1.1; these changes will not be permanent, because increased dissolution of deep-sea carbonate sediments and weathering on land will eventually buffer them. Carbonate dissolution from rocks and sediments, however, takes thousands of years to equilibrate the ocean carbonate system (Caldeira and Wickett, 2003), whereas current rates of increase in atmospheric carbon dioxide are already causing dramatic changes in the ocean carbonate chemistry.

In Earth’s geological history, changes in seawater $p\text{CO}_2$ occurred more slowly than today, allowing weathering and sediment carbonate dissolution to raise carbonate saturation states. Therefore, care should be taken when comparing current changes in carbonate chemistry with those geological periods in the past that had high $p\text{CO}_2$. Only periods with a similar rate and magnitude of change can help us predict the long-term effects of ocean acidification. In order to identify relevant episodes, it is necessary to reconstruct at least two seawater carbonate parameters, as high carbon dioxide concentration in seawater does not imply a low calcium carbonate saturation state (Zeebe and Ridgwell, 2011). An example is the Cretaceous, when very high seawater $p\text{CO}_2$ was combined with high saturation state of calcium carbonate. This combination of factors was due to the slower increase of carbon dioxide compared to the current rates of increase and the fact that high concentrations of carbon dioxide were

maintained for millions of years. When changes in marine carbonate chemistry occur at these timescales, they can be buffered by dissolution of carbonate sediments. This situation had thus a lower potential to affect biological calcification than ocean acidification (Zeebe and Westbroek, 2003; Ridgwell and Schmidt, 2010).

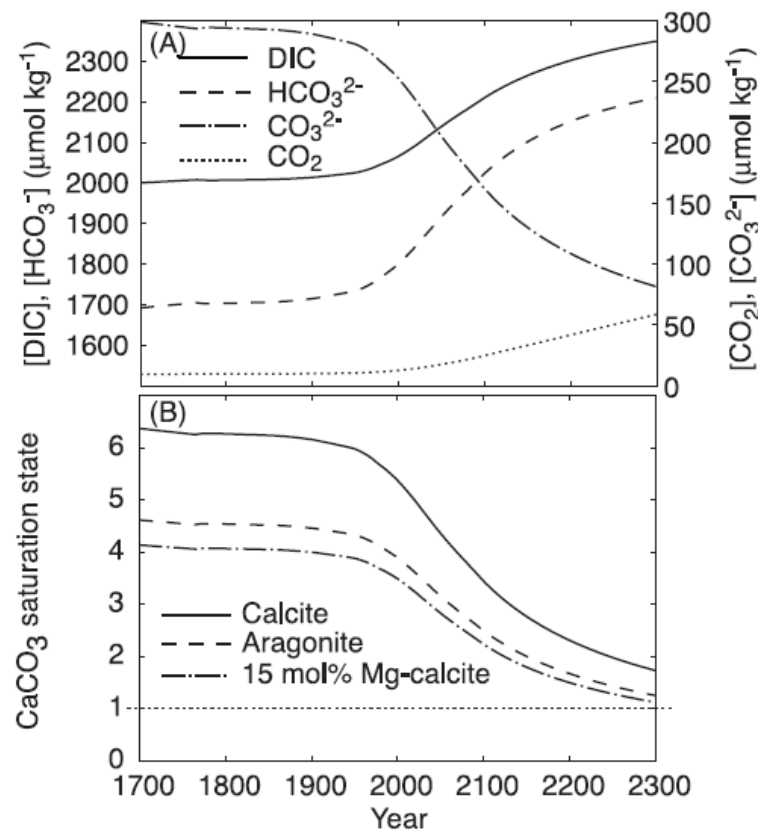


Figure 1.1. Surface water dissolved inorganic carbon chemistry between 1700 and 2300 calculated using a shallow-water ocean carbonate model at 25°C and 35 psu. (A) Total dissolved inorganic carbon concentration [DIC], [CO_2], [HCO_3^-], and [CO_3^{2-}], and (B) surface water saturation state with respect to calcite, aragonite and 15 mol % magnesian calcite (Andersson *et al.*, 2005).

Suitable past ocean acidification analogues are periods of rapid (i.e. less than 10000 years) increase in seawater pCO_2 , which would give no time for compensatory mechanisms to act. The best analogue for ocean acidification

with good geological records is probably the Paleocene-Eocene Thermal Maximum (PETM, ~55.8 million years ago). In this period a temperature increase of 5-9°C over a few thousand years was coupled with massive carbon release. The subsequent decline in seawater pH and CaCO₃ saturation state is similar to ocean acidification in many aspects, albeit rates of change were still slower than the current ones (Zachos *et al.*, 2005). This event did not appear to have significant effects on superficial nanoplankton (Gibbs *et al.*, 2006), but it caused a dramatic decrease in benthic foraminifera species (e.g. Thomas, 2007) and sediment fauna in general (Rodriguez-Tovar *et al.*, 2011). It is not clear, however, if extinctions were caused by changes in carbonate chemistry, oxygen reduction or temperature increase, although it could have been a combination of the above. All things considered, it seems that ocean acidification is an unprecedented phenomenon in our planet's history (Zeebe and Ridgwell, 2011).

Anthropogenic emissions are currently causing rapid changes in ocean carbonate chemistry that are well known and understood (Doney *et al.*, 2009; Orr, 2011), but ocean acidification also has the potential to affect various physical, biogeochemical and biological processes. Predictions of how these processes will respond to an increase in seawater pCO₂ are much less certain, and are an urgent priority for future research (Gattuso *et al.*, 2011). Ocean acidification can affect nutrient availability (Raven *et al.*, 2005; Doney *et al.*, 2009; Hutchins *et al.*, 2009) and trace metal speciation (Raven *et al.*, 2005; Tyrrell, 2008; Doney *et al.*, 2009; Millero *et al.*, 2009; Breitbarth *et al.*, 2010; Shi *et al.*, 2010), as well as sound wave diffusion through seawater (Hester *et al.*, 2008; Brewer and Hester, 2009). Furthermore, many biological processes may be affected, including all pH-dependent physiological functions (e.g. acid-base balance, protein activity) and those processes that use a carbon species as

substrate (e.g. photosynthesis, calcification) (Fabry *et al.*, 2008). Ocean acidification is then likely to affect benthic communities, but their responses are hard to predict because interspecific interactions can cause unexpected changes at the community level (Hale *et al.*, 2011)

1.2 Community effects of ocean acidification on temperate rocky reefs

Laboratory experiments assessing responses to increased CO₂ determine species' relative sensitivities to high CO₂. They can also reveal threshold tolerance values as well as physiological mechanisms involved in biological responses to ocean acidification. It is difficult, however, to scale up from such studies and predict how whole ecosystems will change as our oceans continue to acidify; this approach does not consider interactions between species, which dramatically influence community structure (Kroeker *et al.*, 2013a). Furthermore, the artificial conditions in a laboratory are probably very stressful for some taxa, and this could alter results (Widdicombe *et al.*, 2010).

Consequently, researchers have begun studying ocean acidification effects on community structure using mesocosm experiments. The need to test results obtained in laboratory conditions with simplified communities, however, has also led researchers to manipulate pCO₂ in the field or study areas with naturally high CO₂ concentrations. Such data are being used to develop models to predict how ecosystems will change as seawater carbon dioxide continues to increase.

1.2.1 Laboratory and mesocosm experiments

A community composed of long-lived organisms usually does not change its composition at the timescale of most laboratory and mesocosm experiments (i.e. days to months, rarely years). Therefore, only responses of single species and their interactions to increased pCO₂ can be observed using this approach. In this context, coral reef ecosystems are the most studied: mesocosm experiments lasting up to ten months reported a decrease in coral and coralline algae calcification and growth (Jokiel *et al.*, 2008; Küffner *et al.*, 2008), sometimes leading to net community CaCO₃ loss at low pH (Andersson *et al.*, 2009).

Temperate communities are much less studied, but there is evidence that ocean acidification will cause changes here as well. Macroalgal species show differential sensitivity to increased CO₂; for instance, cover of the calcifying alga *Corallina officinalis* decreased, whereas the non-calcifying *Chondrus crispus* was more abundant as CO₂ increased (Hofmann *et al.*, 2012). Biomass and productivity decreased with increased CO₂ and temperature in communities associated with canopy-forming brown algae, but the invasive *Sargassum muticum* resulted more resistant to both stressors than the native *Cystoseira tamariscifolia* (Olabarria *et al.*, 2013). Community changes are therefore likely even when the dominant species are not calcifiers.

Some macroalgal species seem to be advantaged at elevated CO₂ because they are carbon-limited (Harley *et al.*, 2012). For instance, some turf algae have the potential of outcompeting kelp on Australian rocky shores when CO₂ and nutrients concurrently increase (Falkenberg *et al.*, 2013a). Shading from kelp,

however, reduces turf growth, meaning that a shift from kelp to turf algae is only likely if kelp cover is reduced by other stressors (Falkenberg *et al.*, 2012).

Invertebrate communities have been shown to change as well: for instance, Hale *et al.* (2011) found that organisms associated with turf algae generally reacted to increased pCO₂ consistently with predictions from single species experiments. However, reduced predation rates and competition for space caused nematode abundance to increase unexpectedly. These communities change from being dominated by calcareous organisms to being dominated by non-calcareous organisms at a pH between 7.2 and 7.8 (Christen *et al.*, 2013).

1.2.2 Field pCO₂ manipulation

In recent years, various techniques to increase seawater pCO₂ in the field have been developed for the study of whole communities in their natural environment. In Chesapeake Bay (USA), CO₂ bubbling in open waters was used to assess changes in marine plants chemical defences (Arnold *et al.*, 2012). While this method allows for natural flow conditions, pCO₂ varies with current speed and direction.

Seawater mixed with CO₂ can also be injected into open chambers to better control carbonate chemistry variability while reproducing natural water movement (Campbell and Fourqurean, 2011). This system has been used to test the effects of ocean acidification on the seagrass *Thalassia testudinum*: its growth was not affected by elevated CO₂, whereas nitrogen and phosphorous content significantly decreased with increased CO₂ (Campbell and Fourqurean, 2013). Seagrass epiphytes were more affected by increased CO₂ than by increased nutrients, with calcifying species being substituted by fleshy species (Campbell and Fourqurean, 2014).

A similar system, which uses closed or semi-enclosed chambers, is the Free Ocean Carbon Enrichment system (FOCE); similarly to the previous one, this system can be used to run long term experiments with entire communities exposed to natural levels of light, nutrients and temperature (Waz *et al.*, 2007; Kline *et al.*, 2012). FOCE systems have been successfully used in Australia, where pH was lowered by 0.4 units and dissolution of coralline algae increased at high CO₂ during a short-term experiment (Kline *et al.*, 2012). FOCE systems may be used to assess the effects of ocean acidification on many ecological processes, but are too small to influence some ecosystem properties, such as population connectivity or larval recruitment. So far, no results are available from temperate FOCE systems, even though experiments are being conducted in the Mediterranean Sea using eFOCE (European FOCE) and a shallow water FOCE (swFOCE) system is under development in California (Gattuso *et al.*, 2014).

1.2.3 Areas with naturally elevated pCO₂

Areas with naturally high CO₂ can be used to assess long-term community responses to ocean acidification. Hydrothermal vents are generally characterised by low pH and emit fluids that can contain various gases, especially carbon dioxide, hydrogen sulphide, methane and nitrogen (Tarasov *et al.*, 2005). Increased concentrations of heavy metals in the surrounding sediments are also common (e.g. Dando *et al.*, 2000; Hübner *et al.*, 2004), and macroalgae near such vents can have increased metal concentrations in their tissues (Couto *et al.*, 2010). Vents shallower than 200 m are generally populated by a subset species inhabiting the surrounding area. They are thus very different from deep-sea vents, where chemosynthetic vent-obligated species are abundant (Tarasov *et al.*, 2005).

In shallow areas, usually there is a notable reduction in biodiversity proceeding towards the vents (Melwani and Kim, 2008; Karlen *et al.*, 2010). Here, the most abundant species are those able to resist elevated temperatures and high concentrations of toxic gases and heavy metals. They also have to be resistant to reduced salinity if volcanic emissions are mixed with fresh water (Tarasov *et al.*, 2005). An exception to this trend was reported at vents off Milos (Greece), where sessile macroepibenthos had higher biodiversity near the vents than at the control sites (Morri *et al.*, 1999; Pansini *et al.*, 2000; Bianchi *et al.*, 2011). However, infauna showed an opposite trend, possibly because of the high sulphide concentration in the sediment near the vents (Thiermann *et al.*, 1997). Hot fluid emissions were also indicated as the cause for increased occurrence of warm-water seaweeds near the emissions (De Biasi and Aliani, 2003).

Although many of these areas have high seawater CO₂ concentration, there are very often confounding gradients in temperature, toxic gases, heavy metals or salinity, so their utility to understand community responses to ocean acidification is limited. However, it is possible to find shallow water seeps emitting almost exclusively carbon dioxide without confounding gradients in temperature, salinity, toxic gases and heavy metal contamination. There are only a few published examples of CO₂ seeps at temperate shores used as ocean acidification proxies, such as the two off Italy (Hall-Spencer *et al.*, 2008; Boatta *et al.*, 2013).

There biodiversity, especially that of calcifying taxa, is reduced as pCO₂ increases (Hall-Spencer *et al.* 2008; Martin *et al.*, 2008; Dias *et al.*, 2010; see Figure 1.2) and benthic communities are simpler and more homogeneous as CO₂ increases (Kroeker *et al.*, 2013b). Moreover, shifts in macroalgal dominance along a pCO₂ gradient have been reported (Porzio *et al.*, 2011), and

invertebrate recruitment is heavily influenced as well (Cigliano *et al.*, 2010). Benthic invertebrates also experience a reduction in diversity and biomass, and the community trophic complexity is lower at high CO₂ levels (Kroeker *et al.*, 2011).



Figure 1.2. *Posidonia oceanica* covered in calcareous epiphytes at pH 8.2 at CO₂ vents off Ischia (left) and lacking Corallinaceae at pH 7.6 (right); yellow arrow points to CO₂ bubbles (Hall-Spencer *et al.*, 2008).

Experiments at seeps have revealed different sensitivities of sea urchin species to elevated CO₂: *Paracentrotus lividus*, the main consumer of fleshy algae, is less resistant to elevated carbon dioxide (Calosi *et al.*, 2013a). Changes in herbivore densities have knock-on effects on fleshy macroalgae, such as the calcifying alga *Padina pavonica* (Linnaeus) Thivy. Even though these algae are less calcified at elevated CO₂ levels, their cover in fact increases because they are subject to less herbivore pressure (Johnson *et al.*, 2012). Experiments at seeps can also detect differences in responses to CO₂ as temperature increases: calcification rates in a Mediterranean coral was not affected by pCO₂ in spring, but strongly decreased at elevated CO₂ levels after a very warm summer (Rodolfo-Metalpa *et al.*, 2011).

At volcanic seeps, it is also possible to test differences in ecological processes along pCO₂ gradients. For macroalgal communities, both early recruitment (Porzio *et al.*, 2013) and final community composition after one year (Kroeker *et al.*, 2013c) change greatly with increasing CO₂ due to the direct effects of carbon dioxide and to changes in interspecific interactions. For instance, crustose coralline algae manage to recruit at elevated pCO₂ levels, but their decreased growth rates near the seeps allow fleshy algae to outcompete them (Kroeker *et al.*, 2013c).

Carbon dioxide seeps are proving useful for ocean acidification research because they show us how whole communities change with long-term exposure to high CO₂ levels. They can also be used to test hypotheses developed in laboratory-based experiments. However, seeps are not a perfect reproduction of CO₂-influenced ecosystems, since they are too small to host entire populations. Motile taxa such as fish are not likely to be as heavily influenced by CO₂ as sessile taxa (Riebesell, 2008) and pelagic larvae settling near the seeps can originate from unaffected populations (Cigliano *et al.*, 2010). Moreover, if sites too close to the CO₂ source are chosen, pH can fluctuate rapidly and be very different from what natural ecosystems experience. Hence, care must be taken to select sites appropriately, so that daily and seasonal fluctuations in pH remain as similar as possible to reference sites (Kerrison *et al.*, 2011).

Acidified estuaries are another possibility to study biological responses to ocean acidification in a natural environment. Two types of estuaries have been considered so far, those with high levels of biogenic CO₂ produced by microbial respiration and those exposed to acid sulphate soils runoffs. In the first type pH is lower than in reference estuaries because of increased CO₂ and can cause biological effects such as increased gastropod shell corrosion (Marshall *et al.*,

2008). However, in these areas oxygen levels are generally lower than reference values and nutrients have higher concentrations because of nutrient discharges, potentially confounding the effect of high CO₂ (Mucci *et al.*, 2011). Estuaries can also be subject to acidification episodes if acid sulphate soils are transported by rivers after heavy rainfall events. Although they are not proper ocean acidification analogues, since low pH is episodic and not due to increased CO₂ concentration, hypoxia is not an issue in these sites. Molluscs in these estuaries are less abundant than in control estuaries, although within the natural range of variation reported for that region (Amaral *et al.*, 2011), and mollusc shells are weaker as well (Amaral *et al.*, 2012).

Small-scale analogue systems are very useful to show community effects of ocean acidification, but they cannot be used to assess changes in large scale processes such as population connectivity and larval supply. These processes could be studied in larger high pCO₂ areas, such as upwelling regions, which could be a precious source of information on ecosystems subject to naturally high pCO₂. In temperate regions, undersaturated waters rise from the deep sea along the east coast of USA and Canada and on the Chilean coast (Feely *et al.*, 2008; Mayol *et al.*, 2012). In some cases upwelling waters even penetrate in estuaries, where they have dramatic effects on the pH of waters lacking a carbonate buffer system (Feely *et al.*, 2010). Long-term monitoring of intertidal communities on the Eastern Pacific shores detected a decreased abundance of calcifying organisms when CO₂ is higher (Wootton *et al.*, 2008), and calcifying seaweed epibionts are also less abundant in upwelling areas (Saderne and Wahl, 2013). Elevated CO₂ levels in upwelling waters are compromising oyster aquaculture on eastern US shores (Barton *et al.*, 2012) as well as the fitness of other commercial species such as the Atlantic cod (Frommel *et al.*, 2012).

Some calcifying organisms seem to have adapted to the high pCO₂ recorded in upwelling areas: for instance, mussels are dominant in the Kiel fjord, despite being subject to upwelling episodes during their recruitment season (Thomsen *et al.*, 2010). However, at least some of them already live near their tolerance limit, such as sea urchin living on the USA east coast. Although their larval calcification is not impaired in present-day upwelling conditions, larvae are negatively affected by near future conditions (Evans *et al.*, 2013).

Using this approach could improve our understanding of large scale effect of ocean acidification, although with some limitations. In these systems it is often difficult to decide which environmental factor is driving the observed changes, as many factors usually co-vary with seawater CO₂ concentration. For instance, waters off Chile have high pCO₂, but that is correlated with low oxygen concentration, making the effect of these two concurring factors difficult to disentangle and potentially leading to overestimation of high CO₂ negative effects (Mayol *et al.*, 2012). Furthermore, upwelling waters are generally low in temperature and rich in nutrients, whereas climate change scenarios predict opposite trends (Beardall *et al.*, 2009). Lower temperatures and higher food availability compared with future scenarios could reduce the biological effects of high CO₂, thus leading to underestimation of the detrimental effects of ocean acidification (Thomsen *et al.*, 2010; Melzner *et al.*, 2011).

1.2.4 Modelling approach

Integrating results from single organisms and communities on an ecosystem scale could be done using a modelling approach. Models are widely used in climate change research for physical and chemical factors (e.g. Andersson *et al.*, 2005; Caldeira and Wickett, 2005; Orr *et al.*, 2005), and models involving

also biological factors are currently being developed. Policy makers need to know how marine ecosystems will react not only to ocean acidification, but to concurrent stressors such as increasing temperature, eutrophication and overfishing (Hilmi *et al.*, 2012). Models predicting ecosystem effects of multiple stressors, however, are more difficult to produce because of the system complexity and data scarcity on many factors, e.g. potential for adaptation (Blackford, 2010).

At the moment, there are only a few studies using models to assess ecosystem effects of ocean acidification, but some work has already been done on coral reefs. For instance, a recent study models the potential reef organisms have to influence carbonate chemistry on a local scale (Anthony *et al.*, 2011a). Their results show that the predicted increase in seaweed dominance could actually help calcification in communities downstream, as macroalgae decrease seawater pCO₂ through photosynthesis. These results are consistent with data from Manzello *et al.* (2012), who reported that seagrass beds in Florida take up carbon dioxide and raise the calcium carbonate saturation experienced by inshore coral reefs to pre-industrial levels, although this effect is seasonal because it depends on seagrass productivity.

Models can also be used to predict how interacting stressors will affect communities; for instance, it has been shown that overfishing and eutrophication will decrease coral reef resilience to ocean acidification and increasing temperature. The reason for this is that corals will be less competitive than macroalgae, which will grow faster and will be favoured by decreased fish grazing (Anthony *et al.*, 2011b). Similar results were obtained using a model to analyse how long-term fisheries exploitation and ocean acidification would interact to affect various functional groups (Griffith *et al.*,

2011). This study showed that increased seawater pCO₂ is likely to influence very heavily overfished areas and cause major regime shifts around 2040. It is already possible to see that although in their infancy, models are a promising approach because they can predict large-scale responses that are difficult to test experimentally.

1.3 Mechanisms driving community changes

Community responses to ocean acidification result from the combination of direct effects of carbon dioxide on single species and indirect effects (i.e. biological interactions). While most ocean acidification research has focused on direct effects of elevated CO₂, there is increasing evidence that indirect effects are extremely important in determining community changes (Alsterberg *et al.*, 2013). In the terrestrial environment, biological interactions have been proven to be more important than direct climate change effects (Ockendon *et al.*, 2014), but there is no such evidence for community responses to ocean acidification.

1.3.1 Changes in organism physiology

Most studies on the biological effects of ocean acidification are laboratory experiments that measure physiological responses, most commonly calcification, of a single species. A recent meta-analysis concluded that overall effects of high pCO₂ on organisms' survival, growth, calcification and reproduction are strong and negative (Kroeker *et al.*, 2013a). Moreover, high CO₂ levels have subtler negative effects, such as those on behaviour (Briffa *et al.*, 2012) and neuroreceptors (Munday *et al.*, 2014). Predictions of future ecosystems conditions are also complicated by high taxonomic variability in biological responses to ocean acidification. For example, Ries *et al.* (2009) measured net calcification rates in 18 animal and algal taxa. Calcification rates

decreased in most species, but a wide range of responses was recorded, from negative to parabolic (i.e. highest calcification rates at intermediate pCO₂ values) to positive.

Responses to ocean acidification will not only vary among taxonomic groups (Kroeker *et al.*, 2013a, see Figure 1.3), but in some cases will be species- (Miller *et al.*, 2009), sex- (Holcomb *et al.*, 2011), clone- (Pistevos *et al.*, 2011) or strain-specific (Langer *et al.*, 2009; Hoppe *et al.*, 2011). This high degree of variability in biological responses to ocean acidification has led to conflicting reports: for instance, calcification rates of the coccolithophore *Emiliana huxleyi* have been reported to decrease (De Bodt *et al.*, 2010; Riebesell *et al.*, 2000) or increase (Iglesias-Rodriguez *et al.*, 2008) when exposed to low pH. In the first instance, it was thought that this difference was caused by methodological issues (Iglesias-Rodriguez *et al.*, 2008). However, the two methods used to modify water chemistry in these studies cause very similar changes in the carbonate system (Schulz *et al.*, 2009). Evidence of strain-specific responses was given by Langer *et al.* (2009), and Hoppe *et al.* (2011) confirmed that methodological issues do not cause a variation in *Emiliana huxleyi* responses to ocean acidification.

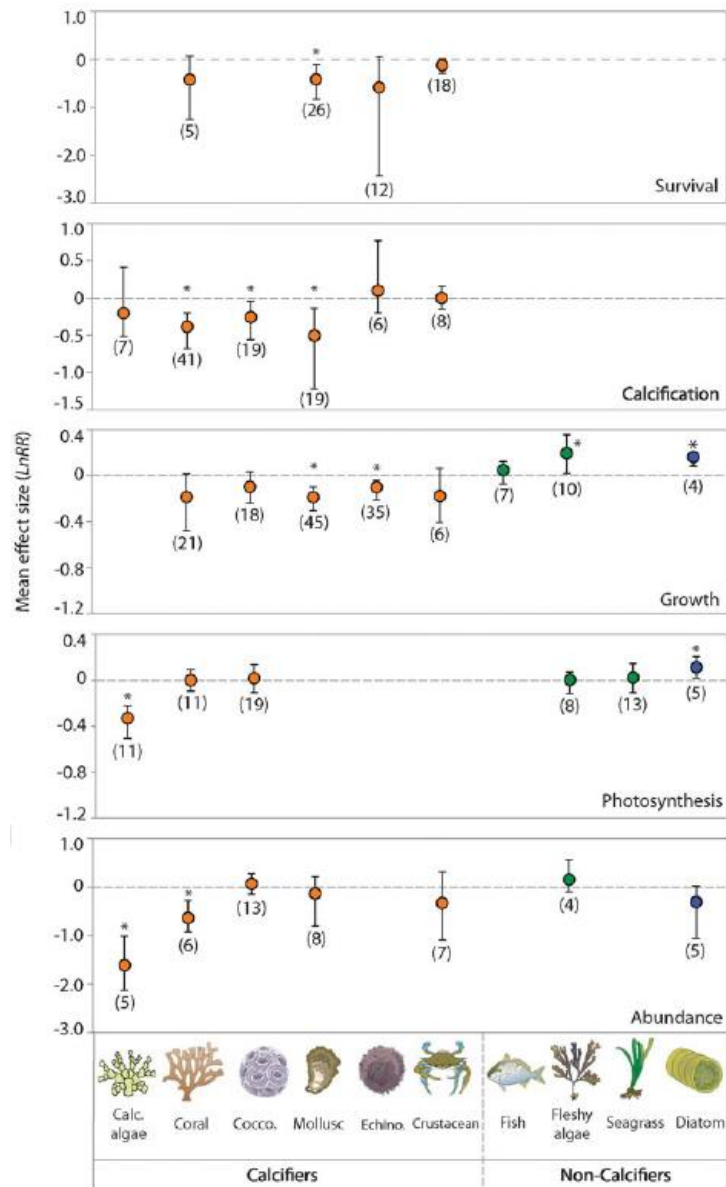


Figure 1.3. Taxonomic variation in effects of ocean acidification. Note the different y-axis scale for growth and photosynthesis. Mean effect size and 95% bias-corrected bootstrapped confidence interval are shown for all organisms combined (overall), calcifiers (orange) and noncalcifiers (green). The calcifiers category includes: calcifying algae, corals, coccolithophores, molluscs, echinoderms and crustaceans. The noncalcifiers category includes: fish, fleshy algae and seagrasses. The number of experiments used to calculate mean effect sizes are shown in parentheses. The mean effect size is significant when the 95% confidence interval does not overlap zero (*); Kroeker *et al.*, 2013a.

Predicting how species and their populations will react to increased CO₂ is complex but necessary if we want to prepare for marine ecosystem changes in the near future. Fortunately, certain traits are proving useful in determining how an organism may respond to ocean acidification. Firstly, very mobile taxa with high metabolic rates usually have efficient mechanisms to regulate pH (Melzner *et al.*, 2009), and are thus likely to be less affected directly by lowered pH compared to non-regulators. A meta-analysis on studies on mobile taxa with good acid-base regulation such as fish and brachyuran crustaceans did not show significant negative responses to high CO₂ levels on survival and growth (Kroeker *et al.*, 2013a), although there is evidence that some tropical fish species have their sensory abilities impaired when carbon dioxide increases (Munday *et al.*, 2014). Negligible effects of elevated CO₂ on growth and calcification were also related to good acid-base regulation in the cephalopod *Sepia officinalis* (Gutowska *et al.*, 2010). In contrast with these results, the giant squid *Dosidicus gigas* has been reported to suffer metabolic depression following short-term exposure to elevated CO₂, possibly because of the very high pH sensitivity of its oxygen-binding pigments (Rosa and Seibel, 2008). Thus, highly pH-sensitive blood pigments insure the rapid oxygen supply necessary to maintain very high metabolic rates, but they could be a disadvantage in a high-CO₂ world if pH regulation is not extremely efficient (Pörtner *et al.*, 2004).

For calcifying organisms, pH regulation at the calcification site will probably determine calcification responses to high CO₂ (Venn *et al.*, 2011). [H⁺] regulation at crystallisation sites has been detected in many taxa, including crabs (Cameron, 1985), coralline red and calcareous green algae (Borowitzka, 1987; McConnaughey & Whelan, 1997), foraminifera (Rink *et al.*, 1998) and

scleractinian corals (Al-Horani *et al.*, 2003; Venn *et al.*, 2011). Differential efficiency in calcification regulation may be one of the causes for the varied calcification responses to high CO₂ between taxa.

At intermediate pCO₂ levels calcification rates can increase (Wood *et al.* 2008; Gooding *et al.* 2009; McDonald *et al.*, 2009; Ries *et al.*, 2009; Findlay *et al.*, 2011; Rodolfo-Metalpa *et al.*, 2011). These responses may be due to the fact that calcification substrata used by many organisms are bicarbonate ions or aqueous carbon dioxide (Wilbur, 1964; Bubel, 1975; Decker & Lennarz, 1988; Al-Horani *et al.*, 2003), both of which will increase following ocean acidification. Alternatively, increased calcification could be a defensive mechanism aiming to compensate for the increased dissolution rates of calcified structures at high CO₂ (McDonald *et al.*, 2009). There are several examples of increased shell dissolution at elevated CO₂ levels in molluscs, echinoderms and corals (Nienhuis *et al.*, 2010; Findlay *et al.*, 2011; Rodolfo-Metalpa *et al.*, 2011). These studies all conclude that the decrease in net calcification rates with increased pCO₂ levels is mostly caused by an increase in dissolution rather than a decrease in the organism's calcification. Organisms that build their skeletons using Mg-calcite, the most soluble form of calcium carbonate, suffer the most from increased dissolution rates as pCO₂ increases (Johnson *et al.*, 2014).

Given the significant increase in carbonate dissolution rates when calcium carbonate saturation state is low, species protecting their shells or skeletons with an organic layer will probably be favoured in an ocean acidification scenario. Rodolfo-Metalpa *et al.* (2011), for instance, showed that coral skeleton and mollusc shells were significantly more damaged in species without or with very limited organic cover. In some cases the organic layer is damaged at high

CO₂ levels, exposing carbonate structures to acidified seawater (Thomsen *et al.*, 2010; Rodolfo-Metalpa *et al.*, 2011)

Even species with very efficient acid-base regulation will require more energy to maintain extracellular pH values in a range compatible with the organism's needs as seawater pH decreases (Thomsen and Melzner, 2010). An organism may manage to maintain most of its physiological functions, but have to down-regulate some others, as reported for the swimming crab *Necora puber* (Small *et al.*, 2010) and in the barnacle *Semibalanus balanoides* (Findlay *et al.*, 2010). In other cases, changes in energy allocation such as compensatory increases in calcification rates could reduce the energy available for other essential physiological processes (Bradassi *et al.*, 2013). Energy can also be allocated depending on the individual; for instance, in the coral *Astrangia poculata* calcification rates decreased with increasing CO₂, but this was more evident in females, probably because they needed energy for egg production (Holcomb *et al.*, 2011). However, up-regulation of physiological processes is not always sustainable in the long term (Lombardi *et al.*, 2011).

Energy availability is extremely important in determining biological responses to ocean acidification, so food supply has an essential role. Increased nutrient or food supply can counter the effects of ocean acidification in corals (Cohen *et al.*, 2009; Holcomb *et al.*, 2010; Chauvin *et al.*, 2011) and molluscs (Thomsen *et al.*, 2010; Thomsen *et al.*, 2013). Increased food availability does not always have a significant effect, but this probably happens when food is not limiting (Holcomb *et al.*, 2011); in some cases, energy supply even outweighs the effects of carbon dioxide (Thomsen *et al.*, 2013).

Photosynthetic organisms could be positively influenced by ocean acidification if they are able to fix more inorganic carbon, and thus have more energy available. Many algal species have carbon concentrating mechanisms (CCMs), so they are less likely to be limited by inorganic carbon concentration (Raven *et al.*, 2012). However, higher seawater pCO₂ would give them a significant advantage, because a greater proportion of their inorganic carbon uptake could derive from passive CO₂ diffusion instead of the energetically expensive CCMs (Cornwall *et al.*, 2012; Harley *et al.*, 2012). The increased energy availability, however, may not be enough to counter the negative effects of ocean acidification in calcifying species faced with the increased energetic costs of calcification at high pCO₂ levels (Bradassi *et al.*, 2013).

The natural pCO₂ variability a species experiences also contributes to its tolerance to ocean acidification. Species exposed to high levels of CO₂ in their habitat could be more resistant to the negative effects of ocean acidification (Maas *et al.*, 2012; Moulin *et al.*, 2011). In addition, short-term experiments are often not representative of the full acclimation potential of a species to ocean acidification. For instance, even a species considered very sensitive to ocean acidification such as the deep-sea coral *Lophelia pertusa* can acclimate to high-CO₂ conditions after some months, while undergoing strong negative effects in the short term (Form and Riebesell, 2011). On the other hand, some short-term responses to high CO₂ could require too much energy to be maintained in the long term (Lombardi *et al.*, 2011).

Most factors considered above can vary during an organism's life cycle, and larvae are more vulnerable than adults in many cases, since their regulatory system is usually less developed than that of adults (Ellis *et al.*, 2009; Melzner *et al.*, 2009). A recent meta-analysis seems to confirm that echinoderm larval

stages are more sensitive to ocean acidification than adults (Dupont *et al.*, 2010). In general, however, differences in responses between life stages are probably less pronounced than those between taxonomic groups, and the most sensitive life stage can vary between taxa (Kroeker *et al.*, 2013a). It is therefore important to consider the whole life cycle of a species before drawing conclusions regarding its sensitivity to increased seawater CO₂.

1.3.2 Changes in biological interactions

Changes in biological communities caused by elevated CO₂ will depend on the responses of single species and the subsequent changes in their interactions. Although only a few studies examine the effect of ocean acidification on biological interactions, there is evidence that competition will be influenced. For instance, elevated CO₂ levels can increase coral mortality due to enhanced competition from seaweeds (Diaz-Pulido *et al.*, 2011) or negatively influence kelp recruitment through increased turf cover (Connell and Russell, 2010). Furthermore, coralline algae with high-Mg calcite skeletons have their fitness reduced when seawater pCO₂ is high, causing them to be outcompeted by non-calcifying algae, commonly fast-growing species (Russell *et al.*, 2009; Hofmann *et al.*, 2012; Kroeker *et al.*, 2013c; Short *et al.*, 2014).

CO₂-related changes in plant-herbivore interactions are poorly known. However, it seems that grazers' consumption rates do not change only because of variations in the animal's metabolic rates, but also as a consequence of the alteration in algal palatability. Since a wide range of reactions to high CO₂ is expected in algal taxa, it is not surprising that gastropod herbivores have increased (Falkenberg *et al.*, 2013b) and decreased (Swanson and Fox, 2007; Russell *et al.*, 2013) feeding rates at high CO₂ when grazing on primary

producers. In one study, the detected decrease in feeding rates is probably caused by an increase in kelp phlorotannins, a class of substances involved with herbivore deterrence in seaweeds (Swanson and Fox, 2007). Seagrasses show an opposite trend since their phenolic protective substances concentrations decrease as CO₂ increases, with potential positive effects on grazing organisms (Arnold *et al.*, 2012). Accordingly, sea urchins have been found to increase their seagrass consumption when pCO₂ increases (Burnell *et al.*, 2013). In other cases, change in pH alone has no significant effects on algal palatability, and changes in feeding rates only occur when interaction between temperature and pH is examined (Poore *et al.*, 2013).

There are also very few studies dealing with the response of predator-prey interactions to increased CO₂ levels. An experiment on four species of reef fish larvae and one of their predators (Ferrari *et al.*, 2011) found that at high CO₂ small fish recruits of all species suffered higher predation rates compared to the control. At the same time, predator's preferences seem to switch from two of the species to the other two. As for the cause of these changes, there is evidence to suggest that high CO₂ impairs some fish sensory perceptions (Munday *et al.*, 2014), but an effect on predator behaviour could not be excluded. CO₂-driven changes in the predator-prey interaction between the intertidal snail *Littorina littorea* and the green crab *Carcinus maenas* have also been recently studied (Bibby *et al.*, 2007; Landes and Zimmer, 2012). Although crabs had reduced claw strength (Landes and Zimmer, 2012) and snails exhibited weaker shells and increased avoidance behaviour with increased CO₂ (Bibby *et al.*, 2007; Landes and Zimmer, 2012), the overall interaction strength between the two species was not affected by pCO₂ (Landes and Zimmer, 2012). Predator-prey

interactions are thus likely to show a wide range of responses to ocean acidification, which are rarely predictable from single-species studies.

1.4 Adaptation potential

Most experiments on ocean acidification effects so far have tested whether present populations of marine organisms can cope with future seawater CO₂ levels. Although this approach gives essential information on the physiological mechanisms involved in coping with ocean acidification, it excludes the possibility an organism could adapt (i.e. genetically change) to increased CO₂. Experiments to test directly for adaptation to ocean acidification have mostly been performed on unicellular phytoplankton due to their extremely rapid generation time (reviewed in Collins *et al.*, 2014). Results so far suggest that taxa negatively affected by ocean acidification, such as calcifying coccolithophores, are under strong adaptive pressure and evolve to partially restore calcification and growth rates (Lohbeck *et al.*, 2012; Benner *et al.*, 2013). On the other hand, non-calcifying taxa such as the diatom *Thalassiosira pseudonana* were able to reduce their usage of energy-expensive carbon-concentrating mechanisms (CCMs), but no genetic adaptation seemed to take place (Crawford *et al.*, 2011).

For organisms with a longer life cycle, experimental evolution is generally not feasible, and alternative approaches need to be used. Variation in responses to ocean acidification among genotypes can hint at a species' potential for adaptation. Variability in fitness with increased CO₂ have been found in bryozoans (Pistevos *et al.*, 2011), oysters (Parker *et al.*, 2012), amphipods (Calosi *et al.*, 2013b) and coccolithophores (Langer *et al.*, 2009). It is also possible to measure within-population genetic diversity as a proxy for their

potential of undergoing rapid evolution (Kelly *et al.*, 2013). Results from these studies revealed that species with shorter generation times do not always have higher adaptation potential than species with longer generation times, but greater genetic diversity (Sunday *et al.*, 2011).

Another approach to assess adaptation or acclimation/acclimatisation potential in marine organisms (for definitions see Box 1) is using natural pCO₂ gradients, such as those found at volcanic seeps or in upwelling areas, to assess whether local populations have acclimated or adapted to elevated CO₂ levels (Reusch, 2014). Individuals from areas with different pH can be exposed to the same CO₂ conditions in the laboratory (“common garden experiments”) or reciprocally transplanted between sites to assess local adaptation (Sanford and Kelly, 2011). So far, both common garden experiments and reciprocal transplants have found significant inter-population differences in responses to pCO₂ in sea urchins, barnacles and polychaetes (Moulin *et al.*, 2011; Calosi *et al.*, 2013c; Evans *et al.*, 2013; Kelly *et al.*, 2013; Pansch *et al.*, 2014). Sea urchins naturally exposed to elevated pCO₂ have offspring that show increased resistance to ocean acidification (Moulin *et al.*, 2011; Evans *et al.*, 2013; Kelly *et al.*, 2013), while tolerant polychaete species transplanted between CO₂ levels can either adapt or acclimatise to high and variable CO₂ (Calosi *et al.*, 2013c). Short-term acclimation or acclimatisation to high pCO₂ can buffer populations against negative impacts of ocean acidification, giving them a chance to survive until adaptation takes place (Sunday *et al.*, 2014). This process, however, can be energetically expensive: barnacles populations not adapted to high and variable pCO₂ could cope with moderate carbonate dioxide levels, but only if food was abundant, whereas the adapted population was unaffected by food levels (Pansch *et al.*, 2014). The adaptation potential to ocean acidification of most

marine organisms is still unknown, and more evidence is urgently needed to fully determine which species will be able to adapt to the rapid environmental changes predicted for the next decades (Kelly and Hofmann, 2012).

Box 1: Acclimation, acclimatisation and adaptation (Angilletta, 2009)

Acclimatisation: the process by which an individual organism adjusts to a gradual change in its environment (such as a change in temperature or pH), allowing it to maintain performance across a range of environmental conditions.

Acclimation: similar to acclimatisation, but refers to changes occurring in response to an artificial or controlled situation.

Adaptation: a process involving the selection on genetic variation that shifts the average phenotype toward the fitness peak.

1.5 Interaction with other anthropogenic stressors

As well as ocean acidification, anthropogenic CO₂ emissions are causing an increase in seawater temperature (IPCC, 2014). Studying how these two factors will interact is essential to understand the future of marine ecosystems. Nonetheless, our knowledge of the combined effect of high pCO₂ and higher temperatures is currently lower than that of the effects of each factor alone. As with responses to changes in carbonate chemistry, interactions with temperature appear to have very variable effects on an organism's physiology, depending on which taxa it belongs to and which physiological responses are measured (e.g. Lischka *et al.*, 2010; Noiset *et al.*, 2013a), although there is a trend towards an increase in negative effects of ocean acidification when organisms are concurrently exposed to elevated temperature (Kroeker *et al.*, 2013a). One possible explanation for this pattern is that the energetic costs of coping with ocean acidification (e.g. maintaining intracellular pH or calcification rates) narrow an organism's aerobic scope (Kelly and Hofmann, 2012).

Hypoxic zones are also expanding in the world oceans, both in coastal areas and in the subsurface open ocean waters (Diaz and Rosenberg, 2008). As hypoxic zones are the result of microbial respiration, decreased oxygen levels are paired with increased pCO₂. Carbon dioxide could then reach levels much higher than those predicted for the world oceans at the end of this century in hypoxic zones, threatening the survival of species otherwise resistant to ocean acidification (Melzner *et al.*, 2013). However, the effects of hypoxia and ocean acidification have mostly been studied in isolation, even though pteropods from hypoxic areas show increased resistance to increased pCO₂, suggesting that carbon dioxide is an important stressor in hypoxic areas (Maas *et al.*, 2012). To date, the only study assessing the combined effect of hypoxia and ocean acidification on marine organisms found that the two stressors interact to affect organisms in ways not predictable from single-stressor experiments (Gobler *et al.*, 2014).

Climate change is also expected to increase the intensity of ultra-violet (UV) radiation in marine systems following depletion of the ozone layer (Austin *et al.*, 1992). Marine organisms utilise many mechanisms for photoprotection against excessive radiation, most of which are energetically expensive and could decrease their resistance to other stressors, including ocean acidification (Häder *et al.*, 2007). The combination of increased CO₂ and UV radiation seems in fact to promote production of protective compounds (phlorotannins) in some brown algae (Swanson and Fox, 2007), even though not all taxa show an enhanced sensitivity to the combination of those stressors (Beardall *et al.*, 2009). For calcifying algae, the synergistic effect of CO₂ and UV radiations could be due to the reduction of the calcified layer as CO₂ increases, which impairs its photoprotective function (Gao *et al.*, 2009; Gao and Zheng, 2010),

even though not all coralline algae are negatively affected by the interaction of elevated carbon dioxide and UV radiations (Yildiz *et al.*, 2013).

Local stressors such as eutrophication and heavy metal pollution can also worsen community responses to ocean acidification, and managing them is essential to improve the resilience of marine ecosystems (Ghedini *et al.*, 2013). While at the single species level increased nutrient levels can offset the negative impacts of ocean acidification (Chauvin *et al.*, 2011; Thomsen *et al.*, 2013; Pansch *et al.*, 2014), elevated energy input often alters the outcome of inter-specific interactions, with more opportunistic species becoming more competitive (Connell and Russell, 2010; Falkenberg *et al.*, 2013a). The interactive effects of ocean acidification and heavy metals have not been studied at the community levels so far, but evidence from single-species experiments suggests that copper will enhance the negative effects of ocean acidification in some marine organisms, such as amphipods and polychaetes (Lewis *et al.*, 2012; Roberts *et al.*, 2013).

1.6 Thesis aims and objectives

Ocean acidification is a relatively new research field and studies on its community effects at temperate rocky reefs are in their infancy. Volcanic seeps are proving useful to study community responses of ocean acidification, but more sites are needed to build confidence in predictions developed using these systems. In addition, there is evidence that indirect effects of carbon dioxide could play a crucial role in the detected community changes, but our knowledge on the relative importance of direct or indirect effects of carbon dioxide is extremely limited. There is also little knowledge on the adaptation potential of

macroalgae and on possible interactions of ocean acidification with other stressors, such as copper pollution.

The overall thesis structure is illustrated in Figure 1.4: this project aimed to determine how benthic communities and their epifauna change along natural CO₂ gradients in the oligotrophic Mediterranean Sea, and investigate whether community changes were caused by direct or indirect effects; the interactive effects of CO₂ and a short-term copper pulse on macroalgae and their epifauna was also assessed. The specific objectives were to:

- Determine whether volcanic seeps off Methana (Greece) are suitable to study the effects of increased pCO₂ on benthic communities by monitoring carbonate chemistry, temperature, salinity, total alkalinity and measuring inorganic nutrients, hydrogen sulphide, as well as total and bioavailable heavy metals (Chapter 2).
- Determine how benthic communities and epifauna of main canopy-forming species change along Mediterranean pCO₂ gradients by assessing community structure and composition (Chapters 3 and 4).
- Determine whether changes in herbivores abundance contribute to the detected changes in benthic communities along pCO₂ gradients by excluding intertidal and subtidal herbivores (Chapter 5).
- Determine whether two abundant macroalgal species, one articulated coralline (*Jania rubens*) and one furoid (*Cystoseira corniculata*), have acclimated to high pCO₂ by transplanting them within and between high CO₂ and reference sites off Methana (Chapter 6).
- Determine whether two abundant macroalgal species, one articulated coralline and one furoid, respond differently to copper exposure at

different pCO₂ levels and how this affects the furoid epifauna by exposing macroalgae to copper *in situ* (Chapter 7).

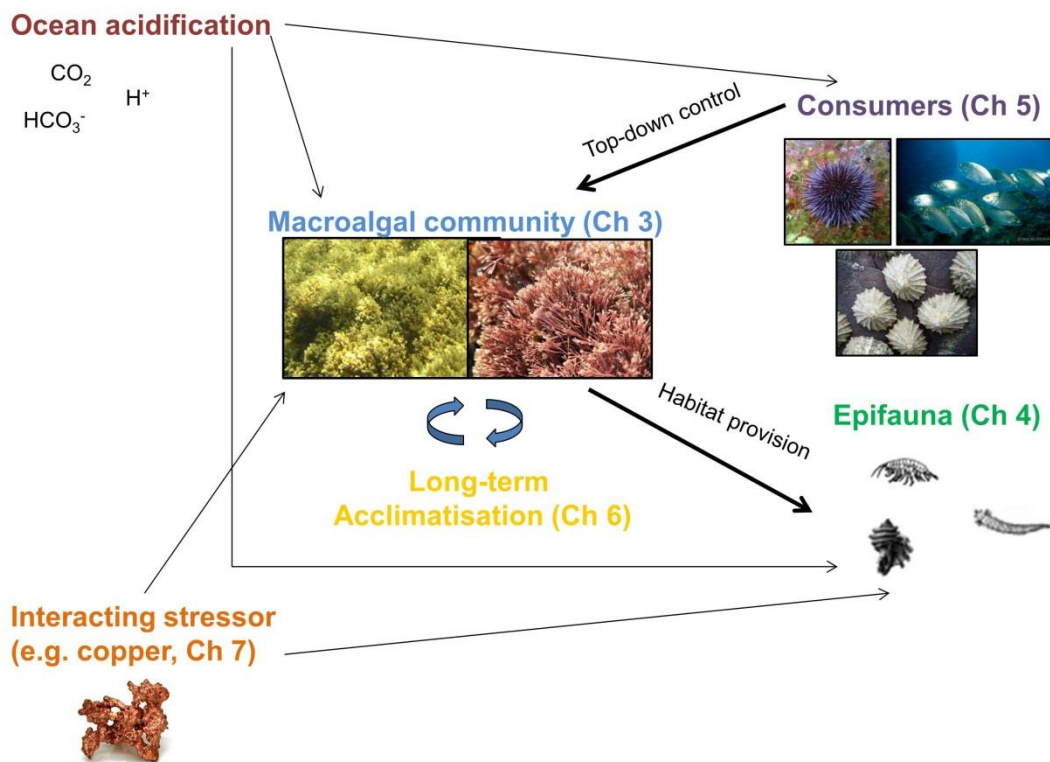


Figure 1.4. Visual abstract of thesis aims; using CO₂ seeps as natural analogues for ocean acidification, I assessed how macroalgal communities (Chapter 3) and their epifauna (Chapter 4) change with increasing pCO₂ levels, and whether long-term acclimatisation to elevated pCO₂ increases adaptation potential of dominant macroalgal species (Chapter 6). I also examined how changes in herbivores densities affect the strength of top-down control on macroalgal communities (Chapter 5), and how interaction of ocean acidification with another stressor (short-term copper pollution) may influence dominant macroalgal species and their epifauna (Chapter 7).

Table 1.1. Summary of this thesis' surveys and experiments, with measured parameters and sample sizes. (A) Summary of sampling for Chapter 2, with sampling date, site, measured parameters and sample sizes: pH, temperature and salinity (pH/T/S), water samples for total alkalinity (TA), water samples for inorganic nutrients (nitrites, nitrates, ammonium, phosphates, silicates), water samples for free sulphides, sediment samples for heavy metals content, macroalgal samples for heavy metals content. (B) Summary of sampling for Chapter 3, with sampling date, sites and number of 20 x 20 cm visual quadrats (Methana) or 20 x 20 cm quadrats scraped from rocky substratum (Vulcano). (C) Summary of sampling for Chapter 4, with sampling dates, sites and species (only Vulcano) and number of 20 x 20 cm quadrats of *Cystoseira corniculata* scraped from the substratum (Methana) or number of collected thalli (Vulcano). (D) Summary of sampling for the two experiments described in Chapter 5. For the limpet exclusion experiment at Vulcano, the table shows sampling dates and number of pH, temperature and salinity measurements (pH/T/S), number of limpet abundance and length measurements, number of experimental plots per treatment where macroalgal cover or biomass were measured (C=controls, P=procedural controls, E=exclusions) and number of wax discs used to quantify limpet grazing. For the herbivore exclusion experiment at Methana, the table shows sampling dates and number of pH, temperature and salinity measurements (pH/T/S), number of transects for sea urchins (*Paracentrotus lividus* and *Arbacia lixula*) abundance and herbivore fish (*Sarpa salpa*, *Siganus luridus* and *Sparisoma cretense*) biomass and number of experimental plots per treatment where macroalgal cover or biomass were measured (C=controls, P=procedural controls, E=exclusions). (E) Summary of sampling for *Cystoseira corniculata* (01-05/10/2012 to 22-25/06/2013) and *Jania rubens* (22-25/06/2013 to 04-09/09/2013) transplants described in Chapter 6. The table shows macroalgal species, treatment (expressed as "Site of origin". "Site of transplant", for a detailed description of the experimental design see Chapter 6), number of thalli used to measure growth and epiphyte cover (*=only epiphytes measured), photosynthetic parameters, pigments content, carbon, nitrogen and phosphorous (C,N,P) content (**P not measured) and total phenols content. N.u.=not used because sample size was too small; lost=all thalli lost; N/A=not applicable. (F) Summary of sampling for the copper exposure experiments described in Chapter 7. For the

environmental monitoring, the table shows experiment dates, sites and number of pH, salinity and temperature measurements (pH/S/T) and number of water samples collected for total alkalinity measurements (TA). For the copper pulse experiments, the table shows macroalgal species (*Cystoseira corniculata* on 18-25/06/2013 and *Jania rubens* on 04-09/09/2013), treatment (expressed as “Site of origin”. “Site of transplant”. “Copper exposure”, for a detailed description of the experimental design see Chapter 7), number of plaster blocks used, number of thalli used to measure copper content, maximum quantum yield, pigments content and epifaunal communities. N.u. treatment not used because sample size was too small; N/A=not applicable.

(A) Chapter 2: Assessing the suitability of a volcanic seep area off Methana (Greece) for ocean acidification studies.							
Date	Site	pH/T /S	TA	Inorganic nutrients	Sulphides	Metals - sediment	Metals - macroalgae
01/09/2011	SEEP	1					
01/09/2011	200 W	1					
01/09/2011	200 E	1					
11-12/02/2012	SEEP	2	3				
11-12/02/2012	200 W	2	3				
11-12/02/2012	200 E	2	4				
22/05/2012 to 06/06/2012	SEEP	11	5			3	5
22/05/2012 to 06/06/2012	200 W	11	6			3	5
22/05/2012 to 06/06/2012	200 E	11	3			3	5
22/05/2012 to 06/06/2012	REF A	1	3			3	5
22/05/2012 to 06/06/2012	REF B	4	3			3	5
27/09/2012 to 05/10/2012	SEEP	11	6				
27/09/2012 to 05/10/2012	200 W	3	6				
27/09/2012 to 05/10/2012	200 E	3	6				
27/09/2012 to 05/10/2012	REF A	8	6				
27/09/2012 to 05/10/2012	REF B	3	3				
18-25/06/2013	SEEP	13	6	3	7		
18-25/06/2013	200 W	7	6	3	3		
18-25/06/2013	200 E	7	6	3	3		
18-25/06/2013	REF A	9	6	3	3		
18-25/06/2013	REF B	8	6	3	3		
04-09/09/2013	SEEP	3	3				
04-09/09/2013	200 W	3	3				
04-09/09/2013	200 E	3	3				
04-09/09/2013	REF A	3	3				

04-09/09/2013	REF B	4	3			
(B) Chapter 3: Changes in subtidal macroalgal communities along pCO₂ gradients at Mediterranean volcanic seeps						
Methana - visual quadrats of benthic communities						
Date	SEEP	200 W	200 E	REF A	REF B	
23-29/05/2012	7	7	7	7	7	
30/09/2012 to 05/10/2012	6	6	6	6	6	
Vulcano - destructively sampled quadrats						
Date	REF A	Mid CO ₂	High CO ₂			
15/05/2010	4	4	4			
(C) Chapter 4: Canopy algal epifauna changes at elevated pCO₂ at two Mediterranean volcanic seeps						
Methana - quadrats of <i>Cystoseira corniculata</i> scraped						
Date	SEEP	200 W	200 E	REF A	REF B	
26/05/2012 to 06/06/2012	3	3	3	3	3	
Vulcano - macroalgal thalli collected						
Date	Species	600 ppm	1200 ppm			
04-08/06/2013	<i>Cystoseira</i> spp.	15	14			
04-08/06/2013	<i>Sargassum vulgare</i>	9	10			
(D) Chapter 5: Effect of herbivores on benthic communities at different pCO₂ levels						
Vulcano - limpets exclusion experiment						
Date	Measured parameter	Treatment	600	1200		
08/05/2012	pH/T/S	N/A	1	1		
18-19/07/2012	pH/T/S	N/A	2	2		
22-23/09/2012	pH/T/S	N/A	2	2		
27/10/2012	pH/T/S	N/A	1	1		
08/05/2012	Limpets abundance/length	N/A	7	9		
18-19/07/2012	Limpets abundance/length	N/A	18	18		
22-23/09/2012	Limpets abundance/length	N/A	9	9		
27/10/2012	Limpets abundance/length	N/A	9	9		
08/05/2012	Macroalgal cover	C	3	3		
08/05/2012	Macroalgal cover	P	3	3		
08/05/2012	Macroalgal cover	E	6	6		
18-19/07/2012	Macroalgal cover	C	3	3		
18-19/07/2012	Macroalgal cover	P	3	3		
18-19/07/2012	Macroalgal cover	E	6	6		
22-23/09/2012	Macroalgal cover	C	3	3		
22-23/09/2012	Macroalgal cover	P	3	3		
22-23/09/2012	Macroalgal cover	E	6	4		
27/10/2012	Macroalgal cover	C	3	3		
27/10/2012	Macroalgal cover	P	3	0		
27/10/2012	Macroalgal cover	E	6	4		
20/11/2012	Macroalgal biomass	C	3	3		
20/11/2012	Macroalgal biomass	P	3	0		
20/11/2012	Macroalgal biomass	E	6	4		
20/11/2012	Limpets grazing rates	N/A	41	34		
Methana - herbivore exclusion experiment						
Date	Measured parameter	Treatment	REF A	SEEP		
30/09/2012 to 05/10/2012 and 20-25/06/2013	Sea urchins abundance	N/A	6 per species	6 per species		
08/09/2013	Fish biomass	N/A	3	3		
20/06/2013	Macroalgal cover/biomass	C	4	4		
20/06/2013	Macroalgal cover/biomass	P	3	3		
20/06/2013	Macroalgal cover/biomass	E	4	3		

(E) Chapter 6: Seaweed acclimatisation to high pCO₂ at volcanic seeps						
Species	Treatment	Growth/ epiphytes	Photosynthetic parameters	Pigments content	C, N, P content	Phenol content
<i>C. corniculata</i>	SEEP.SECP	5	5	5	5	5
<i>C. corniculata</i>	REFB.SECP	8	6	8	7	7
<i>C. corniculata</i>	REFA.SECP	3	3	3	3	3
<i>C. corniculata</i>	REFA.REFA	5	4	5	4	4
<i>C. corniculata</i>	SEEP.REFA	10	9	10	9	10
<i>C. corniculata</i>	REFB.REFB	8	7	8	4	4
<i>C. corniculata</i>	SEEP.REFB	4	3	4	4	3
<i>C. corniculata</i>	SEEP	7*	6	7	7	6
<i>C. corniculata</i>	REFA	7*	7	6	7	7
<i>C. corniculata</i>	REFB	7*	4	7	7	7
<i>J. rubens</i>	SEEP.SECP	4	4	4	4**	N/A
<i>J. rubens</i>	REFB.SECP	4	5	4	3**	N/A
<i>J. rubens</i>	REFA.SECP	n.u.	n.u.	n.u.	n.u.	N/A
<i>J. rubens</i>	REFA.REFA	lost	lost	lost	lost	N/A
<i>J. rubens</i>	SEEP.REFA	lost	lost	lost	lost	N/A
<i>J. rubens</i>	REFB.REFB	5	5	5	9**	N/A
<i>J. rubens</i>	SEEP.REFB	6	5	6	4**	N/A
<i>J. rubens</i>	SEEP	N/A	7	7	5**	N/A
<i>J. rubens</i>	REFA	N/A	7	7	5**	N/A
<i>J. rubens</i>	REFB	N/A	7	7	5**	N/A
(F) Chapter 7: A short-term copper pulse affects macroalgal copper accumulation and indirectly alters epifaunal colonisation at elevated pCO₂						
Environmental monitoring						
Date	Site	pH/T/S	TA			
18-25/06/2013	SEEP	13	6			
18-25/06/2013	REF A	9	6			
18-25/06/2013	REF B	8	6			
04-09/09/2013	SEEP	3	3			
04-09/09/2013	REF A	3	3			
04-09/09/2013	REF B	4	3			
Copper pulse experiments						
Species	Treatment	Plaster	Copper content	Maximum quantum yield	Pigments content	Epi fauna
<i>C. corniculata</i>	REFA.REFA.Cu-	4	5	5	5	4
<i>C. corniculata</i>	REFA.REFA.Cu+		5	5	5	5
<i>C. corniculata</i>	SEEP.REFA.Cu-		5	5	5	N/A
<i>C. corniculata</i>	SEEP.REFA.Cu+		5	5	4	N/A
<i>C. corniculata</i>	REFB.REFA.Cu-		n.u.	3	n.u.	N/A
<i>C. corniculata</i>	REFB.REFA.Cu+		n.u.	3	n.u.	N/A
<i>C. corniculata</i>	REFA.SECP.Cu-	4	5	5	4	N/A
<i>C. corniculata</i>	REFA.SECP.Cu+		5	5	5	N/A
<i>C. corniculata</i>	SEEP.SECP.Cu-		4	4	4	5
<i>C. corniculata</i>	SEEP.SECP.Cu+		5	5	5	5
<i>C. corniculata</i>	REFB.SECP.Cu-		n.u.	4	n.u.	N/A
<i>C. corniculata</i>	REFB.SECP.Cu+		n.u.	5	n.u.	N/A
<i>J. rubens</i>	REFA.REFA.Cu-	4	4	4	5	N/A
<i>J. rubens</i>	REFA.REFA.Cu+		5	4	5	N/A
<i>J. rubens</i>	SEEP.REFA.Cu-		5	5	4	N/A
<i>J. rubens</i>	SEEP.REFA.Cu+		5	5	4	N/A
<i>J. rubens</i>	REFB.REFA.Cu-		4	3	n.u.	N/A
<i>J. rubens</i>	REFB.REFA.Cu+		4	4	n.u.	N/A
<i>J. rubens</i>	REFA.SECP.Cu-	4	5	4	4	N/A
<i>J. rubens</i>	REFA.SECP.Cu+		5	5	3	N/A

<i>J. rubens</i>	SEEP.SECP.Cu-		5	5	4	N/A
<i>J. rubens</i>	SEEP.SECP.Cu+		5	5	5	N/A
<i>J. rubens</i>	REFB.SECP.Cu-		5	5	n.u.	N/A
<i>J. rubens</i>	REFB.SECP.Cu+		5	3	n.u.	N/A

Chapter 2

Assessing the suitability of a volcanic seep area off Methana (Greece) for ocean acidification studies

Aspects of this chapter have been published as:

C. Baggini, M. Salomidi, E. Voutsinas, L. Bray, E. Krasakopoulou, J.M. Hall-Spencer (2014). Seasonality affects macroalgal community response to increases in pCO₂. *PLoS ONE*, 9: e106520.

Abstract

Ocean acidification poses a threat to a wide range of marine systems, but little work has been carried out at the ecosystem level due to logistical constraints. Work in areas with naturally high CO₂ is starting to show community effects of ocean acidification. Replication of these observations across a range of settings is needed to build confidence in predictions developed using these systems as ocean acidification analogues. The aim of this study was therefore to assess whether seeps off Methana, in the oligotrophic Aegean Sea, are appropriate for studying the community effects of ocean acidification. Monitoring of the gradient from 2011 to 2013 showed that median seawater pH decreased from present day values at reference sites (median pH = 8.12) to levels predicted for the end of this century at the seep sites (median pH = 7.69) with no confounding gradients in total alkalinity, salinity, temperature or wave exposure. Most nutrient levels were similar along the pH gradient; silicate levels increased significantly with decreasing pH, but they were high enough at all sites not to limit algal growth. Metal concentrations in sediment and seaweed tissues varied between study sites but did not consistently increase with increasing pCO₂. Methana seeps have the same limitations as other seeps used for ocean acidification studies, i.e. variable pCO₂ and relatively small area influenced. Seeps off Methana, however, influence a relatively large area (~10 km of shore) compared to other seeps used for ocean acidification studies, which may limit the amount of mobile organisms and larvae coming from reference areas. It is therefore concluded that seeps off Methana are suitable for studies into the effects of ocean acidification, provided the limitations of using seep systems in ocean acidification studies are taken into account.

2.1 Introduction

Early work on the effects of ocean acidification involved experiments that focused on single species in laboratory conditions, where pH variability was minimised, for periods of up to 18 months (Kroeker *et al.*, 2013a). This body of work has rapidly advanced our knowledge of the relative sensitivity of different species, which can be used to formulate hypotheses about community responses. Nevertheless, surprising and unpredicted community responses to increased levels of pCO₂ can occur because of interactions between species. For instance, Hale *et al.* (2011) reports that most invertebrate taxa in a community mesocosm experiments responded to increased pCO₂ as expected from single species experiments. Nematodes, however, unexpectedly increased in abundance, probably because of the decreased competition with, and predation by, taxa sensitive to ocean acidification.

Community responses to ocean acidification will also depend on indirect effects of carbon dioxide, such as those which alter animal behaviour (Briffa *et al.*, 2012) and affect their neuroreceptors (Munday *et al.*, 2014). Thus, physiology and ecological niche cannot fully predict a species' susceptibility to environmental changes (Spicer, 2014). Moreover, laboratory and mesocosm experiments are usually too brief to ascertain the effect of increased carbon dioxide on climax communities comprising long-lived organisms (Kroeker *et al.*, 2013a). Hypotheses formulated using data from short-term single-species laboratory experiments thus need to be tested in complex communities, ideally in real marine ecosystems (Garrard *et al.*, 2013).

Areas chronically exposed to high pCO₂ can be used to assess long-term community responses to ocean acidification (Hall-Spencer *et al.*, 2008;

Fabricius *et al.*, 2011; Boatta *et al.*, 2013; Inoue *et al.*, 2013). Although in their infancy, there are widespread opportunities for such studies since hydrothermal seeps characterised by low pH and high pCO₂ levels occur worldwide (Tarasov *et al.*, 2005). However, many of these areas also have gradients in temperature, salinity, total alkalinity, inorganic nutrients, toxic gases and metals (Dando *et al.*, 1999; Karlen *et al.*, 2010), which could confound the ecological effects of carbon dioxide. As a consequence, geochemical baseline surveys are needed to check the extent to which seep systems can be used as natural ocean acidification laboratories (Kerrison *et al.*, 2011; Boatta *et al.*, 2013).

Only a few CO₂ seeps have so far been located that are suitable for use as ocean acidification analogues, namely seeps off Italy (Hall-Spencer *et al.*, 2008; Kerrison *et al.*, 2011; Boatta *et al.*, 2013), Papua-New Guinea (Fabricius *et al.*, 2011) and Japan (Inoue *et al.*, 2013). These studies have shown that increasing levels of seawater pCO₂ reduce benthic biodiversity, especially that of calcifying organisms (Martin *et al.*, 2008; Dias *et al.*, 2010; Fabricius *et al.*, 2014). Replication of such studies in a wider range of settings would strengthen the evidence for the ecosystem effects of increasing pCO₂ at the landscape scale. Data from a natural ocean acidification analogue in the Eastern Mediterranean would be useful due to its extremely low nutrient levels, which could exacerbate the effects of high pCO₂ due to the increased metabolic costs of coping with ocean acidification (Holcomb *et al.*, 2010; Melzner *et al.*, 2011; Kletou and Hall-Spencer, 2012).

The aim of this chapter is to assess the suitability of volcanic seeps off Methana (Saronikos Gulf, Aegean Sea, Greece) for ocean acidification studies. Temperature, pH, salinity, total alkalinity and the concentrations of heavy metals, hydrogen sulphide and major nutrients (nitrite, nitrate, ammonium, phosphate

and silicate) were monitored. In addition, wave exposure was determined using effective fetch (see section 2.2.8) as it affects the distribution of Mediterranean fucoid algae (Spatharis *et al.*, 2011).

2.2 Methods

2.2.1 Study area

The Methana peninsula is the westernmost volcanic system of the northern Aegean Volcanic Arc, derived from the subduction of the African tectonic plate beneath the Eurasian plate. The last volcanic eruption dates back to 230 BC, but the system is still hydrothermally active (Dando *et al.*, 1999). The seeps are shallow (0-5 m depth) and situated on the NE part of the peninsula (Figure 2.1). They appeared shortly after the last volcanic eruption, and the Pausania thermal baths nearby have been used since late Roman times (Bowden and Gill, 1997).

Geothermal fluids rise very slowly from the geological reservoir below Methana (2-3 km underground), where temperatures could be as high as 210 °C; they mix with shallow fluids in the process (D'Alessandro *et al.*, 2008). The released gases are dominated by CO₂, as in most Mediterranean hydrothermal systems (Dando *et al.*, 1999), and are mainly derived from limestone. The estimated CO₂ flux from the whole peninsula is about 0.03 kg s⁻¹, well below the range generally measured worldwide in volcanic/hydrothermal areas (0.2-450 kg s⁻¹; Pecoraino *et al.*, 2005) and lower than those of the rest of the Aegean Volcanic Arc (0.2 kg s⁻¹ at Nea Kameni, Chiodini *et al.*, 1998; 0.6 kg s⁻¹ at Sousaki, D'Alessandro *et al.*, 2006; and 1.0 kg s⁻¹ at Nisyros, Cardellini *et al.*, 2003).

Gas concentrations have been recently measured in Pausanias baths, which are extremely close (<20 meters) to the seeps studied here. Gas emissions

were measured on two occasions, and gas composition was relatively stable over time (D'Alessandro *et al.*, 2008). Gas bubbles in the baths are mostly carbon dioxide, with small amounts of nitrogen, carbon monoxide and methane (Table 2.1). Methane concentrations (17-26 ppm) are much lower than those detected at ocean acidification analogues in Ischia (200 - 800 ppm; Hall-Spencer *et al.*, 2008), Vulcano (1700 ppm; Boatta *et al.*, 2013) and Papua New Guinea (87 - 4360 ppm; Fabricius *et al.*, 2011).

Table 2.1. Composition of gases bubbling at Pausanias baths in ppm (D'Alessandro *et al.*, 2008). These baths are adjacent to the submarine seeps. Carbon dioxide (CO₂) accounts for over 90% of the emitted gases, with smaller percentages of nitrogen (N₂), oxygen (O₂), methane (CH₄), carbon monoxide (CO), helium (He) and hydrogen (H₂). Methane levels are much lower than in other seeps used as ocean acidification proxies.

Date	CO ₂	N ₂	O ₂	CH ₄	CO	He	H ₂
04/06/2006	991000	10700	<400	26	1.6	<5	<5
23/06/2006	970000	30900	5600	17	1.7	<5	<5

The Pausanias bath water composition is moderately enriched in calcium and silicates due to the interaction of thermal waters and limestone and silicate rocks, respectively. Rock-water interactions were responsible for the detected enrichment in K, B and Li as well (D'Alessandro *et al.*, 2008).

2.2.2 Site descriptions

Two preliminary surveys were carried out in September 2011 and February 2012 to characterise carbonate chemistry and find areas with elevated pCO₂ as well as reference sites. These surveys showed that a relatively small area (approximately 20 m of shoreline) near a seep had a pH_{NBS} constantly below 8.0 (Figure 2.1), whereas a much larger area was characterised by variable pH.

This area (shown in light grey in Figure 2.1) had a pH_{NBS} varying from 6.6 to 8.1, with lower values in autumn and higher in winter. Sediment Eh and dissolved oxygen analyses at the sediment-water interface confirmed that volcanic activity did not produce an anoxic layer in the sediment (Krasakopoulou *et al.*, unpublished data).

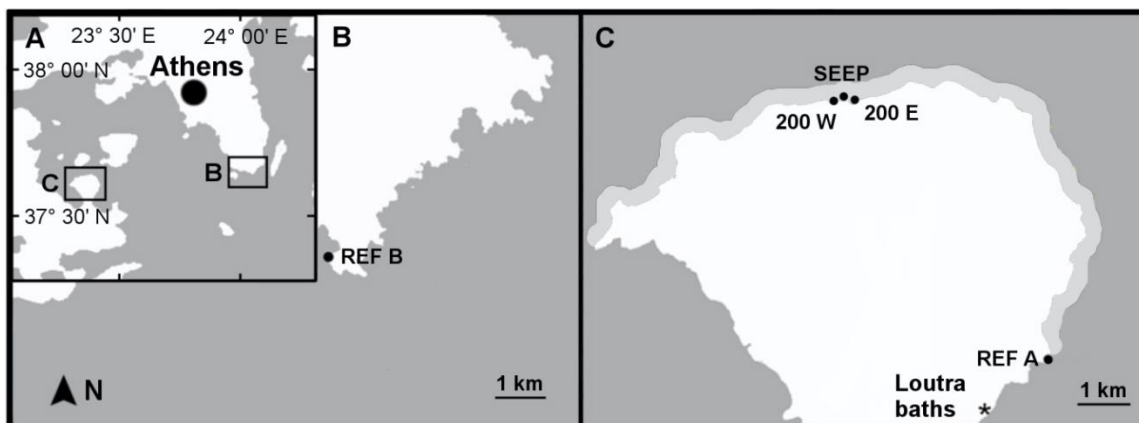


Figure 2.1. (A) Saronikos Gulf, Greece, with study areas marked by rectangles B and C. (B) Study site REF B (black point). (C) Study sites 200 W, SEEP, 200 E and REF A (black points), Loutra baths (*) and area where pH was more variable than at reference sites (light grey).

Five sites with comparable habitats but different pH levels were selected: a site with $pH < 8.0$ near the main seeps (SEEP), two sites with variable pH located approximately 200 m eastwards and westwards of the seep area (200 E and 200 W) and two reference sites, one just outside the variable pH area (REF A) and one at a more distant site unaffected by volcanic activity (REF B). Pictures of the typical benthic communities at SEEP and 200 E are shown in Figure 2.2. All sites had the same type of coastal morphology (large sparse boulders) and similar degrees of urbanisation, as only small villages and hotels were found in their vicinities. The dominant canopy-forming macroalgal species at all sites was *Cystoseira corniculata*, a fucoid alga characteristic of the Eastern

Mediterranean Sea (Taskin *et al.*, 2012). The genus *Cystoseira* indicates good environmental conditions (Ballesteros *et al.*, 2007) and *C. corniculata* is characteristic of sites with high wave exposure (Spatharis *et al.*, 2011).



Figure 2.2. Typical appearance of benthic communities at SEEP (left) and 200 E (right) sites at 0.5 m depth in May 2012 with CO₂ bubbles seeping from the sea floor (arrow). Brown algae (e.g. *Dictyota* sp.) were dominant near the seeps; crustose coralline algae (CCA) became dominant as CO₂ levels decreased. Photos by Laura Bray (May 2012).

2.2.3 Seawater physicochemical parameters

The seeps were monitored from 2011 to 2013 (September 2011, January, February, May and September 2012, June and September 2013 - detailed sampling dates and sample sizes are reported in Table 1.1A); seawater physicochemical parameters were measured at different times of the day and in different meteorological conditions during each trip. Seawater pH, temperature and salinity were measured using a multiprobe (YSI 63) from shore. The probe was calibrated before use with pH 4.01, 7.01 and 10.01 NBS standards. Since

variations of up to 1 pH unit were detected over a few hours at the low pH site, the lack of precision in using the NBS scale for seawater measurements (approximately 0.05 pH, Riebesell *et al.*, 2010) was considered acceptable for this study. For pH, medians and interquartile ranges (IQ) were calculated from hydrogen ion concentrations before re-converting back to pH values following seep monitoring methods provided by Kerrison *et al.* (2011).

Seawater samples for total alkalinity determination were collected in 125 ml borosilicate glass bottles with Teflon caps. Three independent samples per site were collected at each visit, immediately poisoned with HgCl₂ and stored in the dark until analysis. Samples were analysed by Gran titration (AS-ALK 2, Apollo SciTech) and the reliability of the measurements was checked against standard seawater samples provided by A. Dickson (batches 112 and 121). The average total alkalinity value per site and individual pH measurements were used to calculate pCO₂, HCO₃⁻, CO₃²⁻, Ω_{Ar} and Ω_{Ca} using the CO2SYS software (Lewis and Wallace, 1998).

2.2.4 Seawater nutrient concentration

In June 2013 three water samples per site were collected for nutrient analysis; the analyses were performed by the nutrient laboratory staff at the Hellenic Centre for Marine Research. Samples were stored frozen (-20°C), then analysed using a BRAN+LUEBBE II autoanalyser. Inorganic phosphate determination followed the colorimetric method of Murphy and Riley (1962) and nitrite ions (NO₂⁻) were measured colorimetrically according to Bendscheider and Robinson (1952). Determination of nitrate (NO₃⁻) was performed after its reduction to nitrite, which was then determined colorimetrically as above. Silicate was determined by adding a molybdate solution to the sample. The

silicomolybdic acid that formed was then reduced to an intensely blue-coloured complex by adding ascorbic acid as a reducing agent (Mullin & Riley, 1955). The determination of ammonium was performed according to Koroleff (1970) using a Perkin Elmer 25 Lambda spectrophotometer.

2.2.5 Free sulphides in seawater

Free sulphides were determined using a method modified from Cline (1989). Three seawater samples per site were collected using plastic syringes to measure within- and between- site variability in sulphides contents; 2 ml of seawater were injected into a nitrogen-filled septum vial containing a small crystal of cadmium chloride. As the area near the seeps had the highest probability of having high sulphide concentrations, four additional samples were taken on two separate dates (22 and 25 May 2012). In order to validate the method, one sample was taken at the sulphide-rich Loutra thermal baths (location shown in Figure 2.1). For laboratory analysis, most of the water was removed by syringe after allowing the precipitate to settle. The samples were thus reduced to 0.8 ml volume, agitated to suspend all the precipitate and drawn up in a 1 ml disposable syringe which had been flushed with Ar.

Subsequently, 0.2 ml of a solution prepared using 400 mg of N,N-dimethyl-p-phenylene-diamine-dihydrochloride and 600 mg $\text{FeCl}_3 \cdot 6\text{H}_2\text{O}$ dissolved in 100 ml 50% HCl were drawn into the same syringe. The argon bubble in the syringe was used to mix by inverting it a few times. The sample was left to stand for 20 minutes and then injected into a 1 ml semi-microcuvette and read in a Perkin Elmer Lambda 35 UV-VIS spectrometer at 670 nm. Standards were made using a 10 mM sodium sulphide stock solution (249 mg $\text{Na}_2\text{S} \cdot 9 \text{H}_2\text{O}$ in 100 ml

degassed Milli-Q water). The stock solution was diluted immediately before use in degassed seawater to give a range of 0.1 to 100 μM .

2.2.6 Heavy metals in sediment

Sediments were examined for metals that can exhibit increased concentrations in volcanic areas (Al, As, Ca, Cd, Co, Cr, Cu, Fe, Li, Mg, Ni, Pb, Zn; Hübner *et al.*, 2004); S was also analysed to verify whether the area was contaminated by hydrogen sulphide emitted by the seeps, and Cr was analysed to determine sediment quality (see below). In May 2012, sediments were sampled for heavy metal analysis at the three sites where contamination from volcanic activity was likely (SEEP, 200 W and 200 E). Sediment was collected using plastic pots immediately closed with a lid. Three stations were selected for each site to assess within-site variability, and one sample per station was collected. Immediately after sampling, sediment was transferred to polypropylene bags and kept frozen until analysis.

Samples were oven-dried at 30°C until constant mass was reached. They were subsequently reduced to a fine powder and passed through a 180 μm plastic sieve. Triplicate replicates for each station were prepared for analysis by digesting them with aqua regia. First, approximately 0.5 grams of sample were carefully weighed on an analytical balance (precision ± 0.1 mg) and transferred into a pre-cleaned and dry digestion tube (Tecator type). Subsequently, 7.5 ml of hydrochloric acid and 2.5 ml of nitric acid were added. One hour of pre-digestion allowed easily oxidised materials to be destroyed at low temperature. Temperature was then gradually increased in several steps: firstly samples were kept at 60 °C for 30 minutes, then at 85 °C for one hour, then at 105 °C for another hour, then at 120 °C for an hour and finally at 140 °C for a further hour.

After cooling, the digested material was transferred quantitatively to a 50 ml volumetric flask and diluted to volume with distilled water. The blank was prepared following the same steps as above, but without adding sediment. Three replicates of reference material (Harbour Sediment, LGC6156) were prepared following the same procedure.

Digested samples were then analysed for Al, Ca, Cr, Cu, Fe, Mg, Mn, Pb, S and Zn using inductively coupled plasma optical emission spectrometry (ICP-OES, Varian 725-ES; Melbourne, Australia) using a v-groove nebuliser and a Sturman-Masters spray chamber. The analysis parameters were as follows: forward power 1.4 kW, plasma gas flow 15 L min⁻¹, auxiliary gas flow 1.5 L min⁻¹, nebuliser gas flow 0.68 L min⁻¹. Each sample was read three times, with four seconds of replicate read time and a viewing height of 8 mm. Every ten samples analysed, one of the standards was measured again in order to detect any deviation from the initial calibration.

As, Cd, Co, Li and Ni were present in very small quantities, so their concentrations were determined using an inductively coupled plasma mass spectrometry (ICP-MS, Thermo Scientific X series 2, Hemel Hempstead, UK) with a concentric glass nebuliser and a conical spray chamber with an impact bead. The analysis parameters were as follows: forward power 1.4 kW, plasma gas flow 13 L min⁻¹, auxiliary gas flow 0.7 L min⁻¹, nebuliser gas flow 0.8 L min⁻¹. Each sample was read 50 times, with 10 ms read time. Every eleven samples, one of the standards was measured again to detect any deviation from the initial calibration. In addition, an internal reference (iridium) was used to correct for the density difference between standards and digested samples.

Biological effects of heavy metal enrichment of the sediments were examined using an index of ecological risk, the mean Sediment Quality Guidelines-quotient (SQG-Q). This index is an indicator of adverse biological effects caused by different concentrations of heavy metals. This type of numerical SQG can be used to obtain a first approximation of sediment toxicity (Long and MacDonald, 1998; Chapman and Wang, 2001). Mean SQG-Q using two sediment quality guidelines, ERM (effect range-median) and PEL (probable effect levels) was calculated for each site using the following equations (Long and MacDonald, 1998):

$$SQG - Q_{\alpha_PEL} = \frac{\sum_{i=1}^n (PEL - Qi)\alpha}{n} \quad (1)$$

and

$$SQG - Q_{\alpha_ERM} = \frac{\sum_{i=1}^n (ERM - Qi)\alpha}{n} \quad (2)$$

where

$$PEL - Q_{\alpha} = \frac{C}{PEL} \quad (3)$$

and

$$ERM - Q_{\alpha} = \frac{C}{ERM} \quad (4)$$

PEL-Q = Probable effect level quotient

ERM-Q = Effect range-median quotient

C- Heavy metal concentration in each station

PEL - Probable effect level of each heavy metal

ERM - Effect range-median of each heavy metal

n – Number of contaminants used.

PEL and ERM are the concentrations above which adverse effects frequently occur and although they have been calculated with slightly different methods, they both are reliable methods to predict sediment toxicity (Long *et al.*, 1998).

PEL and ERM values for the analysed elements are reported in Table 2.2.

Table 2.2. PEL and ERM threshold values used to calculate the potential biological effect of contaminants (Long *et al.*, 1998). They are concentration expressed as mg/g of dry sediment, and have been calculated from a database of toxicity tests.

	Cd	Cr	Cu	Pb	Ni	Zn
PEL	4.21	160	108	112	42.8	271
ERM	9.6	370	270	218	51.6	410

Each site can be assigned to one of the following impact level categories:

Category 1: $SQG-Q < 0.1$ unimpacted - lowest potential for observing adverse biological effects;

Category 2: $0.1 < SQG-Q < 1$ impacted - moderate potential for observing adverse biological effects;

Category 3: $SQG-Q > 1$ highly impacted - potential for observing adverse biological effects.

2.2.7 Heavy metals in macroalgae

A common phaeophyte, *Dictyota* sp., was analysed for heavy metal concentrations at all five sites. This macroalga was chosen as it was present at all sites and had low epiphyte load. Five individuals per species per site were

collected by snorkelers in May 2012, rinsed with fresh water to eliminate salt, gently brushed to remove epiphytes, kept frozen until transported to the laboratory and then freeze-dried. Freeze-dried macroalgae were ground with pestle and mortar and approximately 0.1 g of each sample was weighed in acid-washed Teflon tubes with a high precision digital scale (0.1 mg accuracy). Two ml of concentrated nitric acid were then added, and the tube containing the digestant was placed in a high-Throughput Microwave Reaction System Run (MARSXpress, CEM Corporation, Matthews, USA) and gently heated to boiling for at least 1 h to ensure full digestion. Samples were allowed to cool and then quantitatively transferred into pre-cleaned 10 ml volumetric flasks and diluted to volume with Milli-Q water. Blanks were prepared following the same procedure, but omitting the sample; a certified reference material (NIES Standard Reference Material No. 3, Chlorella) was simultaneously digested and analysed. Samples were then analysed for content of toxic metals (Al, As, Cd, Cr, Co, Cu, Pb, Ni, Zn; Baumann *et al.*, 2009; Mendes *et al.*, 2013; Khan *et al.*, 2015) and Fe, which had values higher than reference ones and showed between-site variability in the sediment samples. Analyses were performed using ICP-OES and ICP-MS following the procedure outlined in the previous section.

2.2.8 Wave exposure

Wave exposure was estimated using a method from Howes *et al.* (1994), which uses modified effective fetch and maximum fetch to calculate a site-specific index of wave exposure, which is a first approximation of wave exposure. Other factors such as the associated local wind climate and wave refraction are ignored for simplifying the estimate. Modified effective fetch involves the measurement of three fetch distances: the normal to shoreline direction and the

two fetches at 45° to the left and to the right of the normal fetch. The effective fetch is then calculated with the formula:

$$Fe = \frac{\sum_{i=0}^n \cos \alpha_i * Fi}{\sum_{i=0}^n \cos \alpha_i} \quad (5)$$

Where Fe is the effective fetch measure in kilometres, α_i is the angle between the shore normal and the direction i and Fi is the fetch distance in kilometres along direction i . The wave climate of a particular point cannot be characterized by effective fetch alone because waves may be generated in an area remote from the site and propagate into the area. These waves, normally referred to as swell, can be approximated using maximum fetch, which is the maximum fetch distance in kilometres that can be measured from the site. The two indexes are then combined in a matrix (Table 2.3) to determine the wave exposure category for each site. The wave exposure was only calculated for the sites SEEP, REF A and REF B, as the sites 200 W and 200 E are very close to SEEP and have a very similar shore orientation.

Table 2.3. Classification of a shore point wave exposure based on the combination of maximum fetch and modified effective fetch (both in km). Depending on the combination of these two factors, a point on the shore can be classified as very protected, protected, semi-protected, semi-exposed, exposed and very exposed (Howes *et al.*, 1994).

Maximum Fetch (km)	Modified Effective Fetch (km)				
	<1	1-10	10-50	50-500	>500
<1	very protected	n/a	n/a	n/a	n/a
<10	protected	protected	n/a	n/a	n/a
10-50	n/a	semi-protected	semi-protected	n/a	n/a
50-500	n/a	semi-exposed	semi-exposed	semi-exposed	n/a
500-1000	n/a	n/a	semi-exposed	exposed	exposed
<1000	n/a	n/a	n/a	very exposed	very exposed

2.2.9 Statistical analyses

Analysis of nutrient and metal concentration data was performed using separate multivariate analyses of variance (MANOVA) with one factor (site). Normality and homogeneity of variances were tested by visually examining boxplots and residual error plots and using Levene's test, and transformed when necessary. When the data did not meet Mauchly's test of sphericity, the degrees of freedom were corrected using Greenhouse-Geisser estimates of sphericity. Tukey HSD tests were used for multiple comparisons. Analysis of pH data was performed using a non-parametric analysis (Kruskal-Wallis ANOVA) followed by pairwise

multiple comparisons. All of the analyses above were performed using SPSS v. 19 (IBM, USA)

2.3 Results

2.3.1 Seawater physicochemical parameters

The seeps had the lowest median pH_{NBS} (7.69, IQ range 7.57 - 7.85, $n=40$) and were significantly different from the intermediate sites (200 W and 200 E), which had higher median values (7.87, $n=26$ and 7.96, $n=26$ for 200 E and 200 W, respectively) and comparable variability (IQ ranges 7.75 - 8.04 and 7.73 - 8.03 for 200 E and 200 W, respectively). At intermediate sites pH sometimes exceeded 8.0, whereas at SEEP the measured pH never reached 8.0. The reference sites had significantly higher pH values (median values of 8.11, $n=21$ and 8.12, $n=19$ for REF A and REF B, respectively) and lower variability (Figure 2.3).

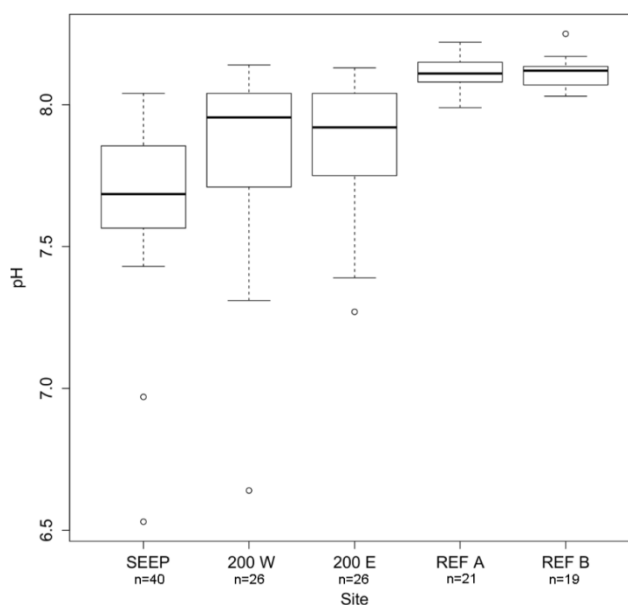


Figure 2.3. Variability in pH at the five study sites off Methana between September 2011 and September 2013. Horizontal line = median, vertical boxes = 25th and 75th percentiles, whiskers = min/max values if smaller than 1.5 times the inter-quartile range and dots = outliers.

Temperature and salinity varied seasonally and were uniform across sites. The minimum temperature was 14.2°C in February, whereas in summer the temperature could reach 26.8°C; salinity varied from 37.5 to 40.0 ppt. Total alkalinity varied from 2.615 to 2.944 mmol kg⁻¹ with no seasonal trend (Table 2.4), with slightly lower values and less variability than CO₂ seeps off Vulcano, where total alkalinity varies between 2.78 to 3.17 mmol kg⁻¹ (Boatta *et al.*, 2013). Seawater pCO₂ had a median value of over 1300 µatm at the SEEP site, almost three times the values calculated for the reference sites. The median saturation state of calcite and aragonite was always > 1, although sites with high and intermediate pCO₂ levels were occasionally under-saturated with respect to both calcite and aragonite (Table 2.4).

Table 2.4. Values of measured (pH and total alkalinity (TA)) and calculated (bicarbonate (HCO₃⁻) and carbonate ions (CO₃²⁻) concentrations, pCO₂, saturation state of calcite (Ω_{Ca}) and aragonite (Ω_{Ar})) carbonate system parameters at the five sites using data from six surveys from September 2011 to September 2013. Sample sizes for pH and total alkalinity are shown below site name.

Site		pH (NBS)	TA (mmol kg ⁻¹)	pCO ₂ (µatm)	HCO ₃ ⁻ (mmol kg ⁻¹)	CO ₃ ²⁻ (mmol kg ⁻¹)	Ω _{Ar}	Ω _{Ca}
SEEP (n _{pH} =40, n _{TA} =23)	Min	6.53	2.639	24092	2.771	0.006	0.09	0.13
	Median	7.69	2.794	1754	2.538	0.104	1.16	2.45
	Max	7.99	2.944	691	2.243	0.225	3.45	5.20
200 W (n _{pH} =26, n _{TA} =24)	Min	6.64	2.696	18652	2.773	0.007	0.11	0.17
	Median	7.96	2.771	872	2.366	0.177	2.70	4.12
	Max	8.14	2.941	526	2.138	0.271	4.18	6.29
200 E (n _{pH} =26, n _{TA} =22)	Min	7.27	2.693	4505	2.658	0.038	0.57	0.88
	Median	7.88	2.739	1042	2.403	0.152	2.30	3.50
	Max	8.13	2.836	532	2.114	0.263	4.05	6.10
REF A (n _{pH} =21, n _{TA} =18)	Min	7.99	2.640	773	2.261	0.183	2.84	4.30
	Median	8.11	2.708	550	2.106	0.246	3.78	5.70
	Max	8.22	2.769	393	2.049	0.269	4.04	6.18
REF B (n _{pH} =19, n _{TA} =15)	Min	8.03	2.615	674	2.254	0.185	2.81	4.30
	Median	8.12	2.697	539	2.145	0.231	3.54	5.33
	Max	8.25	2.858	362	2.024	0.280	4.23	6.46

2.3.2 Seawater nutrient concentrations

Nutrient concentrations were similar to background levels in the Saronikos Gulf (Friligos, 1991) except for silicate, which was mostly higher than the background value of 1.22 μM even at one of the reference sites (Table 2.5). When values were < LOQ. (Limit Of Quantification) they were substituted with LOQ/2; LOQ. = 0.126 μM for $\text{NO}_2^- + \text{NO}_3^-$ and 0.102 μM for NH_4^+ . Statistically significant differences between sites were only detected for nitrite and silicate. Nitrite, however, had a very small range, varying from $0.040 \pm 0.005 \mu\text{M}$ in REF B to $0.054 \pm 0.002 \mu\text{M}$ in 200 E, and these were the only two sites that were significantly different. Silicate had a wider range (from $1.180 \pm 0.269 \mu\text{M}$ in REF B to $6.371 \pm 1.841 \mu\text{M}$ in 200 W); only site 200 W was significantly different from the reference sites according to pairwise comparisons. No significant differences and relatively uniform values were measured for phosphate, whereas nitrate and ammonium showed higher values at 200 E, although these differences were not significant, possibly due to high within-site variability.

Table 2.5. Average seawater nutrient concentrations (\pm SD, n=3) at Methana in June 2013. For the five sites, nitrite (NO_2^-), nitrate (NO_3^-), ammonium (NH_4^+), phosphate (PO_4^{3-}) and silicate (SiO_4^{4-}) concentrations are shown. Background values (Bgd) for the Aegean Sea from Friligos (1991). Different letters indicate significant differences according to post-hoc pairwise comparisons; n.d. = not determined.

	SEEP	200 W	200 E	REF A	REF B	Bgd
NO_3^- (μM)	0.070 ± 0.062	0.094 ± 0.069	0.559 ± 0.297	0.054 ± 0.054	0.085 ± 0.045	0.42
NO_2^- (μM)	$0.054 \pm 0.003^{a,b}$	$0.044 \pm 0.005^{a,b}$	0.059 ± 0.004^b	$0.042 \pm 0.004^{a,b}$	0.040 ± 0.009^a	n.d.
NH_4^+ (μM)	0.232 ± 0.172	0.265 ± 0.189	1.075 ± 0.318	0.203 ± 0.189	0.298 ± 0.091	0.36
PO_4^{3-} (μM)	0.025 ± 0.008	0.031 ± 0.011	0.038 ± 0.009	0.024 ± 0.006	0.044 ± 0	0.12
SiO_4^{4-} (μM)	$4.018 \pm 0.671^{a,b}$	6.371 ± 3.189^a	1.607 ± 0.288^c	$1.883 \pm 0.221^{b,c}$	1.180 ± 0.466^c	1.22

2.3.3 Free sulphides in seawater

Free sulphides concentrations were below the measurable limit for this method (1 μM) at all five sites. In contrast, the sample from Loutra thermal baths had a concentration of free sulphides of 35 μM .

2.3.4 Heavy metals in sediment

Results in mg kg^{-1} of dry sediment (normalised to dry mass) are reported in Table 2.6 for each site and compared to the minimum values reported in a survey of heavy metal concentrations in sediments from the Aegean Sea (Karageorgis *et al.*, 2005). As and Mn results were not considered reliable, as the concentrations determined in the reference material exceeded the confidence interval of the certified values, and are therefore not reported.

Table 2.6. Concentration of analysed elements in mg kg^{-1} of dry sediment from three sites with low (SEEP) and intermediate (200 W, 200 E) pH compared to reference values for the Aegean Sea (minimum values reported by Karageorgis *et al.*, 2005; n.m. = not measured); for SEEP, 200 W and 200 E values are expressed as average \pm standard deviation, $n=3$.

Element	SEEP	200 W	200 E	Reference values
Al	43916 \pm 545	41804 \pm 775	43166 \pm 739	27000
Ca	25056 \pm 428	23119 \pm 282	24463 \pm 380	46900
Cd	0.07 \pm 0.04	0.06 \pm 0.01	0.05 \pm 0.01	n.m.
Co	2.85 \pm 0.35	3.53 \pm 0.35	2.24 \pm 0.16	10
Cr	11.71 \pm 0.57	15.46 \pm 1.00	9.37 \pm 0.87	39
Cu	3.67 \pm 0.32	4.41 \pm 0.37	3.95 \pm 0.95	4
Fe	9436 \pm 266	17802 \pm 1084	8443 \pm 257	13700
Li	7.39 \pm 1.02	7.28 \pm 0.70	7.11 \pm 0.43	n.m.
Mg	2444 \pm 153	2943 \pm 123	2271 \pm 29	17900
Ni	5.32 \pm 0.81	5.89 \pm 0.59	3.72 \pm 0.31	35
Pb	14.99 \pm 3.94	16.30 \pm 2.56	10.76 \pm 5.08	17
S	796.45 \pm 100.16	561.06 \pm 49.52	1746.45 \pm 247.45	n.m.
Zn	13.31 \pm 0.52	20.43 \pm 0.78	12.43 \pm 0.87	33

Average values of the two ecological risk indicators (SQG-Q_PEL and SQG-Q_ERM) are shown in Figure 2.4; all three sites are unimpacted according to

both indexes, except for the site 200 W, which is classified as impacted according to the SQG-Q_PEL index.

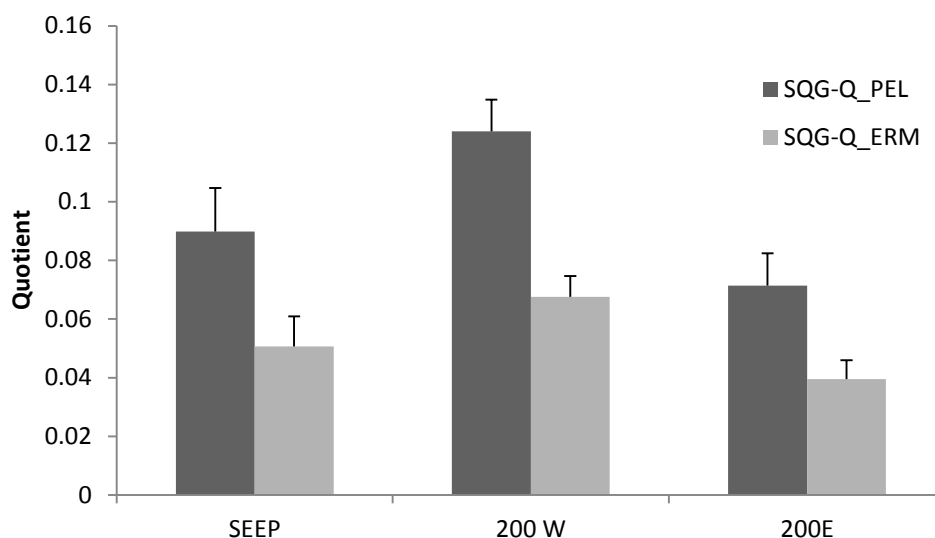


Figure 2.4. Mean (\pm SD) Sediment Quality Guidelines-quotient (SQG-Q) calculated with PEL and ERM for each site. If the index value is below 0.1, biological effects of heavy metals are unlikely. This is the case of the average value for most samples analysed here, except for 200 W, which is considered impacted according to the SQG-Q_PEL index. N=9 for all sites except SEEP, where n=6.

2.3.5 Heavy metals in macroalgae

Log-transformed metal concentrations were significantly different between sites for all elements analysed. Average concentration of elements in *Dictyota* sp. tissues and results of pairwise comparisons test are shown in Table 2.7. There was large spatial variability in metal content, but no specific metal concentration consistently increased with decreasing pH. Elevated concentrations were recorded at station 200 W for aluminium, arsenic and iron, and at REF A for aluminium and zinc.

Table 2.7. *Dictyota* sp. metal content at the five sites. Means (\pm SD; mg kg⁻¹ dry mass; n=5) are shown for each metal and site; different letters indicate significant differences according to Tukey HSD test.

Element	SEEP	200 W	200 E	REF A	REF B
Al	66.58 \pm 66.58 ^a	391.84 \pm 497.99 ^b	75.01 \pm 31.78 ^{a,b}	314.62 \pm 243.57 ^{a,b}	89.77 \pm 39.92 ^{a,b}
As	15.90 \pm 2.30 ^a	39.02 \pm 5.06 ^d	25.79 \pm 6.00 ^c	18.41 \pm 2.91 ^{a,b}	22.52 \pm 0.83 ^{b,c}
Cd	0.014 \pm 0.004 ^a	0.018 \pm 0.006 ^{a,b}	0.034 \pm 0.013 ^{b,c}	0.573 \pm 0.228 ^c	0.067 \pm 0.035 ^d
Co	0.059 \pm 0.051 ^a	0.107 \pm 0.044 ^a	0.096 \pm 0.029 ^a	1.613 \pm 0.706 ^b	0.119 \pm 0.036 ^a
Cr	0.857 \pm 0.156 ^{a,b}	2.526 \pm 1.179 ^c	0.579 \pm 0.112 ^a	1.204 \pm 0.544 ^b	1.093 \pm 0.489 ^{a,b}
Cu	2.069 \pm 0.510 ^a	3.160 \pm 0.602 ^{a,b}	3.435 \pm 1.273 ^{a,b}	7.726 \pm 3.337 ^c	4.771 \pm 0.678 ^{b,c}
Fe	587.1 \pm 95.7 ^b	5659.8 \pm 1350.3 ^a	485.5 \pm 104.6 ^{b,c}	316.3 \pm 197.9 ^{c,d}	146.3 \pm 72.8 ^d
Ni	0.916 \pm 0.223 ^a	1.325 \pm 0.281 ^a	1.338 \pm 0.231 ^a	4.181 \pm 1.292 ^b	2.554 \pm 0.596 ^b
Pb	2.704 \pm 0.480 ^a	17.605 \pm 21.164 ^b	2.378 \pm 0.616 ^a	25.979 \pm 26.174 ^b	10.820 \pm 12.842 ^b
Zn	10.95 \pm 11.73 ^a	11.70 \pm 1.19 ^a	8.22 \pm 1.85 ^a	42.02 \pm 20.75 ^b	14.68 \pm 1.33 ^{a,b}

Values higher than ranges reported in the literature for seaweed tissues from unpolluted sites (Table 2.8) were found for aluminium, arsenic and iron at 200W and for aluminium and zinc in REF A.

Table 2.8. Comparison of metal concentration (mg kg⁻¹ dry mass) in *Dictyota* spp. measured in this study with values found in the literature for unpolluted sites (n.d. = not determined; b.d.l. = below detection limit).

Element	This study (means range)	Abdallah <i>et al.</i> , 2005 (mean \pm SD, n= 3)	McDermid and Stuercke, 2003 (range)	Raman <i>et al.</i> , 2013 (mean \pm S.D., n=3)	Maher and Clarke, 1984
Al	66 – 391	n.d.	n.d.	n.d.	n.d.
As	15 – 39	n.d.	n.d.	n.d.	26.3
Cd	0.014 – 0.573	0.98 \pm 0.3	n.d.	3.9 \pm 0.3	n.d.
Co	0.059 – 1.613	4.3 \pm 1.2	n.d.	5.5 \pm 0.2	n.d.
Cr	0.579 – 2.526	1.1 \pm 0.3	n.d.	b.d.l.	n.d.
Cu	2 – 8	1.3 \pm 0.4	5	6.4 \pm 0.3	n.d.
Fe	316 – 5659	n.d.	438 - 608	504 \pm 12.4	n.d.
Ni	0.916 – 4.181	2.2 \pm 0.6	n.d.	27 \pm 0.4	n.d.
Pb	2 – 25	19.2 \pm 5.5	n.d.	28.5 \pm 3.5	n.d.
Zn	8 – 42	4.9 \pm 1.2	13 - 16	11.7 \pm 0.3	n.d.

2.3.6 Wave exposure

Values of modified effective fetch and maximum fetch for the three sites examined are shown in Table 2.9. All sites are classified as semi-exposed with regards to wave exposure.

Table 2.9. Table showing modified effective fetch (in km) and maximum fetch (in km) for the three sites examined. Fetch values were not calculated for the sites 200 W and 200 E because they were extremely close and with a very similar orientation to SEEP. All sites are considered semi-exposed according to the classification in table 2.3.

Site	Modified effective fetch (km)	Maximum fetch (km)
SEEP	11.17	51.37
REF A	18.91	130.42
REF B	15.81	53.12

2.4 Discussion

Seeps off northern Methana had a median pH value (7.69) similar to that predicted for 2100 according to the IPCC “business as usual” scenario (Caldeira and Wickett, 2005), whereas the reference sites had median values above 8. The seeps had no confounding gradients in temperature, salinity, total alkalinity, hydrogen sulphide or wave exposure. The low pH area off Methana had pCO₂ levels comparable to those reported at other ocean acidification analogues (Hall-Spencer *et al.*, 2008; Kroeker *et al.*, 2011; Fabricius *et al.*, 2011; Kerrison *et al.*, 2011; Boatta *et al.*, 2013), making it suitable to assess community responses to increased pCO₂.

Enrichment in silicate, which was significantly different from reference values in one of the intermediate sites, is likely due to water-rock interactions common in

hydrothermal environments (D'Alessandro *et al.*, 2008). However, it is unlikely that silicate is limiting in the Aegean Sea; for instance, Si becomes limiting to diatoms when the N:Si ratio in seawater is higher than two (Gilpin *et al.*, 2004), whereas the background ratio for the Aegean Sea is 0.64 (Friligos, 1991). Significant differences in nitrite concentrations among sites are unlikely to explain the community changes either, as their range is very small (0.040 – 0.059 μM). Mediterranean organisms are normally not limited by silicate or inorganic nitrogen, but by phosphate (Zohary and Robarts, 1998), for which no confounding gradient was found.

No free sulphides were detected near the seeps, although they were present at the Loutra thermal baths, over 10 km from the study site. Hydrogen sulphide is toxic for cellular respiration, and it is often emitted from Mediterranean volcanic vents (Dando *et al.*, 1999; Caramanna *et al.*, 2011). However, sulphides are extremely reactive and oxidise quickly to sulphates in oxygenated waters. It is therefore common to find very low or undetectable sulphide concentrations just a few meters away from volcanic seeps. For instance, at Vulcano sulphides become undetectable at 30 m from the main vents, even though hydrogen sulphide gas has a concentration of 400 ppm at the main bubbling site (Boatta *et al.*, 2013).

No enrichment in sediment heavy metal in the low and intermediate pH sites was detected, even though sediment enriched in various elements have been reported from a nearby area (Hübner *et al.*, 2004). In addition, analysis of *Dictyota* sp. shows that no metal consistently increased in concentration as pCO_2 increased. Brown algae are considered a good indicator of bioavailable metals since they greatly bioaccumulate metals, often proportionally to metals concentration in surrounding seawater (Phillips, 1990). Values higher than

ranges reported in the literature were found for aluminium, arsenic and iron at 200 W and for aluminium and zinc in REF A (Table 2.8). Aluminium variability is likely to be related to local mineralogy (Karageorgis *et al.*, 2005), while enrichment in the other elements has previously been linked to hydrothermal activity (Hübner *et al.*, 2004). Metal bioaccumulation is a common occurrence at shallow and deep hydrothermal vents (Tarasov *et al.*, 2005; Couto *et al.*, 2010), but at Methana metal enrichment did not seem to have major effects at the community and species level. The intermediate and reference sites enriched in some elements (200 W and REF A) were not significantly different from the other intermediate and reference sites (200 E and REF B) with regards to key species percent cover and overall community structure (see Chapter 3).

As with other carbon dioxide seeps used as natural analogues for ocean acidification, Methana has some limitations. Motile taxa such as fish are able to move in and out of high CO₂ areas (Riebesell, 2008) and pelagic larvae can come from unaffected populations (Cigliano *et al.*, 2010). Moreover, carbonate chemistry is much more variable near the seeps than in reference conditions, as changes in current direction and intensity influence the dispersal of the dissolved gas emissions. Compared to other volcanic seeps, at Methana seawater pCO₂ is high and variable on a greater scale (>15 vs <0.3 km of shoreline; Hall-Spencer *et al.*, 2008; Fabricius *et al.*, 2011; Boatta *et al.*, 2013). Thus, Methana might offer an opportunity to study ecological processes such as recruitment in a high CO₂ area probably less influenced by unaffected populations than smaller sites.

The need to translate results from laboratory experiments to more realistic systems has led to several areas with naturally high pCO₂ to be used to infer biological community responses to ocean acidification. Examples include

estuaries acidified by acid sulphate soils (Amaral *et al.*, 2011), groundwater submarine springs (Crook *et al.*, 2012), upwelling regions (Manzello, 2010; Thomsen *et al.*, 2010; Mayol *et al.*, 2012) and rockpools with different carbonate chemistry (Moulin *et al.*, 2011; Evans *et al.*, 2013). None of the above are perfect ocean acidification analogues, as they can have confounding gradients in salinity and alkalinity (groundwater springs) or in temperature and nutrients (upwelling areas). In addition, low pH recorded in groundwater springs and acidified estuaries is not always caused by increased carbon dioxide concentrations, so only the effects of low pH on biological communities can be tested. However, studies from low pH/high CO₂ sites mostly report decreased abundance and diversity of calcifying organisms, in accord with findings from CO₂ seeps and laboratory experiments (Hall-Spencer *et al.*, 2008; Kroeker *et al.*, 2013a; Fabricius *et al.*, 2014). General patterns of community responses to ocean acidification can then be detected using areas with naturally low pH, even though confounding factors should always be taken into account.

Overall, our data show that the examined seeps off Methana offer an opportunity to study the effects of high pCO₂ levels on natural benthic communities in an oligotrophic environment. The general limitations of using CO₂ seeps should, however, be taken into account. These seeps could also be used to study how ecological processes are influenced by carbon dioxide on a scale of kilometres, not tens of meters as the other seeps currently used as ocean acidification analogues.

Chapter 3

Changes in subtidal macroalgal communities along pCO₂ gradients at Mediterranean volcanic seeps

Aspects of this chapter have been published as:

C. Baggini, M. Salomidi, E. Voutsinas, L. Bray, E. Krasakopoulou, J.M. Hall-Spencer (2014). Seasonality affects macroalgal community response to increases in pCO₂. *PLoS ONE*, 9: e106520.

Abstract

Shifts in macroalgal communities have been detected along $p\text{CO}_2$ gradients at volcanic seeps in a few temperate (Italy) and tropical (Papua New Guinea) settings. However, replication of these observations is needed to expand our ability to predict how marine ecosystems will change due to ocean acidification. The present study determined macroalgal diversity and abundance along $p\text{CO}_2$ gradients caused by volcanic seeps off Methana (Greece) and Vulcano (Italy) using visual census and destructive sampling methods, respectively. At Methana, *Cystoseira corniculata* was dominant in autumn and *Sargassum vulgare* C.Agardh was dominant in spring near the seeps. The articulated coralline alga *Jania rubens* had significantly higher cover at reference sites, but only in autumn. Diversity decreased with increasing CO_2 regardless of sampling season. At Vulcano, the main habitat-forming algal species changed as CO_2 level increased: at the reference site *Cystoseira* spp. and *Dictyopteris polypodioides* (A.P.De Candolle) J.V.Lamouroux were dominant, at elevated $p\text{CO}_2$ levels *Sargassum vulgare* greatly increased in abundance replacing *D. polypodioides*. These data are consistent with results from laboratory experiments and observations at other Mediterranean CO_2 seep sites in that benthic communities decreased in calcifying algal cover with increasing $p\text{CO}_2$. This chapter demonstrates that natural $p\text{CO}_2$ gradients can help us envisage how benthic communities will be affected by ocean acidification in a range of environmental conditions, and that benthic community responses to ocean acidification can be strongly affected by season.

3.1 Introduction

Studies on single species can be very useful for formulating hypotheses about how biological communities may respond to ocean acidification. However, work on global warming demonstrates that most temperature-associated causes of severe population decline originate not from direct physiological responses to heat, but result from modified species interactions (Cahill *et al.*, 2013). Similar trends arise in lake acidification (Locke and Sprules, 2000) and it is anticipated that consequences of ocean acidification will be similar (Gaylord *et al.*, 2014). Responses of seaweed species to increased carbon dioxide are poorly known (Harley *et al.*, 2012; Koch *et al.*, 2013), with laboratory experiments to date concentrated on calcifying red and green algae (Gao *et al.*, 1993; Büdenbender *et al.*, 2011; Price *et al.*, 2011). So far, evidence indicates that calcifying algae will be negatively affected by ocean acidification while some fleshy algae may thrive (Kroeker *et al.*, 2013a; Brodie *et al.*, 2014). There is very little information on brown seaweed responses to elevated pCO₂ despite the fact that they are key species in temperate rocky habitats worldwide (Steneck *et al.*, 2002). In addition, a species can respond differently to ocean acidification in single species experiments and in natural communities because of inter-specific interaction; for instance, crustose coralline algae may cope with elevated CO₂, but be outcompeted by fleshy algae (Kroeker *et al.*, 2013c).

Our limited ability to predict community responses of macroalgal communities to ocean acidification worldwide and the few experiments performed on Mediterranean species add value to studies examining community responses using CO₂ seeps in the Mediterranean Sea. Results from surveys at seeps off Ischia and Vulcano (both in Italy) show how increased carbon dioxide is likely to cause shifts in macroalgal communities. As CO₂ increases at these sites,

coralline algae are replaced by canopy-forming brown algae such as *Sargassum vulgare* in the shallow subtidal off Ischia (Porzio *et al.*, 2011) or brown foliose algae such as *Dictyota* spp. and non-calcified *Padina* sp. off Vulcano (Johnson *et al.*, 2012; Graziano *et al.*, unpublished data). This response to increased CO₂ differs from shifts towards opportunistic green macroalgal species such as *Ulva* spp. or mat-forming algae reported in stressed marine benthic ecosystems, such as those exposed to eutrophication (Airoldi and Beck, 2007; Connell *et al.*, 2008), where decreased floral complexity can have detrimental effects on local biodiversity (Schermer *et al.*, 2013) and indirectly affect the abundance of many commercial species (Harley *et al.*, 2012). On the other hand, increased abundance of brown perennial algae near volcanic CO₂ seeps suggests that carbon dioxide may be a useful resource that can benefit perennial habitat-forming algae (Porzio *et al.*, 2011; Connell *et al.*, 2013).

This study aims to assess changes in macroalgal communities along pCO₂ gradients off Greece and Italy. I characterised benthic communities at a shallow subtidal site in the Eastern Mediterranean Sea (Methana, Greece) in spring and autumn as well as those off Vulcano (Italy) at a depth of 3-5 metres in spring. I was mindful of the fact that responses to increased carbon dioxide in these two environments could be substantially different from those previously recorded, since the Aegean Sea has lower average nutrient concentrations than those in the Tyrrhenian Sea (Moutin and Raimbault, 2002). Food limitation has been shown to exacerbate the negative influence of ocean acidification on benthic invertebrates (Melzner *et al.*, 2011; Rodolfo-Metalpa *et al.*, 2011), so nutrient limitation may act in combination with ocean acidification to negatively affect seaweed communities. At ambient levels of CO₂ around Methana and Vulcano,

subtidal brown algae such as *Cystoseira* spp. and *Dictyopteris polypodioides* have the highest biomass (Pérès and Picard, 1964). These subtidal species are expected to be less sensitive to ocean acidification than calcifying algae (Kroeker *et al.*, 2013a), but they could be more sensitive to ocean acidification than intertidal brown algae. As subtidal habitats are more stable than intertidal ones, subtidal organisms are generally thought to be more vulnerable to environmental changes (Lobban and Harrison, 1994).

In addition, there are very few studies dealing with the seasonal patterns of benthic community changes along pCO₂ gradients, even though temperate coastal waters vary greatly among seasons (Coma *et al.*, 2000). These ecosystems undergo large yearly changes in light and temperature regimes, which indirectly influence other factors important for biological communities, such as nutrient levels (Pingree *et al.*, 1976). In the Mediterranean Sea, these three factors strongly influence macroalgal communities: macroalgal biomass peaks in late spring, and community composition changes among seasons (Sala and Boudouresque, 1997). Specifically, many mat-forming algae disappear and most erect algae decrease in cover during the cold season (Piazzi *et al.*, 2004).

3.2 Methods

3.2.1 Methana experimental design and data analysis

The first part of the work for this thesis chapter was conducted along a pCO₂ gradient off Methana (Greece). Five sites at three pCO₂ levels were used: SEEP (high CO₂ level), 200 W and 200 E (intermediate CO₂ level), REF A and REF B (reference CO₂ level); for a detailed description of study sites, see Chapter 2. Benthic community composition was assessed in May and

September 2012 using visual census (detailed sampling dates and sample sizes are reported in Table 1.1B): samples were collected between 0.7 and 1.0 m below mean sea level using 20x20 cm quadrats on horizontal and sub-horizontal rocky substrata (Fraschetti *et al.*, 2005). A frame with 25 4x4 cm squares was used to assess percentage cover (C%) and number of taxa (S). Percentage cover of algae and sessile invertebrates was determined by assigning each taxon a score ranging from 0 to 4 within each square and summing the 25 estimates (Dethier *et al.*, 1993). Final values were expressed as percentages. Taxa were identified to the lowest possible level, usually species, except for turf algae; this functional group was defined as sparse to thick mats of small and juvenile algae less than 2 cm high (Steneck and Dethier, 1994). Seven replicate quadrats randomly chosen but placed at least 4-5 m from each other were assessed for every site in May 2012 and six replicates were collected in September 2012. The selected sample size represented the maximum number of samples that could be randomly collected from sub-horizontal surfaces at the smallest site (SEEP, ~20 m of shoreline) at the selected depth (0.7-1.0 m below sea level). Samples were collected in May, when Mediterranean seaweeds reach their biomass peak (Ballesteros, 1984) and September, when Greek shallow benthic communities have been exposed for over three months to temperatures > 25°C (Maria Salomidi, personal communication).

Differences in community structure and composition were assessed using Permutational Multivariate Analysis of Variance (PERMANOVA, (Anderson *et al.*, 2003); PRIMER 6 and PERMANOVA + package (Clarke and Gorley, 2006)). The analysis had two fixed factors: season (two levels) and site (five levels). The analyses were performed on Bray-Curtis measures of square root

transformed data, using 9999 permutations of residuals under a reduced model. Pair-wise comparisons were then performed for significant factors with more than two levels. Since site was a significant factor in the PERMANOVA, its levels were compared using a SIMPER analysis to identify the taxa driving dissimilarities.

Macroalgal cover data were used to calculate Shannon diversity (Shannon and Weaver, 1949) and Pielou's evenness (Pielou, 1966) for each sample. The two indices were analysed using an ANOVA followed by a Tukey HSD test for multiple comparisons. After testing for normality and homoscedasticity, canopy-forming and calcifying algae arcsin-transformed percent cover was analysed using a two-way ANOVA with site and functional group as fixed factors; seasons were tested separately. The site*species interaction was then decomposed to obtain multiple comparisons among sites for each season separately. The same analysis was then performed for selected single species. All univariate analyses were performed using SPSS v19 (IBM, USA).

3.2.2 Vulcano study site

The second part of the work for this thesis chapter was conducted along a pCO₂ gradient off the island of Vulcano in the Eolian archipelago (Italy). This island is an active volcano formed in the collision of the Eurasian and Asian plates. The gradient is caused by submarine volcanic seeps emitting over 97% CO₂ (Inguaggiato *et al.*, 2012; Boatta *et al.*, 2013), which lower seawater pH to 5.5-5.6 at the main bubbling site. The hydrothermal fluids also contain hydrogen sulphide (Italiano *et al.*, 1984; Capaccioni *et al.*, 2001), which is potentially toxic to cellular respiration. However, hydrogen sulphide rapidly oxidises to sulphate; sulphide concentrations are in fact very low (< 50 µMol kg⁻¹) at > 20 m from the main seeps as water is well-oxygenated all over the bay (Boatta *et al.*, 2013). I

chose an area for this study that was a ~200 m stretch of rocky shore at >30 m from the main seeps, where pH ranges from 7.55 to 8.2 (Boatta *et al.*, 2013). Along this gradient, the three sites (pH \pm S.D.) shown in Figure 3.1 were selected, one with high (High CO₂; pH 7.57 \pm 0.23, n = 19), one with intermediate (Mid CO₂; pH 7.94 \pm 0.16, n = 18) and one with reference pCO₂ (REF A; pH 8.14 \pm 0.05, n = 11); pH data are from monitoring conducted in September 2009 and April 2010 from Graziano *et al.* (unpublished data).

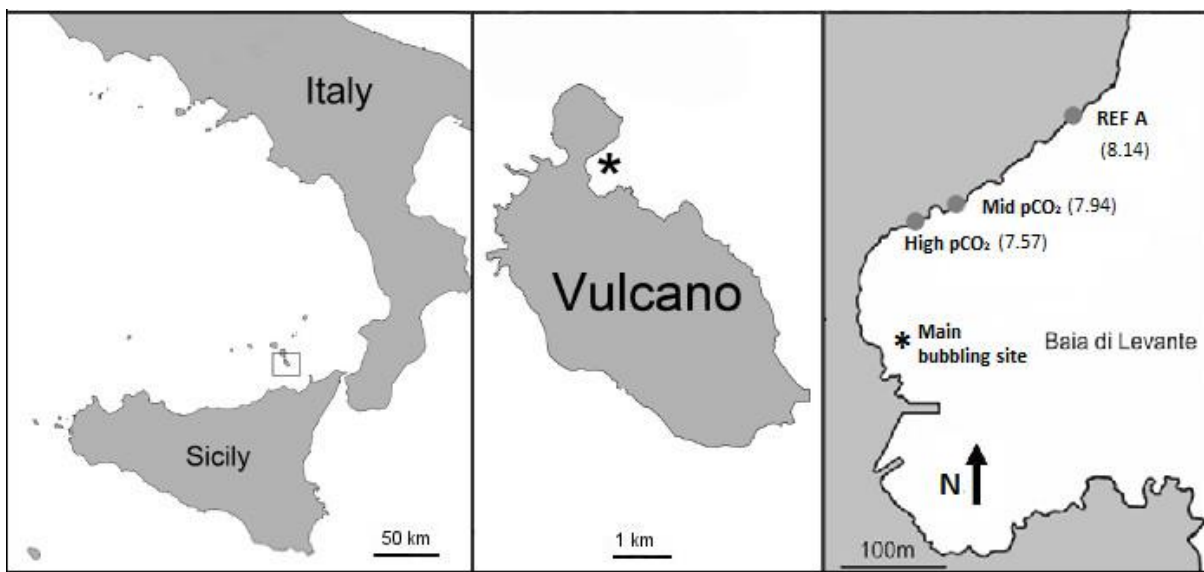


Figure 3.1. Vulcano Island (Sicily, Southern Italy) and study sites; the asterisk marks the main bubbling area, whereas grey circles indicate the three sampling sites and their average pH, with decreasing pCO₂ moving away from the bubbling area.

Geochemical surveys in Levante bay in 2011 have shown that these seeps do not influence the main seawater elements and data in Table 3.1A demonstrate that temperature, salinity and total alkalinity do not change significantly among the sites used for this chapter (Boatta *et al.*, 2013). Nutrients were also measured (Table 3.1B); nitrite and silicate concentrations were significantly different among sites, while nitrate levels were relatively stable along the CO₂ gradient and phosphate levels remained below detection limit (~10 nmol L⁻¹) at

all sites (Johnson, 2012). The increase in nitrates was very small (0.01 μM), and silicates are not believed to be limiting for marine organisms at the reference site, as phosphates are the limiting nutrient in Mediterranean waters (Zohary and Robarts, 1998).

Table 3.1. (A) Mean ($\pm\text{SD}$) seawater temperature (T), salinity (S) and total alkalinity (TA) recorded from September 2009 to July 2011 at three sites used for this chapter (data from Boatta *et al.*, 2013). (B) Mean ($\pm\text{SD}$) dissolved nutrient concentrations at three studied sites at Vulcano (n = 5-6). Phosphate was also determined but at all stations was below the detection limit of the AutoAnalyser, i.e. $\sim 10\text{ nmol L}^{-1}$ (data from Johnson, 2012).

A)	Site	T ($^{\circ}\text{C}$)	S (‰)	n	TA ($\mu\text{Eq kg}^{-1}$)	n
	High CO_2	21.71 \pm 4.93	37.49 \pm 0.64	41	2524.7 \pm 0.6	9
	Mid CO_2	21.67 \pm 4.93	37.59 \pm 0.58	41	2520.5 \pm 6.6	9
	REF A	21.66 \pm 4.22	37.45 \pm 0.66	22	2532.5 \pm 20.9	7

B)	Site	Nitrite (μM)	Nitrate (μM)	Silicate (μM)
	High CO_2	0.02 \pm 0.002	0.33 \pm 0.22	19.39 \pm 2.77
	Mid CO_2	0.02 \pm 0.007	0.16 \pm 0.13	15.12 \pm 5.48
	REF A	0.01 \pm 0.002	0.24 \pm 0.11	3.43 \pm 0.11

As for minor seawater elements, there was a marked increase in iron concentration, which reached values up to three orders of magnitude higher than ambient concentrations reported for the Mediterranean Sea (Sarhou and Jeandel, 2001; Figure 3.2). Iron is an essential micronutrient for marine algae and is a limiting factor for their growth in many areas in the world ocean (Geider and La Roche, 1994). In the Mediterranean Sea, however, iron is only limiting in special circumstances (Bennet and Guien, 2006) due to the very low phosphate concentrations in the region (Zohary and Robarts, 1998). The minimum iron value measured off Vulcano during a recent geochemical survey was 57 nMol/kg (Boatta *et al.*, 2013), much higher than phosphate concentrations in the area ($< 10\text{ nMol/kg}$; Johnson, 2012). According to the modified Redfield ratio

(Martin *et al.*, 1990), iron is limiting when its concentration is lower than 10% of that of phosphate, which is not the case in Vulcano.

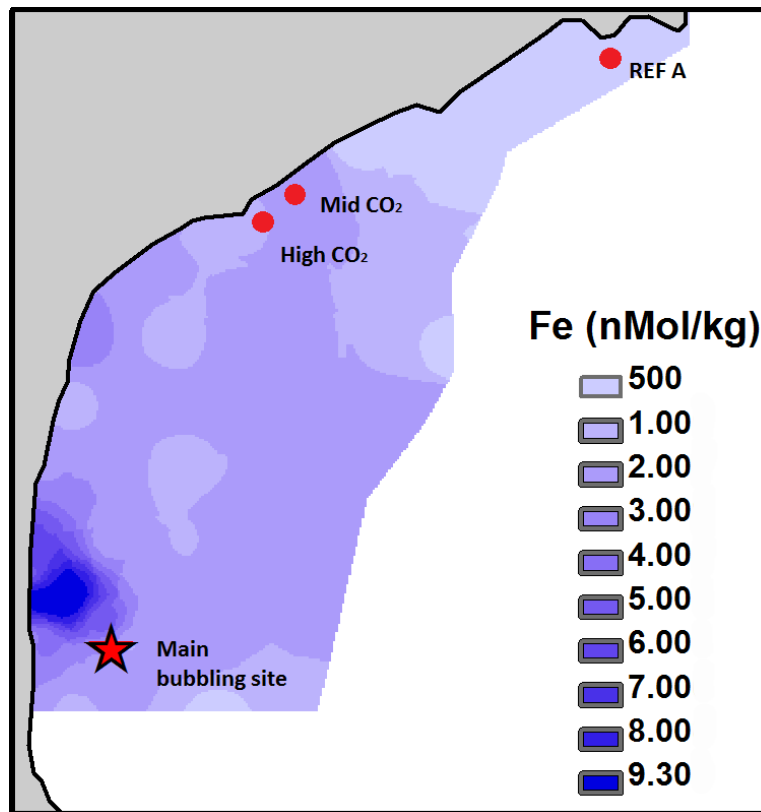


Figure 3.2. Distribution map adapted from a recent geochemical survey (Boatta *et al.*, 2013) in the Baia di Levante showing the iron concentrations measured in the area in April 2011. The sites used for this thesis have been superimposed (red dots); the red star indicates the main bubbling site. Data for these maps were collected from around 70 sampling points within the bay.

Elevated heavy metal concentrations are also a common feature of volcanic areas (Tarasov *et al.*, 2005). A recent geological survey of Baia di Levante (Figure 3.3) revealed that parts of the bay have sediment of poor or bad quality according to the Marine Sediment Pollution Index (MSPi; Shin and Lam, 2001). The sites chosen for the present study have average or good sediment condition, which only have a moderate potential for causing adverse biological effects according to the Sediment Quality Guideline Quotient (SQG-Q, for its

definition see Chapter 2; Vizzini *et al.*, 2013). The change in pCO₂ values caused by the seeps is therefore the most likely driver of any biological change observed at the study sites.

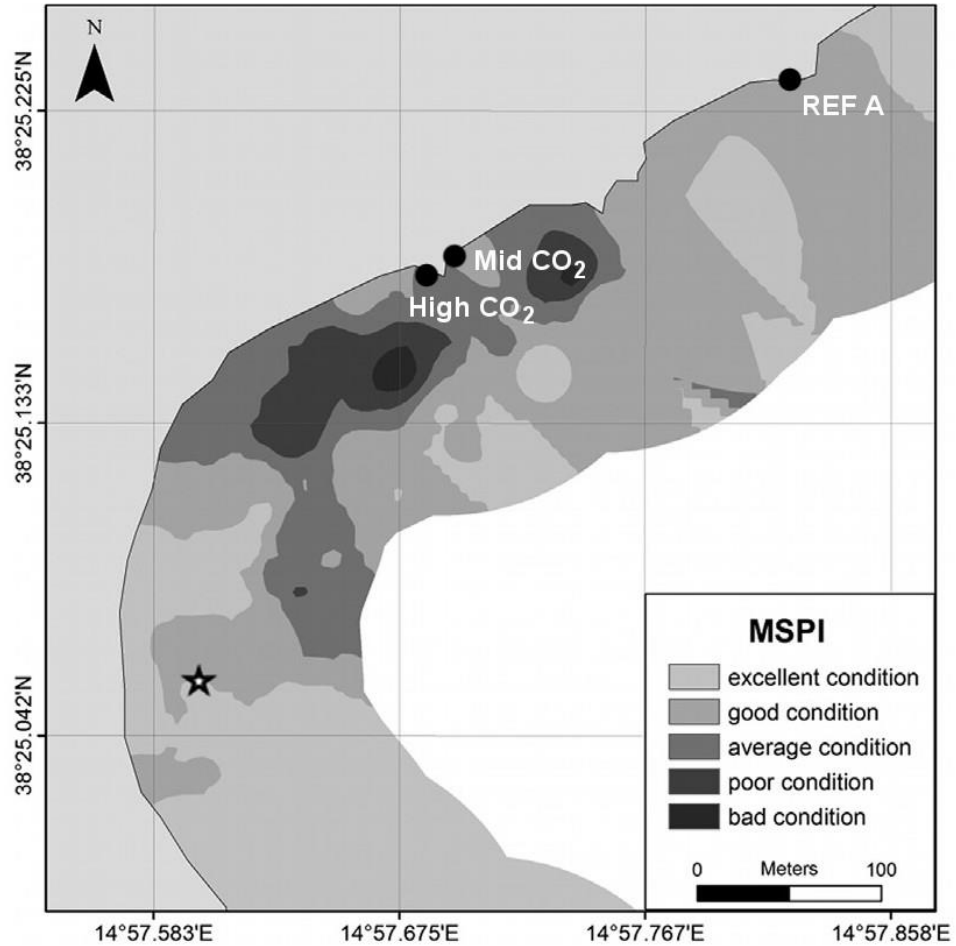


Figure 3.3. Results from a recent geochemical survey in the Baia di Levante showing the Marine Sediment Pollution Index (MSPI) from sediment collected in autumn 2011. The sites used for this thesis have been superimposed (black dots); the star indicates the main bubbling site. Data for these maps were collected from 50 sampling points within the bay (Vizzini *et al.*, 2013).

3.2.3 Vulcano experimental design and data analysis

Macroalgae were collected by scraping 20 x 20 cm squares of rock with hammer and chisel following a method developed for this type of Mediterranean shore (Ballesteros, 1986). Four replicates were collected in three sites in May

2010 by Mariagrazia Graziano and Kristy Kroeker, immediately frozen and transported to the laboratory (detailed sampling dates and sample sizes are reported in Table 1.1B). Samples were then sorted and identified to the lowest possible taxonomic level, mostly to the species level, except for turf algae; this functional group was defined as sparse to thick mats of small and juvenile algae less than 2 cm high (Steneck and Dethier, 1994). For biomass determination, dry biomass of each taxon was obtained drying the identified samples in an oven at 60°C for 24 hours. The obtained data was analysed using the same procedure outlined above for Methana, but using an experimental design with one fixed factor with three levels (“Site”) and log-transforming the biomass data for functional groups and single species analyses.

3.3 Results

3.3.1 Methana benthic community

Overall, 18 macroalgal taxa and three invertebrate taxa (two sponges and one hydrozoan) were recorded. Benthic communities significantly differed among sites and seasons (Table 3.2A), with a significant interaction between the two factors (pseudo- $F_{4,55}=1.754$, $p(\text{perm})=0.0457$). In spring the high $p\text{CO}_2$ site was significantly different from the reference sites, while the intermediate $p\text{CO}_2$ sites were not significantly different from any of them. In autumn, the high $p\text{CO}_2$ site was significantly different from all other sites (Table 3.2B). Site had a significant effect on diversity ($p = 0.049$, Table 3.3) with a clear decrease as CO_2 increased (0.94 ± 0.10 , $n=26$ to 0.55 ± 0.08 , $n=13$; mean \pm SE).

Table 3.2. (A) PERMANOVA analysis on square-root transformed percentage cover of Methana benthic communities. The first table shows main factors and their interaction and degrees of freedom (df), sum of squares (SS), pseudo-F, permutational p and unique permutations for each of them. Season, site and their interaction all have a significant effect. (B) Results from pair-wise comparisons between sites for each season (different letters represent significantly different groups).

(A)	Source	df	SS	Pseudo-F	p (perm)	Unique perms
	Season	1	31069	19.234	0.0001	9949
	Site	4	21820	3.377	0.0001	9918
	Season x Site	4	11330	1.754	0.0457	9916
	Residual	55	88840			
	Total	64	1.5273E5			

(B)	Season	Sites			
	Spring	SEEP ^a	200 W ^{a,b}	200 E ^{a,b}	REF A ^b REF B ^b
	Autumn	SEEP ^a	200 W ^b	200 E ^b	REF A ^b REF B ^b

Shannon diversity (H') and Pielou's evenness (J') of benthic communities off Methana were pooled among seasons and sites as no significant differences were detected between seasons and between sites with the same CO₂ level (Figure 3.4). Although the factor 'site' had a significant effect on Shannon diversity (Table 3.3), no significant differences were detected by the Tukey test. However, both indices show a clear decreasing trend in the diversity of the rocky shore sessile communities from reference to high CO₂ levels, with Shannon's diversity index almost halving (0.94 ± 0.40 to 0.55 ± 0.37; mean ± SD).

Table 3.3. ANOVA results for (A) Shannon diversity (H') and (B) Pielou's evenness (J') of Methana benthic communities. The Tables show main factors and their interactions and sum of squares (SS), degrees of freedom (df), Mean Squares (MS), F-ratios (F) and p values. Significant p values (< 0.05) are highlighted. Results from pairwise comparisons among sites were never significant and are not reported.

A) Source	Type III SS	df	MS	F	p
Site	1.438	4	0.359	2.557	0.049
Season	0.261	1	0.261	1.859	0.178
Site x Season	0.232	4	0.058	0.413	0.798
Error	7.731	55	0.141		
Total	9.664	64			

B) Source	Type III SS	df	MS	F	p
Site	0.282	4	0.071	1.285	0.287
Season	0.166	1	0.166	3.022	0.088
Site x Season	0.119	4	0.030	0.539	0.708
Error	3.022	55	0.055		
Total	3.568	64			

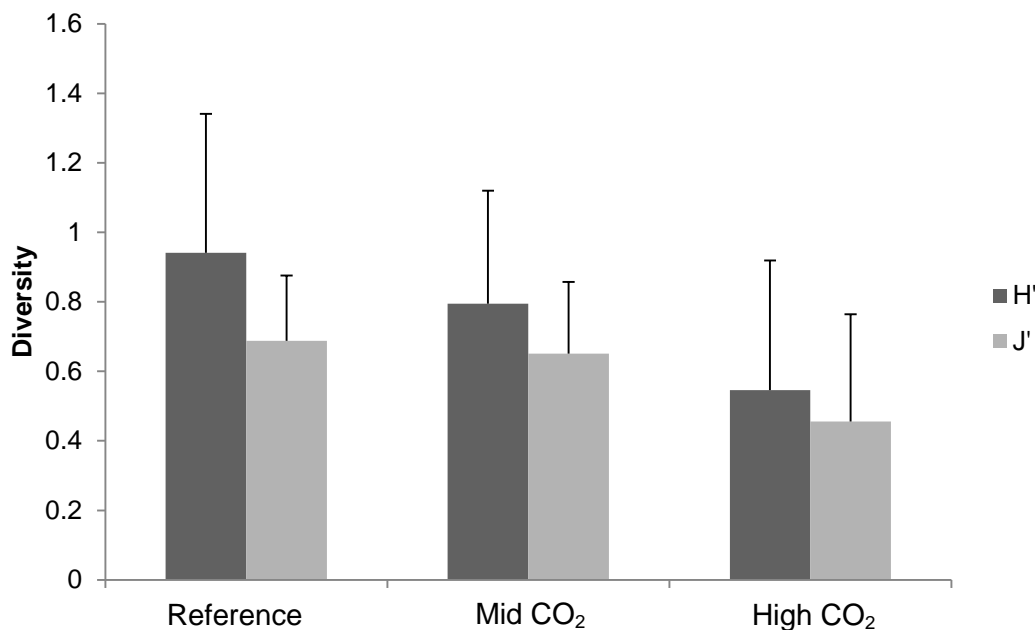


Figure 3.4. Mean (\pm SD) Shannon diversity (H') and Pielou's evenness (J') at high ($n=13$), intermediate ($n=26$) and reference ($n=26$) CO₂ at Methana rocky shores at depths between 0.7 and 1.0 m pooling sites and season.

The SIMPER analysis among sites shows which taxa contributed most to the detected differences (Table 3.4). The main drivers of differences between groups were canopy-forming algae such as *Cystoseira corniculata* and *Sargassum vulgare* and calcareous algae such as coralline crustose algae (CCA), the articulated coralline alga *Jania rubens* and the calcified brown alga *Padina pavonica*.

Table 3.4. SIMPER analysis of Methana benthic communities showing the average dissimilarities between each pair of sites and which species contributed up to 90% of the dissimilarity. For each taxon, the average abundance in the two groups that are being compared, their average dissimilarity, the dissimilarity to standard deviation ration and the taxon contribution and cumulative contribution are shown. CCA stands for coralline crustose algae.

Groups SEEP & 200 E; Average dissimilarity = 65.40						
Taxon	SEEP	200 E	Av.Diss	Diss/SD	Contrib%	Cum.%
	Av.Abund	Av.Abund				
<i>Cystoseira corniculata</i>	5.27	6.76	14.85	1.28	22.71	22.71
CCA	0.11	2.86	8.80	0.88	13.45	36.16
<i>Sargassum vulgare</i>	2.58	0.85	8.46	0.74	12.93	49.09
<i>Jania rubens</i>	0.00	2.63	7.70	0.78	11.77	60.85
<i>Dictyota</i> sp.	1.16	1.59	6.14	0.91	9.38	70.24
<i>Sargassum</i> sp.	1.50	0.00	4.28	0.45	6.54	76.78
<i>Padina pavonica</i> (not calcified)	1.12	0.27	3.93	0.51	6.02	82.79
Bare substratum	1.08	0.00	3.16	0.60	4.83	87.62
<i>Falkenbergia</i> sp.	0.46	0.00	1.38	0.51	2.10	89.73
<i>Cladophora</i> sp.	0.50	0.00	1.36	0.39	2.08	91.80

Groups SEEP & 200 W; Average dissimilarity = 63.83						
Taxon	SEEP	200 W	Av.Diss	Diss/SD	Contrib %	Cum.%
	Av.Abund	Av.Abund				
<i>Cystoseira corniculata</i>	5.27	6.52	14.63	1.30	22.92	22.92
<i>Sargassum vulgare</i>	2.58	0.59	8.96	0.70	14.04	36.96
<i>Cladostephus spongiosus</i>	0.36	1.95	6.54	0.85	10.24	47.20
<i>Dictyota</i> sp.	1.16	1.56	6.18	0.85	9.68	56.88
<i>Jania rubens</i>	0.00	1.90	5.46	0.65	8.56	65.44
CCA	0.11	1.57	4.81	0.63	7.53	72.97
<i>Sargassum</i> sp.	1.50	0.55	4.27	0.52	6.69	79.65

<i>Padina pavonica</i> (not calcified)	1.12	0.26	3.96	0.51	6.21	85.86
Bare substratum	1.08	0.64	2.89	0.58	4.53	90.39

Groups 200 E & 200 W; Average dissimilarity = 43.27

Taxon	200 E		200 W		Contrib%	Cum.%
	Av.Abund	Av.Abund	Av.Diss	Diss/SD		
<i>Cystoseira corniculata</i>	6.76	6.52	9.58	1.11	22.14	22.14
CCA	2.86	1.57	8.68	0.92	20.06	42.21
<i>Cladostephus spongiosus</i>	0.00	1.95	5.86	0.82	13.54	55.74
<i>Jania rubens</i>	2.63	1.90	3.41	0.60	7.87	63.61
<i>Dictyota</i> sp.	1.59	1.56	3.11	0.66	7.18	70.80
<i>Sargassum vulgare</i>	0.85	0.59	2.81	0.74	6.50	77.30
Bare substratum	0.00	0.64	1.62	0.40	3.75	81.05
<i>Padina pavonica</i> (not calcified)	0.27	0.26	1.54	0.40	3.56	84.61
<i>Halopteris scoparia</i>	0.15	0.42	1.54	0.39	3.56	88.17
<i>Sargassum</i> sp.	0.00	0.55	1.44	0.49	3.33	91.49

Groups SEEP & REF A; Average dissimilarity = 74.58

Taxon	SEEP		REF A		Contrib%	Cum.%
	Av.Abund	Av.Abund	Av.Diss	Diss/SD		
<i>Cystoseira corniculata</i>	5.27	5.01	15.26	1.36	20.46	20.46
<i>Jania rubens</i>	0.00	3.77	11.28	0.94	15.13	35.59
<i>Sargassum vulgare</i>	2.58	0.34	8.76	0.70	11.75	47.34
Bare substratum	1.08	1.71	6.83	1.29	9.15	56.50
<i>Dictyota</i> sp.	1.16	1.98	6.49	0.76	8.70	65.20
CCA	0.11	1.83	5.13	0.87	6.87	72.07
<i>Sargassum</i> sp.	1.50	0.00	4.28	0.45	5.74	77.81
<i>Padina pavonica</i> (not calcified)	1.12	0.00	3.27	0.44	4.38	82.19
<i>Cystoseira amentacea</i>	0.00	0.93	2.93	0.53	3.93	86.12
<i>Padina pavonica</i> (calcified)	0.00	0.75	2.44	0.52	3.27	89.40
<i>Halopteris scoparia</i>	0.00	0.66	2.03	0.40	2.73	92.12

Groups 200 E & REF A; Average dissimilarity = 46.56

Taxon	200 E		REF A		Contrib%	Cum.%
	Av.Abund	Av.Abund	Av.Diss	Diss/SD		
<i>Cystoseira corniculata</i>	6.76	5.01	11.28	1.21	24.22	24.22
CCA	2.86	1.83	6.48	0.78	13.93	38.15
Bare substratum	0.00	1.71	5.02	0.99	10.77	48.92
<i>Dictyota</i> sp.	1.59	1.98	4.84	0.84	10.39	59.31
<i>Jania rubens</i>	2.63	3.77	4.39	0.86	9.43	68.74
<i>Sargassum vulgare</i>	0.85	0.34	3.15	0.77	6.77	75.50
<i>Cystoseira amentacea</i>	0.00	0.93	2.81	0.53	6.04	81.55
<i>Padina pavonica</i> (calcified)	0.00	0.75	2.34	0.52	5.04	86.58
<i>Halopteris scoparia</i>	0.15	0.66	2.30	0.48	4.95	91.53

Groups 200 W & REF A; Average dissimilarity = 53.21

Taxon	200 W	REF A	Av.Diss	Diss/SD	Contrib%	Cum.%
	Av.Abund	Av.Abund				
<i>Cystoseira corniculata</i>	6.52	5.01	10.33	1.20	19.42	19.42
CCA	1.57	1.83	6.12	0.92	11.50	30.92
Bare substratum	0.64	1.71	5.85	1.14	10.99	41.91
<i>Jania rubens</i>	1.90	3.77	5.74	0.80	10.78	52.69
<i>Cladostephus spongiosus</i>	1.95	0.00	5.66	0.81	10.64	63.33
<i>Dictyota</i> sp.	1.56	1.98	4.96	0.78	9.32	72.65
<i>Cystoseira amentacea</i>	0.00	0.93	2.82	0.53	5.31	77.96
<i>Halopteris scoparia</i>	0.42	0.66	2.56	0.48	4.82	82.77
<i>Sargassum vulgare</i>	0.59	0.34	2.40	0.58	4.51	87.29
<i>Padina pavonica</i> (calcified)	0.00	0.75	2.35	0.52	4.42	91.71

Groups SEEP & REF B; Average dissimilarity = 72.33

Taxon	SEEP	REF B	Av.Diss	Diss/SD	Contrib%	Cum.%
	Av.Abund	Av.Abund				
<i>Cystoseira corniculata</i>	5.27	4.64	15.07	1.30	20.84	20.84
<i>Sargassum vulgare</i>	2.58	0.60	8.90	0.71	12.31	33.15
<i>Sargassum</i> sp.	1.50	1.86	7.36	0.81	10.18	43.33
CCA	0.11	2.44	6.80	1.15	9.41	52.73
<i>Jania rubens</i>	0.00	2.09	5.96	0.79	8.24	60.97
<i>Dictyota</i> sp.	1.16	1.61	5.76	0.76	7.97	68.94
Bare substratum	1.08	1.46	4.65	0.88	6.42	75.36
<i>Padina pavonica</i> (calcified)	0.00	1.18	3.66	0.87	5.06	80.42
<i>Padina pavonica</i> (not calcified)	1.12	0.00	3.26	0.44	4.51	84.92
<i>Halopteris scoparia</i>	0.00	0.97	2.98	0.43	4.12	89.04
<i>Falkenbergia</i> sp.	0.46	0.00	1.32	0.51	1.82	90.86

Groups 200 E & REF B; Average dissimilarity = 53.38

Taxon	200 E	REF B	Av.Diss	Diss/SD	Contrib%	Cum.%
	Av.Abund	Av.Abund				
<i>Cystoseira corniculata</i>	6.76	4.64	12.03	1.18	22.55	22.55
CCA	2.86	2.44	7.52	1.06	14.08	36.62
<i>Sargassum</i> sp.	0.00	1.86	5.37	0.69	10.06	46.69
<i>Jania rubens</i>	2.63	2.09	4.08	0.76	7.64	54.33
Bare substratum	0.00	1.46	4.00	0.70	7.49	61.81
<i>Sargassum vulgare</i>	0.85	0.60	3.96	0.68	7.42	69.23
<i>Dictyota</i> sp.	1.59	1.61	3.96	0.79	7.41	76.64
<i>Padina pavonica</i> (calcified)	0.00	1.18	3.50	0.87	6.56	83.20
<i>Halopteris scoparia</i>	0.15	0.97	3.12	0.49	5.84	89.04
<i>Padina pavonica</i> (not calcified)	0.27	0.00	0.83	0.30	1.55	90.59

Groups 200 W & REF B; Average dissimilarity = 57.06

Taxon	200 W	REF B		Diss/SD	Contrib%	Cum.%
	Av.Abund	Av.Abund	Av.Diss			
<i>Cystoseira corniculata</i>	6.52	4.64	11.48	1.23	20.13	20.13
CCA	1.57	2.44	6.89	1.09	12.07	32.20
<i>Cladostephus spongiosus</i>	1.95	0.00	5.55	0.82	9.73	41.93
<i>Sargassum</i> sp.	0.55	1.86	5.48	0.80	9.60	51.54
Bare substratum	0.64	1.46	4.21	0.78	7.38	58.92
<i>Dictyota</i> sp.	1.56	1.61	4.17	0.76	7.32	66.24
<i>Jania rubens</i>	1.90	2.09	4.04	0.75	7.09	73.32
<i>Halopteris scoparia</i>	0.42	0.97	3.83	0.54	6.71	80.03
<i>Padina pavonica</i> (calcified)	0.00	1.18	3.49	0.87	6.12	86.15
<i>Sargassum vulgare</i>	0.59	0.60	3.22	0.52	5.64	91.79

Groups REF A & REF B; Average dissimilarity = 54.82

Taxon	REF A	REF B		Diss/SD	Contrib%	Cum.%
	Av.Abund	Av.Abund	Av.Diss			
<i>Cystoseira corniculata</i>	5.01	4.64	10.88	1.19	19.84	19.84
<i>Jania rubens</i>	3.77	2.09	6.05	0.89	11.03	30.87
Bare substratum	1.71	1.46	6.03	1.13	10.99	41.86
<i>Sargassum</i> sp.	0.00	1.86	5.24	0.68	9.55	51.41
<i>Dictyota</i> sp.	1.98	1.61	4.95	0.75	9.03	60.44
CCA	1.83	2.44	4.91	1.23	8.95	69.39
<i>Halopteris scoparia</i>	0.66	0.97	4.17	0.61	7.60	76.99
<i>Padina pavonica</i> (calcified)	0.75	1.18	3.78	0.93	6.89	83.88
<i>Cystoseira amentacea</i>	0.93	0.00	2.65	0.53	4.84	88.71
<i>Sargassum vulgare</i>	0.34	0.60	2.58	0.40	4.70	93.42

Taxa driving community differences among sites (Table 3.4) were grouped into two categories; canopy-forming algae (*Cystoseira corniculata*, *Cystoseira amentacea* (C.Agardh) Bory de Saint-Vincent, *Sargassum vulgare* and *Cladostephus spongiosum* (Hudson) C.Agardh) and calcifying algae (CCA, *Jania rubens*, *Corallina* sp., *Amphiroa* sp. and *Padina pavonica*). The two categories are shown for May (Figure 3.5A) and September (Figure 3.5B). As no significant differences were found within intermediate and reference sites, $p\text{CO}_2$ levels were pooled for clarity. Both categories showed very strong seasonal patterns: no differences in canopy-forming algal cover were detected

in May, but in September the high $p\text{CO}_2$ site had higher canopy cover than the reference sites. Likewise, calcifying algae showed no significant difference among $p\text{CO}_2$ levels in spring, but in autumn the high $p\text{CO}_2$ site had a significantly lower cover of calcareous algae compared to intermediate and control $p\text{CO}_2$ levels.

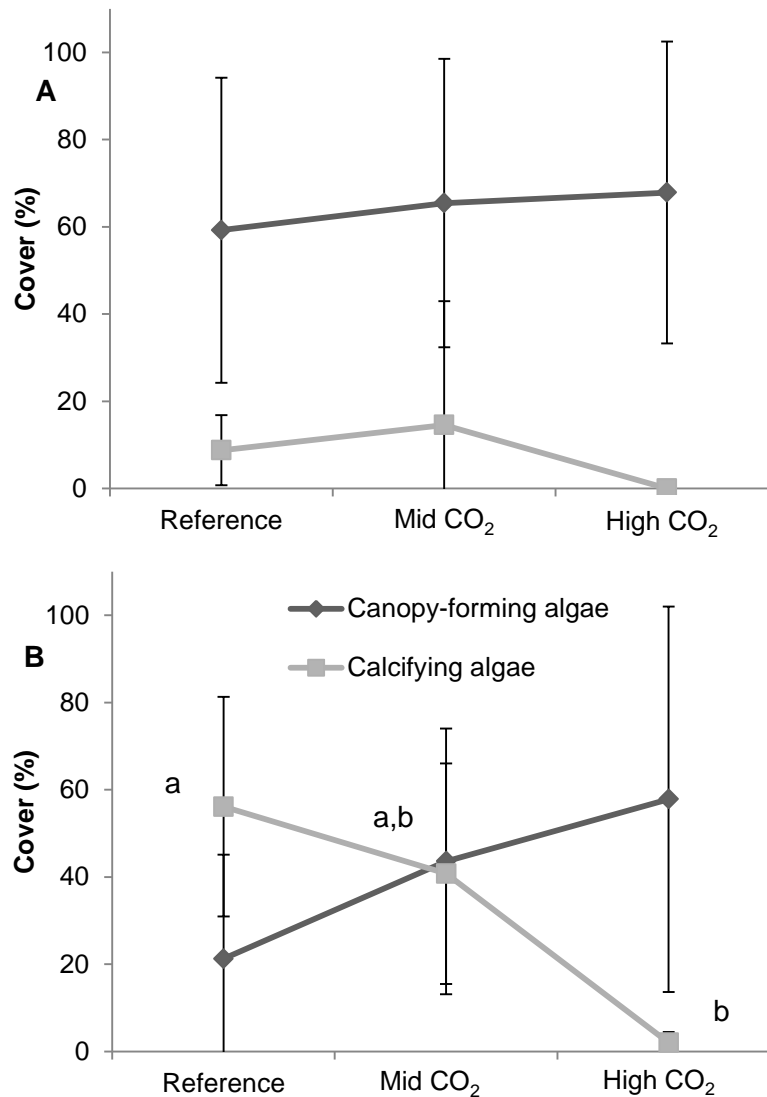


Figure 3.5. Mean percentage cover (\pm SD) of canopy-forming algae (black) and calcifying algae (grey) in May (a) and September (b) at high (n=6), intermediate (n=14) and reference (n=14) CO₂ conditions off Methana. Different letters indicate significant differences between groups.

The species forming these two categories changed along the $p\text{CO}_2$ gradient depending on the season, and the main canopy-forming and calcareous species covers are shown for May and September in Figure 3.7A and 3.7B, respectively. As no significant differences were found within intermediate and reference sites, $p\text{CO}_2$ levels were pooled for clarity. In spring, *S. vulgare* was more abundant at the high $p\text{CO}_2$ site, but it was almost absent from all sites in autumn. In contrast, *C. corniculata* cover significantly increased in the high $p\text{CO}_2$ site from spring to autumn, while the opposite was true for the intermediate and reference sites, where *C. corniculata* cover decreased from spring to autumn. As for the coralline algae, CCAs recruited earlier than *J. rubens* and reached their maximum cover in spring at the intermediate sites, while in the reference sites their cover increased from spring to autumn. The articulate coralline alga *J. rubens* had extremely low abundances at all sites in spring, while in autumn its percent cover decreased with increasing $p\text{CO}_2$ levels (Figure 3.6).

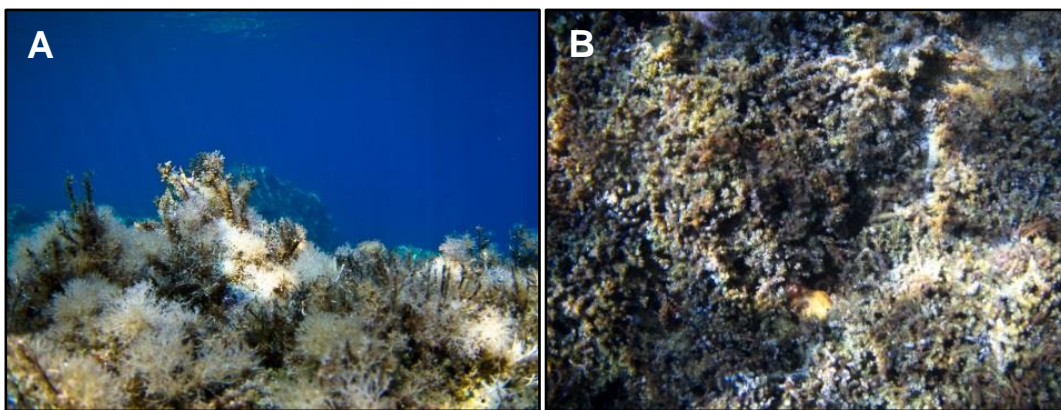


Figure 3.6. Typical appearance of macroalgal communities off Methana in autumn at (A) reference sites, with high cover of the articulated coralline alga *J. rubens*, and (B) near the CO_2 seeps, where *C. corniculata* is dominant (photos by Maria Salomidi).

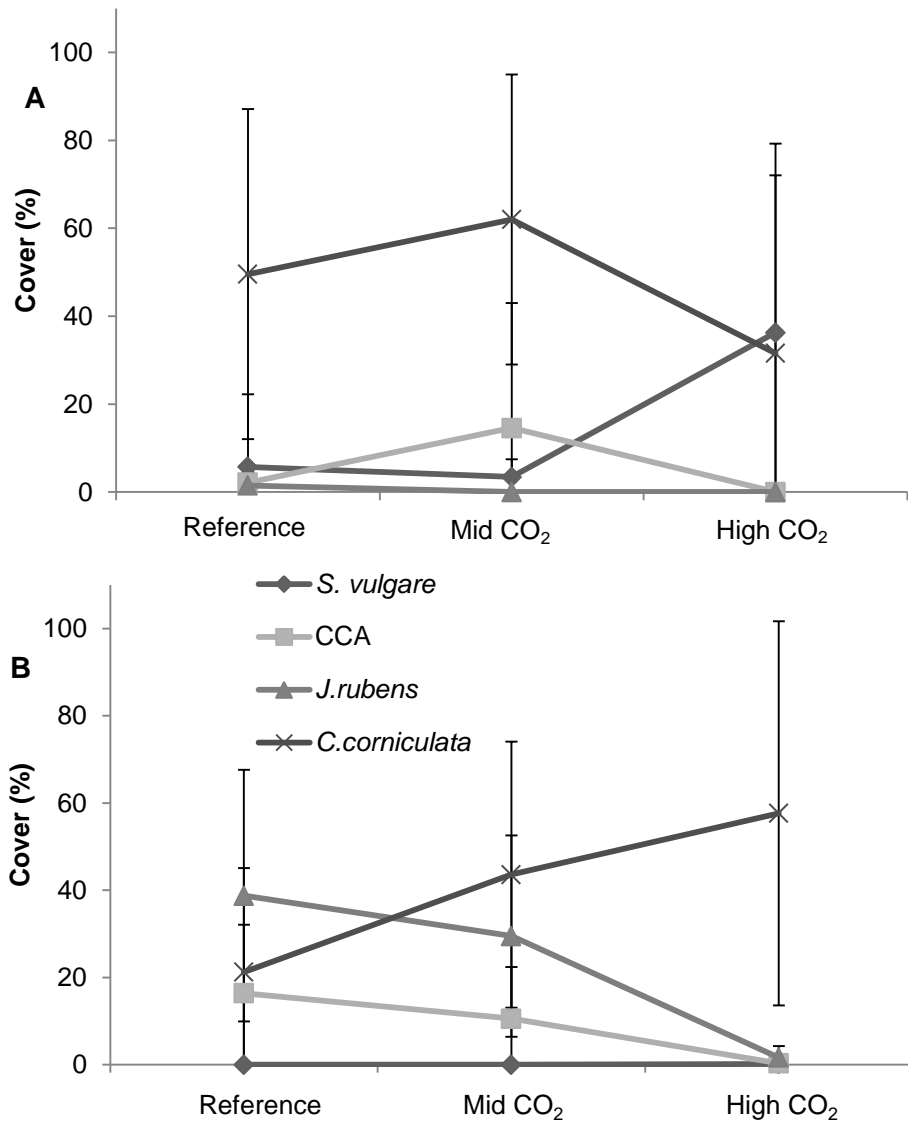


Figure 3.7. Mean percentage cover (\pm SD) of dominant macroalgal species in May (A) and September (B) at high ($n=6$), intermediate ($n=14$) and reference ($n=14$) levels of CO₂ in Methana. Different letters and numbers indicate significant differences between groups.

3.3.2 Vulcano macroalgal communities

At Vulcano, 32 macroalgal taxa were recorded, five of which were calcifying algae. Results from PERMANOVA analysis on square-root transformed data (Table 3.5a) show that macroalgal communities were significantly different among sites (pseudo- $F_{2,9}=2.702$, $p(\text{perm})=0.0005$). Pair-wise comparisons (Table 3.5b) show that there was a significant difference between the

communities at the High CO₂ and reference sites ($t_{2,6}=1.793$, $p(\text{MC})=0.045$), whereas the Mid CO₂ site was intermediate between the other two.

Table 3.5. (A) PERMANOVA analysis on square-root transformed biomass of Vulcano benthic communities. The Table shows degrees of freedom (df), sum of squares (SS), pseudo-F, permutational p and unique permutations for the factor “pCO₂ level”. (B) Since “Site” had a significant effect ($p<0.05$), pair-wise comparisons between CO₂ levels were carried out and are shown in the lower part of the table. Since the number of possible permutations was low (<100), Monte Carlo p ($p(\text{MC})$) was used as the most reliable p value, and shows that the t-values of High CO₂ and reference site were significantly different.

(A)	Source	df	SS	MS	Pseudo-F	p (perm)	Unique perms
	Site	2	6950.7	3475.4	2.7017	0.005	4732
	Residual	9	11577	1286.4			
	Total	11	18528				

(B)	Groups	t	p (perm)	Unique perms	p (MC)
	High CO ₂ , Mid CO ₂	1.5833	0.0277	35	0.0692
	High CO ₂ , REF A	1.7925	0.0291	35	0.0450
	Mid CO ₂ , REF A	1.5589	0.0259	35	0.0912

Shannon diversity (H') and Pielou's evenness (J') were not significantly different among sites (Table 3.6), and Figure 3.8 shows that no specific trend was detectable.

Table 3.6. ANOVA results for (A) Shannon diversity (H') and (B) Pielou's evenness (J') of Vulcano macroalgal communities. The Tables show main factors and their interactions and sum of squares (SS), degrees of freedom (df), Mean Squares (MS), F-ratios (F) and p values.

(A)	Source	Type III SS	df	MS	F	p
	Site	0.657	2	0.328	0.911	0.436
	Error	3.245	9	0.361		
	Total	3.902	11			
(B)	Source	Type III SS	df	MS	F	p
	Site	0.087	2	0.043	0.963	0.418
	Error	0.405	9	0.045		
	Total	0.491	11			

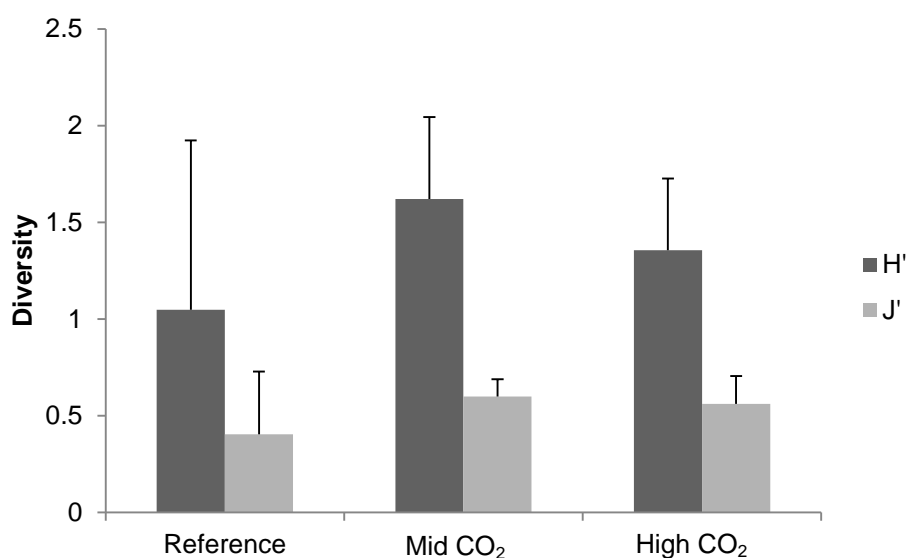


Figure 3.8. Mean (\pm SD, $n = 4$) Shannon diversity (H') and Pielou's evenness (J') at high, intermediate and reference pCO_2 at Vulcano.

SIMPER analysis shows which taxa contribute most to the detected differences among sites (Table 3.7). Dissimilarity levels are highest between the high CO_2 and reference sites (60.20), followed by the dissimilarity between reference and intermediate sites (59.77); intermediate and high pCO_2 sites were the most similar groups (average dissimilarity = 58.03). These results are consistent with

the pair-wise comparison of macroalgal communities (see Table 3.5b). The main drivers of differences between groups were canopy-forming algae such as *Cystoseira* sp., *Sargassum vulgare* and *Dictyopteris polypodioides*, calcifying algae such as crustose coralline algae (CCA) and the calcified brown alga *Padina pavonica*, green algae such as *Flabellia petiolata* (Turra) Nizamuddin, *Caulerpa prolifera* (Forsskål) J.V.Lamouroux and *Caulerpa racemosa* (Forsskål) J.Agardh and turf algae.

Table 3.7. SIMPER analysis of Vulcano benthic communities showing average dissimilarities between each pair of pCO₂ levels and which species contributed to the dissimilarity by up to 90%. For each taxon, the average abundance at the two groups that are being compared, their average dissimilarity, the dissimilarity to standard deviation ratio and the taxon contribution and cumulative contribution are shown.

Groups High CO₂ & Mid CO₂; Average dissimilarity = 58.03						
	High CO ₂	Mid CO ₂				
Taxa	Av.Ab	Av.Ab	Av.Diss	Diss/SD	Contr%	Cum%
<i>Cystoseira</i> sp.	4.39	1.91	12.11	1.57	20.87	20.87
<i>Flabellia petiolata</i>	2.45	0.61	7.62	1.74	13.13	34.00
<i>Sargassum</i> sp.	1.29	0.00	5.03	0.95	8.66	42.66
<i>Caulerpa prolifera</i>	1.40	0.40	4.86	1.37	8.37	51.04
CCA	0.38	1.05	4.01	1.17	6.91	57.94
<i>Peyssonnelia</i> sp.	0.06	0.74	3.08	0.70	5.31	63.25
Turf algae	2.05	1.61	2.96	1.70	5.10	68.36
<i>Cystoseira</i> with <i>Peyssonnelia</i> epiphyte	0.00	0.53	2.27	0.54	3.92	72.28
<i>Dictyopteris</i> <i>polypodioides</i>	0.00	0.55	2.21	1.51	3.81	76.09
<i>Dictyota</i> sp.	0.80	0.87	2.01	1.32	3.47	79.56
<i>Caulerpa racemosa</i>	0.07	0.49	1.86	1.14	3.20	82.76
<i>Taonia atomaria</i>	0.34	0.15	1.75	0.86	3.02	85.78
<i>Padina pavonica</i>	0.00	0.29	1.25	2.72	2.16	87.94
<i>Halopteris scoparia</i>	0.00	0.31	1.25	0.54	2.15	90.08
Groups High CO₂ & REF A; Average dissimilarity = 60.20						
	High CO ₂	REF A				
Taxa	Av.Ab	Av.Ab	Av.Diss	Diss/SD	Contr%	Cum%
<i>Cystoseira</i> sp.	4.39	4.77	12.64	1.08	21.00	21.00
<i>Flabellia petiolata</i>	2.45	0.37	7.77	2.03	12.9	33.91

<i>Caulerpa prolifera</i>	1.40	0.00	5.97	2.24	9.92	43.83
Turf algae	2.05	0.80	5.04	1.54	8.37	52.20
<i>Sargassum</i> sp.	1.29	0.41	4.91	1.09	8.16	60.35
<i>Dictyopteris polypodioides</i>	0.00	1.17	4.50	0.92	7.47	67.82
<i>Halopteris scoparia</i>	0.00	0.73	2.80	0.90	4.66	72.48
CCA	0.38	0.75	2.77	1.12	4.60	77.08
Articulated coralline	0.00	0.56	2.32	2.04	3.85	80.93
<i>Taonia atomaria</i>	0.34	0.25	1.82	0.97	3.02	83.95
<i>Dictyota</i> sp.	0.80	0.78	1.80	1.22	2.99	86.94
<i>Dictyota fasciola</i>	0.00	0.36	1.33	0.75	2.21	89.15
<i>Cystoseira</i> with <i>Peyssonnelia</i> epiphyte	0.00	0.28	1.03	0.54	1.72	90.86

Groups Mid CO₂ & REF A; Average dissimilarity = 59.77

Taxa	Mid CO ₂	REF A	Av.Diss	Diss/SD	Contr%	Cum%
	Av.Ab	Av.Ab				
<i>Cystoseira</i> sp.	1.91	4.77	13.93	1.19	23.31	23.31
<i>Dictyopteris polypodioides</i>	0.55	1.17	5.19	1.44	8.68	31.99
Turf algae	1.61	0.80	4.07	1.26	6.82	38.80
CCA	1.05	0.75	3.77	1.28	6.31	45.11
<i>Halopteris scoparia</i>	0.31	0.73	3.27	1.00	5.47	50.58
<i>Peyssonnelia</i> sp.	0.74	0.00	3.24	0.70	5.43	56.01
<i>Cystoseira</i> with <i>Peyssonnelia</i> epiphyte	0.53	0.28	3.00	0.74	5.02	61.03
<i>Dictyota</i> sp.	0.87	0.78	2.72	1.23	4.55	65.58
<i>Flabellia petiolata</i>	0.61	0.37	2.67	1.25	4.47	70.05
Articulated coralline	0.00	0.56	2.62	2.28	4.38	74.42
<i>Caulerpa racemosa</i>	0.49	0.00	2.03	1.04	3.40	77.83
<i>Sargassum</i> sp.	0.00	0.41	1.73	0.59	2.89	80.72
<i>Caulerpa prolifera</i>	0.4	0.00	1.70	0.86	2.84	83.56
<i>Dictyota fasciola</i>	0.00	0.36	1.49	0.76	2.49	86.05
<i>Padina pavonica</i>	0.29	0.02	1.25	3.17	2.09	88.14
<i>Taonia atomaria</i>	0.15	0.25	1.15	1.27	1.93	90.07

Taxa driving differences among sites were grouped in four categories, canopy-forming algae, calcifying algae, non-calcifying green algae and turf algae. The canopy-forming algae category consisted of the sum of the biomass of *Cystoseira* sp., *Dictyopteris polypodioides* and *Sargassum vulgare*; the calcifying algae group included CCA, articulate coralline algae, *Padina*

pavonica, *Peyssonnelia* sp. and *Acetabularia acetabulum* P.C.Silva. Non-calcifying green algae consisted of *Flabellia petiolata*, *Caulerpa prolifera* and *Caulerpa racemosa*, while turf algae were already grouped in one category. Biomass of these categories is shown below (Figure 3.9), and the pattern is consistent with that of Methana in spring. Canopy-forming algae did not show a clear pattern and calcifying algae had the highest biomass at the intermediate site, although this difference was not significant (see Figure 3.5a). Non-calcifying green algae had a significant increase as pCO₂ increased, and turf algae biomass was significantly higher in the high pCO₂ site than in the control, with the Mid CO₂ site having intermediate values between the other two sites.

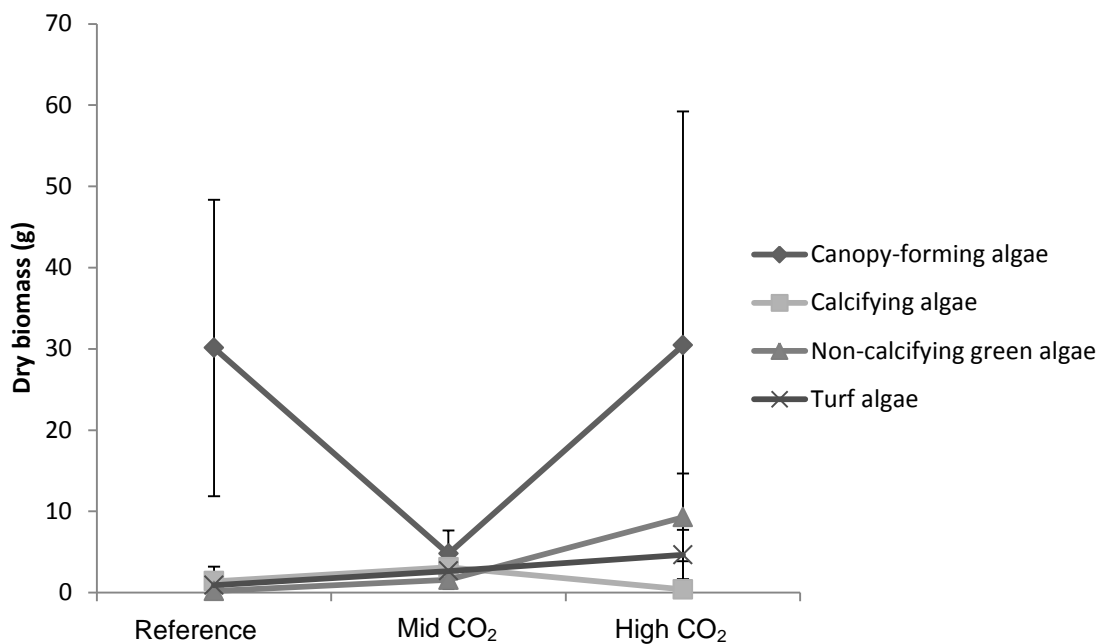


Figure 3.9. Mean (\pm SD, n=4) biomass of canopy-forming algae, calcifying algae, non-calcifying green algae and turf algae at sites with high, mid and reference pCO₂ at Vulcano.

The most representative canopy-forming and non-calcifying green algae biomass is shown below (Figure 3.10). The two canopy-forming algae *S. vulgare* and *D. polypodioides* showed opposite trends, with the first substituting the latter as pCO₂ increased. On the other hand, the two most abundant non-

calcifying green algae (*F. petiolata* and *C. prolifera*) had a significant increase in biomass at the high CO₂ site compared to the reference site.

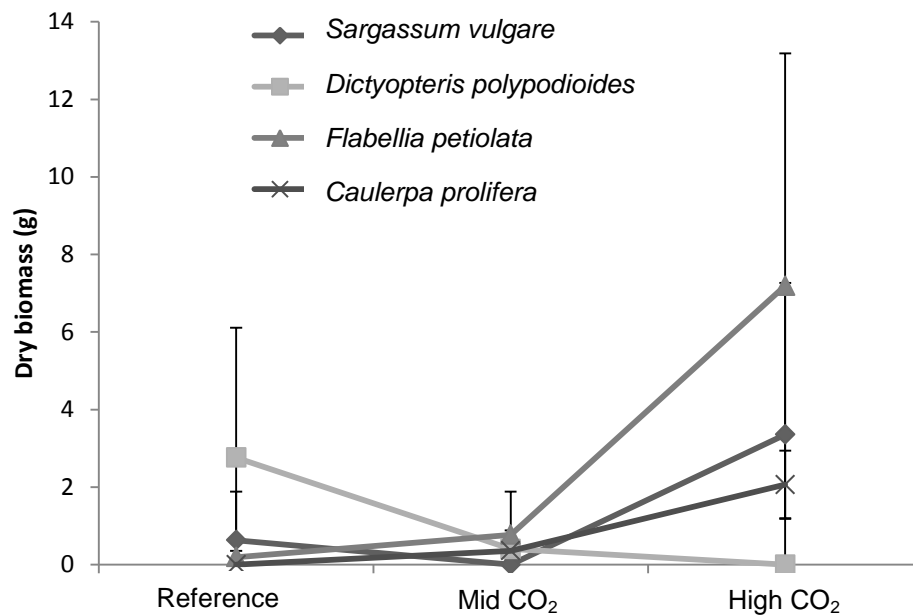


Figure 3.10. Mean (\pm SD, n=4) biomass of *Sargassum vulgare*, *Dictyopteris polypodioides*, *Flabellia petiolata* and *Caulerpa prolifera* at sites with high, mid and reference pCO₂ at Vulcano.

3.4 Discussion

These results show that increased seawater pCO₂ can have profound effects on macroalgal communities in oligotrophic conditions and that sampling season strongly affects the response of benthic communities to ocean acidification. At Methana, coralline algal cover decreased while canopy-forming algae became more abundant as pCO₂ increased, but the difference was only statistically significant in autumn. Macroalgal communities off Methana had year-round decreased diversity, especially of calcifying species, as carbon dioxide increased, in line with results from surveys at other CO₂ seeps (Porzio *et al.*, 2011; Fabricius *et al.*, 2011,2014) and from laboratory experiments (Hale *et al.*, 2011; Kroeker *et al.*, 2013a).

The seasonal effects of ocean acidification on macroalgal communities have not been detected until now since most field studies have been carried out in one season, while laboratory and mesocosm experiments rarely last long enough to incorporate seasonality effects. Godbold and Solan (2013) found that seasonality greatly affected invertebrate responses to both ocean acidification and increased temperature. A recent study showed that in tropical seagrass epiphyte communities fleshy algae substituted coralline algae as CO₂ increased, and that this pattern was more pronounced in winter (Campbell and Fourqurean, 2014). One of the very few long-term studies of algal physiological responses to ocean acidification showed that coralline algae respond differently to increased pCO₂ depending on season: net calcification was negatively affected by the interaction of increased pCO₂ and temperature in summer, but not in the other seasons (Martin *et al.*, 2013).

At Vulcano, where samples were only collected in spring, results are consistent with Methana; calcifying algal biomass decreased with increasing pCO₂ whereas biomass of canopy-forming algae did not show any specific trend, although the dominant canopy-forming species shifted with increasing CO₂. Here, more taxa were detected because of the different method used, revealing that less conspicuous species such as non-calcifying green algae (e.g. *Flabellia petiolata*) and turf algae increased with increasing seawater pCO₂.

Non-calcifying green algal biomass increased at elevated pCO₂; this trend was particularly evident for *Flabellia petiolata* and *Caulerpa prolifera*. Increased *F. petiolata* abundance at intermediate pCO₂ levels was also reported from Ischia, where this species becomes dominant when pH drops to about 7.8 (Porzio *et al.*, 2011); this is consistent with findings from Vulcano, where average pH at the high CO₂ site is about 7.6 (Boatta *et al.*, 2013). The reason why *F. petiolata*

benefits from increased CO₂ is not currently known, but previous studies have shown that this species is unlikely to use carbon concentrating mechanisms (CCMs; Raven *et al.*, 2002; Mercado *et al.*, 2009). It is therefore possible that increased CO₂ levels give this species a competitive advantage as they would have more substratum available for photosynthesis (Cornwall *et al.*, 2012; Koch *et al.*, 2013).

The increase in fleshy algae with increasing pCO₂ recorded in Vulcano is consistent with previous results from volcanic seeps (Porzio *et al.*, 2011; Graziano *et al.*, unpublished data). Shifts towards fleshy macroalgae in response to ocean acidification have also been reported in laboratory and mesocosm studies, where small fleshy algae increase their biomass and percent cover by outcompeting coralline crusts as CO₂ goes up (Connell and Russell, 2010). Since these algae can have a negative effect on kelp recruitment, ocean acidification has the potential to cause dramatic phase shifts in temperate habitats (Connell and Russell 2010), although nutrient and light levels will determine their significance (Russell *et al.*, 2009; Russell *et al.*, 2011). In contrast, at Methana turf-forming algae cover did not increase as CO₂ increased. Another shallow subtidal survey off Italian CO₂ seeps (Porzio *et al.*, 2011) detected a decrease in turf-forming algal biomass at pCO₂ levels of about 1000 ppm. This shows that shifts to turf-forming algae do not necessarily happen at intermediate pCO₂ levels, especially if not associated with increased nutrient levels (Connell and Russell, 2010) or other disturbances disrupting fucoid algal cover (Falkenberg *et al.*, 2012).

Decreased abundance of calcifying algae at high CO₂ sites off Vulcano and Methana is consistent with previous results from volcanic seeps off Ischia, in Italy (Porzio *et al.*, 2011). Here, the articulated coralline *Jania rubens* was one

of the dominant species at reference CO₂ levels, but it was absent at elevated CO₂. At Methana, this species was not completely absent from the high CO₂ site, possibly because here the average pH was higher than in Ischia (see Chapter 2). Cover of crustose coralline algae (CCA) decreased with increasing pCO₂ as well both in Italy and in Greece, confirming that calcifying algae are likely to be threatened by ocean acidification (Gao *et al.*, 1993; Anthony *et al.*, 2008; Kuffner *et al.*, 2008; Martin *et al.*, 2008; Ries *et al.*, 2009; Martin and Gattuso, 2009; Gao and Zheng, 2010), especially those species living near their thermal limit (Koch *et al.*, 2013). CCA producing Mg-calcite appear to be extremely sensitive to ocean acidification, whereas those species containing dolomite-rich calcium carbonate seem more resistant to dissolution in high CO₂ conditions (Nash *et al.*, 2012). Intermediate pCO₂ levels seem to increase CCA abundance in spring both off Vulcano and Methana, possibly because carbon fertilisation could enhance calcification. This pattern has been observed in some laboratory studies (Ries *et al.*, 2009; Hofmann *et al.*, 2012) when pCO₂ is below 1000 µatm. However, calcifying algae appear unable to cope with the high energetic demands of calcification when pCO₂ reaches levels above 1000 µatm (Bradassi *et al.*, 2013). Recent studies found that CCA are more sensitive to rates, not magnitude, of ocean acidification (Kamenos *et al.*, 2013) and that fluctuating pH reduces growth in an articulated coralline alga (Cornwall *et al.*, 2013): high variability in pCO₂ at the seeps could therefore lead to an over-estimation of its negative effects on coralline algae.

The increase in canopy-forming algal cover at high CO₂ was mostly caused by an increased abundance of *Sargassum vulgare* in spring along both pCO₂ gradients and of *Cystoseira corniculata* in autumn at Methana. *Sargassum vulgare* was more abundant at high CO₂ also at volcanic seeps off Ischia

(Porzio *et al.*, 2011). However, this species was absent at Methana in autumn because of its pronounced seasonal cycle (Belegratis *et al.*, 1999). As for *C. corniculata*, it is likely that the higher autumnal cover at the elevated pCO₂ site was due to the absence of *S. vulgare* and *J. rubens*. In fact, the genus *Sargassum* can be advantaged over *Cystoseira* when competing for space (Engelen *et al.*, 2008), while *J. rubens* is an epiphyte that can overgrow canopy-forming algae and become dominant in autumn (Belegratis *et al.*, 1999). Physiological responses of *J. rubens* to high pCO₂ are likely to be the main determinant of its decrease in cover, but enhanced defensive compound production by *C. corniculata* cannot be excluded. It has in fact been shown that some furoid algae are carbon limited, and elevated CO₂ can cause a sharp increase in their defensive compound contents (Swanson and Fox, 2007).

At Vulcano, *Dictyopteris polypodioides* biomass sharply decreased as pCO₂ increased. This is surprising, as *Dictyota* sp. did not seem to be affected by ocean acidification at Vulcano and actually increase its biomass with increasing CO₂ at Ischia (Porzio *et al.*, 2011). This pattern could be either explained by differences in these species' physiologies or by their different palatability to herbivores, as abundances of their main consumer, the sea urchin *Paracentrotus lividus*, decrease with increasing pCO₂ at Vulcano (Johnson *et al.*, 2012; Calosi *et al.*, 2013a). Since no studies on this species' physiological responses to ocean acidification have been conducted so far, there is no information available on the underlying physiological mechanisms. This is a further proof that biological response to ocean acidification can greatly vary even within families (Miller *et al.*, 2009; Kroeker *et al.*, 2011), and that some non-calcifying species can be as sensitive to increased pCO₂ as calcifiers.

Overall, this study shows that phase shifts in benthic communities as seawater pCO₂ increases are likely to be consistent between Western and Eastern Mediterranean Sea and between intertidal and shallow subtidal (2-3 metres depth) habitats. Loss of diversity and reduced abundance of ecologically important calcifying algae at elevated carbon dioxide levels found in this study add to a growing body of evidence showing that ocean acidification is likely to alter community composition (Hall-Spencer *et al.*, 2008; Fabricius *et al.*, 2011; Kroeker *et al.*, 2011; Porzio *et al.*, 2011; Hofmann *et al.*, 2012; Brodie *et al.*, 2014). Changes in benthic community structure have potential profound effects on biological processes such as food web dynamics, nutrient cycling and primary productivity (Tilman, 1999), thus affecting ecosystem functioning.

Chapter 4

Canopy algal epifauna changes at elevated pCO₂ at two Mediterranean volcanic seeps

Abstract

Only a few studies have dealt with epifaunal community responses to ocean acidification, and they have not reported consistent results. As for canopy-forming algal epifauna, there is virtually no information on their responses to elevated pCO₂. This chapter investigates how epifauna of the main canopy-forming macroalgae at volcanic seeps in Italy and Greece changed with increasing pCO₂. Rocky shores at both sites were dominated by fucoid algae; at Vulcano (Italy) there was a change from *Dictyopteris polypodioides* to *Sargassum vulgare* with increasing pCO₂, while the genus *Cystoseira* remained abundant at all sites, but there was a shift in species. In contrast, *Cystoseira corniculata* was the main canopy-forming alga at volcanic seeps off Methana (Greece) and at nearby reference sites. Canopy-forming algal samples were collected at Methana (*C. corniculata*) and Vulcano (*Cystoseira* spp. and *S. vulgare*) to examine their epifaunal communities. The hypotheses tested were: (i) abundance and diversity of calcifiers will decrease as CO₂ increases; (ii) the magnitude of change in epifaunal communities will differ depending on the macroalgal species they inhabit. At both sites fauna was collected in spring, from 20 x 20 cm quadrats off Methana and by collecting individual thalli of fucoid algae off Vulcano. Although macroalgal morphology and mobile epifauna changed significantly with increasing pCO₂, sessile epiphyte communities did not show consistent changes among pCO₂ levels. The lack of a clear CO₂ effect on epiphytes could be due to the ability of canopy-forming algae to locally raise pH due to photosynthesis; epifauna may still be affected by changes in pCO₂ because it is more mobile than epiphytes and therefore often leaves the macroalgal boundary layer. The abundance of calcifying organisms was strongly affected by increasing pCO₂, whereas non-calcified taxa such as many

polychaetes were more abundant at high CO₂, probably because of reduced competition for space and resources. However, at Vulcano the structure of epifaunal communities inhabiting *S. vulgare* did not change significantly with pCO₂, unlike epifaunal communities living on *Cystoseira* spp. at Vulcano and *C. corniculata* at Methana. Thus, canopy-forming macroalgae and their associated communities are expected to change as seawater carbon dioxide levels increase, but the magnitude of change is expected to differ depending on the macroalgal host.

4.1 Introduction

Although research on biological responses to ocean acidification is in its infancy, there is evidence that an increase in seawater pCO₂ often has strong negative effects on calcifying organisms (Kroeker *et al.*, 2013a). Evidence from volcanic CO₂ seeps used as ocean acidification analogues supports this conclusion (e.g. Hall-Spencer *et al.*, 2008; Cigliano *et al.*, 2010; Fabricius *et al.*, 2011; Kroeker *et al.*, 2011; Inoue *et al.*, 2013), although abundant food supplies can help animals to cope with increased pCO₂: for example, mussels and barnacles can remain dominant in eutrophic conditions despite being exposed to high CO₂ levels in Kiel fjord (Thomsen *et al.*, 2010). Community responses do not always reflect single species responses that would be predicted from laboratory-based physiological tests because of biological interactions. For instance, in a mesocosm study of communities from artificial substrata mimicking mat-forming algae Hale *et al.* (2011) reported an unexpected increase in nematode abundance at high CO₂ because of reduced competition for space with taxa sensitive to hypercapnia, such as molluscs. In a field study of turf-associated fauna along pCO₂ gradients in the Mediterranean Sea, Kroeker *et al.* (2011) found that small crustaceans such as amphipods and

tanaisids, not nematodes, increased in abundance at low pH. Crustaceans in the mesocosm study (Hale *et al.*, 2011) decreased with increasing pCO₂. There are therefore great uncertainties in predicting the responses of benthic communities to ocean acidification, although both studies report a strong decrease in calcifying organisms' abundance and diversity at increased pCO₂ (Hale *et al.* 2011; Kroeker *et al.*, 2011).

Marine macroalgae are dominant on temperate rocky reefs worldwide (Steneck *et al.*, 2002) and are considered ecosystem engineers because they add structural complexity to the substratum. Invertebrate communities associated with macroalgae have higher species richness and diversity than unvegetated substrata (Dean and Connell, 1987). Epifaunal abundance and diversity can be influenced by hydrodynamics and sedimentation rate (Sánchez-Moyano *et al.*, 2000), and is usually correlated with the complexity of their macroalgal habitat. For instance, densely branched Mediterranean macroalgae host more diverse invertebrate communities because of reduced predation risk and hydrodynamism (Chemello and Milazzo, 2002). Differences in epifaunal communities can also be determined by other seaweed characteristics, such as the presence of defensive compounds (Hay *et al.*, 1987; Jormalainen *et al.*, 2001). Macroalgae and seagrasses raise pH near their fronds through photosynthesis; this process controls calcification rates of their coralline algal epiphytes (Semesi *et al.*, 2009) and has been proven to reduce the negative effects of ocean acidification on some macroalgae, especially if water movement is slow (Cornwall *et al.*, 2014). Invertebrates living on macroalgae might be exposed to smaller changes in ambient pCO₂ compared to animals living in the water column or on bare substrata, and community changes may therefore be less dramatic.

At volcanic seeps off Vulcano (Italy), dominant macroalgae change along a pCO₂ gradient: *Cystoseira* spp. and *Dictyopteris polypodioides* are abundant at reference sites, whereas *Sargassum vulgare* becomes extremely abundant at high pCO₂ (see Chapter 3). On the other hand, no such change was recorded at volcanic seeps off Methana (Greece), where *Cystoseira corniculata* remains the dominant canopy-forming species, even though *Sargassum vulgare* cover increases with pCO₂ (see Chapter 3). Macroalgal communities associated with *Sargassum muticum* have been proven to cope better with ocean acidification than those associated with *Cystoseira tamariscifolia* (Olabarria *et al.*, 2013), but responses of canopy-forming algae epifauna to ocean acidification have not been studied yet.

Based on previous evidence, I expect that canopy-forming algae will not be negatively affected as the oceans acidify (Kroeker *et al.*, 2013a). However, diversity of biological communities can still decrease as pCO₂ increases even if their habitat resists ocean acidification (Martin *et al.*, 2008; Fabricius *et al.*, 2014). Epifaunal communities are the main constituent of diets for seagrass-associated fish, and are therefore an important link to higher trophic level organisms, such as juvenile fish (Yamada *et al.*, 2010). The aim of this study was to assess changes in epifauna of the main canopy-forming algal species along two pCO₂ gradients at volcanic seeps off Vulcano (Italy) and Methana (Greece) given their importance for coastal ecosystem functioning and fisheries. The hypotheses tested are; (i) invertebrate diversity and abundance will decrease with increasing CO₂, and (ii) the manner of these changes in diversity and abundance will depend on the host macroalgal species.

4.2 Methods

4.2.1 Methana

In May 2012, samples were collected by scraping 20 x 20 cm quadrats of *C. corniculata* (Figure 4.2A) growing on horizontal or sub-horizontal rock using a hammer and chisel while covering the area with a 200 µm mesh size nylon net to avoid loss of vagile fauna. Three samples were collected from each of the five sites described in Chapter 2 (SEEP, 200 W, 200 E, REF A and REF B); detailed sampling dates and sample sizes are reported in Table 1.1C. Samples were fixed in 4% buffered formaldehyde for approximately 48 h, transferred to 70% IMS (Industrial Methylated Spirit) and stored until analysis. Samples were then sorted, separating *C. corniculata* from its epiphytic algae, which were assigned to functional groups, and from its epifauna. *Cystoseira corniculata* and its epiphytes were then dried at 50°C for 72 h and weighed (± 1 mg accuracy) to obtain dry mass. Over 29000 individual invertebrates were sorted under a stereoscope and identified to the lowest possible taxonomic level, hereafter termed the operational taxonomic unit (OTU). Amphipods were identified using keys from Bellan-Santini *et al.* (1982, 1989, 1993, 1998), molluscs were identified using the key from Doneddu and Trainito (2005) and taxonomic expertise by Prof. Renato Chemello (University of Palermo, Italy), and all other taxa were identified using the guide from Riedl (1991). The invertebrates collected included foraminiferans, sipunculids, molluscs (bivalves and gastropods), polychaetes (including serpulid worms), crustaceans (amphipods, decapods, isopods, tanaids and copepods) and echinoderms.

4.2.2 Vulcano

In June 2013, samples were collected by placing nets (200 µm mesh size) over 15 individual thalli per site of *Cystoseira* spp. (Figure 4.2B) and on 10 thalli per site of *Sargassum vulgare* (Figure 4.2C) and delicately detaching the thallus from the rock with a chisel. Two sites shown in Figure 4.1 were used, one with high pCO₂ (1200 ppm) and one with lower pCO₂ (600 ppm); detailed sampling dates and sample sizes are reported in Table 1.1C. Samples were sieved and transferred to 70% Industrial Methylated Spirit (IMS) for storage. Over 14000 individual invertebrates were sorted under a stereoscope and identified to the lowest possible taxonomic level, hereafter termed the operational taxonomic unit (OTU). Amphipods were identified using keys from Bellan-Santini *et al.* (1982, 1989, 1993, 1998), molluscs were identified using the key from Doneddu and Trainito (2005) and taxonomic expertise by Prof. Renato Chemello (University of Palermo, Italy), and all other taxa were identified using the guide from Riedl (1991). The invertebrates collected included molluscs (bivalves and gastropods), polychaetes, crustaceans (amphipods, decapods, isopods and tanaids) and echinoderms.

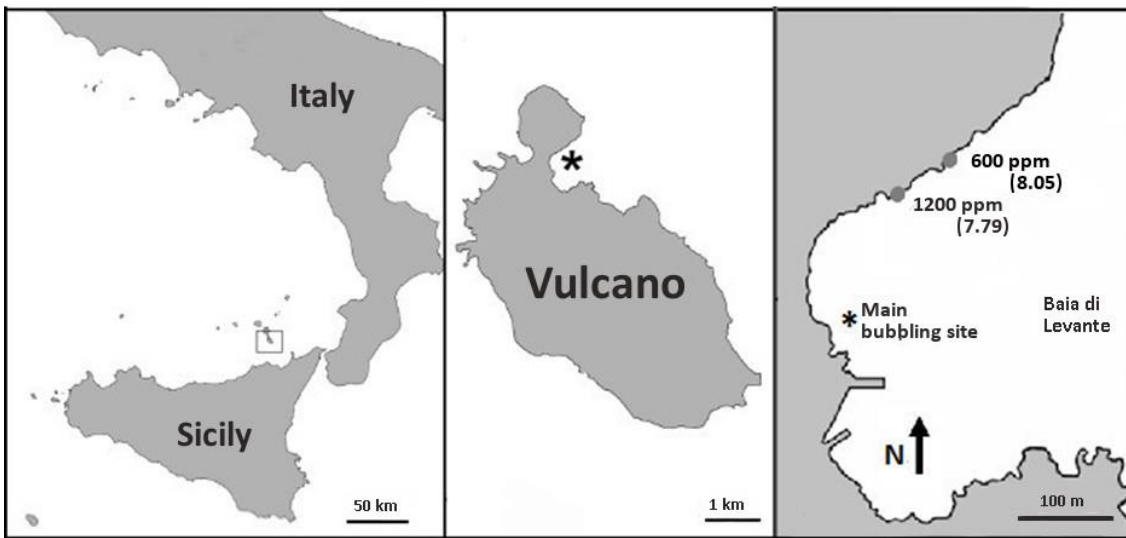


Figure 4.1. Location of Vulcano Island (Sicily, Southern Italy) and of the study area. Asterisk marks the main venting site, grey circles show two experimental sites, with decreasing $p\text{CO}_2$ moving away from the bubbling site. Average pH from environmental monitoring performed in 2012 (data reported in Chapter 5).

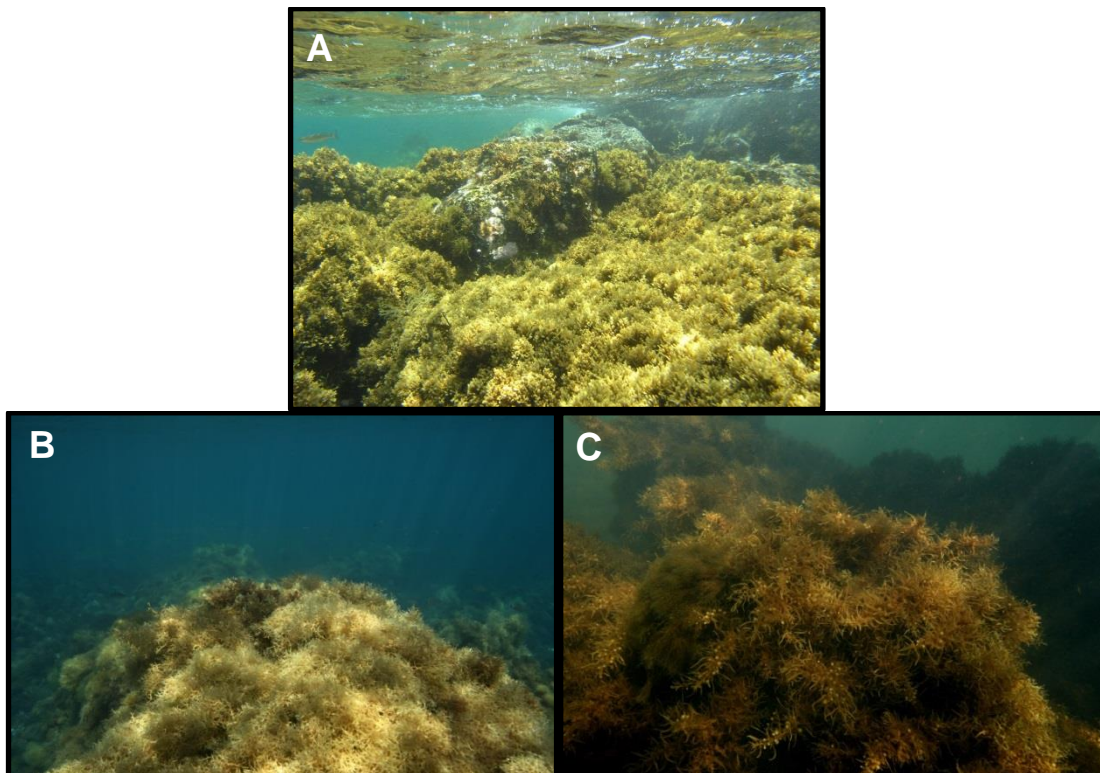


Figure 4.2. Macroalgal species sampled for epifauna at Methana in May 2012 (*Cystoseira corniculata*; A) and at Vulcano in June 2013 (*Cystoseira* spp. and *Sargassum vulgare*; B and C).

Several algal morphological parameters that could influence invertebrate density were measured for each thallus; parameters were selected based on Chemello and Milazzo (2002). Macroalgal biomass was measured with a balance (± 0.001 g accuracy) after it was blot-dried (fresh mass) and dried in an oven for 72 h at 50°C (dry mass). The other morphological parameters used were:

- Axis length: length of main axis measured in mm, measured by spreading the macroalgal thalli on graph paper;
- Frond density: number of primary branches on longest frond/axis length;
- Branching arrangement: total tip number/frond density;
- Canopy volume: maximum height (mm) x maximum length (mm) x maximum width (mm), measured by spreading the macroalgal thalli on graph paper;
- Volume: ml of water displaced, measured in a graduated cylinder;
- Interstitial volume: canopy volume - volume;
- Index of compactness: canopy volume/volume;
- Order of branching: counted from the distal branch to the stem. The final branches were classed first order, and whenever two branches of the same order joined, the order of the resultant branch was increased by one;
- Fractal dimension: calculated from black and white photos using the box counting method with the Fractalyse 2.4 software (CNRS, France).

4.2.3 Statistical analyses

ANOVA was used to analyse the biomass of *C. corniculata* samples from Methana (fixed factor: site) and morphological parameters influencing epifauna

on algal thalli from Vulcano (fixed factors: site and species) after checking they complied with the normality and variance homogeneity requirements of ANOVA. These analyses were performed using SPSS v19 (IBM, USA).

The structure and composition of epiphytic communities from Methana samples and patterns in morphological parameters in samples from Vulcano were tested using a PERMANOVA on square-root (Methana) and normalised (Vulcano) data, with the same experimental designs outlined above. Type III sums of squares with 9,999 unrestricted permutations of the raw data were used for Methana data to account for small sample sizes, whereas Vulcano morphological data were analysed using 9,999 permutations of residuals under a reduced model. Pairwise tests were performed when a factor with more than two levels was significant.

The same procedure was used to analyse epifaunal community data, but a BIO-ENV analysis (Clarke and Ainsworth, 1993) was first used to determine the best combination of variables (epiphyte community and *C. corniculata* biomass for Methana samples, morphological parameters for Vulcano samples) to use as covariates for PERMANOVA (i.e. the combination of variables that explained the most epifaunal variation); when covariates were used, type I sums of squares were used. Epifaunal diversity (Vulcano) and changes in abundance of individual broad taxonomic groups (Vulcano and Methana) were also analysed using the experimental design described above. Where appropriate and meaningful, nMDS plots were used to visually inspect similarities among samples. All analyses above were performed using PRIMER 6 with PERMANOVA+ extension (Plymouth Routines In Multivariate Ecological Research, version 6).

4.3 Results

4.3.1 Methana

Dry mass of *C. corniculata* growing in 20 x 20 cm quadrats off Methana showed significant differences among study sites (Table 4.1). Pairwise comparisons among sites then showed no consistent differences between different pH levels, although average dry mass of *C. corniculata* decreased from the seep site (mean \pm SE, n=3: 78.967 \pm 12.782 g) to the reference sites (mean \pm SE, n=6: 44.700 \pm 8.996 g), as shown in Figure 4.3.

Table 4.1. ANOVA on biomass of *C. corniculata* from 20 x 20 cm quadrats in May 2012. The Table shows the main factor, sum of squares (SS), degrees of freedom (df), Mean Squares (MS), F-ratios (F) and p values. The p values < 0.05 are highlighted. The lower part of the Table shows subsets detected by post-hoc pairwise comparisons, with different letters representing significantly different groups.

Source	Type III SS	df	MS	F	p
Site	5163.609	4	1290.902	5.333	0.015
Error	2420.427	10	242.043		
Total	7584.036	14			
Subsets	SEEP ^a	200 W ^{a,b}	200 E ^a	REF A ^{a,b}	REF B ^b

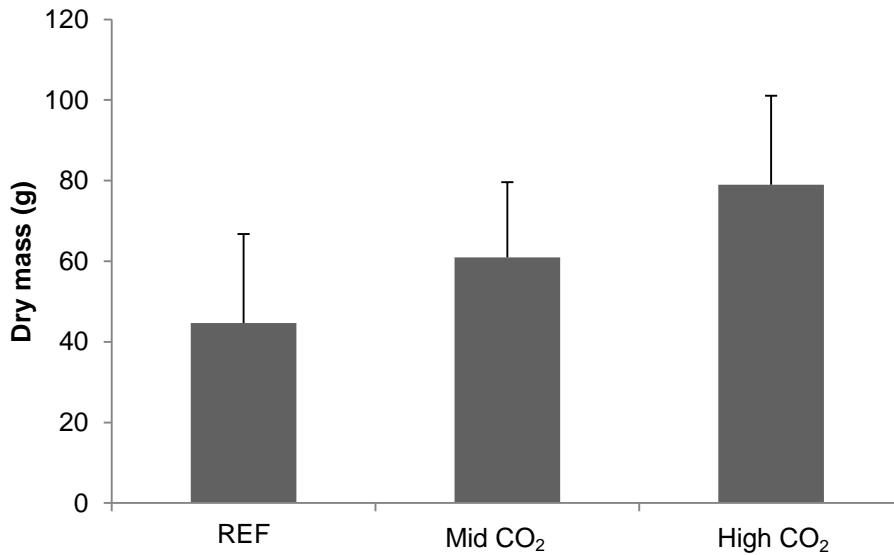


Figure 4.3. Mean (\pm SD) dry mass of *C. corniculata* from 20 x 20 cm quadrats scraped from rock in May 2012 at reference (REF, n=6), intermediate (n=6) and high CO₂ (n=3) off Methana.

Epiphyte communities on *C. corniculata* also showed significant differences among sites, but no consistent effect of pCO₂ was revealed by pairwise comparisons (Table 4.2).

Table 4.2. PERMANOVA on epiphyte communities of *C. corniculata* from 20 x 20 cm quadrats scraped from rocky substratum in May 2012. The table shows the main factor, degrees of freedom (df), sum of squares (SS), Mean Squares (MS), pseudo F-ratios (Pseudo-F), permutational p and number of unique permutations. Significant p values (< 0.05) are highlighted. The lower part of the table shows subsets detected by post-hoc pairwise comparisons, with different letters representing significantly different groups.

Source	df	SS	MS	Pseudo-F	P(perm)	Unique perms
Site	4	9361.90	2340.50	2.5891	0.0095	9903
Residual	10	9039.90	903.99			
Total	14	18402.00				
Subsets		SEEP ^a	200 W ^{a,b}	200 E ^{a,b}	REF A ^b	REF B ^{a,b}

BIO-ENV analysis showed that among the measured covariates, dry biomass of Porifera epiphytes (white species) explained most of the variability between samples. Spearman correlation coefficient for this analysis was 0.101, meaning that white Porifera epiphytes explained 10.1% of the variability of invertebrate abundance among samples. PERMANOVA of the invertebrate data using white Porifera epiphytes as a covariate showed a significant effect of site (Table 4.3). Pairwise comparisons showed that invertebrate communities at SEEP were significantly different from those at reference sites, while sites with intermediate pCO₂ were not significantly different from either SEEP or the closest reference site (REF A).

Table 4.3. PERMANOVA on epifaunal communities of *C. corniculata* from 20 x 20 cm quadrats scraped from rocky substratum in May 2012 using biomass of epiphytic Porifera (white) as covariate. The Table shows the main factors and their interaction, degrees of freedom (df), sum of squares (SS), Mean Squares (MS), pseudo F-ratios (Pseudo-F), permutational p and number of unique permutations. Significant p values (< 0.05) are highlighted. The lower part of the Table shows subsets detected by post-hoc pairwise comparisons, with different letters representing significantly different groups.

Source	df	SS	MS	Pseudo-F	P(perm)	Unique perms
Porifera	1	946.61	946.61	2.5386	0.0283	9951
Site	4	8207.80	2052.00	5.5030	0.0001	9930
Porifera x Site	3	726.85	242.28	0.6498	0.8743	9918
Residual	6	2237.30	372.88			
Total	14	12119.00				
Subsets		SEEP ^a	200 W ^{a,b}	200 E ^{a,b}	REF A ^{b,c}	REF B ^c

To further explore general patterns of changes in invertebrate communities along the Methana pCO₂ gradient, the community analysis was repeated grouping OTUs into general categories. BIO-ENV analysis of these data showed that among the measured covariates, dry biomass of Porifera epiphytes

(white species) and of Porifera epiphytes (yellow species) explained most of the variability between samples. Spearman correlation coefficient for this analysis was 0.122, meaning that white and yellow Porifera epiphytes explained 12.2% of the variability in invertebrate abundance among samples. However, PERMANOVA of the invertebrate data using the two categories above as covariates showed that they did not have a significant effect. PERMANOVA was then repeated without covariates, and a significant effect of site was detectable (Table 4.4). Pairwise comparisons showed that invertebrate communities at SEEP were significantly different from those at reference sites. Sites with intermediate pCO₂ levels were not significantly different from each other, but 200 W was also not significantly different from SEEP.

Table 4.4. PERMANOVA on invertebrate communities of *C. corniculata* from 20 x 20 cm quadrats in May 2012 grouping taxa into broad taxonomic groups. The Table shows the main factor, degrees of freedom (df), sum of squares (SS), Mean Squares (MS), pseudo F-ratios (Pseudo-F), permutational p and number of unique permutations. Significant p values (< 0.05) are highlighted. The lower part of the Table shows subsets detected by post-hoc pairwise comparisons, with different letters representing significantly different groups.

Source	df	SS	MS	Pseudo-F	P(perm)	Unique perms
Site	4	4742.7	1185.70	8.0678	0.0001	9918
Residual	10	1469.6	146.96			
Total	14	6212.4				
Subsets		SEEP ^a	200 W ^{a,b}	200 E ^b	REF A ^c	REF B ^c

A MDS plot of these data (Figure 4.4) is consistent with pairwise comparisons; it shows that reference sites were clearly different from sites with intermediate and high pCO₂ levels, while the latter were only loosely separated.

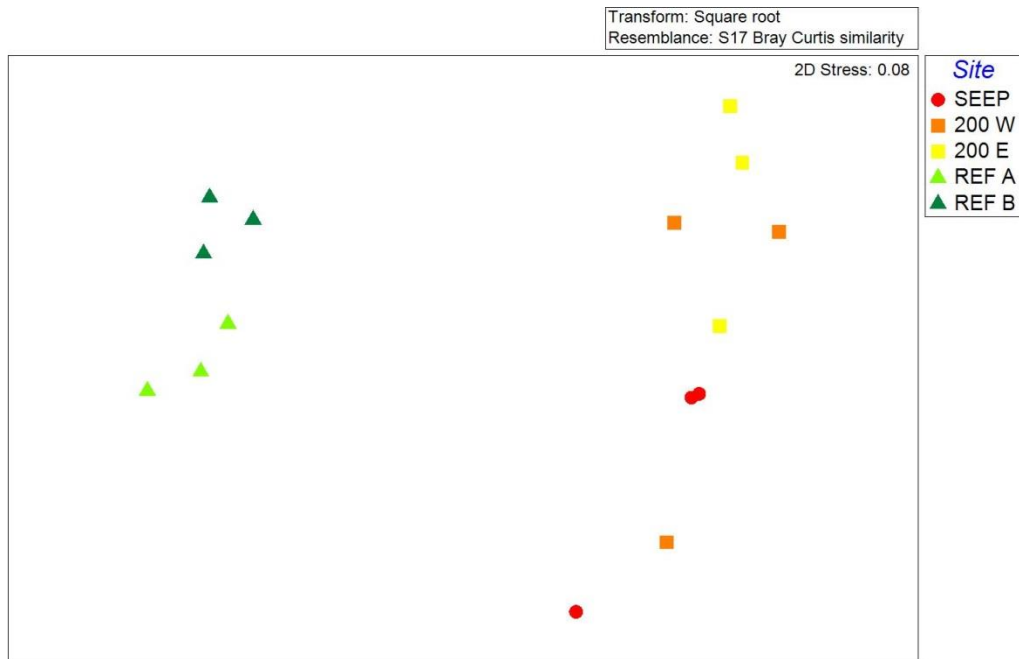


Figure 4.4: MDS plot of invertebrate assemblages on *C. corniculata* thalli collected from 20 x 20 cm quadrats at SEEPS, 200 W, 200 E, REF A and REF B at Methana in May 2012.

Abundances of invertebrate categories that showed significant responses to increased $p\text{CO}_2$ are reported in Figure 4.5. The most abundant invertebrates were amphipods, polychaetes and foraminifera (Figure 4.5A), while bivalves, ophiuroids, sipuncula, gastropods and serpulids were present in lower abundances (Figure 4.5B). In general, heavily calcified taxa (foraminifera, bivalves, gastropods and serpulids) showed decreased abundances with increasing $p\text{CO}_2$, while others (amphipods, polychaetes, ophiuroids) had a parabolic pattern (with highest abundances at intermediate CO_2) whilst sipunculids showed no clear trend in relation to carbon dioxide levels.

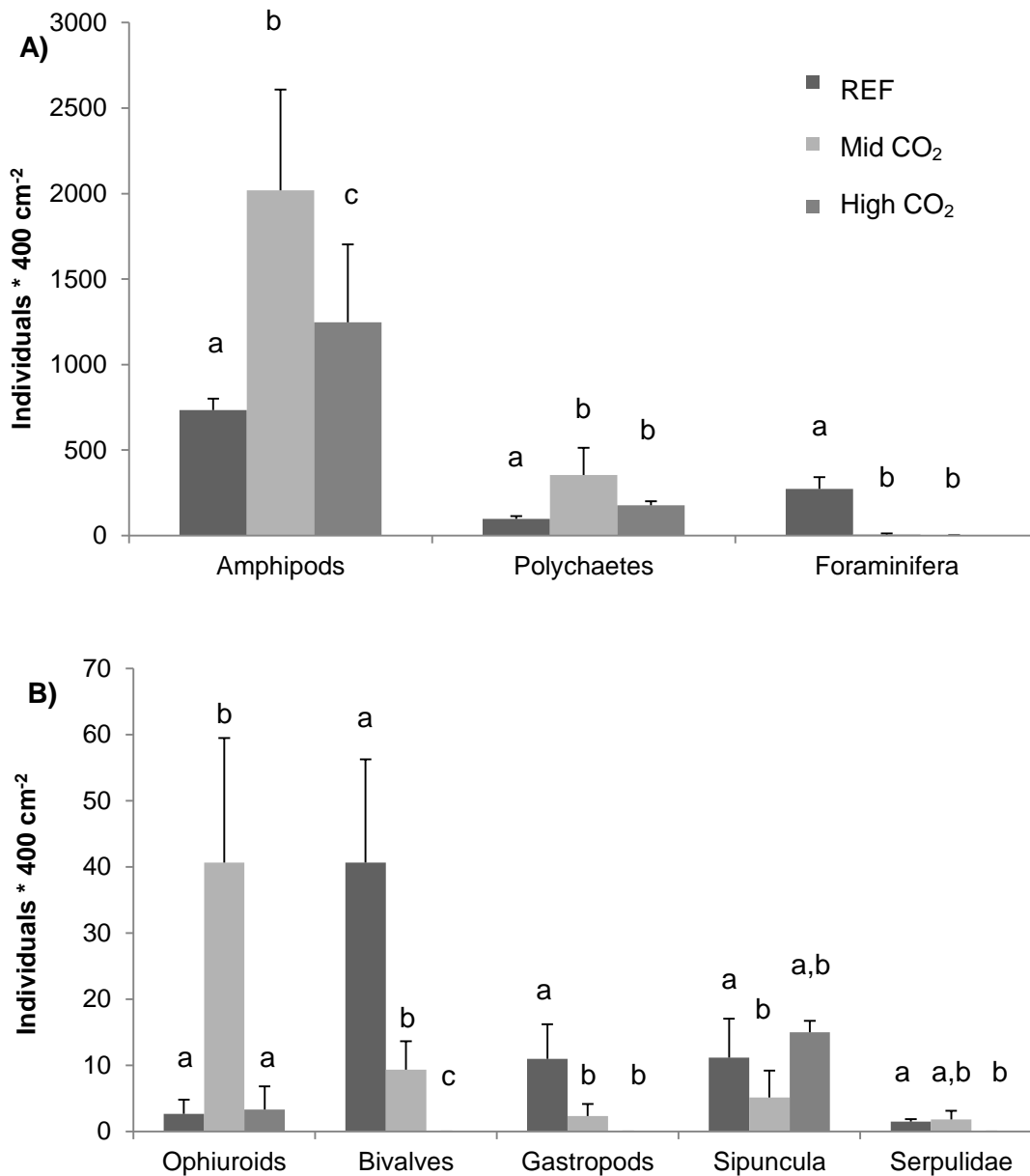


Figure 4.5. Mean (\pm SD, $n=3$) number of individuals for each of the main taxonomic groups of invertebrates found on *C. corniculata* from 20 x 20 cm quadrats in May 2012 at reference (REF, $n=6$), intermediate ($n=6$) and high CO₂ levels ($n=3$). The groups are divided depending whether they could have more (A) or less (B) than 100 individuals per sample. Different letters represent significantly different groups according to pairwise comparisons.

4.3.2 Vulcano

Normalised morphological parameters of macroalgae were significantly different between sites, and changed differently in *Cystoseira* spp. and *S. vulgare* (Table 4.5). All combinations of site and species were significantly different in pairwise comparisons (Table 4.5). The MDS plot clearly shows that while all combinations of site and species were different from each other, *Cystoseira* spp. samples were more tightly grouped than those of *S. vulgare*, which were separated into two very distinct groups (600 and 1200; Figure 4.6).

Table 4.5. PERMANOVA on morphology of *Cystoseira* spp. and *S. vulgare* thalli collected at Vulcano in June 2013. The table shows the main factors and their interaction, degrees of freedom (df), sum of squares (SS), Mean Squares (MS), pseudo F-ratios (Pseudo-F), permutational p and number of unique permutations. Significant p values (< 0.05) are highlighted. The lower part of the table shows subsets detected by post-hoc pairwise comparisons, with different letters representing significantly different groups.

Source	df	SS	MS	Pseudo-F	p(perm)	Unique perms
Site	1	32.662	32.662	5.9684	0.0003	9935
Species	1	45.812	45.812	8.3715	0.0001	9942
Site x Species	1	114.23	114.23	20.874	0.0001	9940
Residual	44	240.79	5.4724			
Total	47	415.99				
Pairwise comparisons	600 S ^a	1200 S ^b	600 C ^c	1200 C ^d		

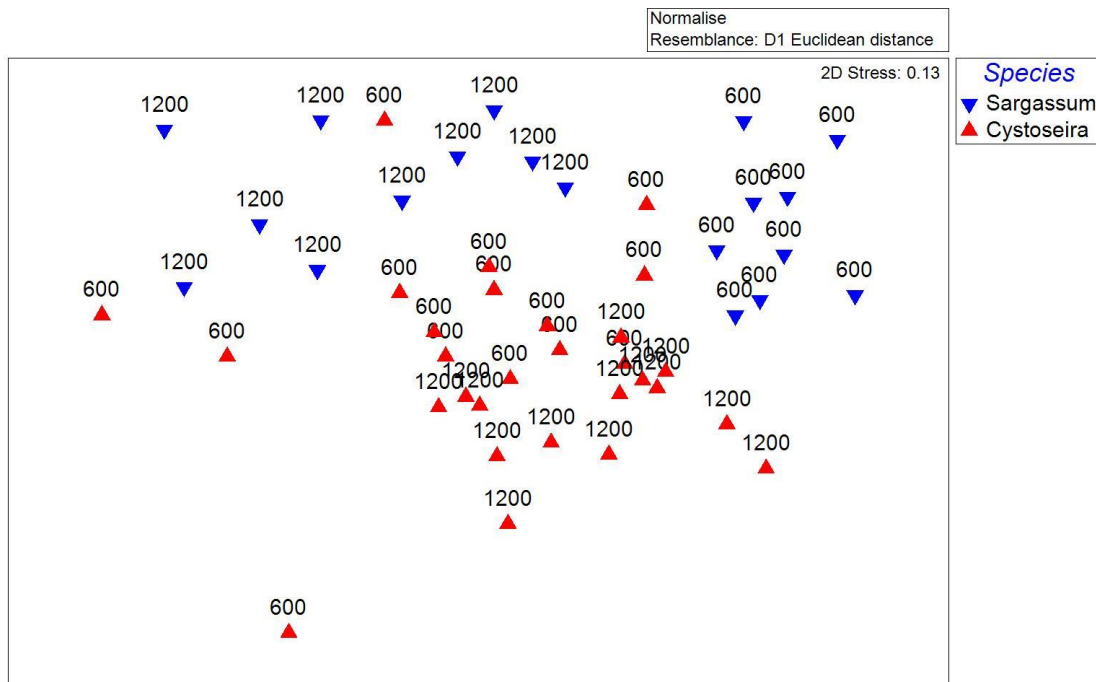


Figure 4.6: MDS plot of macroalgal morphology of *Cystoseira* spp. and *S. vulgare* thalli collected at Vulcano in June 2013 at sites with 600 and 1200 ppm average seawater pCO₂.

The morphological variables best explaining epifaunal patterns were axis length, order of branching and frond density; these three parameters explained 29.3% of the epifauna variability according to the BIO-ENV analysis. ANOVAs of the parameters above showed that axis length of *Cystoseira* spp. and *S. vulgare* exhibited opposite patterns. Main axes of *S. vulgare* were longer at elevated CO₂, increasing from under 150 mm to over 400 m, whereas those of *Cystoseira* spp. were shorter at the high CO₂ site (Figure 4.7A). Order of branching was mostly similar for all sites and species, but *S. vulgare* at the low pCO₂ site had a much simpler structure (Figure 4.7B). On the other hand, frond density was not significantly different between sites, but was significantly higher in *Cystoseira* spp. than in *S. vulgare* (Figure 4.7C).

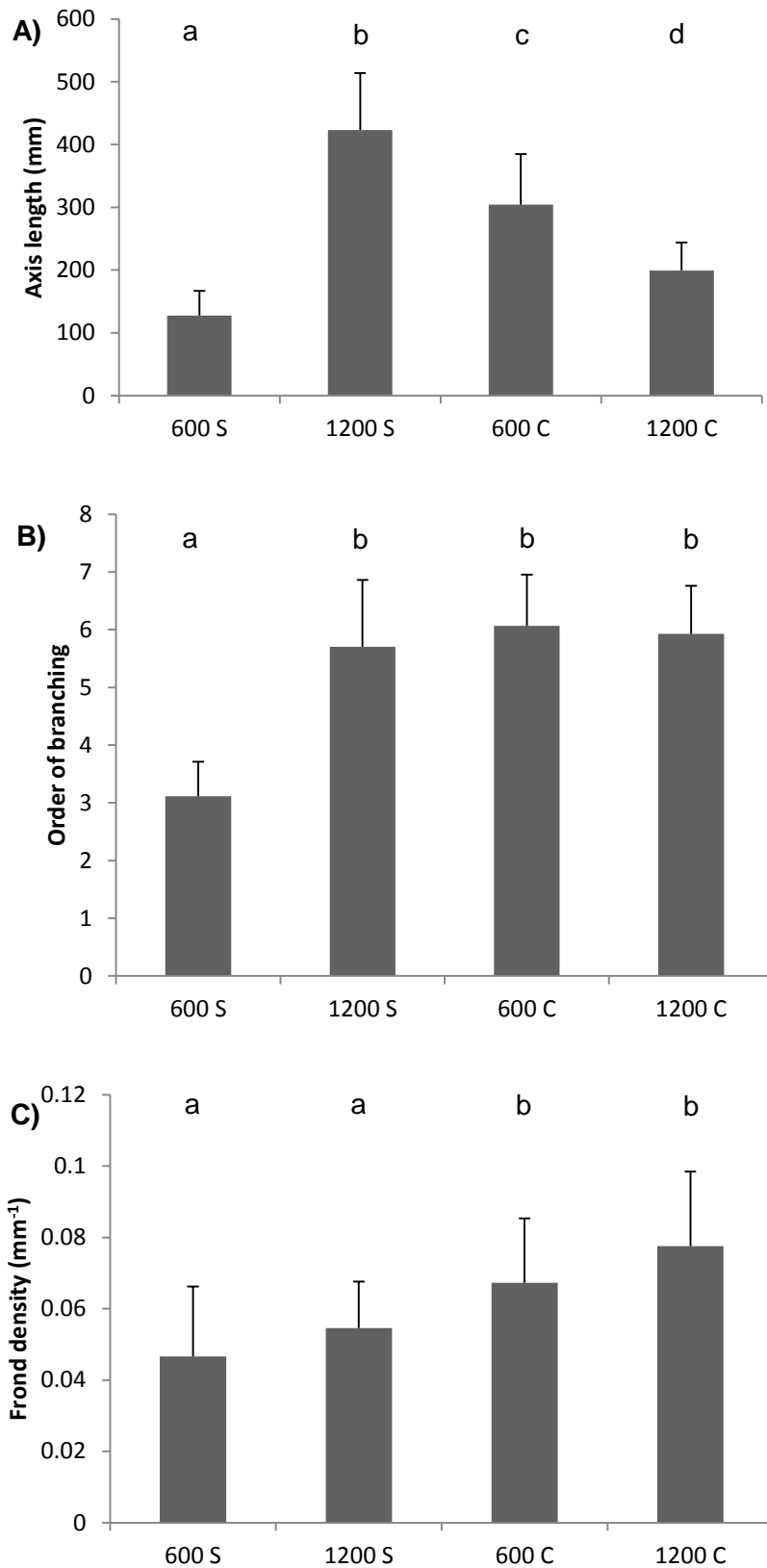


Figure 4.7: Mean (\pm SD, $n=9-15$) axis length (A), order of branching (B) and frond density (C) of *Cystoseira* spp. and *S. vulgare* thalli collected at Vulcano in June 2013 at sites with 600 and 1200 ppm average seawater pCO₂. Different letters represent significantly different groups identified by pairwise comparisons.

As for the invertebrate community analysis, no significant interactions between factors and covariates were detected; those interactions were therefore removed from the analysis. The results show that after taking into account the three covariates, invertebrate communities were significantly different between sites and between species, but the two factors did not interact (Table 4.6). Pairwise comparisons revealed that while epifauna of *Cystoseira* spp. was significantly different between sites, epifauna of *S. vulgare* did not change significantly as pCO₂ increased, and its community structure was not significantly different from that of *Cystoseira* spp. (Table 4.6). As analysis of broad taxonomic categories gave the same results, they are not reported here.

Table 4.6. PERMANOVA on invertebrate communities of *Cystoseira* spp. and *S. vulgare* thalli collected at Vulcano in June 2013 using axis length, order of branching and frond density as covariates. The table shows the main factors and their interaction, degrees of freedom (df), sum of squares (SS), Mean Squares (MS), pseudo F-ratios (Pseudo-F), permutational p and number of unique permutations. Significant p values (< 0.05) are highlighted. The lower part of the table shows subsets detected by post-hoc pairwise comparisons, with different letters representing significantly different groups.

Source	df	SS	MS	Pseudo-F	p(perm)	Unique perms
Axis length	1	5313.9	5313.9	6.1971	0.0001	9926
Order of branching	1	4385.8	4385.8	5.1148	0.0001	9925
Frond density	1	2865.6	2865.6	3.3419	0.0003	9935
Site	1	7833.2	7833.2	9.1352	0.0001	9926
Species	1	4895.1	4895.1	5.7088	0.0002	9934
Site x Species	1	1245.6	1245.6	1.4527	0.1366	9924
Residual	41	35156	857.47			
Total	47	61696				
Pairwise comparisons	600 S ^{a,b}	1200 S ^{a,b}	600 C ^a	1200 C ^b		

Epifaunal diversity was not significantly affected by any morphological parameters, so covariates were removed from the analysis. Similarly to the epifaunal community structure, Shannon diversity was significantly affected by site and species, but the two factors did not interact (Table 4.7). Although epifauna of both macroalgae had lower diversity at elevated CO₂, the difference was clearer in *Cystoseira* spp. (Figure 4.8).

Table 4.7. ANOVA on epifaunal diversity of *Cystoseira* spp. and *S. vulgare* thalli collected at Vulcano in June 2013. The table shows the main factors and their interaction, degrees of freedom (df), sum of squares (SS), Mean Squares (MS), pseudo F-ratios (Pseudo-F), permutational p and number of unique permutations. Significant p values (< 0.05) are highlighted. The lower part of the table shows subsets detected by post-hoc pairwise comparisons, with different letters representing significantly different groups.

Source	df	SS	MS	Pseudo-F	p(perm)	Unique perms
Site	1	0.67246	0.6724 6	6.9354	0.0113	9824
Species	1	0.39158	0.3915 8	4.0385	0.0485	9830
Site x Species	1	0.10733	0.1073 3	1.1069	0.3002	9835
Residual	44	4.2662	0.097			
Total	47	5.5516				
Pairwise comparisons	600 S ^{a,b}	1200 S ^b	600 C ^a	1200 C ^c		

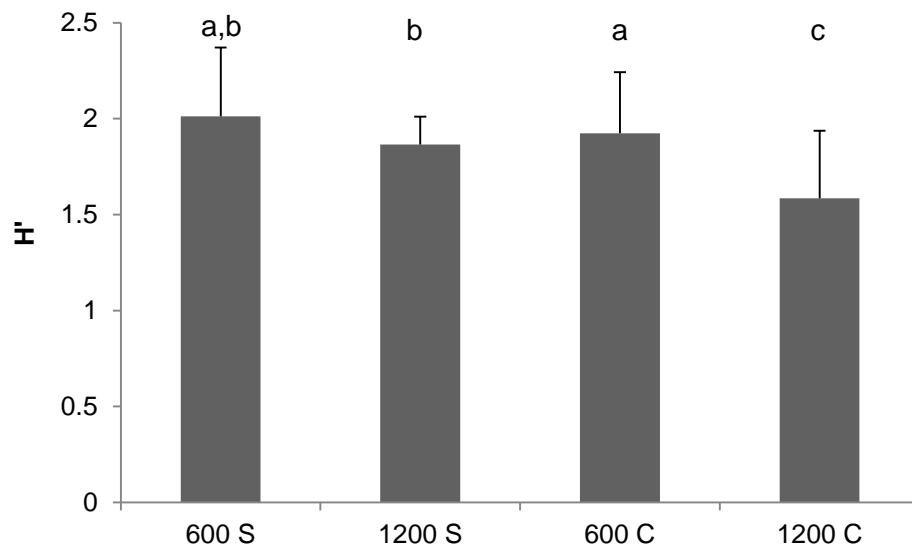


Figure 4.8: Mean (\pm SD, n=9-15) diversity of epifaunal communities on *Cystoseira* spp. and *S. vulgare* thalli collected at Vulcano in June 2013 at sites with 600 and 1200 ppm average seawater pCO₂. Different letters represent significantly different groups identified by pairwise comparisons.

Graphs of the number of individuals of the most abundant taxa are shown in Figure 4.9. Values are reported as individuals per ml of water displaced by the macroalga, as this was the morphological parameter that seemed to influence invertebrate abundance the most (BIO-ENV analyses on single taxa, results not shown). Amphipods and tanaids showed a clear decrease with increasing pCO₂ on *S. vulgare*, but a trend towards increasing abundance on *Cystoseira* spp.. Gastropods decreased at the high CO₂ site in both macroalgal species, whereas polychaetes and isopods became more abundant as CO₂ increased.

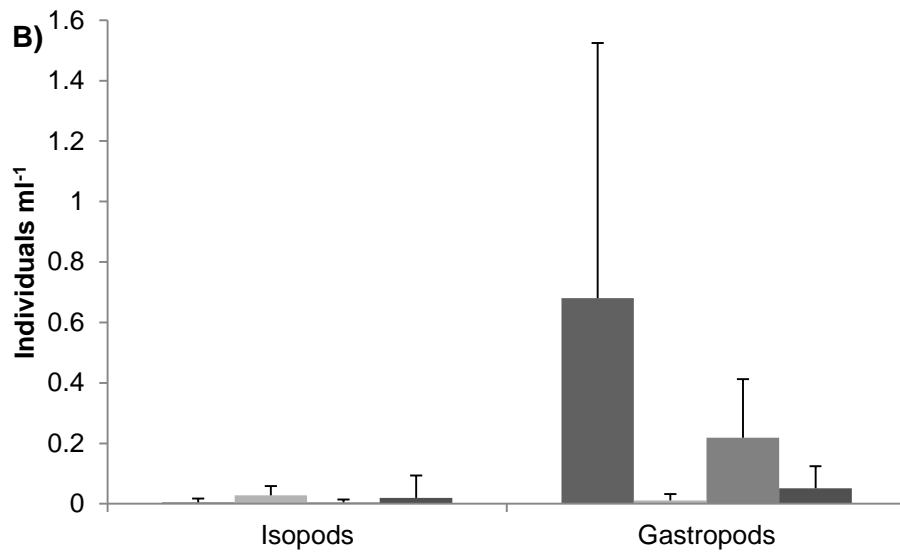
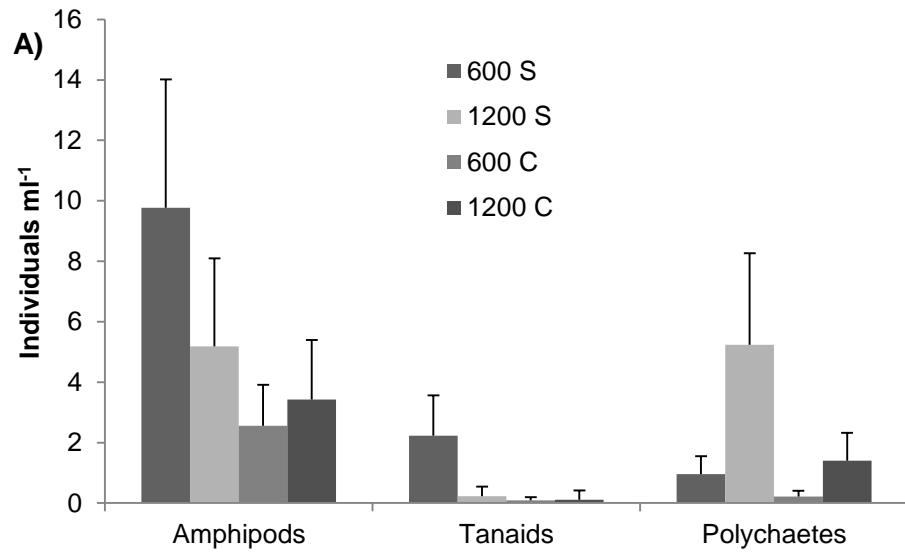


Figure 4.9. Mean (\pm SD, $n=9-15$) number of individuals for each of the main taxonomic groups of invertebrates per ml of water displaced by thalli of *Cystoseira* spp. and *S. vulgare* collected at Vulcano in June 2013 at sites with 600 and 1200 ppm average seawater pCO_2 . The groups are divided depending whether they had more (A) or less (B) than 1 individual per ml of water displaced.

4.4 Discussion

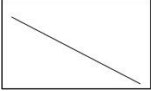
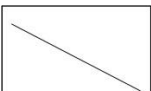
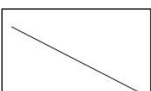
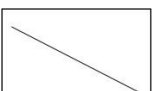
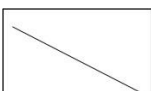
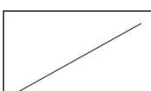
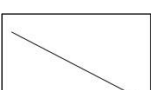
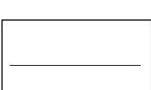
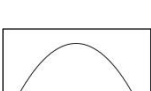
This is the first study to assess how epifauna of different canopy-forming algae responds to elevated CO₂ levels. Epifauna of macroalgae and seagrasses represents the main food source for many commercial fish, especially for juvenile individuals (Yamada *et al.*, 2010); changes in their abundance and specific composition could therefore have dramatic consequences for coastal ecosystems and fisheries. Epifauna of *Cystoseira* spp. collected at two CO₂ seeps was significantly affected by elevated carbon dioxide levels, but epifauna of *Sargassum vulgare* was not affected by changes in pCO₂. This has implications for ecosystem functioning, as epifauna can contribute 70-98% of secondary productivity on temperate rocky reefs (Taylor, 1998).

Community structure of *Cystoseira* spp. epifauna significantly changed with increasing pCO₂ at both sites, but at Vulcano *S. vulgare* epifauna did not change significantly with pCO₂ levels. The changes in epifaunal communities are in accord with previous studies on epifaunal responses to ocean acidification, which reported significant changes in community structure (Hale *et al.*, 2011; Kroeker *et al.*, 2011). A pH < 7.2 can cause communities to shift from net calcification to net dissolution, although total invertebrate biomass does not change with pCO₂ (Kroeker *et al.*, 2011; Christen *et al.*, 2013). At Vulcano, epifaunal diversity significantly decreased at the high CO₂ site on *Cystoseira* spp. thalli, but epifauna of *S. vulgare* did not show significant changes in community structure and diversity between sites. Although invertebrate communities often decrease in diversity as CO₂ increases (Cigliano *et al.*, 2010; Hale *et al.*, 2011; Kroeker *et al.*, 2011), *Cystoseira*-associated macroalgal communities are more sensitive to ocean acidification compared to those associated with *Sargassum muticum* (Olabarria *et al.*, 2013). In addition, the

increase in *S. vulgare* structural complexity at the high CO₂ site might have helped maintain epifaunal diversity, as morphological complexity of macroalgal hosts has been linked with higher diversity and abundance of their associated epifauna (Chemello and Milazzo, 2002; Bates, 2009).

Heavily calcified taxa decreased in abundance with increasing pCO₂, both at Methana and Vulcano (results summarised in Table 4.8). The only taxa that increased in abundance at elevated pCO₂ were polychaetes and amphipods, although the former showed a clearer increase. Compensatory increase in abundance of CO₂-resistant taxa in ocean acidification conditions has been reported by Hale *et al.* (2011) and Kroeker *et al.* (2011) for nematodes and crustaceans, respectively. These results show that different taxa can be advantaged as CO₂ increases depending on system characteristics; specifically, different taxa can be advantaged by decreased predation rates or reduced competition for space and resources (Micheli *et al.*, 1999). Taxa producing carbonate structures are negatively affected by elevated CO₂ (Kroeker *et al.*, 2013a), whereas crustaceans experience less severe effects because their chitinous skeletons are less prone to dissolution than calcium carbonate structures (Whiteley, 2011). At both study sites, crustaceans indeed showed small or unclear changes in abundance at different CO₂ levels. At Vulcano, changes in epifaunal densities with increased CO₂ were more marked in *S. vulgare*, possibly because its increase in thallus length and complexity at the high CO₂ site increased available habitat for epifauna, therefore masking direct effects of carbon dioxide on their abundance.

Table 4.8. Response to increasing CO₂ of the main epifaunal taxa living on *Cystoseira corniculata* (Methana) or *Cystoseira* spp. and *Sargassum vulgare* (Vulcano); symbols indicate increase (↗), decrease (↘) or no change (—) with elevated CO₂; n.f. = not found.

Taxon	Methana	Vulcano	
	<i>Cystoseira corniculata</i>	<i>Cystoseira</i> spp.	<i>Sargassum vulgare</i>
Foraminifera		n.f.	n.f.
Sipunculida		n.f.	n.f.
Bivalves		n.f.	n.f.
Gastropods			
Polychaetes			
Serpulids		n.f.	n.f.
Amphipods			
Isopods			
Tanaids			
Copepods		n.f.	n.f.
Ophiuroids		n.f.	n.f.

At Methana, biomass of *C. corniculata* and of its epiphytes did not change consistently among pCO₂ levels, even though there were clear differences among sites. *C. corniculata* biomass increased, albeit not significantly, at elevated CO₂. This is consistent with a recent meta-analysis showing that some fleshy algae exhibit faster growth rates at elevated pCO₂ levels (Kroeker *et al.*, 2013a). The lack of significant effects of pCO₂ on *C. corniculata* epiphytes is surprising, as it contrasts with the clear decrease in calcifying epiphytes off Vulcano as CO₂ increased (Papworth, 2012), for macroalgal communities (Chapter 3) and epifauna (this chapter). Other factors may be influencing epiphyte communities and masking direct effects of CO₂; for instance, epiphytes are often controlled by grazers such as amphipods or gastropods (Fong *et al.*, 2000; Whalen *et al.*, 2012), whose abundances varied among sites. Another possibility is that *C. corniculata* photosynthesis raises pH near its fronds (Hendriks *et al.*, 2014; Cornwall *et al.*, 2014). This may have reduced the impacts of ocean acidification on epiphytes, but not on mobile epifauna, which often swim in and out of macroalgal fronds (Edgar, 1992).

At Vulcano, macroalgal morphology clearly changed at elevated pCO₂. *Sargassum vulgare* was competitively advantaged at high CO₂, as it increased in length and complexity (i.e. order of branching) at the 1200 ppm site. In contrast, *Cystoseira* spp. decreased in length at elevated CO₂, but their frond densities were higher than that of *S. vulgare* at both sites. While *S. vulgare* was the only species of the genus *Sargassum* present at both study sites, several *Cystoseira* species were present off Vulcano. Specifically, *C. compressa* was very abundant at the 1200 ppm site and *C. humilis* was very abundant at the 600 ppm site. Part of the morphological variability of *Cystoseira* spp. could

therefore be attributed to changes in species composition rather than direct effects of pCO₂ on one species' morphology. Other factors, chiefly wave exposure and light, have long been known to influence macroalgal morphology (Hurd, 2000; Monro and Poore, 2005), but neither changes between the two study sites (Johnson *et al.*, 2013). On the other hand, seasonal changes only have a minor influence on most macroalgal morphological parameters (Wernberg and Vanderklift, 2010), so results from this study are unlikely to be influenced by sampling season. *Sargassum vulgare* cover increased with increasing pCO₂ at other Mediterranean seeps (Porzio *et al.*, 2011; Chapter 3), but this is the first evidence that pCO₂ levels can influence fleshy algal morphology as well.

Magnitude of change in communities associated with canopy-forming algae also depends on the type of community, as macroalgal epiphytes did not change among pCO₂ levels, whereas epifaunal communities did. At Vulcano, epifauna of *Cystoseira* spp. and *S. vulgare* were not significantly different within pCO₂ levels. Epifauna of macroalgal species belonging to the same functional group are indeed not likely to be significantly different (Bates and DeWreede, 2007). However, *S. vulgare* epifauna changed between sites less than that of *Cystoseira* spp., hinting at host-specific patterns of epifaunal change with increasing CO₂. In addition, the concurrent increase in *S. vulgare* abundance at elevated pCO₂ will amplify changes in epifaunal communities, with knock-on effects on ecosystem functioning (Taylor, 1998).

Chapter 5

Effect of herbivores on benthic communities at different pCO₂ levels

Parts of this chapter are currently under review as:

C. Baggini, Y. Issaris, M. Salomidi, J.M. Hall-Spencer (2014). Herbivore diversity improves benthic community resilience to ocean acidification. *Journal of Experimental Marine Biology and Ecology* (accepted pending revisions).

Abstract

Marine volcanic seeps exhibit profound changes in benthic communities along gradients of increasing pCO₂ on intertidal and subtidal rocky shores. As grazing by fish, sea urchins and gastropods can also structure benthic communities, decreased herbivore densities due to intolerance to acidified conditions may interact with direct CO₂ effects to determine benthic community structure in a high CO₂ world. Here, two exclusion experiments were used to test effects of herbivory in benthic communities along pCO₂ gradients. Limpets were excluded on intertidal shores at volcanic seeps off Vulcano (Italy) to examine their role in changes from coralline to fleshy algal assemblages. At volcanic seeps off Methana (Greece), herbivore exclusions were used to test whether herbivores affect subtidal algal recruitment differently as carbon dioxide levels increase. Off Vulcano, spatial heterogeneity and seasonality of benthic intertidal communities at a reference site was much higher than at a high CO₂ site. Limpets had weak effects on benthic communities at ambient CO₂ levels, and no effect at the high CO₂ site. Limpet abundances significantly decreased as pCO₂ levels increased, but higher limpet grazing rates at elevated CO₂ were not sufficient to maintain top-down control on benthic communities. Conversely, sea urchins and herbivorous fish dramatically reduced macroalgal biomass at Methana. This effect was not hampered by increased pCO₂ despite lower sea urchin densities near the CO₂ seeps, probably because fish grazing increased. In summary, we found that as long as herbivore fish are present, carbon dioxide levels up to about 2000 μatm are unlikely to significantly reduce the importance of herbivory in structuring Mediterranean benthic communities, even when herbivores strongly control benthic communities. A shift from sea urchin to fish as main

grazers highlights that ocean acidification may cause complex responses at the community level.

5.1 Introduction

Ocean acidification is expected to have profound effects on marine ecosystems worldwide (Kroeker *et al.*, 2013a). Studies at volcanic seeps have shown that increased seawater pCO₂ causes changes in benthic macroalgal and invertebrate communities (Kroeker *et al.*, 2011; Porzio *et al.*, 2011). These changes could be caused by physiological effects of CO₂ on macroalgae, altered competitive interactions (Kroeker *et al.*, 2013c), changes in chemical plant defences (Arnold *et al.*, 2012), or a combination of the above. In addition, grazers may have a determining role in the observed community changes given the strong role of herbivory in marine ecosystems (Poore *et al.*, 2012). Some herbivores, such as amphipods, become more abundant as CO₂ increase at volcanic seeps (Cigliano *et al.*, 2010; Kroeker *et al.*, 2011; Suaria *et al.*, unpublished data). Conversely, key grazers such as limpets and sea urchins decrease in abundance with increased CO₂ (Hall-Spencer *et al.*, 2008; Johnson *et al.*, 2012; Calosi *et al.*, 2013a; Graziano *et al.*, unpublished data), but their contribution to community changes along pCO₂ gradients has not previously been tested experimentally.

Coastal environments have low functional redundancy, even when diversity is relatively high (Micheli *et al.*, 2014). Decrease of limpet and sea urchin densities as seawater CO₂ increases thus leave marine ecosystem vulnerable to phase shifts, especially in the absence of herbivorous fish (Hughes, 1994). Numerous dramatic changes to benthic communities due to reduction in grazing rates have

been reported; for instance, tropical coral reefs can be overgrown by macroalgae if grazing pressure is removed (Hughes *et al.*, 2007).

Limpets of the genus *Patella* are abundant grazers in intertidal Mediterranean shores. Three species are particularly common: *P. aspera*, *P. rustica* and *P. caerulea* (Figure 5.1a). They can greatly influence benthic communities, although their influence varies in space and time (Benedetti-Cecchi *et al.*, 2000) and the algal functional groups affected change depending on several factors. For instance, Benedetti-Cecchi *et al.* (1996) showed how limpets strongly affect coarsely branched and coralline algal abundance, but not filamentous algae, whereas the opposite is true for a study performed in the same area, but on artificial structures (Bulleri *et al.*, 2000).

Limpets are negatively affected by increasing CO₂ levels and the consequent decrease in seawater calcium carbonate saturation; their densities decrease with increasing pCO₂ at seeps off Ischia and Vulcano (Hall-Spencer *et al.*, 2008; Graziano *et al.*, unpublished data). They can survive elevated pCO₂ conditions and up-regulate their calcification rates to counter increased shell dissolution rates (Rodolfo-Metalpa *et al.*, 2011). Some gastropod herbivores increase their feeding rates when pCO₂ increases (Falkenberg *et al.*, 2013b), possibly to sustain the higher energetic cost of calcification. The increase in benthic microalgal chlorophyll concentration recorded at volcanic seeps as CO₂ increases (Johnson *et al.*, 2013) could therefore give limpets a significant advantage in coping with high CO₂ conditions through increased food availability. There is thus a possibility that limpets will still affect benthic communities in a high CO₂ ocean, even with decreased densities, by means of increased feeding rates.

In Mediterranean subtidal environments, high densities of the sea urchins *Paracentrotus lividus* and *Arbacia lixula* can cause a shift from photophilic algal assemblages to “barren grounds”, impoverished assemblages dominated by encrusting algae (Sala *et al.*, 1998; Figure 5.1b). Sea urchin grazing can cause a shift to barren grounds in temperate rocky reefs worldwide, which are considered an alternative stable state to kelp beds (Filbee-Dexter and Scheibling, 2014). Once established, barren grounds can be maintained by relatively low sea urchin densities (Chiantore *et al.*, 2008), although these can change back to macroalgal beds if the biomass of carnivorous fish exceeds a critical threshold (Guidetti and Sala, 2007). Herbivorous fish are normally thought to exert weaker top-down control on temperate benthic communities compared to sea urchins (Floeter *et al.*, 2005). However, in the warm-temperate Mediterranean Sea herbivorous fish can limit the distribution of some macroalgal species (Vergés *et al.*, 2009). The main herbivorous fish in the Mediterranean Sea are the sparid *Sarpa salpa* (Figure 5.1c) and the scarid *Sparisoma cretense*, as well as the lessepsian migrants *Siganus luridus* and *Siganus rivulatus*, which can account for over 90% of herbivorous fish biomass in Greek coastal waters (Kalogirou *et al.*, 2012). Increased temperatures in the Mediterranean Sea are helping *Siganus* spp. to expand their range; these fish are therefore causing and maintain barren grounds in the Eastern Mediterranean (Sala *et al.*, 2011; Vergés *et al.*, 2014).

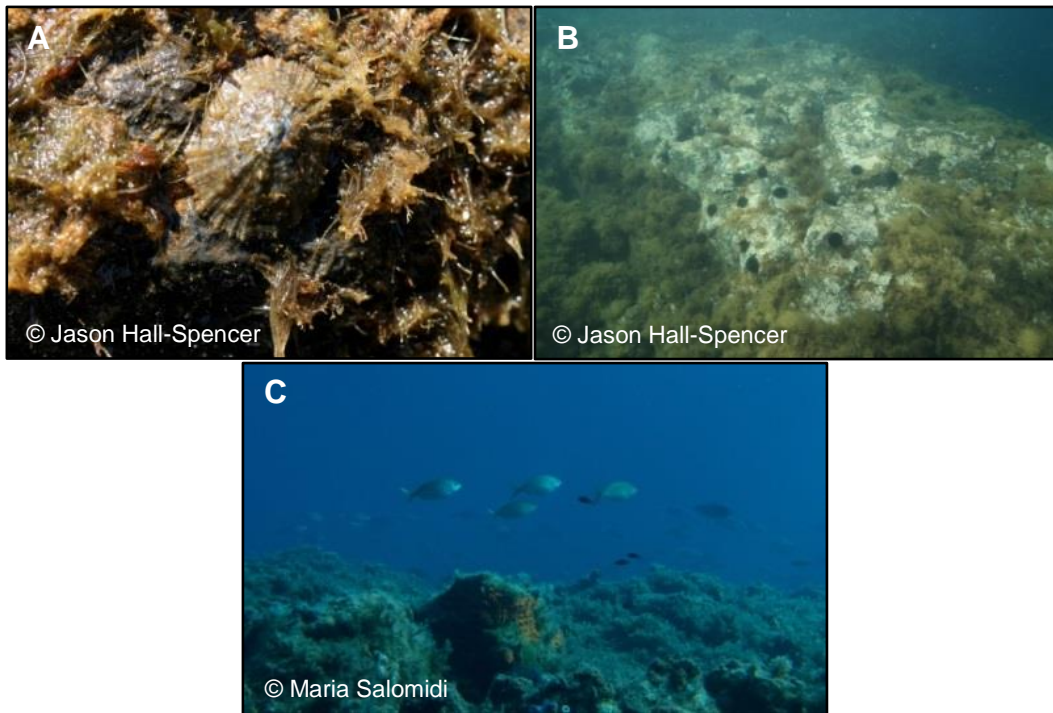


Figure 5.1. Main grazers on Mediterranean intertidal and subtidal shores: (A) Limpet on intertidal shore off Vulcano (Italy); (B) sea urchins reducing macroalgal biomass at shores off Vulcano (Italy); (C) herbivorous fish (*Sarpa salpa*) near CO₂ seeps off Methana (Greece).

Ocean acidification has a detrimental effect on the physiology of many sea urchin species (Dupont *et al.*, 2010) and their densities often decrease as seawater pCO₂ increases (Johnson *et al.*, 2012; Calosi *et al.*, 2013a). On the other hand, many adult fish seem to tolerate carbon dioxide levels predicted for the end of this century (Melzner *et al.*, 2009). Despite this, near-future levels of CO₂ can have profound effects on fish behaviour and sensory functions, particularly at larval and juvenile stages, making many fish species less alert to predators even after prolonged exposure at CO₂ seeps (McCormick *et al.*, 2013; Munday *et al.*, 2014). However, the structure of fish communities seems to be more affected by indirect effects on habitat complexity of ocean acidification than by observed direct effects of elevated pCO₂ on the behaviour of chronically exposed fish (Munday *et al.*, 2014). Being able to move in and out a pCO₂

gradient adult herbivorous fish could be advantaged by high CO₂ conditions because of increased food availability following decreased competition with sea urchins (Johnson *et al.*, 2012) and decreased plant chemical defences (Arnold *et al.*, 2012)

Our understanding of algal community change due to elevated CO₂ has evolved through a series of studies at volcanic seeps. Initial work led researchers to conclude that a shift from coralline algae dominated to fleshy algal communities was driven by dissolution effects on calcified algae (Hall-Spencer *et al.*, 2008; Martin *et al.*, 2008; Porzio *et al.*, 2011). Subsequent work investigating macroalgal succession indicated that certain coralline algae were able to withstand dissolution at CO₂ levels predicted for the end of this century, but fleshy algae were able to outcompete them at high CO₂ (Kroeker *et al.*, 2013c). In a comparison of a tropical and a temperate CO₂ seep system, Johnson *et al.* (2012) found that *Padina* spp. cover was higher at elevated CO₂ levels despite lower calcium carbonate content of thalli at the high CO₂ site. They postulated that this was possible since sea urchins, their main grazers, were unable to tolerate high CO₂ conditions (see Calosi *et al.*, 2013a; Bray *et al.*, 2014). More recent work demonstrates that most evidence of community changes does not originate from direct physiological responses of species to ocean acidification, but from indirect ocean acidification effects on habitat changes or trophic interactions (Alsterberg *et al.*, 2013; Fabricius *et al.*, 2014; Munday *et al.*, 2014; Gaylord *et al.*, 2014). Volcanic CO₂ seeps can be used to disentangle the direct and indirect effects of ocean acidification on marine benthic communities. Here we formally test these effects of ocean acidification in experiments along natural pCO₂ gradients with and without grazers present on rocky Mediterranean shores. Specifically, two separate exclusion experiments were used to test

effects of herbivory in benthic communities along pCO₂ gradients. Limpets were excluded on intertidal shores at volcanic seeps off Vulcano (Italy) to examine their role in changes from coralline to fleshy algal assemblages. At volcanic seeps off Methana (Greece), herbivore exclusions were used to test whether herbivores differently affect subtidal algal recruitment as carbon dioxide levels increase.

5.2 Methods

5.2.1 Vulcano

5.2.1.1 Study site

The aim of this experiment was to examine the role of limpet grazing in driving changes from coralline to fleshy algal assemblages as CO₂ levels increase, and it was conducted in an area off Vulcano Island described in Chapter 3. Along this gradient, the two sites shown in Figure 5.2 were selected, one with average pH_{NBS} of about 7.8 (named “1200 ppm”) and one located about 50-60 m farther away from the main seeps (named “600 ppm”), with an average pH of approximately 8.05, slightly lower and more variable than most Mediterranean coastal waters (Boatta *et al.*, 2013). The sites were visited four times during the experiment (start of experiment, i.e. May 2012; July 2012; September 2012; November 2012 - detailed sampling dates and sample sizes are reported in Table 1.1D), and each time pH (NBS scale), temperature and salinity were measured at about 0.5 m depth using a calibrated YSI (556 MPS) pH meter. For pH, means were calculated from hydrogen ion concentrations and then re-converted to pH. The other carbonate chemistry parameters were calculated with CO2Sys (Lewis and Wallace, 1998) using the average total alkalinity value

resulting from monitoring at the site in 2011 ($2.525 \text{ mMol kg}^{-1}$, Boatta *et al.*, 2013).

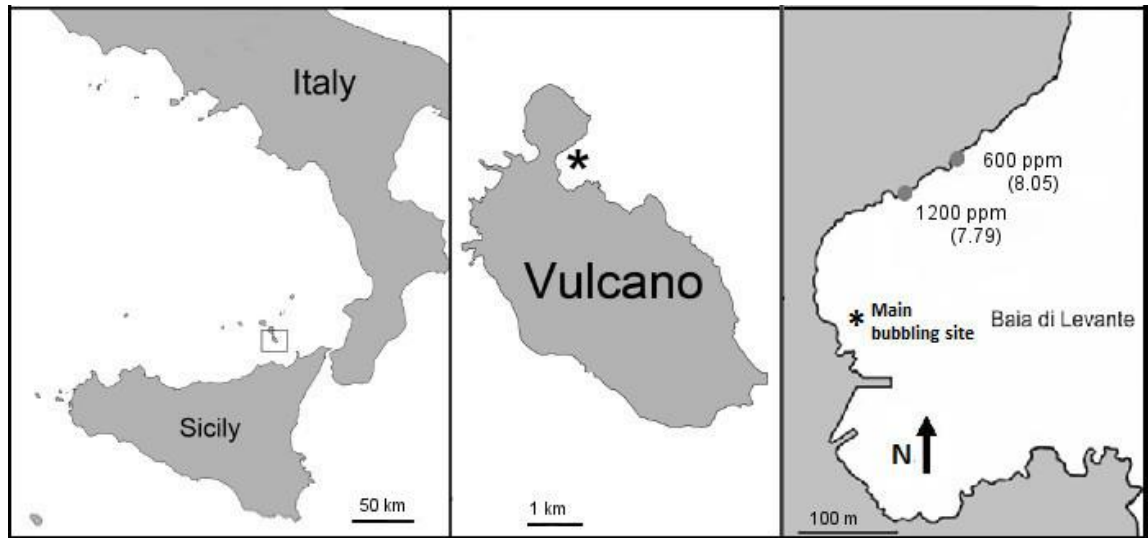


Figure 5.2. Position of Vulcano Island (Sicily, Southern Italy) and of the study area. Asterisk marks the main venting site, grey circles show the two experimental sites, with decreasing pCO_2 moving away from the bubbling site (modified from Graziano *et al.*, unpublished data). Average pH measured during the experiment shown in parentheses ($n=6$).

5.2.1.2 Limpet exclusion

At each site, twelve 15 cm diameter circular plots were selected in the intertidal zone (defined as the area 10 cm above the limit of the canopy-forming algae, *Cystoseira* spp.). All plots were chosen on vertical flat surfaces with similar wave exposure, as limpet grazing is more intense on vertical surfaces (Marco Milazzo, personal communication). Six of these plots were enclosed using 5 cm high copper rings, which are very rarely crossed by limpets (Harley, 2002). The rings were screwed to the substratum and any space between the ring and the rock was filled using epoxy putty. Half rings were attached in the same way to three of the remaining plots to serve as procedural controls, while the three remaining plots were marked with epoxy putty at the corners and were used as controls (Figure 5.3).

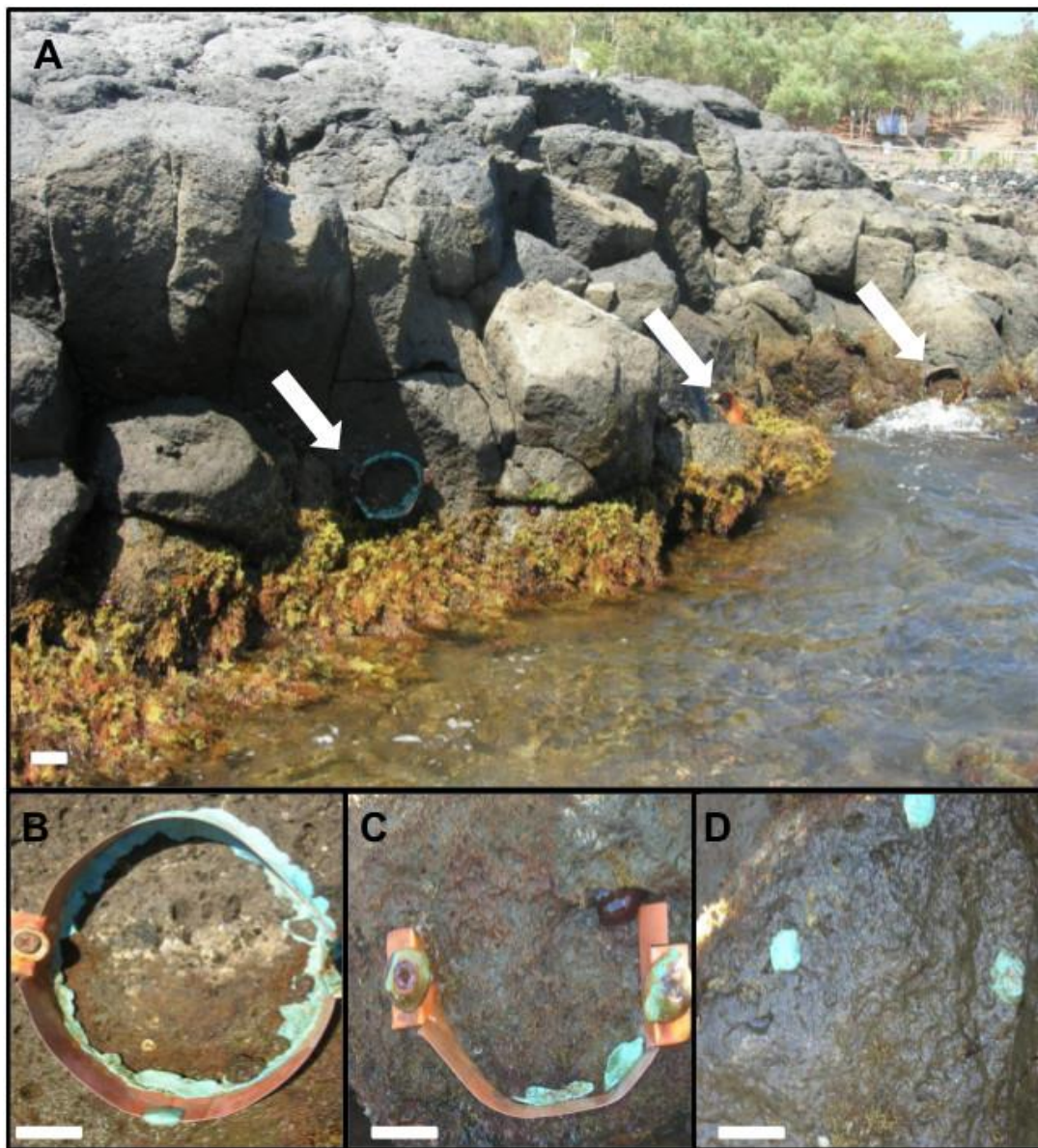


Figure 5.3. Rocky shore on Vulcano showing experimental units (arrows) at the 1200 ppm site during low tide (A). In the lower part of the figure the three treatments are shown: limpet exclosure (15 cm diameter, B), procedural control (C) and control (D); scale bars = 5 cm.

The experiment lasted six months; benthic diversity and abundance in the plots were assessed using visual census approximately every two months (start of experiment, i.e. May 2012; July 2012; September 2012; November 2012). In November 2012, a 10 x 10 cm quadrat in the centre of each plot was denuded of all macroalgae using a hammer and chisel. The samples were preserved in

70% ethanol and were identified to the lowest possible taxonomic level in the laboratory. After identification, algae from each taxon were left to dry at 60°C in the oven for 72h and weighed to obtain dry mass.

5.2.1.3 Limpet abundances and feeding rates

During each visit, limpet abundance was determined at low tide in nine haphazardly chosen replicate plots per site. The plots were the same size as the experimental plots. Limpets were counted and their shell length measured using a Vernier calliper (accuracy ± 1 mm). In July, limpet densities were also determined at high tide to determine whether there was a significant difference in limpet densities related to this parameter.

In November 2012, limpet feeding rates were also measured using wax discs (Thompson *et al.*, 1997). Individually numbered 14 mm diameter plastic holders filled with wax were placed in holes drilled in the rocky substratum. In each site, three grids of 16 holes in which wax discs could be placed were drilled, in a 4x4 configuration with 15 cm gaps between each hole. Discs were left for 14 days on the shore and then collected, and in the laboratory number of grazed discs and percentage cover of grazing marks were determined.

5.2.1.4 Statistical analyses

Benthic species composition and abundance from visual census was tested using a three-factor PERMANOVA. "Site" and "treatment" were considered fixed factors with two (600 and 1200 ppm) and three (exclusion, procedural control and control) levels, respectively, whereas "date" was a random orthogonal factor. A square-root transformation was used to reduce the influence of abundant taxa in the community, a Bray-Curtis dissimilarity matrix was built and

Type III sums of squares with 9,999 unrestricted permutations of the raw data were used to account for small sample sizes. Although the design includes repeated measures on the same plots, sphericity and normality are not necessary for PERMANOVA because the test uses a permutation procedure to generate a distribution for the pseudo-F statistic (analogous to the F statistic in ANOVA). When a limited number of permutations (<100) was available, Monte Carlo p-values were preferred over permutational p-values, which are not reliable in these cases (Anderson *et al.*, 2003). The scraping samples were analysed in the same way, but the experimental design only included the “treatment” and “site” factors. Percent changes in key groups of macroalgae were also analysed using this design.

Variance derived from significant interactions was then decomposed to determine which factor determined the significant interaction, and pairwise tests were performed when necessary. A SIMPER analysis was then used to determine the contribution of each taxon to the average Bray-Curtis dissimilarity between levels of a factor if the PERMANOVA analysis was significant. The same procedure was used to analyse scrapings data, but the design was modified to include only the “site” and “treatment” factors. All analyses above were performed using PRIMER 6 with PERMANOVA+ extension (Plymouth Routines In Multivariate Ecological Research, version 6).

Limpet abundance and length as well as percent cover of marks on wax discs and macroalgal biomass from scrapings were analysed using a two-way ANOVA with “site” and “date” as factors after checking they complied with the normality and variance homogeneity requirements of the analysis. However, no “date” factor was used for the analysis of limpet grazing rates and macroalgal biomass. All the analyses above were performed using SPSS v19.

5.2.2 Methana

To assess whether subtidal herbivores differently affect algal recruitment at different carbon dioxide levels, we conducted a second exclusion experiment at Methana CO₂ seeps.

5.2.2.1 Herbivore surveys

Off Methana, herbivore densities were determined at a site near the seeps (SEEP) and at a reference site (REF A; see Chapter 2 for sites description - detailed sampling dates and sample sizes are reported in Table 1.1D). Densities of *Paracentrotus lividus* and *Arbacia lixula* were determined separately using transects: individuals present between 1 and 2 m depth were counted by snorkelers along five transects (5 m long and 1 m wide) per site per species in September 2012 and June 2013. Fish community composition and biomass were quantified in September 2013 by Maria Salomidi and Yiannis Issaris using a standard visual census technique (while SCUBA diving) within belt transects of 25 m length and 5 m width placed at 3m depth (three replicates, 125 m² surface each). The observer conducting the fish survey moved at constant speed identifying, counting and attributing all individuals to 5 cm size classes within 2.5 m on either side of the 25 m transect line (La Mesa and Vacchi, 1999; Giakoumi *et al.*, 2012). Length estimates of fish from the visual surveys were converted to wet biomass by using the allometric length-biomass conversion: $B = a L^b$, where B is biomass in grams and L is total length in cm. The constant parameters a and b corresponding to the closest geographical area were obtained from Morey *et al.* (2003).

5.2.2.2 Herbivore exclusion

Four sterile 10 x 10 cm ceramic tiles were attached to rocks using epoxy putty and deployed at the two Methana study sites at ~ 2 m depth by snorkelers as

controls; four tiles per site were enclosed in a 1 cm mesh cage to exclude herbivores, and four additional tiles per site were enclosed in a cage missing one side to act as procedural controls (Figure 5.4). The cages were painted using non-toxic antifouling paint (EP-2000, ePaint, Florida) to prevent epiphytes from growing and shading the tiles. Tiles were deployed in September 2012 and recovered in June 2013, when seaweed biomass reaches its annual peak (Ballesteros, 1984).

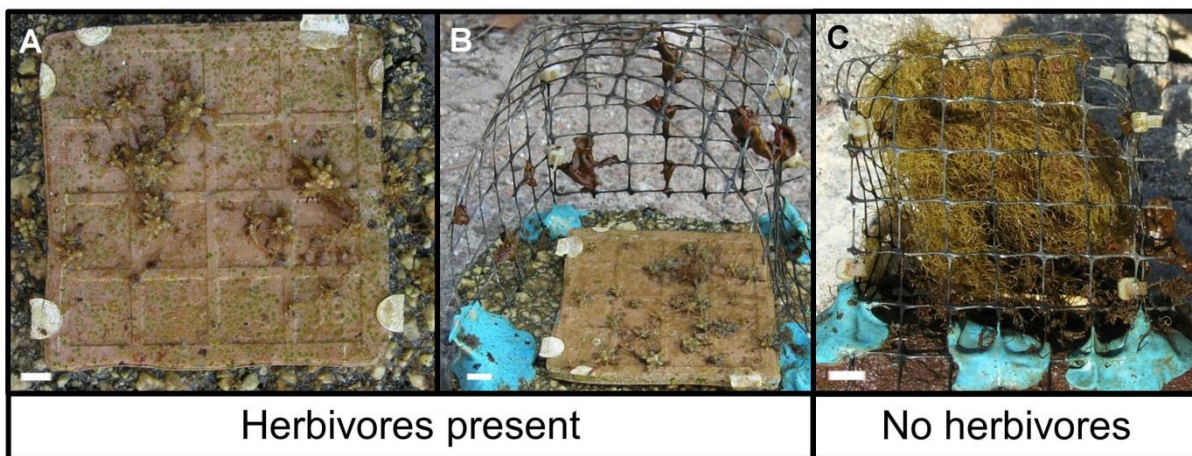


Figure 5.4. Pictures of the three treatments for the herbivore exclusion experiment at Methana taken at the end of the experiment (June 2013): control tile (10 x 10 cm; A), procedural control (B) and herbivore exclusion (C); scale bars = 1 cm.

After recovery, tiles were detached from the rock, put in individual zip-lock bags and stored frozen. In the laboratory, their cover was visually assessed and quantified as percent cover of functional groups. The functional groups used were: fucoid algae (mostly *Cystoseira* sp.), erect brown algae, fleshy brown algae (mostly *Dictyota* sp.), calcifying brown algae (mostly *Padina pavonica*), turf algae (mat-forming algae shorter than 2 cm, mostly *Halopteris scoparia* (Linnaeus) Sauvageau), encrusting black, encrusting green, filamentous green, articulated coralline algae, coralline crustose algae (CCA), serpulid worms, biofilm, bare substratum. The biomass of turf and erect algae was measured by

scraping the algae from the tiles, drying them at 60°C for 72 h and weighing them to obtain dry mass.

5.2.2.3 Statistical analyses

Sea urchin data were analysed with a three-way ANOVA after transforming them (fourth root) to comply with the normality and variance homogeneity requirements of ANOVA. The ANOVA had three fixed factors (species, date and site). Log-transformed biomass of the three recorded herbivorous fish was also analysed using an ANOVA with site and species as fixed factors. All the analyses above were performed using SPSS v19.

Tiles species composition and abundance from visual census was tested using a two-factor PERMANOVA with “site” and “treatment” as fixed factors. A square-root transformation was used to reduce the influence of abundant taxa in the community, a Bray-Curtis dissimilarity matrix was built and Type III sums of squares with 9,999 unrestricted permutations of the raw data were used to account for small sample sizes. Pairwise tests were performed when a factor with more than two levels was significant. A nMDS plot was used to visually inspect the similarities among samples. The same procedure was used to analyse biomass data.

Percent cover or biomass changes in key groups of macroalgae were analysed with a permutational ANOVA using the experimental design described above, but using dissimilarity matrices based on Euclidean distances. Percent cover was used for those functional groups that could not be reliably scraped from the tile (i.e. CCA, encrusting green, encrusting black, biofilm and bare substratum). All analyses above were performed using PRIMER 6 with PERMANOVA+ extension (Plymouth Routines In Multivariate Ecological Research, version 6).

5.3 Results

5.3.1 Vulcano

5.3.1.1 Environmental parameters

Measured and calculated carbonate chemistry parameters are shown in Table 5.1. Over the experiment duration, pH in the 1200 ppm site was approximately 7.8, more than 0.2 points lower than the 600 ppm site. In contrast, measured temperature and salinity were not significantly different between the two sites. At the elevated CO₂ site, seawater pCO₂ was double than in the reference site, even though seawater was still saturated with respect to both calcite and aragonite.

Table 5.1. Mean (\pm SD, n=6) pH, temperature (T) and salinity (S) measured during the experiment at Vulcano between May - October 2012 and pCO₂, bicarbonate ions (HCO₃⁻), carbonate ions (CO₃²⁻), seawater saturation with respect to calcite (Ω_{Ca}) and aragonite (Ω_{Ar}) calculated using CO2Sys.

	pH _{NBS}	T (°C)	S (ppt)	pCO ₂ (μ atm)	HCO ₃ ⁻ (mmol kg ⁻¹)	CO ₃ ²⁻ (mmol kg ⁻¹)	Ω_{Ca}	Ω_{Ar}
600 ppm	8.05 \pm 0.04	25.03 \pm 1.20	38.72 \pm 0.15	602 \pm 51	2025 \pm 39	205 \pm 16	4.77 \pm 0.37	3.16 \pm 0.25
1200 ppm	7.79 \pm 0.17	25.20 \pm 2.78	38.72 \pm 0.39	1211 \pm 192	2200 \pm 53	133 \pm 22	3.10 \pm 0.50	2.06 \pm 0.33

5.3.1.2 Limpet exclusion, abundance and feeding rates

Copper rings were highly effective at excluding limpets from experimental plots. No limpets were found in the enclosure plots during subsequent visits, except for July, when 1-2 small limpets (length < 2 mm) had recruited into three enclosure plots at the 600 ppm site, but they were removed and no limpets crossed the copper rings. The visual census data and the scraping data had

similar results, so only the visual census data analysis is reported for simplicity. Results from the PERMANOVA analysis (Table 5.2) show that the experimental treatment had a different effect at the two sites (Site*Treatment pseudo- $F_{2,68} = 3.997$, $p(\text{perm}) = 0.0086$).

Table 5.2. PERMANOVA analyses of square-root transformed percentage benthic cover in the experimental plots for the experiment performed at Vulcano from May to October 2012. The first table shows main factors and their interactions and degrees of freedom (df), sum of squares (SS), pseudo-F, permutational p and unique permutations for each of them. Treatment x Date interaction and Date both have a significant effect ($p < 0.05$). The second table shows pair-wise comparisons between treatments at both sites with no significant differences between the t-values of any of the treatments at the 1200 ppm site, while all comparisons were significant at the 600 ppm site.

Source	df	SS	Pseudo-F	p(perm)	Unique perms
Site	1	11014.0	8.3517	0.0054	6367
Treatment	2	3322.3	2.5128	0.0926	9950
Date	3	20601.0	5.9490	0.0001	9930
Site x Treatment	2	2337.8	3.9974	0.0086	9955
Site x Date	3	3996.6	1.1541	0.3159	9938
Treatment x Date	6	3827.9	0.5527	0.9450	9905
Site x Treatment x Date**	5	1374.9	0.2382	0.9989	9927
Res	68	78493.0			
Total	90	133570.0			

** Term has one or more empty cells

Within level '1200 ppm' of factor 'Site'			
Groups	t	p(perm)	Unique perms
exclosure, proc control	0.81312	0.5255	1259
exclosure, control	1.2114	0.2832	4344
proc control, control	1.0702	0.3976	420

Within level '600 ppm' of factor 'Site'			
Groups	t	P(perm)	Unique perms
exclosure, proc control	7.4724	0.0016	840
exclosure, control	2.021	0.0444	840
proc control, control	4.2419	0.0019	840

There was also a significant difference between sampling dates (pseudo- $F_{3,68}=5.949$, $p(\text{perm})=0.0001$), which was consistent among sites and

treatments. Pair-wise comparisons between treatments in each site obtained by decomposing the variance in the site*treatment interaction are shown in the lower part of Table 5.2. It is evident that the 600 ppm site had a much higher heterogeneity compared to the elevated CO₂ site because all pairwise comparisons were significant in the former site. However, this means that no conclusion on the overall treatment effect can be drawn.

The SIMPER analysis between sites and among treatment levels at the 600 ppm site showed which taxa contributed the most to the detected differences (Table 5.3). The main drivers of differences between sites were bare rock and brown turf, which together account for almost 40% of the total variability. Both categories increased at the 1200 ppm site, whereas *Padina*, CCA, *Dictyotales* and *Cystoseira* showed the opposite trend. The main drivers of differences among treatments were the dominant categories such as turf algae and bare substratum. Those taxa that changed most among treatment levels such as the calcareous brown alga *Padina pavonica* and the barnacle *Chtamalus stellatus* were also important determinants of the differences between treatments.

Table 5.3. SIMPER analysis showing the average dissimilarities between sites, as well as that among treatments at the 600 ppm site at Vulcano in 2012 pooling dates and which cover group contributes to the dissimilarity up to 90%. For each species, the average abundance in the two groups that are being compared, their average dissimilarity, the dissimilarity to standard deviation ration and the taxon contribution and cumulative contribution are shown.

Groups 600 ppm and 1200 ppm; Average dissimilarity = 53.94						
Taxa	1200 ppm	600 ppm	Av.Diss	Diss/SD	Contrib%	Cum.%
	Av.Abund	Av.Abund				
Bare rock	5.22	4.14	10.81	1.30	20.04	20.04
Brown turf	6.26	5.10	9.56	1.25	17.72	37.77
<i>Padina</i>	0.64	2.64	7.08	1.10	13.13	50.89
CCA	0.60	2.49	6.68	1.33	12.38	63.28

<i>Dictyotales</i>	0.19	1.22	3.59	0.80	6.66	69.94
<i>Cystoseira</i>	0.51	0.68	2.89	0.62	5.36	75.30
<i>Anadyomene</i>	0.53	0.55	2.38	0.80	4.40	79.70
<i>Chthamalus</i>	0.05	0.76	2.26	0.59	4.19	83.89
<i>Dasycladus</i>	0.09	0.73	2.16	0.58	4.00	87.89
Green turf	0.43	0.05	1.45	0.31	2.68	90.57
Groups exclosure and control; Average dissimilarity = 42.52						
	Exclosure	Control				
Taxa	Av.Abund	Av.Abund	Av.Diss	Diss/SD	Contrib%	Cum.%
Bare rock	4.04	4.82	9.06	1.4	21.31	21.31
Brown turf	5.35	4.97	6.45	1.07	15.17	36.48
<i>Padina</i>	2.73	1.32	5.87	1.24	13.81	50.29
<i>Dictyotales</i>	1.02	1.86	4.72	0.96	11.1	61.39
CCA	2.68	3.01	3.93	1.11	9.24	70.63
<i>Chthamalus</i>	1.28	0.19	3.04	0.74	7.14	77.77
<i>Cystoseira</i>	0.9	0.26	2.85	0.64	6.71	84.47
<i>Dasycladus</i>	0.74	0.48	2.28	0.69	5.36	89.83
<i>Anadyomene</i>	0.55	0.29	1.34	0.64	3.16	92.99
Groups exclosure and proc control; Average dissimilarity = 45.14						
	Exclosure	Proc control				
Taxa	Av.Abund	Av.Abund	Av.Diss	Diss/SD	Contrib%	Cum.%
<i>Padina</i>	2.73	3.77	7.66	1.22	16.98	16.98
Bare rock	4.04	3.69	7.51	1.11	16.63	33.6
Brown turf	5.35	4.75	6.56	1.06	14.53	48.14
CCA	2.68	1.59	5.28	1.23	11.71	59.84
<i>Dictyotales</i>	1.02	0.97	3.17	0.89	7.03	66.87
<i>Chthamalus</i>	1.28	0.29	3.06	0.76	6.78	73.65
<i>Cystoseira</i>	0.9	0.66	2.99	0.8	6.62	80.27
<i>Dasycladus</i>	0.74	0.94	2.97	0.75	6.58	86.84
<i>Anadyomene</i>	0.55	0.8	1.77	0.8	3.92	90.76
Groups control and proc control; Average dissimilarity = 48.22						
	Control	Proc control				
Taxa	Av.Abund	Av.Abund	Av.Diss	Diss/SD	Contrib%	Cum.%
Bare rock	4.82	3.69	9.59	0.99	19.88	19.88
<i>Padina</i>	1.32	3.77	9.31	1.14	19.31	39.2
Brown turf	4.97	4.75	7.23	0.88	15	54.19
CCA	3.01	1.59	5.12	0.97	10.62	64.81
<i>Dictyotales</i>	1.86	0.97	4.91	0.96	10.18	74.99
<i>Dasycladus</i>	0.48	0.94	2.93	0.64	6.07	81.06
<i>Cystoseira</i>	0.26	0.66	2.24	0.71	4.65	85.71
<i>Anadyomene</i>	0.29	0.8	2.04	0.85	4.24	89.95
<i>Chthamalus</i>	0.19	0.29	0.94	0.49	1.96	91.91

Some individual species showed patterns related to the experimental treatment (Figure 5.5). The treatments had a significant effect on percent cover of *Padina pavonica* and *Dictyota* sp., but there was no pattern coherent with grazing reduction (i.e. control and procedural control had different values), meaning that these two taxa likely responded to some artefact effect such as changes in light

or water circulation. On the other hand, the barnacle *Chthamalus stellatus* and the red alga *Laurencia* sp. significantly increased their cover when limpets were excluded, the former only at the 600 ppm site and the latter showing a diminished effect at the elevated CO₂ site.

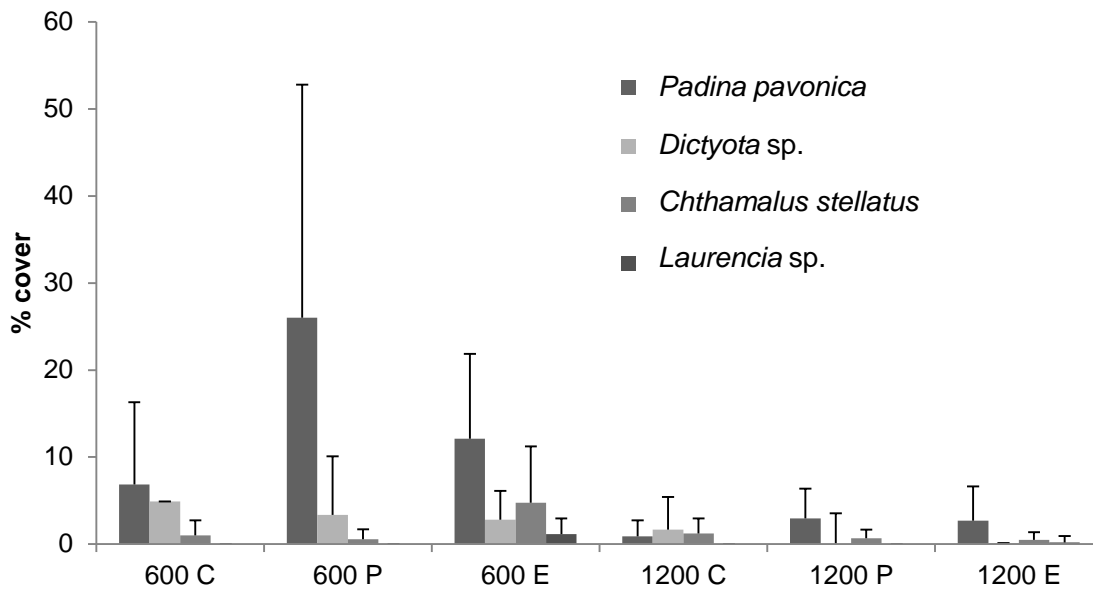


Figure 5.5. Mean percent cover (\pm SD, n=9-18) of species significantly affected by experimental treatments at the exclusion experiment at Vulcano in 2012 (C is control, P is procedural control, E is exclusion) pooling sampling dates at the 600 ppm and 1200 ppm sites.

Statistical analysis of limpet abundance data shows that both site (pseudo- $F_{1,4}=18.223$, $p(\text{perm})=0.006$) and date (pseudo- $F_{4,78}=3.5842$, $p(\text{perm})=0.01$) had a significant effect. Pairwise comparisons confirm that at the 1200 ppm site there was no significant seasonal pattern. Conversely, at the 600 ppm site limpet abundances were higher than those in the 1200 ppm site in spring and summer, but in autumn there was a sudden drop in limpet densities, bringing their values close to those of the 1200 ppm site (Figure 5.6). Limpet abundances sampled at high and low tide in July did not differ significantly.

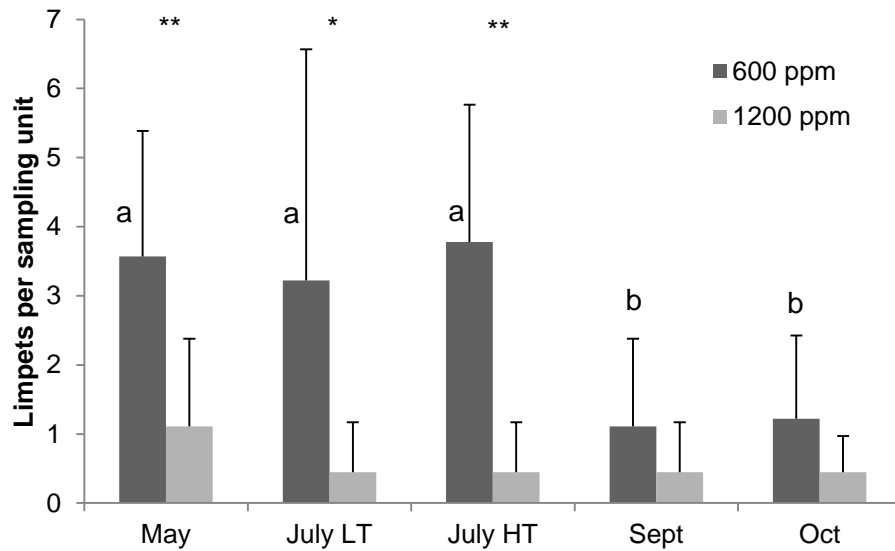


Figure 5.6. Mean (\pm SD, $n=9$) limpet abundance per sampling unit on the four sampling dates for 600 ppm and 1200 ppm sites at Vulcano during the exclusion experiment (May-October 2012). In July limpet densities were assessed twice, once at low tide (LT) and once at high tide (HT) to determine the variability of limpet abundances within a tidal cycle; all other densities were determined at low tide. Different letters mean that limpet abundances are significantly different among sampling dates. Asterisks show when the two sites are significantly different (* = $p < 0.05$; ** = $p < 0.01$).

As for limpet length measurements, the permutational ANOVA results report only a significant effect of site (pseudo- $F_{1,7}=17.861$, $p(\text{perm})=0.028$). Limpets from the 1200 ppm site were bigger than those living in the 600 ppm site, especially in spring and summer. This difference, however, was never significant in pairwise comparisons and was strongly reduced in autumn (Figure 5.7).

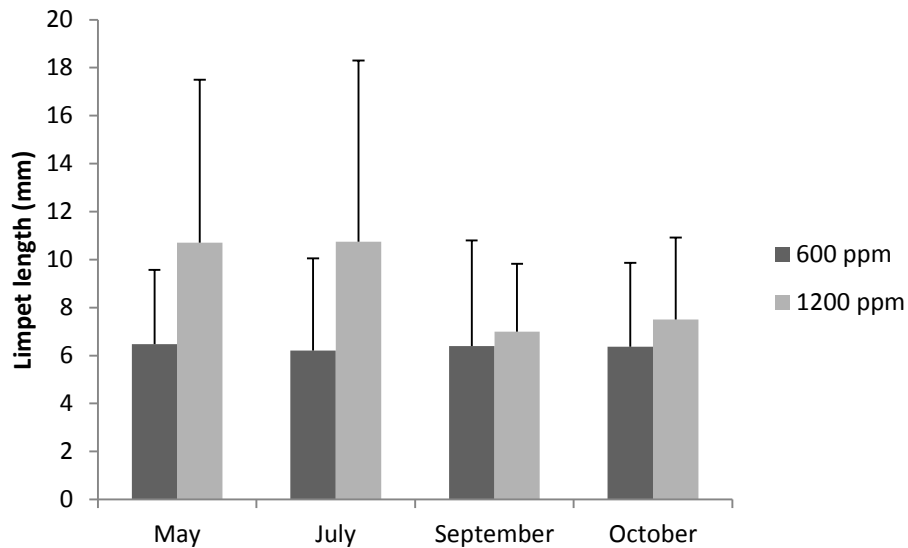


Figure 5.7. Mean (\pm SD) limpet length in the four sampling dates (May, July, September and October 2012) at the 600 and 1200 ppm sites off Vulcano. Limpets in the 1200 ppm site are slightly longer than those in the 600 ppm site. N=4-29.

After verifying that quadrat and position of disc in the quadrat (high or low) had no significant effect on the percentage of grazed disc, arcsin-transformed data were analysed using a one-way ANOVA. Results from the analysis show that there was no significant difference in grazing rates between sites, even though there was a clear trend for higher grazing rates at the 600 ppm site (Figure 5.8).

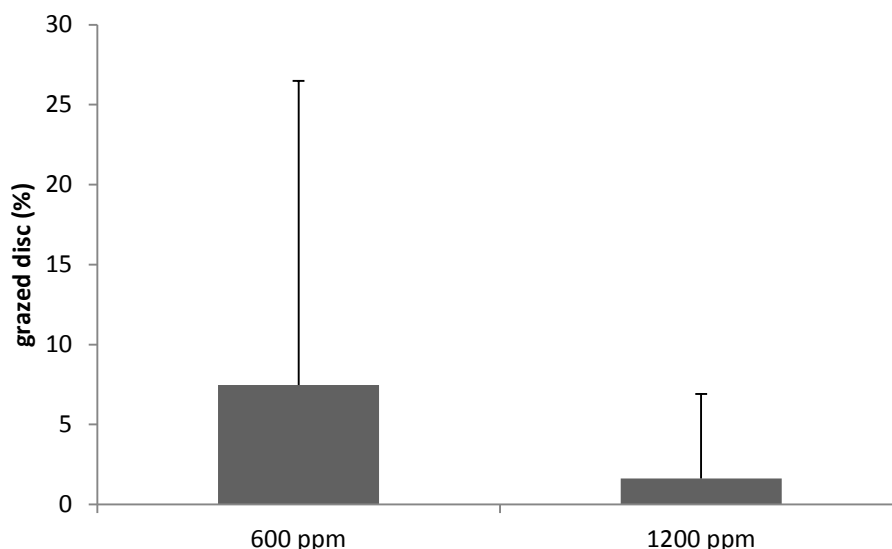


Figure 5.8: Mean (\pm SD) percentage of wax disc grazed by limpets in the 600 ppm site (n=41) and the 1200 ppm site (n = 34) at Vulcano in November 2012.

5.3.2 Methana

5.3.2.1 Environmental parameters

Measured and calculated carbonate chemistry parameters are shown in Table 5.4. The mean pH near the seeps was approximately 7.7, more than 0.3 points lower than the reference site. On the other hand, temperature and salinity were not significantly different between the two sites. At the high CO₂ site, seawater pCO₂ was double that of the reference site, even though on average seawater was still saturated with respect to both calcite and aragonite.

Table 5.4. Mean (\pm SD, n=11-24) pH, temperature (T) and salinity (S) measured at Methana in September 2012 and June 2013 as well as pCO₂, bicarbonate ions (HCO₃⁻), carbonate ions (CO₃²⁻), seawater saturation with respect to calcite (Ω_{Ca}) and aragonite (Ω_{Ar}) calculated using CO2Sys.

	pH _{NBS}	T (°C)	S (ppt)	pCO ₂ (μ atm)	HCO ₃ ⁻ (mmol kg ⁻¹)	CO ₃ ²⁻ (mmol kg ⁻¹)	Ω_{Ca}	Ω_{Ar}
SEEP	7.70 \pm 0.16	25.34 \pm 0.85	38.77 \pm 0.93	1676.8 \pm 643.5	2485.4 \pm 112.4	125.0 \pm 46.5	2.91 \pm 1.06	1.93 \pm 0.71
REF A	8.09 \pm 0.06	25.01 \pm 1.05	38.94 \pm 0.87	586.9 \pm 106.7	2140.5 \pm 63.3	232.1 \pm 25.9	5.40 \pm 0.59	3.57 \pm 0.39

5.3.2.2 Herbivore surveys

Sea urchin densities significantly differed between REF A and SEEP, and the densities of the two species were significantly different as well (Table 5.5). On the other hand, no effect of date was detected, and the lack of significant interactions indicates that both *A. lixula* and *P. lividus* densities changed consistently between sites. As no significant effect of date was detected, sea urchin densities were pooled between dates for easier representation.

Table 5.5. ANOVA on fourth-root transformed sea urchin densities measured at Methana in September 2012 and June 2013. The table shows main factors and their interactions and sum of squares (SS), degrees of freedom (df), Mean Squares (MS), F-ratios (F) and p values. Significant p values (< 0.05) are highlighted.

Source	SS	df	MS	F	p
Site	5.629	1	5.629	17.047	< 0.001
Date	0.704	1	0.704	2.131	0.153
Species	3.952	1	3.952	11.969	0.001
Site * Date	0.085	1	0.085	0.257	0.615
Site * Species	0.029	1	0.029	0.089	0.767
Date * Species	0.487	1	0.487	1.476	0.232
Site * Date * Species	0.068	1	0.068	0.206	0.653
Error	11.887	36	0.330		
Total	51.118	44			

Densities of *A. lixula* were consistently higher than those of *P. lividus* (Figure 5.9), with average densities of the former species ranging from 1.9 to 7.5 individuals in a five-metre transect. On the other hand, *P. lividus* densities ranged from 0.2 to 1.6 individuals. There was also a clear reduction in the densities of both species near the seeps, with *P. lividus* being almost absent at the high CO₂ site.

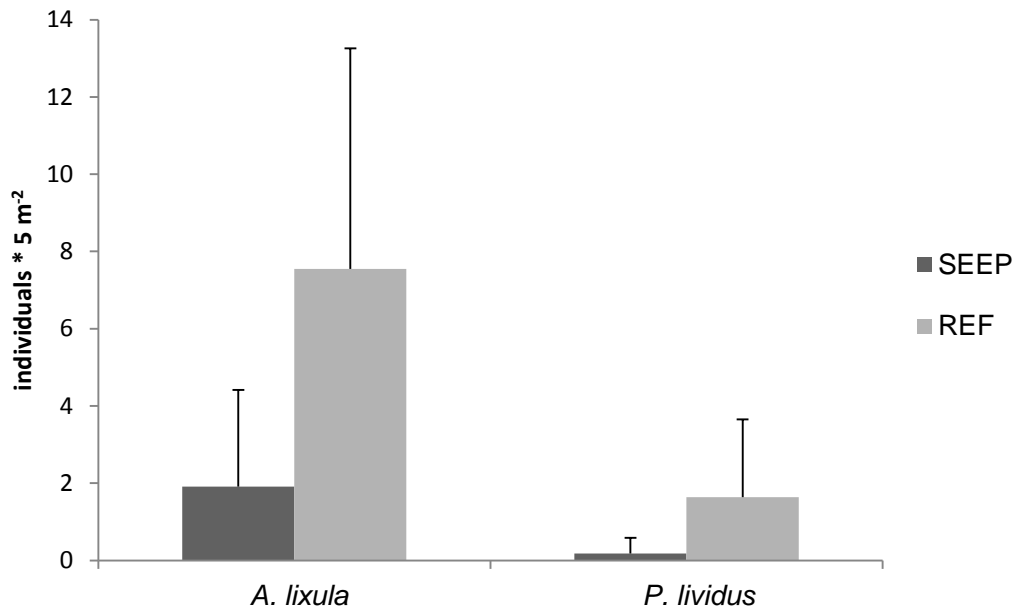


Figure 5.9. Average number (\pm SD, n=11) of sea urchin individuals along a 5 m transect at Methana study sites (SEEP and REF A) pooling data from September 2012 and June 2013.

Three herbivorous fish species were recorded at the study sites: *Sarpa salpa*, *Siganus luridus* and *Sparisoma cretense*. Results from ANOVA (Table 5.6) show that, just as with sea urchins, both site and species had a significant effect on fish biomass. No significant interactions were found, meaning that changes in all species' biomass between sites followed a similar pattern.

Table 5.6. ANOVA on log-transformed herbivorous fish biomass at Methana in June 2013 showing main factors and their interactions and sum of squares (SS), degrees of freedom (df), Mean Squares (MS), F-ratios (F) and p values. Significant p values (< 0.05) are highlighted.

Source	SS	df	MS	F	p
Species	52.403	2	26.201	4.291	0.039
Site	35.608	1	35.608	5.831	0.033
Species * Site	17.190	2	8.595	1.408	0.282
Error	73.279	12	6.107		
Total	363.430	18			

All herbivorous fish species increased in biomass (i.e. total biomass per 25 m transect) near the seeps (Figure 5.10), but the magnitude of the change was very different among species: while *S. cretense* had a low biomass that changed very little between sites, the two other species had very marked changes in biomass between sites. *S. luridus* was present at both sites and its mean biomass increased from 65 to 1565 g from REF A to SEEP. *S. salpa* was absent from REF A, while at SEEP it was the dominant species in terms of biomass (2009 ± 3145 g).

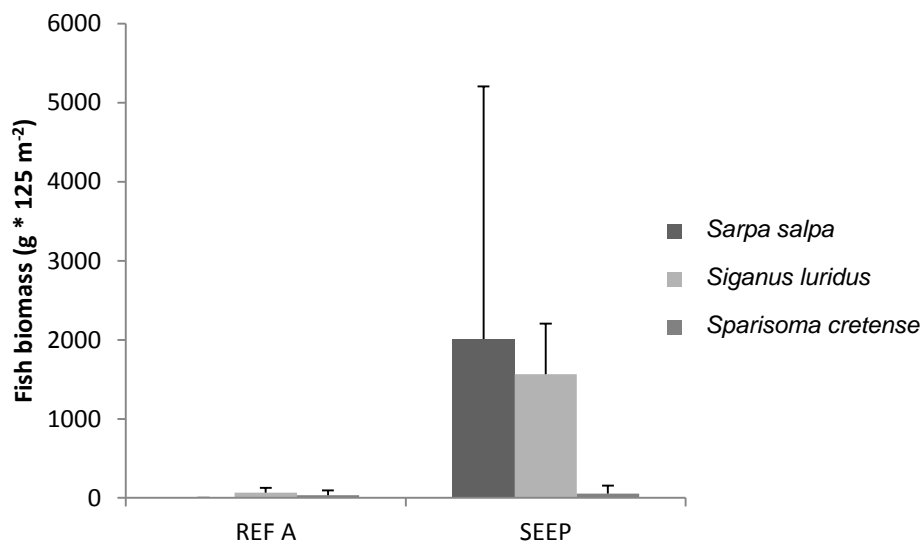


Figure 5.10. Average total biomass (\pm SD, n=3) of herbivorous fish (*Sarpa salpa*, *Siganus luridus* and *Sparisoma cretense*) per 25 m transect at REF A and SEEP in September 2013.

5.3.2.3 Herbivore exclusion

PERMANOVA analysis of tiles cover (Table 5.7) shows that both site and treatment had a significant effect on benthic assemblages, but there was no interaction between the two factors. Since the treatment factor was significant, pairwise comparisons were performed among treatment levels to detect which

pairs were significantly different. The results (Table 5.7, lower part) show that exclusions were significantly different from both control and procedural control, which did not differ between each other.

Table 5.7. PERMANOVA on square-root transformed percentage cover of the uncaged and caged tiles deployed at Methana from September 2012 to June 2013. The first table shows main factors and their interactions and degrees of freedom (df), sum of squares (SS), Mean Square (MS), pseudo-F, permutational p and unique permutations for each of them. The second table shows pair-wise comparisons between treatments pooling sites; for each comparison the t value, p value and number of unique permutations are shown.

Source	df	SS	MS	Pseudo-F	P(perm)	Unique perms
Site	1	5380.7	5380.7	5.3584	0.0003	9938
Treatment	2	11675	5837.4	5.8133	0.0001	9937
Site x Treatment	2	2318.5	1159.2	1.1544	0.3204	9945
Residual	15	15062	1004.2			
Total	20	34487				

Groups	t	P(perm)	Unique perms
Control, Exclusion	2.7397	0.0001	9937
Control, Proc control	1.2182	0.2271	9918
Exclusion, Proc control	2.3722	0.0009	9878

The MDS plot (Figure 5.11) shows that SEEP and REF A were clearly different for all treatments. Controls and procedural controls were closely grouped whereas exclusion tiles were very different. At the SEEP site, a different group of algae (erect brown algae, fleshy brown algae, calcifying brown algae) was dominant in each exclusion tile, whereas at the reference site there was mostly an increase in calcifying brown algal cover when herbivores were excluded.

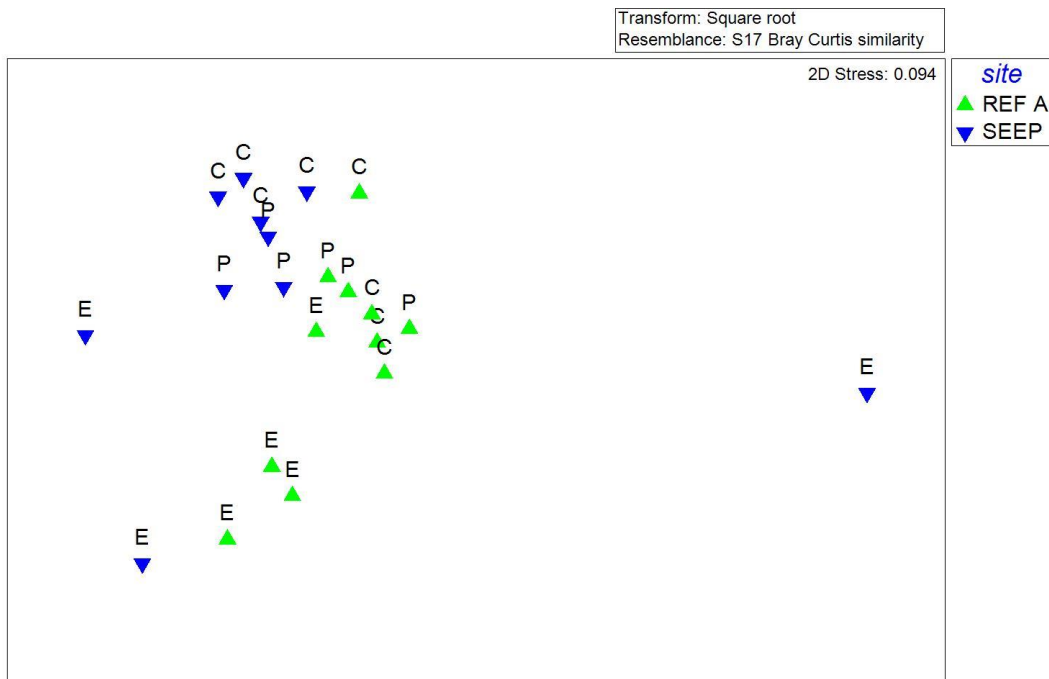


Figure 5.11: MDS plot for the herbivore exclusion experiment performed at Methana from September 2012 to June 2013; green triangles represent tiles placed in REF A, blue triangles are tiles placed in SEEP. Letters above the symbols represent the treatments: C is control, P is procedural control, E is exclusion.

Statistical analysis of the scraping data produced results analogous to the percent cover data at the community level, so only the latter are reported as they are more comprehensive (i.e. they also include encrusting forms). Total biomass significantly differed among treatments (Table 5.8), ranging from about 0.1 g in the controls to approximately 3 g in the exclusions (Figure 5.12). However, at the reference site procedural controls had values intermediate between controls and exclusions.

Table 5.8. PERMANOVA on square-root transformed biomass of macroalgae growing on uncaged and caged tiles deployed at Methana from September 2012 to June 2013. The table shows main factors and their interactions and degrees of freedom (df), sum of squares (SS), Mean Square (MS), pseudo-F, permutational p and unique permutations for each of them.

Source	df	SS	MS	Pseudo-F	p(perm)	Unique perms
Site	1	0.2548	0.2548	1.5942	0.2271	9835
Treatment	2	8.3648	4.1824	26.166	0.0002	9955
Site x Treatment	2	0.3737	0.1869	1.1691	0.334	9959
Residual	15	2.3976	0.1598			
Total	20	11.706				

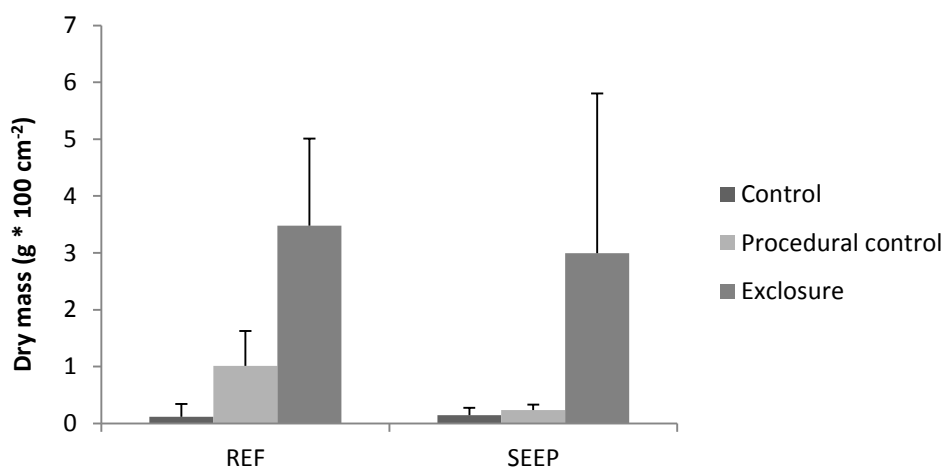


Figure 5.12. Average biomass (\pm SD) of fleshy and erect algae grown on tiles for all three treatments of the herbivore exclusion experiment conducted at Methana from September 2012 to June 2013; $n = 3-4$.

Eight functional groups were significantly different between treatments or sites, four turf or erect and four encrusting forms. Overall, turf and erect algae increased in herbivore exclusions (Figure 5.13A), whereas encrusting forms showed the opposite trend (Figure 5.13B). Biofilm percent cover did not show any clear effect of herbivore exclusion, but it significantly increased at the high CO₂ site. The effect of herbivore exclusion was always clear at SEEP, while at

REF A some functional groups (turf algae, CCA and bare substratum) had biomass or cover values similar between exclusion and procedural control. There were significant differences between sites as well, with turf algae, calcifying brown algae and CCA decreasing as CO₂ increased and fucoid algae, fleshy brown algae, biofilm and bare substratum showing the opposite trend.

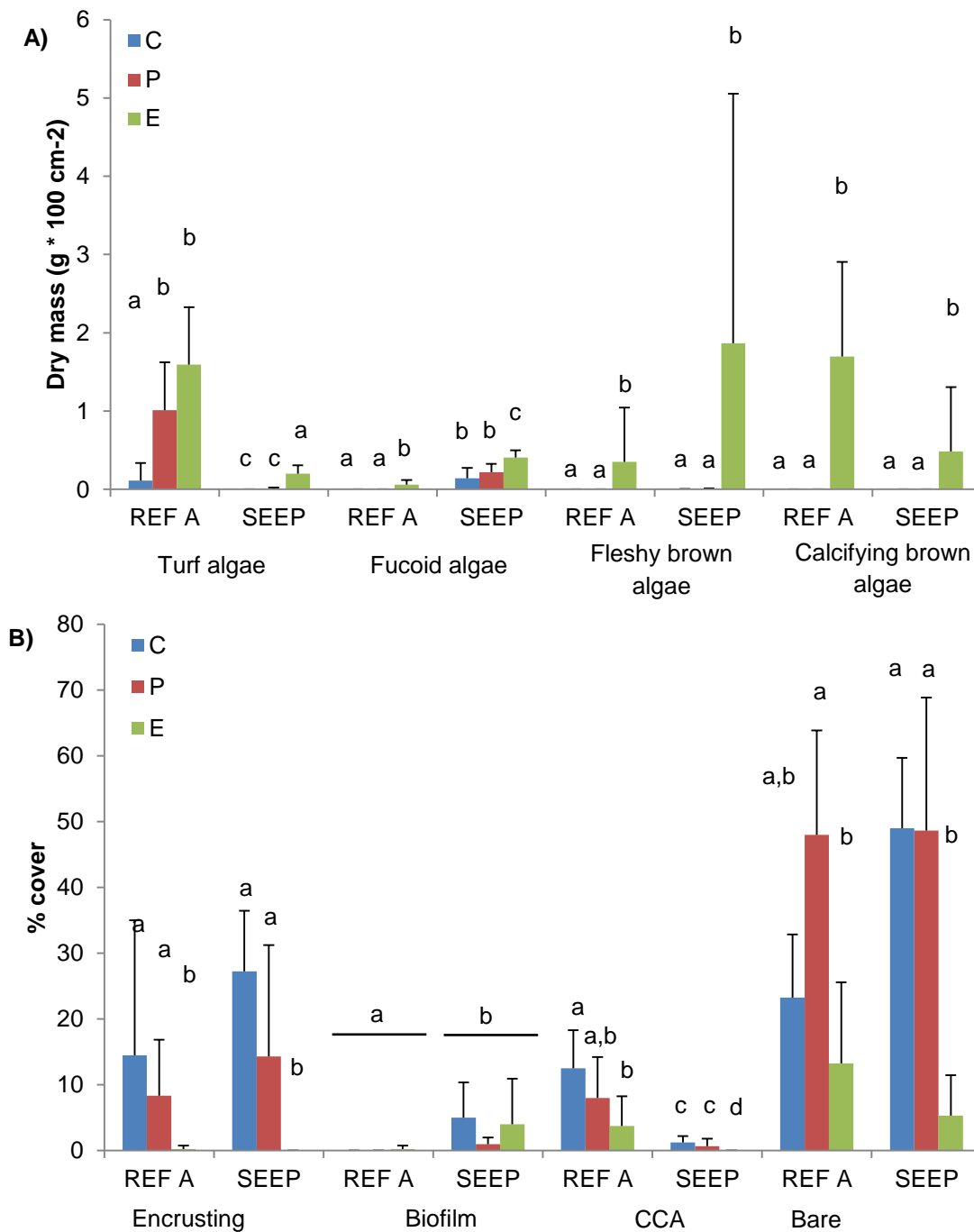


Figure 5.13. Mean (\pm SD, n=3-4) biomass (A) or percent cover (B) of functional groups that showed significant differences between sites (REF A and SEEP) or treatments (C=controls;

P=procedural controls; E=herbivore exclusions). Different letters indicate significantly different sub-groups within a functional group.

5.4 Discussion

The relative role of bottom-up and top-down processes in shaping marine ecosystems has long been a critical issue in marine ecology research. Previous research has shown that relative importance of these two types of processes is highly context-dependant (Burkepile and Hay, 2006). This study shows that in Mediterranean intertidal and subtidal rocky reefs increased pCO₂ (bottom-up) has a significant effect on benthic communities. On the other hand, limpet herbivory (top-down) only had a weak influence on benthic communities at an intertidal rocky shore off Vulcano (Italy), but sea urchin and fish grazing strongly controlled seaweed biomass and community structure in a subtidal habitat off Methana (Greece), even though herbivore community composition changed dramatically as CO₂ levels increased.

Direct effects of carbon dioxide were mostly consistent between Vulcano and Methana. In both areas, bare substratum increased and CCA cover decreased with increasing CO₂. Many crustose coralline algae are well known to be sensitive to ocean acidification (Kroeker *et al.*, 2010; Brodie *et al.*, 2014), and even tolerant species can be outcompeted by non-calcifying algae at elevated CO₂ levels (Kroeker *et al.*, 2013c). The “bare substratum” functional group used at Vulcano included biofilms, which are known to increase in high CO₂ environments (Johnson *et al.*, 2013; Kroeker *et al.*, 2013; Taylor *et al.*, 2014).

At Methana, fleshy brown and furoid algae also significantly increased near the seeps, whereas *Padina pavonica* abundance decreased with increased CO₂ at both sites. Furoid algae are commonly found in high abundances near volcanic

CO₂ seeps (Porzio *et al.*, 2011; Chapter 3), while fleshy brown algae may have increased in cover at high CO₂ after outcompeting *P. pavonica*. Recently, Johnson *et al.* (2012) reported increasing *P. pavonica* densities as CO₂ increased in shallow subtidal waters off Vulcano, possibly because of lower consumption by sea urchins. The decreased *P. pavonica* cover at elevated CO₂ found at Vulcano may be due to the different sampling depth (personal observation): *Paracentrotus lividus*, the species that mostly grazes on *P. pavonica* (Chiantore *et al.*, 2008), is easily dislodged by waves (Bulleri *et al.*, 1999). Intertidal shores off Vulcano are subject to high wave activity, so *P. pavonica* is not likely to be influenced by sea urchin grazing there. On the other hand, *P. pavonica* (the main calcifying brown alga) biomass decreased with increasing CO₂ at Methana, but only when herbivores were excluded, unlike in the study from Johnson *et al.* (2012). This probably happened because fleshy brown algae (*Dictyota* sp.) had a competitive advantage over the calcifier *P. pavonica* as CO₂ increased.

On the other hand, turf algae showed opposite responses to increased CO₂, as their cover increased at Vulcano and decreased at Methana. Turf algae are often advantaged by increased CO₂, as many turf species are extremely fast-growing and possibly carbon-limited (Connell *et al.*, 2013). However, a recent survey at seeps off Ischia reported decreased turf biomass at high CO₂ levels (Porzio *et al.*, 2011). Turf algae is a functional group that includes many species, some of which may be palatable to grazers (Falkenberg *et al.*, 2014), and therefore exhibit very different responses to ocean acidification.

Limpets exerted a weak top-down control on benthic communities off Vulcano in reference conditions, whereas carbon dioxide caused major changes in benthic community structure. Limpets have a decreasing influence on benthic

communities as latitude decreases (Coleman *et al.*, 2006), and in the Mediterranean Sea their effect is not consistent in space and time (Benedetti-Cecchi *et al.*, 2001). When consistent negative effects on filamentous algae were recorded in the Mediterranean Sea, limpet densities were much higher than in this study (Bulleri *et al.*, 2000). Moreover, when the physical environment is stressful limpet grazing has weaker effects on macroalgae (Bazterrica *et al.*, 2007); this could be the case at Vulcano, where communities are exposed to strong wave action.

At Vulcano, limpets influenced percent cover of the barnacle *Chthamalus stellatus* and of a red alga (*Laurencia* sp.). At the 600 ppm site, percent cover of both taxa decreased when limpets were present, while at elevated CO₂ limpets did not have any significant influence on the experimental plots. Limpets can reduce barnacle recruitment by dislodging young individuals (Menge *et al.*, 2010), but at elevated CO₂ levels barnacle recruitment was strongly reduced and no significant effect of limpets was detectable. This may be due to negative effects of elevated carbon dioxide on barnacles in a food-limited habitat (Pansch *et al.*, 2014), decreased limpet densities at elevated CO₂ (this study) or a combination of the above. The genus *Laurencia* is probably vulnerable to grazing, as limpets are thought to control the upper limit of the *Laurencia-Gigartina* belt found in some parts of Britain (Lewis, 1964). At the 1200 ppm site, *Laurencia* sp. percent cover was extremely low even in the control plots; consequently, lack of significant differences among experimental treatments at this site is probably due to this taxon response to elevated carbon dioxide rather than to decreased limpet grazing. So far, no experiments have been performed on this genus' response to ocean acidification, but at volcanic seeps off Ischia

Laurencia obtusa is only present at pH 8.1 and disappears even at moderate pCO₂ levels (Porzio *et al.*, 2011).

The slight increase in limpet length with high CO₂ confirms findings from seeps off Ischia (Hall-Spencer *et al.*, 2008) and could partly explain the trend towards increased grazing rates detected in this study. Increased feeding rates at elevated CO₂ levels have already been reported for some sea snails (Falkenberg *et al.*, 2013b), whereas other species decrease their food consumption at high CO₂ (Russell *et al.*, 2013). Changes in herbivore feeding rates may be due to altered food quality rather than to direct effects of CO₂ on their metabolism (Falkenberg *et al.*, 2013b; Poore *et al.*, 2013), and changes in macroalgal nutritional value at Vulcano could explain the higher feeding rates of limpets living at the 1200 ppm site. Increased calcification costs (Wood *et al.*, 2010), compensatory hyper-calcification at high CO₂ levels (Rodolfo-Metalpa *et al.*, 2011) and shifts in limpet shell mineralogy from calcite to the more energy-expensive aragonite (Langer *et al.*, 2014) could also explain increased limpet grazing rates.

Subtidal herbivore exclusion at Methana dramatically changed benthic communities grown on tiles after nine months. Previous studies show that herbivores have a greater influence on recruiting compared to established macroalgal communities (Korpinen *et al.*, 2008), and subtidal herbivores exert a stronger top-down control than limpets, whose effect is very variable (Benedetti-Cecchi *et al.*, 2001). Herbivore exclusion caused an increase in algal biomass regardless of site, but in the reference site only calcifying brown algae (*Padina pavonica*) colonised the caged tiles. On the other hand, every caged tile at the high CO₂ site was colonised by a different species (*Padina pavonica*, *Dictyota* sp. and erect brown algae). This confirms that non-calcifying algae become

more abundant as $p\text{CO}_2$ increases, likely because of a decreased competitiveness of calcifying species (Porzio *et al.*, 2011; Kroeker *et al.*, 2013).

Herbivory is known to alter outcomes of macroalgal competition, favouring less palatable species (Hereu *et al.*, 2008). At Methana, herbivore-resistant encrusting algae became more abundant at both CO_2 levels when herbivores were present. In addition, macroalgal communities at Methana showed smaller differences between CO_2 levels when herbivores were present (Figure 5.10). Recent evidence shows that grazers can indeed dampen the effects of environmental changes on primary producers, both in terrestrial and in marine ecosystems (Post and Pedersen, 2008; Anthony *et al.*, 2011; Falkenberg *et al.*, 2014).

At Methana, both sea urchin species had reduced densities near the seeps regardless of sampling date, which is in accord with their predicted sensitivity to high CO_2 resulting from laboratory experiments (Dupont *et al.*, 2010). There is a partial disagreement with results from Vulcano, where *P. lividus* densities decreased, but *A. lixula* densities increased with increasing CO_2 (Calosi *et al.*, 2013a). Increased sea urchin densities near volcanic seeps have previously been correlated with low structural complexity of high- CO_2 habitats (Fabricius *et al.*, 2014); *A. lixula* may therefore tolerate moderate carbon dioxide enrichment, but high habitat complexity may prevent its colonisation at seeps off Methana. Sea urchins were replaced by herbivorous fish at high CO_2 levels; functional redundancy of herbivores can maintain top-down control on macroalgal biomass and reduce the effects of multiple stressors on benthic communities (Blake and Duffy, 2010; Eriksson *et al.*, 2011). Fish, however, are highly mobile and could swim in and out of the high CO_2 area (Riebesell, 2008), masking

potential negative effects of ocean acidification such as those on many species' neuroreceptors (Shaw *et al.*, 2013).

Coastal assemblages often have low functional redundancy, and the loss of a few species can negatively affect ecosystem functioning (Micheli and Halpern, 2005). Taxonomic diversity can help marine community resilience to increased temperatures (Allison, 2004), but there is no evidence this applies to community responses to ocean acidification. Here we show that taxonomic diversity helps improving resilience to ocean acidification: herbivorous fish kept grazing pressure high at elevated CO₂, even though sea urchin densities decreased near the seeps. Overfishing of apex predators has led to higher abundances of Mediterranean sea urchins and herbivorous fish, as they are usually not targeted by commercial fisheries (Guidetti and Dulčić, 2007; Guidetti and Sala, 2007). High herbivore densities can often lead to impoverished macroalgal communities, very different from unexploited Mediterranean coastal ecosystems (Sala *et al.*, 2012). Thus, unvaried grazing pressure at different CO₂ levels may maintain suboptimal community structure. However, at a global level herbivorous fish abundance is strongly reduced by overfishing (Micheli and Halpern, 2005), and when this is combined with other herbivores disappearing (e.g. sea urchin mass mortality in Jamaica) benthic habitat can experience dramatic phase shifts (Hughes, 1994).

Bottom-up control (i.e. increase in CO₂) seemed to be the main factor influencing benthic community structure regardless of herbivore consumption levels. Recent research has shown that indirect effects can be as important as the direct effects of CO₂ in shaping community responses to ocean acidification (Kroeker *et al.*, 2013). However, herbivores have the strongest effect and when they are present other indirect effects are reduced or disappear altogether

(Alsterberg *et al.*, 2013). Here we show that carbon dioxide still affects the specific composition of benthic communities in subtidal habitats even when herbivore pressure is strong, even though grazing reduced community structure variability. The most striking finding of this study is that herbivore functional redundancy can offset indirect effects of ocean acidification; this, however, is only possible in unpolluted ecosystems, as diversity is reduced in contaminated marine systems (Johnston and Roberts, 2009). Although neither of the sites studied in this Chapter is a nature reserve, these areas are not heavily impacted by human activities (author's personal observation); it is therefore possible that impacts of ocean acidification on benthic communities will be more severe in polluted areas. Managing local stressors (e.g. eutrophication, heavy metals) is thus essential to maintain high diversity and increase ecosystem resilience to environmental change (Ghedini *et al.*, 2013).

Chapter 6

Seaweed acclimatisation to high pCO₂ at volcanic seeps

Abstract

Most experiments on organism responses to ocean acidification have been conducted for a relatively short time, so there is little evidence for most species' potential for long-term acclimatisation or adaptation, except for some species of phytoplankton. Volcanic seeps can expose benthic communities to increased CO₂ for centuries, and are starting to be used to study adaptive effects of elevated CO₂ on marine organisms. This chapter aims to determine whether dominant macroalgal species at volcanic seeps off Methana (Greece) show evidence of long-term acclimatisation. Ten thalli of the canopy-forming alga *Cystoseira corniculata* and ten thalli of the articulated coralline alga *Jania rubens* were transplanted within and between one high CO₂ and two reference sites, and their physiological performance was assessed after long-term transplants. Neither species showed signs of non-reversible acclimatisation to elevated CO₂ levels, since there were only very small differences between thalli depending on their site of origin. *C. corniculata* seemed to be favoured by increased CO₂, as it had reduced epiphyte cover and higher rETR_{max} (maximum relative electron transport rate) when transplanted near the seeps. At high CO₂, this species also had increased chlorophyll *c* and antheraxanthin content, as well as increased C:N ratios. *Jania rubens* also showed an increase in some pigment concentrations (chlorophyll *a*, violaxanthin, zeaxanthin and phycocyanin) at high CO₂ levels, but in this species all other parameters were unaffected by the transplant. *Cystoseira corniculata* and *Jania rubens* appear not to permanently acclimatise to ocean acidification, but their different physiological responses may alter their competitive interactions. This would help explain the reduction in *J. rubens* cover recorded at increased CO₂ levels off Methana.

6.1 Introduction

Currently, most of the work on ocean acidification biological responses is performed using short-term experiments. As a consequence, there is limited information on the potential for marine algae to permanently acclimatise or adapt to ocean acidification, except for short-lived organisms. For example, the coccolithophore *Emiliania huxleyi* adapted after being exposed to high pCO₂ for about 500 generations. Actually, calcification rates at high CO₂ were always lower than those in reference conditions, but adapted organisms had much higher calcification rates than non-adapted ones (Lohbeck *et al.*, 2012). For longer-lived macroalgae a solution could be studying individuals from volcanic seeps, which can have high CO₂ levels for centuries (Dando *et al.*, 2000).

Genetic adaptation and non-reversible acclimatisation are thought to be rare in marine environments due to their connectivity, which increases the genetic exchange of adults, larvae or other propagules (Palumbi, 1994). However, there are only a few examples of gene flow preventing or slowing down local adaptation in marine species, whereas local adaptation, especially to temperature, is relatively common in marine environments (Sanford and Kelly, 2011). Connectivity of marine environments is therefore unlikely to be as high as previously thought, and speciation can occur over relatively short distances (e.g. Tellier *et al.*, 2011). Moreover, short dispersal distances decrease inter-population gene flow, increasing the likelihood of local adaptation (Endler, 1977). Dominant macroalgal species at seeps off Methana, *Cystoseira corniculata* and *Jania rubens*, have short dispersal distances (< 5 km; Jones and Moorjani, 1973; Susini *et al.*, 2007). It is thus possible that these two species have acclimatised to high and variable pCO₂, as seeps off Methana influence approximately 10 km of shoreline (Baggini *et al.*, 2014).

Porzio (2010) showed that brown algae of the genus *Dictyota* had altered their morphology and had distinct genotypes when seawater pCO₂ was high. In fact, macroalgae exposed to other stressors on relatively short time scales can undergo permanent changes in their physiology or genome. For instance, exposure to low salinity in the Baltic Sea has led to the evolution of a new *Fucus* species after only a few thousand years (Bergström *et al.*, 2005). In another case, *Fucus serratus* individuals from copper-contaminated areas and their offspring are more tolerant to this heavy metal compared with individuals from more pristine areas, although it is not known whether this is transgenerational acclimation or genetic adaptation (Nielsen *et al.*, 2003).

Non-reversible acclimatisation to high pCO₂ might therefore occur in macroalgae, and studying species from volcanic seeps might give us an insight on the possible mechanisms. The aim of this chapter is to assess whether two dominant seaweed species growing near CO₂ seeps off Methana (Greece) were permanently acclimatised to high and variable pCO₂ conditions using reciprocal transplantations (Sanford and Kelly, 2011). Hypotheses tested were:

- 1) Growth rates and maximum quantum yield (F_v/F_m) are higher in individuals transplanted at the same CO₂ level they are acclimatised to, since acclimatised populations perform best in their origin conditions (Leimu and Fischer, 2008);
- 2) Pigment content is higher in coralline algae acclimatised to reference conditions and decreases at elevated CO₂ (*Jania rubens*; Gao and Zheng, 2010), whereas chlorophyll in brown algae increases as seawater pCO₂ increases (*Cystoseira corniculata*; Johnson *et al.*, 2012);

- 3) Total phenolic compounds, such as phlorotannins, are higher in brown algae acclimatised to high pCO₂ (Swanson and Fox, 2007);
- 4) Carbon:nitrogen ratio increases in seaweed exposed to elevated carbon dioxide in the long term because there is more inorganic carbon available, not as a result of acclimatisation (Koch *et al.*, 2013);
- 5) Inorganic carbon content in *J. rubens* decreases in individuals from reference conditions transplanted to the high CO₂ area because of skeleton dissolution, whereas individuals from high CO₂ have higher inorganic carbon content when transplanted to the reference sites because of persistent hyper-calcification (Rodolfo-Metalpa *et al.*, 2011).

Evidence from macroalgae that have acclimatised to high CO₂ conditions is essential to assess the adaptation potential of macroalgae to ocean acidification. There is relatively little information on long-term responses of macroalgae to elevated CO₂, and only a few studies have tackled the issue using field-based experiments. To date, evidence from laboratory experiments indicates that temperate macroalgal communities will change their specific composition as seawater pCO₂ increases; this has potential knock-on effects on marine food webs, nutrient cycling and carbon storage (Brodie *et al.*, 2014). However, there is very little information on macroalgal adaptation potential to increased CO₂, meaning that coastal ecosystems might not change as much as anticipated if macroalgae can acclimatise to elevated pCO₂ levels (Sunday *et al.*, 2014).

6.2 Methods

6.2.1 Experimental design and field sampling

Two common and abundant macroalgal species in Methana were examined for signs of long-term acclimatisation to high pCO₂; detailed sampling dates and sample sizes are reported in Table 1.1E. Ten thalli for each species were transplanted within and between one high CO₂ site (SEEP) and two reference sites (REF A and REF B) as shown in Figure 6.1; see Chapter 2 for site descriptions. All specimens were transplanted by detaching thalli with a small chip of rock still attached using hammer and chisel and attaching them to rocky substratum in the target site using epoxy putty (Z-Spar A-788 Splash Zone Epoxy Putty). This method has been previously used for *Cystoseira* in the Mediterranean Sea and has a good success rate (Sales *et al.*, 2011). Physiological parameters were then measured in the transplanted seaweeds and in seven unmanipulated thalli of each species per site; the number of unmanipulated thalli was selected to reflect the average number of transplanted thalli left at the end of the experiments.

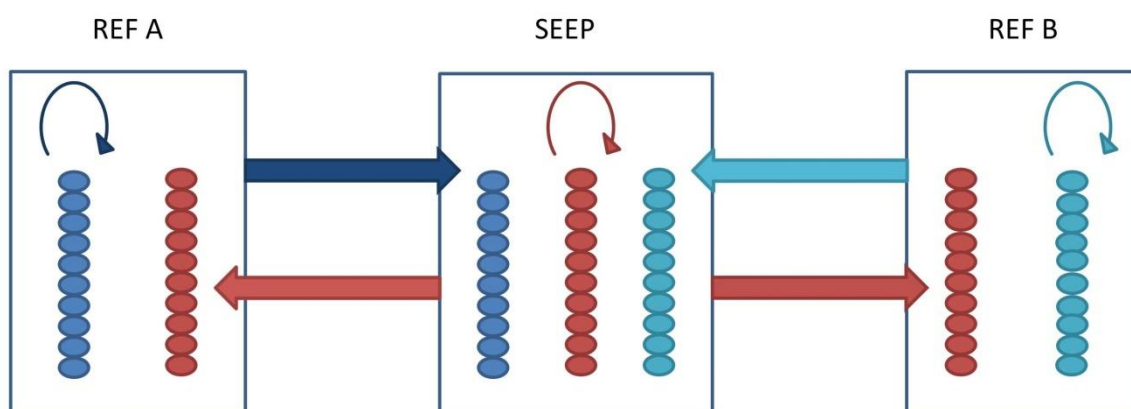


Figure 6.1. Scheme of the experimental design for reciprocal transplantations of *Cystoseira corniculata* transplanted from September 2012 to June 2013 and *Jania rubens* transplanted from June to September 2013. Ten individuals of each species from the high CO₂ site

(SEEP) and the two reference sites (REF A and REF B) were transplanted within their site of origin as procedural controls (round arrows). Ten individuals per species from both reference sites were also transplanted to the SEEP site (blue and light blue arrows). Furthermore, ten individuals per species originally from the high CO₂ site were transplanted to REF A and other ten individuals were transplanted to REF B (red arrows).

Cystoseira corniculata is a furoid alga and this genus is the main canopy-former in the Mediterranean Sea, where it indicates relatively pristine environmental conditions (Benedetti-Cecchi *et al.*, 2001). It was the dominant macroalgal species at seeps off Methana, and has a biomass maximum between May and June in the region (Haritonidis *et al.*, 1986). This species was transplanted in September 2012 and physiological parameters were measured in June 2013 (in correspondence to its biomass peak). The articulate coralline alga *Jania rubens* is an epiphytic thermophilic species and is extremely common in the study area in spring and summer, with a bloom around August (Beleggratis *et al.*, 1999). *Jania rubens* thalli were transplanted in June 2013 (when thalli are large enough to be visible) and their physiological parameters were measured in September 2013 (in correspondence to its biomass peak); thalli of this species transplanted to REF A were all lost due to stormy weather, so only samples from SEEP and REF B were analysed.

Difference in maximum thallus height between the beginning and the end of transplantation was measured placing thalli on graph paper (accuracy ± 1 mm) and used to calculate relative growth for *C. corniculata* and *J. rubens*. Tips were checked for grazer marks. While measuring growth, epiphyte cover of *C. corniculata* thalli was also evaluated using a scale from 1 (epiphyte cover < 25%) to 4 (epiphyte cover > 75%). Chlorophyll *a* fluorescence of the macroalgae was measured with a pulse amplitude modulated fluorometer

(Diving PAM, Walz, Effeltrich, Germany). The maximum photochemical quantum yield of photosystem II (F_v/F_m) was measured after 15 minutes of dark adaptation (Schreiber *et al.*, 1995), then rapid light curves (eight points at 20 s intervals, E1=16, E2=24, E3=34, E4=52, E5=77, E6=118, E7=176 and E8=250 $\mu\text{mol photon m}^{-2} \text{s}^{-1}$) were conducted and non-photochemical quenching (NPQ) was measured. The physiological parameters I_k , $rETR_{\text{max}}$ and α_{ETR} (saturation irradiance for ETR, maximum relative electron transport rate and photochemical efficiency, respectively) were calculated using a non-linear regression analysis (Eilers and Peeters, 1988).

Tissue samples for laboratory analyses were collected between 8:00 and 10:00 to avoid the confounding effect of mid-day photoinhibition on pigments (Häder *et al.*, 1996) and dried with silica gel for C:N ratio analysis (for all species), total phenolic compounds and tissue P analyses (*C. corniculata* only) and inorganic carbon content (*J. rubens*). More tissue was placed in liquid nitrogen and stored at -60 °C for pigment analysis (all species).

6.2.2 Laboratory analyses

The total carbon and nitrogen content in dried samples of *C. corniculata* and the organic carbon and nitrogen content of *J. rubens* thalli was measured using a CHN Analyzer (CE Instruments EA1110 elemental analyser). Approximately 1-3 mg of tissue were ground to a powder and packed into aluminum capsules for analysis of total carbon and nitrogen. For organic carbon and nitrogen content of *J. rubens*, approximately 10 mg of sample was ground to powder, placed in silver capsules, acidified with 20 μl of 2M HCl 12 times at 6-12 hours intervals and dried in an oven at 60°C. Separate tissue samples from *J. rubens* were dried for 72 h at 60°C, weighed to obtain dry mass and then put for 24h in a

muffle furnace at 400°C to burn all organic matter and obtain the mass of inorganic carbon. For total phenolic compounds analysis, ~100 mg of freeze-dried tissue was ground and extracted in methanol at 4°C for 24 h. Total phenolic compounds of *C. corniculata* were then analysed using a method modified from Kamal (2011). Seaweed extracts were diluted in distilled water (10% methanol extract, 90% distilled water) and absorbance at 765 nm was measured using a 96 well plate and a FLUOstar Omega microplate reader (BMG Labtech). Each well contained 20 µl 50% Folin-Ciocalteu reagent (Folin and Ciocalteu, 1927), 10 µl Na₂CO₃ (1.5 M) and 10 µl sample solution. Phloroglucinol (1,3,5-trihydroxybenzene) was used as a standard. Plates were refrigerated overnight before measurement, and eight replicate measurements per sample were made.

Samples of *C. corniculata* and *J. rubens* for pigment analysis were freeze-dried in the dark for 24h, after which they were ground in pure acetone using a mortar and pestle. Extraction occurred at 4°C for 24 h in the dark. After extraction, samples were centrifuged at 4000 rpm for 15 min at 4°C. Pigment content was then analysed using the Gauss-Peak Spectra method (Küpper *et al.*, 2007). Samples were scanned in a dual-beam spectrophotometer from 350 nm to 750 nm at 1 nm steps. The absorbance spectra were introduced in the GPS fitting library, using SigmaPlot. The employment of this library allowed to identify and quantify Chlorophyll *a*, Chlorophyll *c*₁ and *c*₂, Pheophytin *a*, Fucoxanthin, Antheraxanthin, β-carotene, Violaxanthin and Zeaxanthin for *C. corniculata* (Küpper *et al.*, 2007) and Chlorophyll *a*, Pheophytin *a*, β-cryptoxanthin, Antheraxanthin, β-carotene, Violaxanthin and Zeaxanthin for *J. rubens*. *J. rubens* carotenoids were selected based on Schübert *et al.* (2006). For phycobiliproteins in *J. rubens* samples approximately 0.5 g of tissue was

homogenised in 10 mL 0.1 M phosphate buffer (pH 6.8). After being left at 4°C in the dark overnight, extracts were centrifuged for 10 minutes at 1000g and then read in the spectrophotometer at the wavelengths determined by Beer and Eshel (1985).

6.2.3 Statistical analyses

All data were checked for compliance with ANOVA assumptions (normality by visually inspecting data and homogeneity of variance using Levene's test) and transformed when necessary. Growth was analysed using a two way ANOVA with 'site of origin' and 'site of destination' as fixed factors. When a factor had a significant effect, a Tukey HSD pair-wise test was performed. Epiphyte cover of *C. corniculata* was analysed using a Kruskal-Wallis analysis with 'treatment' as a fixed factor. Separate MANOVAs were used to analyse treatment effects on C:N and N:P ratios (*C. corniculata*), C and N content (*J. rubens*), photochemical parameters (both species), pigments content (both species) and phycobilins (*J. rubens*). When the data did not meet Mauchly's test of sphericity, the degrees of freedom were corrected using Greenhouse-Geisser estimates of sphericity. CaCO₃ content (*J. rubens*) and total phenolic compounds (*C. corniculata*) were analysed using one-way ANOVAs with 'treatment' as a fixed factor.

6.3 Results

6.3.1 Growth and epiphyte cover

Relative growth of *C. corniculata* thalli was significantly different among transplantation sites (Table 6.1). Pairwise comparisons showed that thalli transplanted to the high CO₂ site (SEEP) and one reference site (REF A) grew more than those transplanted to the other reference site (REF B; Figure 6.2).

Different pCO₂ did not seem to have significant effects on linear growth of this macroalgal species.

Table 6.1. ANOVA results for transplanted *C. corniculata* thalli growth. The table shows main factors and their interactions and sum of squares (SS), degrees of freedom (df), Mean Squares (MS), F-ratios (F) and p values. Significant p values (< 0.05) are highlighted. The last row shows results from pairwise comparisons between sites of destination, different letters represent significantly different groups.

Source	Type III SS	df	MS	F- ratio	p
Origin	0.065	2	0.032	1.028	0.368
Destination	0.614	2	0.307	9.766	<0.001
Origin * Destination	0.114	2	0.057	1.822	0.176
Error	1.131	36	0.031		
Total	1.826	42			
Post-hoc subsets	REF B ^a	REF A ^b	SEEP ^b		

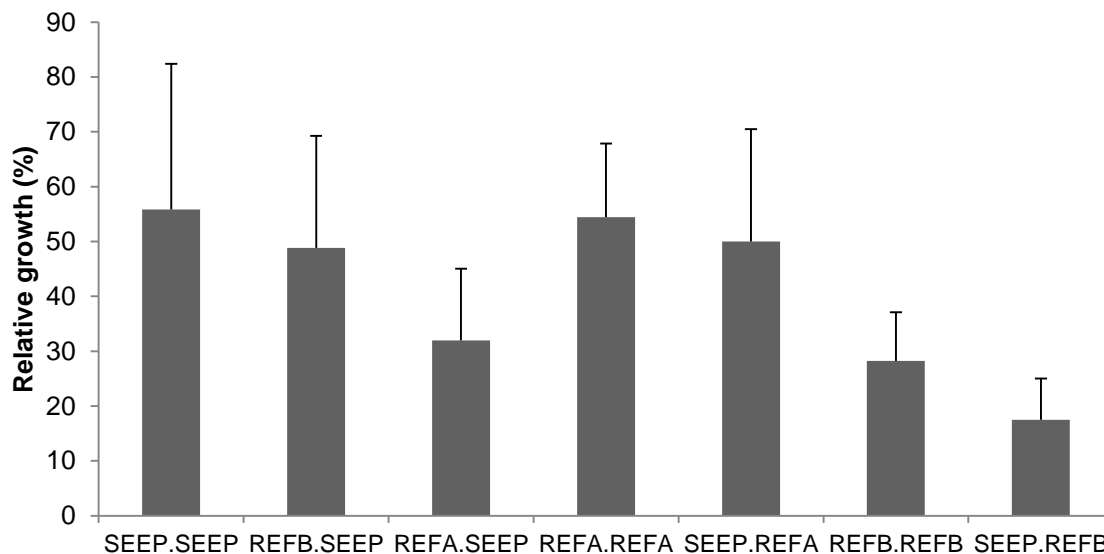


Figure 6.2. Mean relative growth (\pm SD, n=3-10) of *C. corniculata* thalli transplanted at Methana from September 2012 to June 2013 within and between two reference sites (REF A and REF B) and one high CO₂ site (SEEP). Treatments are shown as “Site of origin.Site of transplant”.

Transplanted *J. rubens* thalli did not exhibit any significant difference in relative growth (Table 6.2). Even though thalli transplanted from SEEP had higher

average growth than those transplanted from the reference site (REF A), the two groups did not show any significant difference as variability was very high (Figure 6.3).

Table 6.2. ANOVA results for transplanted *J. rubens* thalli growth. The table shows main factors and their interactions and sum of squares (SS), degrees of freedom (df), Mean Squares (MS), F-ratios (F) and p values.

Source	Type III SS	df	MS	F-ratio	p
Origin	1869.486	1	1869.486	2.312	0.149
Destination	5.400	1	5.400	0.007	0.936
Origin * Destination	75.479	1	75.479	0.093	0.764
Error	12130.052	15	808.670		
Total	14019.002	18			

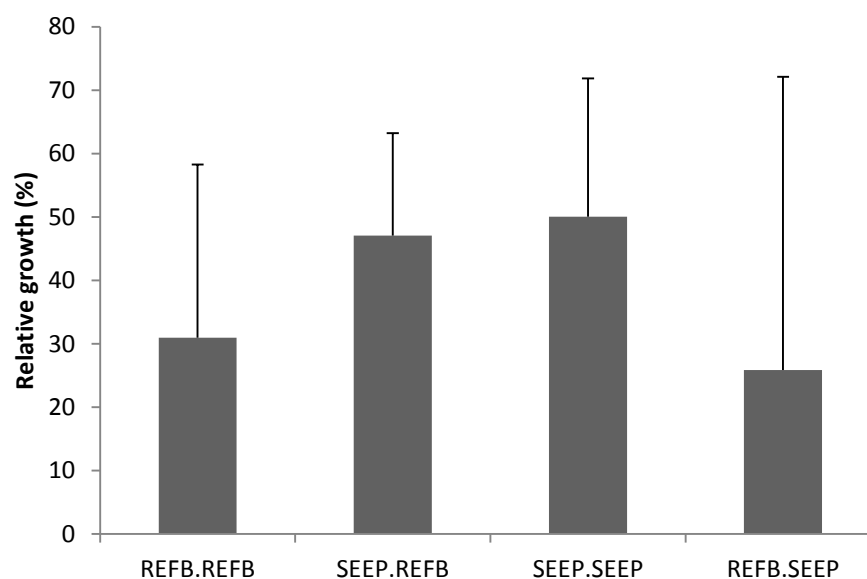


Figure 6.3. Mean relative growth (\pm SD, n=4-6) of *J. rubens* thalli transplanted at Methana from June 2013 to September 2013 within and between one reference site (REF B) and one high CO₂ site (SEEP). Treatments are shown as “Site of origin.Site of transplant”.

Epiphytes cover of *C. corniculata* thalli was significantly different among treatments according to a Kruskal-Wallis test. In general, thalli collected from or transplanted to the high CO₂ site (SEEP) had lower epiphytes cover compared

to those collected from or transplanted to the two reference sites (REF A and REF B). Macroalgae transplanted from high CO₂ levels to the reference sites (i.e. SEEP.REFA and SEEP. REFB) have lower epiphytes cover than those transplanted within the same reference site (i.e. REFA.REFA and REFB.REFB; Figure 6.4).

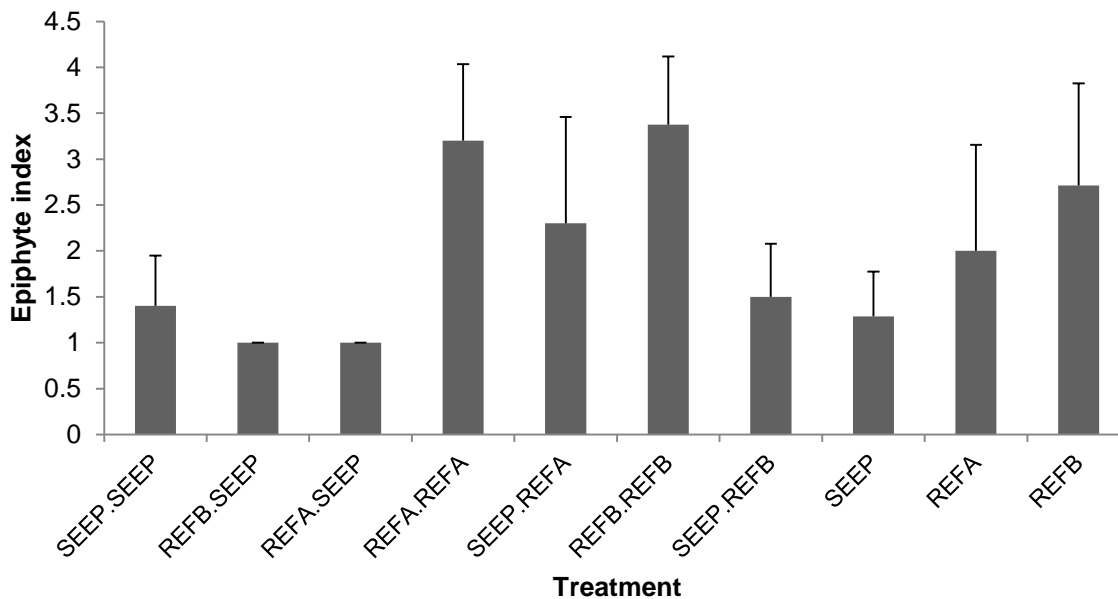


Figure 6.4. Mean epiphyte cover (\pm SD, n=3-10) of *C. corniculata* thalli transplanted at Methana from September 2012 to June 2013 within and between two reference sites (REF A and REF B) and one high CO₂ site (SEEP). Treatments are shown as “Site of origin.Site of transplant”; the last three treatments (SEEP, REF A and REF B) are unmanipulated thalli collected in June 2013.

6.3.2 Photosynthetic parameters

Maximum relative electronic transport rate ($rETR_{max}$) and saturation irradiance for ETR (I_k) were significantly different among treatments for *C. corniculata* transplanted at Methana from September 2012 to June 2013 (Table 6.3). The main differences in relative electron transport rates were connected with site of transplant, with thalli transplanted to SEEP generally having higher values of

rETR_{max} than those transplanted to the reference sites (Table 6.4). On the other hand, I_k did not show any consistent trend related to the experimental treatments.

Table 6.3. MANOVA on photosynthetic parameters in *C. corniculata* thalli transplanted at Methana from September 2012 to June 2013 within and between two reference sites (REF A and REF B) and one high CO₂ site (SEEP). F-ratios (F) and p values are reported when significant (p<0.05).

Response variable	Treatment
rETR _{max}	F(9,44)=4.01; p=0.001
I _k	F(9,44)=2.46; p=0.023
α	-
NPQ	-
F _v /F _m	-

Table 6.4. Mean photosynthetic parameters (± SD, n=3-9) of *C. corniculata* thalli transplanted at Methana from September 2012 to June 2013 within and between two reference sites (REF A and REF B) and one high CO₂ site (SEEP). Treatments are shown as “Site of origin.Site of transplant”; the last three treatments (SEEP, REF A and REF B) are unmanipulated thalli collected in June 2013.

Origin.Destination	rETR _{max} (μmol e m ⁻² s ⁻¹)	I _k (μmol photons m ⁻² s ⁻¹)	α _{ETR}	NPQ	F _v /F _m
SEEP.SEEP	21.7 ± 12.2	87.4 ± 44.1	0.247 ± 0.052	0.065 ± 0.104	0.644 ± 0.053
REFB.SEEP	19.3 ± 11.4	66.0 ± 37.2	0.305 ± 0.059	0.104 ± 0.109	0.665 ± 0.053
REFA.SEEP	15.5 ± 3.4	62.2 ± 5.2	0.247 ± 0.036	0.231 ± 0.041	0.664 ± 0.022
REFA.REFA	9.6 ± 3.6	53.5 ± 22.1	0.185 ± 0.033	0.379 ± 0.240	0.594 ± 0.035
SEEP.REFA	17.0 ± 13.5	100.7 ± 94.3	0.194 ± 0.078	0.280 ± 0.292	0.587 ± 0.083
REFB.REFB	13.3 ± 25.7	108.0 ± 248.3	0.369 ± 0.417	0.313 ± 0.192	0.672 ± 0.069
SEEP.REFB	7.3 ± 3.7	67.6 ± 37.8	0.132 ± 0.072	0.219 ± 0.240	0.590 ± 0.123
SEEP	30.5 ± 16.7	133.3 ± 62.5	0.225 ± 0.055	0.293 ± 0.193	0.628 ± 0.064
REFA	13.3 ± 5.3	60.4 ± 33.0	0.364 ± 0.374	0.311 ± 0.206	0.610 ± 0.098
REFB	3.8 ± 0.7	17.2 ± 7.0	0.242 ± 0.075	0.176 ± 0.097	0.588 ± 0.041

No significant differences among treatments were detected using a MANOVA for *J. rubens* transplanted from June to September 2013 (Table 6.5). The

measured (NPQ, F_v/F_m) and calculated ($rETR_{max}$, I_k , α_{ETR}) parameters for *J. rubens* are reported in Table 6.6, and all parameters are generally lower in *J. rubens* than in *C. corniculata* (Table 6.4).

Table 6.5. MANOVA on photosynthetic parameters in *J. rubens* thalli transplanted at Methana from June 2013 to September 2013 within and between one reference site (REF B) and one high CO₂ site (SEEP). F-ratios (F) and p values are reported when significant ($p < 0.05$).

Response variable	Treatment
$rETR_{max}$	-
I_k	-
α	-
NPQ	-
F_v/F_m	-

Table 6.6. Mean photosynthetic parameters (\pm SD, $n=3-4$) of *J. rubens* thalli transplanted at Methana from June 2013 to September 2013 within and between one reference site (REF B) and one high CO₂ site (SEEP). Treatments are shown as "Site of origin.Site of transplant"; the last three treatments (SEEP, REF A and REF B) are unmanipulated thalli collected in September 2013.

Origin.Destination	$rETR_{max}$ ($\mu\text{mol e m}^{-2} \text{s}^{-1}$)	I_k ($\mu\text{mol photons m}^{-2} \text{s}^{-1}$)	α_{ETR}	NPQ	F_v/F_m
SEEP.SEPE	5.2 \pm 5.2	39.9 \pm 44.7	0.136 \pm 0.031	0.095 \pm 0.083	0.485 \pm 0.018
REFB.SEPE	5.4 \pm 4.1	57.7 \pm 47.0	0.163 \pm 0.126	0.147 \pm 0.140	0.441 \pm 0.078
REFB.REFB	10.1 \pm 13.5	76.4 \pm 83.7	0.110 \pm 0.038	0.094 \pm 0.162	0.454 \pm 0.054
SEEP.REFB	6.9 \pm 4.8	128.7 \pm 155.2	0.489 \pm 0.826	0	0.394 \pm 0.119
SEEP	3.5 \pm 3.2	48.4 \pm 21.4	0.069 \pm 0.041	0.110 \pm 0.056	0.383 \pm 0.080
REFA	2.4 \pm 0.5	35.4 \pm 16.1	0.077 \pm 0.032	0.158 \pm 0.106	0.397 \pm 0.042
REFB	3.1 \pm 0.4	30.7 \pm 18.4	0.136 \pm 0.089	0.253 \pm 0.116	0.458 \pm 0.046

6.3.3 Pigment contents

Chlorophyll *c* and antheraxanthin content of *C. corniculata* transplanted from September 2012 to June 2013 significantly differed among treatments, while all other pigments were not significantly affected (Table 6.7). Thalli transplanted to

reference sites had lower chlorophyll *c* and antheraxanthin content than those transplanted to the high CO₂ site (Figure 6.5). Unmanipulated thalli, however, did not show a similar pattern, with very small differences among sites.

Table 6.7. MANOVA on pigments content in *C. corniculata* thalli transplanted at Methana from September 2012 to June 2013 within and between two reference sites (REF A and REF B) and one high CO₂ site (SEEP). F-ratios (F) and p values are reported when significant (p<0.05).

Response variable	Treatment
Chl a	-
Chl c	F(9,53)=3.552 p=0.002
Pheophytin a	-
β-carotene	-
Fucoxanthin	-
Violaxanthin	-
Antheraxanthin	F(9,53)=4.117 p<0.001
Zeaxanthin	-

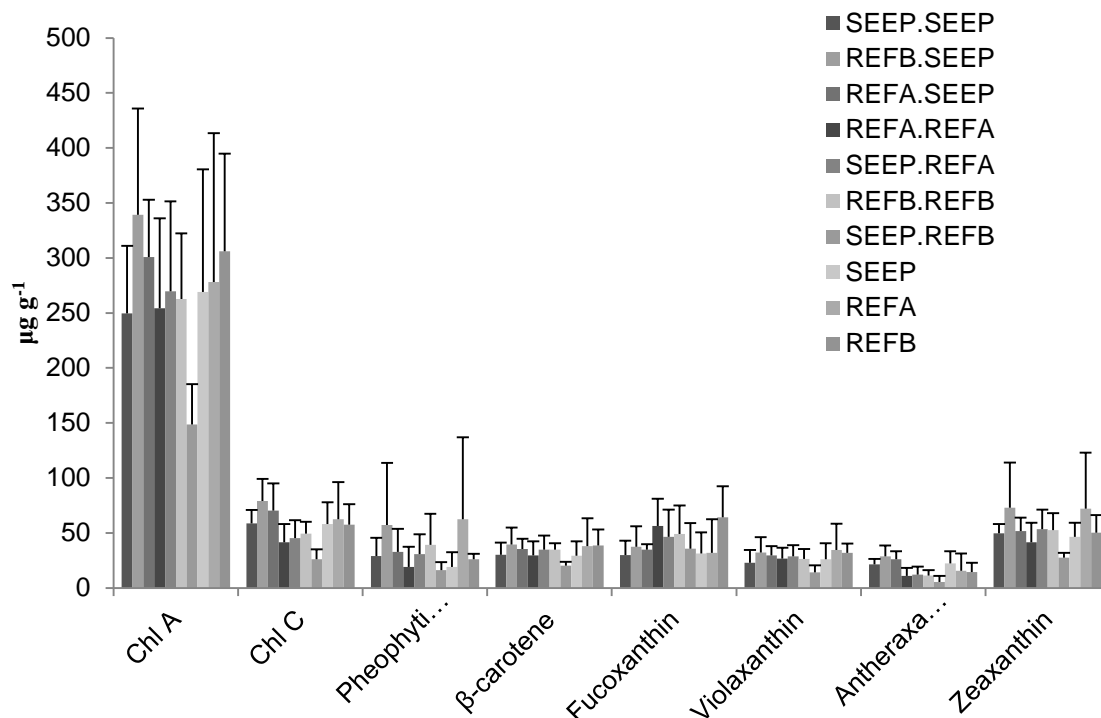


Figure 6.5. Mean pigments content (\pm SD, n=3-10) of *C. corniculata* thalli transplanted at Methana from September 2012 to June 2013 within and between two reference sites (REF

A and REF B) and one high CO₂ site (SEEP). Treatments are shown as “Site of origin.Site of transplant”; the last three treatments (SEEP, REF A and REF B) are unmanipulated thalli collected in June 2013.

MANOVA on log-transformed pigments content for *J. rubens* transplanted at Methana from June to September 2013 showed that treatment had a significant effect on all pigments analysed except for β -cryptoxanthin and antheraxanthin (Table 6.8). Chlorophyll *a*, violaxanthin and zeaxanthin content was higher in thalli transplanted to the high CO₂ site (SEEP), especially in those which also came from the high CO₂ site (SEEP.SEPE) and the unmanipulated thalli collected from that site (Figure 6.6). Pheophytin *a* and β -carotene were mostly present in higher quantities in unmanipulated thalli or in those transplanted to their site of origin (e.g. SEEP.SEPE) compared to those transplanted to a different site.

Table 6.8. MANOVA on pigments content in *J. rubens* thalli transplanted at Methana from June 2013 to September 2013 within and between one reference site (REF B) and one high CO₂ site (SEEP). F-ratios (F) and p values are reported when significant ($p < 0.05$).

Response variable	Treatment
Chl <i>a</i>	F(6,33)=8.874 $p < 0.001$
Pheophytin <i>a</i>	F(6,33)=14.414 $p < 0.001$
β -cryptoxanthin	-
β -carotene	F(6,33)=3.925 $p = 0.005$
Violaxanthin	F(6,33)=7.151 $p < 0.001$
Antheraxanthin	-
Zeaxanthin	F(6,33)=10.702 $p < 0.001$

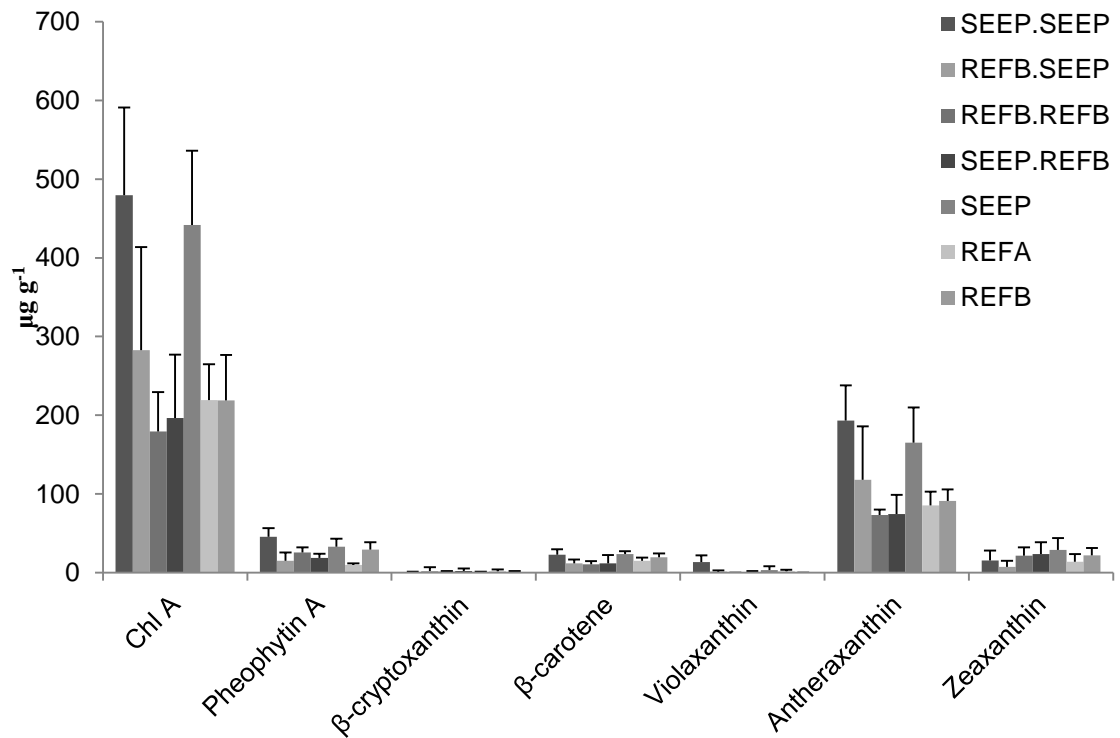


Figure 6.6. Mean pigments content (\pm SD, $n=4-7$) of *J. rubens* thalli transplanted at Methana from June 2013 to September 2013 within and between one reference site (REF B) and one high CO₂ site (SEEP). Treatments are shown as “Site of origin.Site of transplant”; the last three treatments (SEEP, REF A and REF B) are unmanipulated thalli collected in September 2013.

MANOVA on log-transformed phycobilins content for *J. rubens* transplanted at Methana from June to September 2013 showed that treatment had a significant effect on phycocyanin (Table 6.9). Similarly to some pigments, phycocyanin content was higher in thalli transplanted to the high CO₂ site or unmanipulated thalli collected from SEEP (Figure 6.7).

Table 6.9. MANOVA on phycobilins content in *J. rubens* thalli transplanted at Methana from June 2013 to September 2013 within and between one reference site (REF B) and one high CO₂ site (SEEP). F-ratios (F) and p values are reported when significant (p<0.05).

Response variable	Treatment
Phycoerythrin	-
Phycocyanin	F(6,32)=5.542 p<0.001

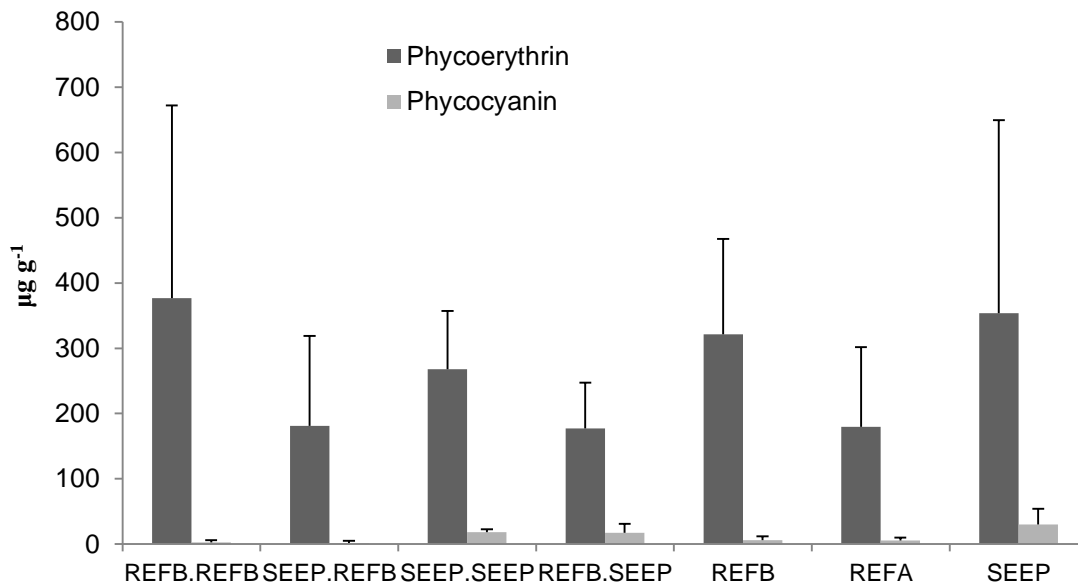


Figure 6.7. Mean phycobilins content (\pm SD, n=3-7) of *J. rubens* thalli transplanted at Methana from June 2013 to September 2013 within and between one reference site (REF B) and one high CO₂ site (SEEP). Treatments are shown as “Site of origin.Site of transplant”; the last three treatments (SEEP, REF A and REF B) are unmanipulated thalli collected in September 2013.

6.3.4 Carbon, nitrogen and phosphorus content

There was a significant difference among treatments for C:N ratio of *C. corniculata* thalli transplanted at Methana from September 2012 to June 2013, but not for N:P ratio (Table 6.10). C:N ratio was in fact higher in unmanipulated thalli collected at SEEP compared to those collected at reference sites (Figure

6.8). Similarly, thalli transplanted to the high CO₂ site had higher C:N ratio than those transplanted to the reference sites.

Table 6.10. MANOVA on C:N and N:P ratios in *C. corniculata* thalli transplanted at Methana from September 2012 to June 2013 within and between two reference sites (REF A and REF B) and one high CO₂ site (SEEP). F-ratios (F) and p values are reported when significant (p<0.05).

Response variable	Treatment
C:N	F(9,44)=5.404 p<0.001
N:P	-

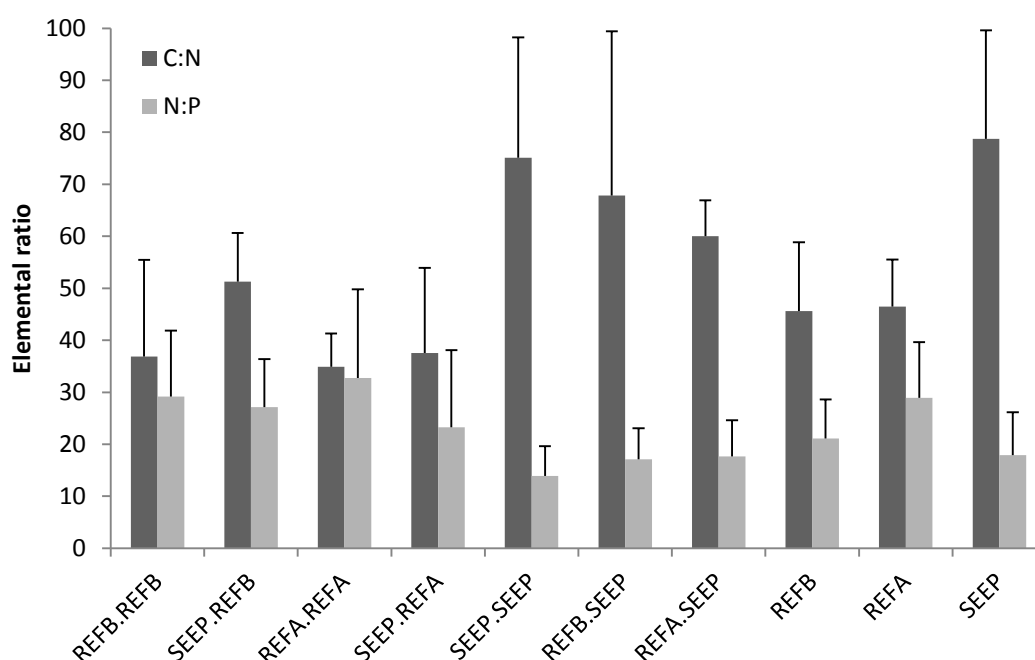


Figure 6.8. Mean C:N and N:P ratios (\pm SD, n=3-9) of *C. corniculata* thalli transplanted at Methana from September 2012 to June 2013 within and between two reference sites (REF A and REF B) and one high CO₂ site (SEEP). Treatments are shown as “Site of origin.Site of transplant”; the last three treatments (SEEP, REF A and REF B) are unmanipulated thalli collected in June 2013.

Calculating C:N ratios was not possible for many *J. rubens* samples because the nitrogen content was below detection limit; C and N were therefore analysed separately using a MANOVA, and results are reported in Table 6.11. Nitrogen content was significantly different among treatments, and it was higher in thalli

transplanted within the high CO₂ site and in unmanipulated thalli collected at SEEP (Figure 6.9).

Table 6.11. MANOVA on C and N content in *J. rubens* thalli transplanted at Methana from June 2013 to September 2013 within and between one reference site (REF B) and one high CO₂ site (SEEP). F-ratios (F) and p values are reported when significant (p<0.05).

Response variable	Treatment
C	-
N	F(6,22)=3.021; p=0.026

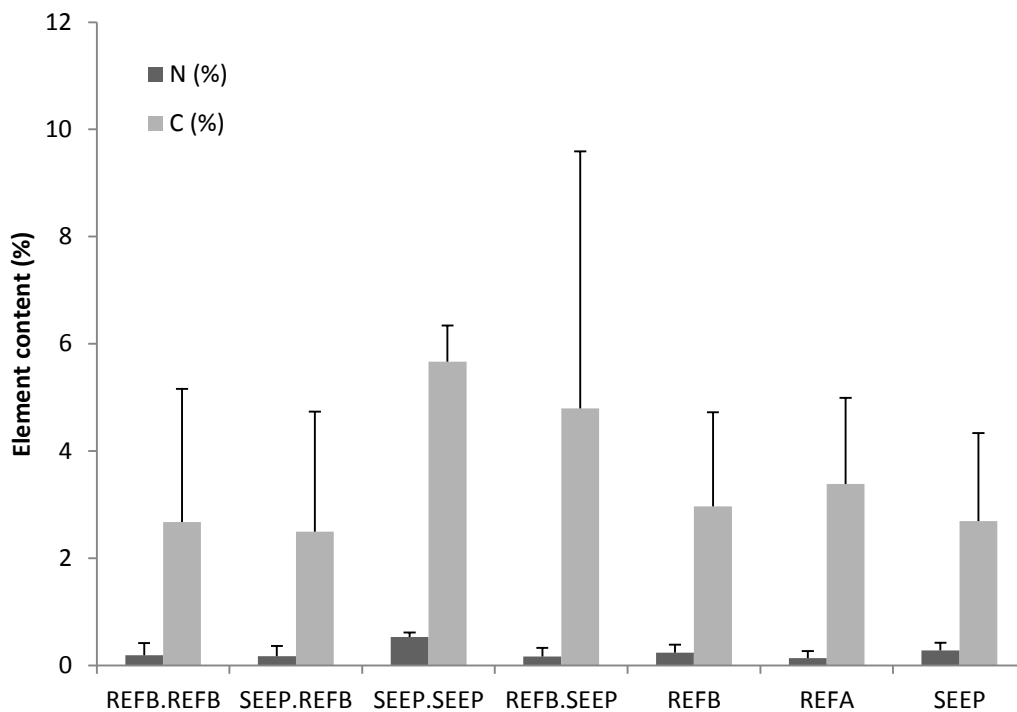


Figure 6.9. Mean C and N percent content (\pm SD, n=3-5) of *J. rubens* thalli transplanted at Methana from June 2013 to September 2013 within and between one reference site (REF B) and one high CO₂ site (SEEP). Treatments are shown as “Site of origin.Site of transplant”; the last three treatments (SEEP, REF A and REF B) are unmanipulated thalli collected in September 2013.

On the other hand, no significant differences among treatments were detected for inorganic carbon content of *J. rubens* transplants (Table 6.12). Percent

inorganic carbon content varies little among treatment, as it is around 80% for all of them (Figure 6.10).

Table 6.12. ANOVA results for transplanted *J. rubens* thalli inorganic carbon content. The table shows the source of variation and sum of squares (SS), degrees of freedom (df), Mean Squares (MS), F-ratios (F) and p values.

Source	Type III SS	df	MS	F	p
Treatment	124.378	8	15.547	1.756	0.129
Error	247.854	28	8.852		
Total	372.232	36			

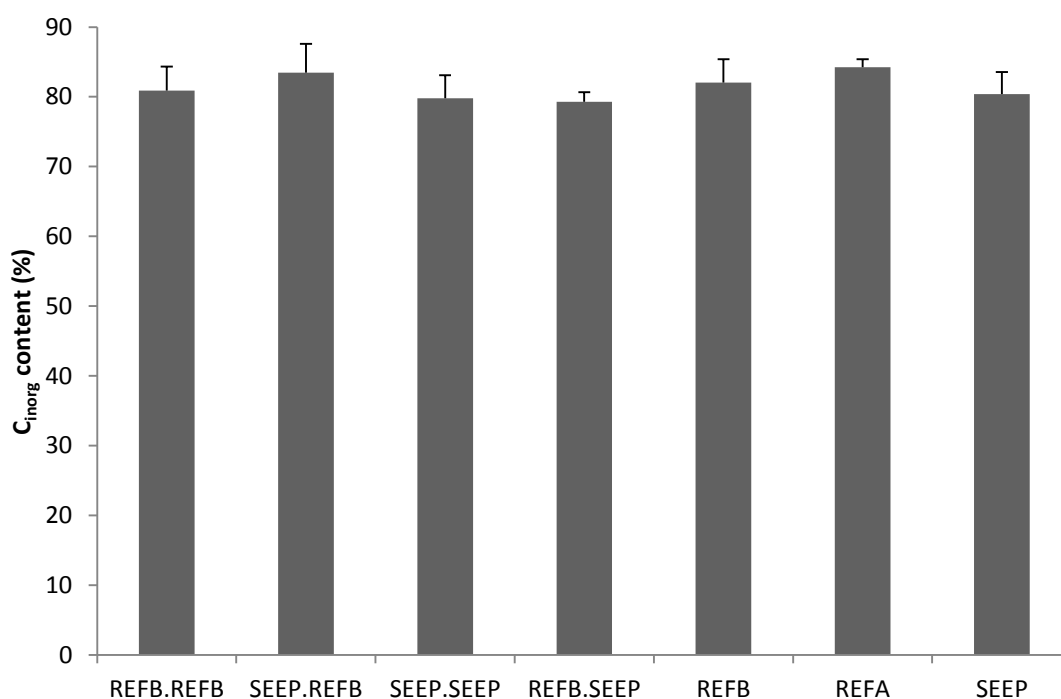


Figure 6.10. Mean inorganic carbon percent content (\pm SD, $n=3-7$) of *J. rubens* thalli transplanted at Methana from June 2013 to September 2013 within and between one reference site (REF B) and one high CO₂ site (SEEP). Treatments are shown as “Site of origin.Site of transplant”; the last three treatments (SEEP, REF A and REF B) are unmanipulated thalli collected in September 2013.

6.3.5 Total phenolic compounds

Total phenolic compounds of *C. corniculata* thalli were significantly different among treatments (Table 6.13). In general, thalli transplanted to the high CO₂ site (SEEP) had higher phenols content compared to those transplanted to the two reference sites (REF A and REF B). However, macroalgae transplanted from high CO₂ levels to the reference sites (i.e. SEEP.REFA and SEEP. REFB) had higher phenols content than those transplanted within the same reference site (i.e. REFA.REFA and REFB.REFB), whereas unmanipulated thalli did not show clear patterns, possibly because of high within-site variability (Figure 6.11).

Table 6.13. ANOVA on phenols content of *C. corniculata* thalli transplanted at Methana from September 2012 to June 2013 within and between two reference sites (REF A and REF B) and one high CO₂ site (SEEP). The table shows the source of variation and sum of squares (SS), degrees of freedom (df), Mean Squares (MS), F-ratios (F) and p values.

Source	Type III SS	df	MS	F	p
Treatment	10.922	9	1.214	3.202	0.004
Error	18.189	48	0.379		
Total	29.111	57			

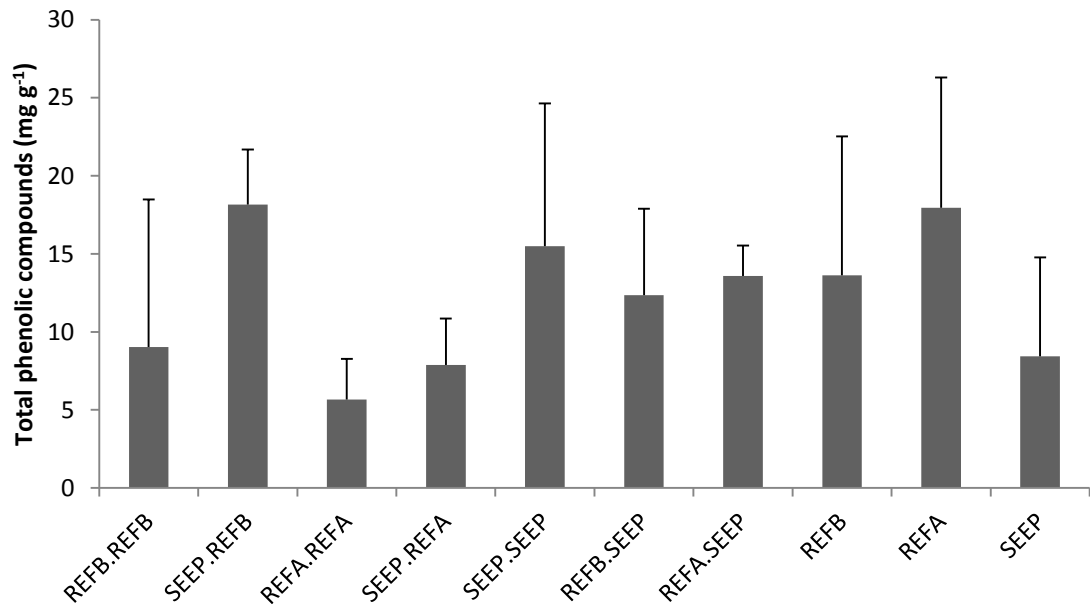


Figure 6.11. Mean phenols concentration (\pm SD, $n=3-10$) of *C. corniculata* thalli transplanted at Methana from September 2012 to June 2013 within and between two reference sites (REF A and REF B) and one high CO₂ site (SEEP). Treatments are shown as “Site of origin.Site of transplant”; the last three treatments (SEEP, REF A and REF B) are unmanipulated thalli collected in June 2013.

6.4 Discussion

For the first time, long-term acclimatisation of macroalgae to ocean acidification has been assessed using reciprocal transplantations within and between areas with reference and elevated CO₂ levels. Results from these experiments suggest that phenotypic plasticity allowed *C. corniculata* and *J. rubens* to alter their physiological performance depending on the carbonate chemistry at the site of transplant. Although both species could survive $p\text{CO}_2$ levels up to 1700 μatm , *C. corniculata* seemed to be favoured at elevated CO₂; this might lead to reduced abundances of *J. rubens* and increased abundances of *C. corniculata* at elevated $p\text{CO}_2$ as a consequence of altered inter-specific competition.

In contrast with the initial hypothesis, linear growth and photosynthetic performance of both species were not higher in thalli transplanted within $p\text{CO}_2$ levels. No effects of site were detected for *J. rubens* growth, while *C. corniculata* growth was significantly lower at one of the reference sites (REF B). These findings are in contrast with recent studies reporting decreased growth of articulated coralline algae (Gao and Zheng, 2010; Hofmann *et al.*, 2011; Hofmann *et al.*, 2012; Cornwall *et al.*, 2014; Johnson *et al.*, 2014) and fucoid algae (Gutow *et al.*, 2014) at elevated CO_2 levels. However, responses to ocean acidification in macroalgae present high inter-specific variability (Kroeker *et al.*, 2013a), and fucoid algae can show no change or increase in growth rates as CO_2 increases (Swanson and Fox, 2007; Chen and Zou, 2014). In addition, experiments have mostly been conducted in laboratories for relatively short periods of time, whereas this field experiment lasted three and nine months for *J. rubens* and *C. corniculata*, respectively. In the field, many macroalgae do not reach their maximum potential frond size as their linear growth is limited by external factors, such as wave motion or nutrient limitation (Fisher and Martone, 2014). As *C. corniculata* dry biomass showed an increasing trend with increasing seawater $p\text{CO}_2$ at Methana (see Chapter 4), biomass of transplanted seaweeds might have shown a response to $p\text{CO}_2$ levels. However, measuring biomass change was not possible in this study, as the seaweeds were permanently attached to the substratum using epoxy putty, which remained on the transplanted thalli after they were collected at the end of the experiment.

Photosynthetic performance of *J. rubens* was unaffected by the transplant, whereas *C. corniculata* had higher $r\text{ETR}_{\text{max}}$ when transplanted to elevated CO_2 . This is in accord with recent findings by Johnson *et al.* (2014), who did not find strong and consistent effects of ocean acidification on algal photophysiology.

Previous studies on articulated coralline algae have shown that although photosynthetic parameters are often not affected by increased CO₂ (Hofmann *et al.*, 2012), oxygen production can be negatively affected by ocean acidification (Hofmann *et al.*, 2011). However, oxygen production in articulated coralline algae is less affected by increased CO₂ compared to crustose forms (Noisette *et al.*, 2013b), and algae acclimatised to elevated CO₂ in tidal pools do not show changes in their productivity as carbon dioxide increases (Egilsdottir *et al.*, 2013). As for brown algae, maximum quantum yield (F_v/F_m) is normally not affected by elevated CO₂, although it can decrease in combination with elevated temperature (Johnson *et al.*, 2012; Olabarria *et al.*, 2013). Similarly to *C. corniculata*, increased photosynthetic capacity (rETR_{max}) at high CO₂ has been reported for *Padina pavonica* at seeps off Vulcano (Johnson *et al.*, 2012).

Both macroalgal species showed an increase in some pigment contents when transplanted to elevated CO₂ levels. This is in accord with the initial hypothesis for *C. corniculata*, but not for *J. rubens*, possibly because most information about coralline algal responses to ocean acidification comes from laboratory studies, while there are a few field studies on brown algae. *Cystoseira corniculata* thalli transplanted to the seeps had increased chlorophyll *c* and antheraxanthin, although unmanipulated thalli did not show any CO₂-dependent pattern. Antheraxanthin is an intermediate and volatile compound in the xanthophyll cycle (Goss and Jakob, 2010); its increase is thus unlikely to have physiological significance, especially since de-epoxidation state did not change significantly among treatments (data not shown). *J. rubens* thalli transplanted to SEEP had higher chlorophyll *a*, violaxanthin, zeaxanthin and phycocyanin content. Some pigments of *J. rubens* were affected by the transplant: thalli transplanted to their site of origin had higher pheophytin *a* and β-carotene

content than those transplanted to another site. Few studies have examined changes in macroalgal pigment content with increased CO₂; laboratory experiments performed so far have not found significant effects of ocean acidification on pigments in brown and red algae (Egilsdottir *et al.*, 2013; Noisette *et al.*, 2013a; Noisette *et al.*, 2013b; Yildiz *et al.*, 2013; Bender *et al.*, 2014). However, the only study examining macroalgal pigment content at volcanic seeps found increased chlorophyll *a* and *c* content in *Padina pavonica* grown at elevated CO₂ (Johnson *et al.*, 2012). Most laboratory experiments were conducted over a relatively short time (up to three months); it is then possible that macroalgae increase some species' pigment production at increased CO₂ levels, but only in the long term. However, the crustose coralline alga *Lithophyllum cabiochae* did not show significant changes in chlorophyll *a* concentration after being exposed to elevated CO₂ for one year (Martin *et al.*, 2013); more studies are therefore needed to test this phenomenon.

Epiphyte cover of *C. corniculata* was lower in thalli transplanted near the seeps, and was slightly lower in thalli transplanted from the SEEP site than in thalli from reference sites. This could be partly explained by the increase in total phenolic compounds in thalli transplanted to SEEP and the smaller phenols increase in those transplanted from SEEP; increased total phenolic compounds with elevated CO₂ have already been found in other brown algae, although not all species exhibit this pattern (Swanson and Fox, 2007; Poore *et al.*, 2013). Although phenolic compounds, mostly phlorotannins, have been proven to inhibit grazers and protect brown seaweeds from UV radiation (Halm *et al.*, 2010), their effect on seaweed epiphyte load is not clear (Jennings and Steinberg, 1997; Brock *et al.*, 2008). In fact, epiphyte settlement on macroalgae

is likely controlled by other factors, including macroalgal morphology and polar secondary metabolites such as terpenoids (Jennings and Steinberg, 1997).

Phenols are carbon-dense compounds, and their increase could explain the increased C:N ratio in *C. corniculata* thalli transplanted to SEEP. The increase in C:N ratio was caused by increased carbon and decreased nitrogen content in thalli transplanted to SEEP. This is in contrast with other studies reporting decreased C:N ratio in macroalgae exposed to high CO₂; in one case this was caused by decreased nitrogen content with increased CO₂ (Falkenberg *et al.*, 2013b; Gutow *et al.*, 2014). Decreased nitrogen content with increased CO₂ is also reported by Kübler *et al.* (1999) for the red alga *Lomentaria articulata*, but coupled with decreased carbon content. However, increased CO₂ did not change carbon and nitrogen content in many brown and red macroalgae (Olabarria *et al.*, 2013; Poore *et al.*, 2013). The strong grazing pressure at Methana could have driven an enhanced carbon-dense chemical defences production at SEEP thanks to increased CO₂ availability (Connell *et al.*, 2013); chemical defences of brown algae and seagrasses may therefore be differently affected by ocean acidification, as the latter had lower defensive compound contents at elevated pCO₂ levels (Arnold *et al.*, 2012).

Unaltered inorganic carbon content of *J. rubens* among treatments suggests that this species is not locally adapted to elevated pCO₂ and can maintain calcification rates at high CO₂ and counter increased dissolution rates at volcanic seeps. Work to date has shown that articulated coralline algal calcification is less affected by increased CO₂ than that of crustose forms; although net calcification rates of articulated coralline algae can decrease at elevated CO₂, crustose coralline algae often start dissolving at pCO₂ levels above 1000 µatm (Hofmann *et al.*, 2011; Noisette *et al.*, 2013b; Johnson *et al.*,

2014). However, maintaining calcification rates at decreased calcium carbonate saturation is energetically expensive (Bradassi *et al.*, 2013), and *J. rubens* thalli grown at reference sites might not be able to maintain them when exposed to elevated CO₂ for longer periods. Some coralline algae exposed to high CO₂ for two months or more have lower proportions of very soluble high-Mg calcite in their skeletons (Egilsdottir *et al.*, 2013; Diaz-Pulido *et al.*, 2014). *Jania rubens* transplanted near seeps at Methana could therefore have modified mineralogy or increased the production of calcification-inducing compounds to improve survival at elevated CO₂ levels (Koch *et al.*, 2013). However, articulated coralline algae appear to increase their Mg content with increasing seawater temperatures (Williamson *et al.*, 2014). The concurrent increase in seawater pCO₂ levels and temperatures predicted for 2100 may therefore impair the ability of articulated coralline algae to modify their mineralogy to better resist to ocean acidification.

To summarise, the two seaweeds examined changed their physiology depending on the environmental conditions at the site of transplant. The possibility of genotypic differentiation among populations of these macroalgal species depending on their acclimatisation to elevated CO₂ cannot be excluded until genetic studies are performed. Species with high phenotypic plasticity could in fact have genetically adapted to elevated CO₂ levels, but show similar physiological performances, a phenomenon named “phenotypic buffering” (Sunday *et al.*, 2014). Changes in the physiological performance of dominant macroalgal species are likely to alter the outcome of competition between them; this is reflected by the macroalgal community composition near seeps off Methana. Here, *J. rubens* cover decreased, whereas *C. corniculata* cover increased with increasing pCO₂ (Chapter 3; Figure 6.12). This study therefore

shows that even after centuries of exposure to high CO₂ levels, two dominant macroalgal species did not appear to have permanently acclimatised to elevated carbon dioxide levels. This is likely to heavily influence temperate coastal ecosystems, as the observed changes in benthic community structure are likely to indirectly influence upper trophic levels and ecosystem processes such as nutrient cycling or carbon sequestration.

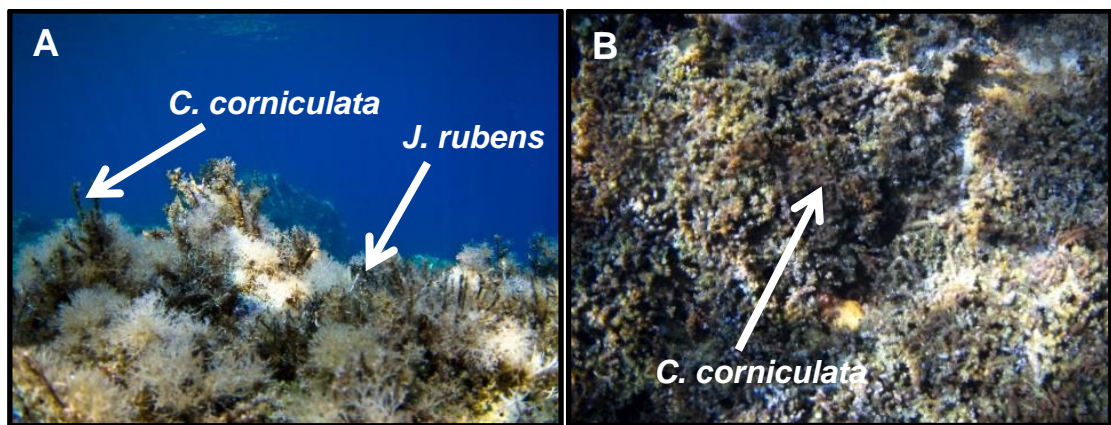


Figure 6.12. Typical macroalgal assemblage off Methana in September 2013 at reference sites (A) with abundant *J. rubens* overgrowing *C. corniculata*, and near the seeps (B), where *C. corniculata* could grow undisturbed; photos by Maria Salomidi.

Chapter 7

A short-term copper pulse affects macroalgal copper accumulation and indirectly alters epifaunal colonisation at elevated pCO₂.

Abstract

Ocean acidification is expected to interact with other anthropogenic stressors to modify marine ecosystems. Copper is toxic to marine organisms, and copper pulses are a common source of pollution in coastal areas. In this study, calcifying and non-calcifying seaweeds acclimatised to high CO₂ at volcanic seeps or from reference sites were exposed to elevated CO₂ and a 36-hour copper pulse in two field experiments. Invertebrate re-colonisation of a fucoid alga exposed to copper at different pCO₂ levels was also assessed. *Cystoseira corniculata* and *Jania rubens* accumulated more copper in high CO₂ conditions. *Jania rubens* grown near the seeps accumulated more copper than those transplanted from reference sites. These changes had no effect on maximum quantum yield of both species. *Cystoseira corniculata* pigment contents changed little, but total carotenoids decreased in *J. rubens* thalli exposed to copper at both sites. Phycoerythrin content in *J. rubens* slightly increased in thalli exposed to copper at the reference site, whereas it decreased following copper exposure at elevated CO₂ levels. Previous acclimatisation to high CO₂ did not influence seaweed responses to copper. However, copper accumulation at high CO₂ altered epifaunal community structure near the seeps, but not in reference conditions. Thus, multiple stressors can interact and increase the magnitude of changes in benthic communities.

7.1 Introduction

Macroalgal responses to increased CO₂ differ in calcifying and non-calcifying species (Porzio *et al.*, 2011). Carbon concentrating mechanisms (CCMs) are used by most macroalgae to convert bicarbonate ions into carbon dioxide; these are energy expensive, so increased dissolved CO₂ decreases the energy needed to obtain the substratum for photosynthesis (Cornwall *et al.*, 2012). On the other hand, calcifying algae face increased energetic costs of calcification as calcium carbonate saturation levels fall due to ocean acidification (Bradassi *et al.*, 2013; Koch *et al.*, 2013). The combination of increased carbon availability and higher energetic cost of calcification may cause shifts from coralline-dominated to fleshy seaweed communities as atmospheric CO₂ increases (Connell *et al.*, 2013), not only because of reduced coralline algae growth (Küffner *et al.*, 2008; Martin *et al.*, 2008; Kroeker *et al.*, 2010), but also because of altered competitive interactions between calcified and non-calcified algae (Kroeker *et al.*, 2013c; Short *et al.*, 2014).

Acclimatisation or adaptation to high pCO₂ could improve the ecological performance of calcifying algae as oceans become acidified (Hofmann *et al.*, 2010). Algae living in high-CO₂ environments could therefore be helpful in determining the potential for acclimatisation in these organisms. So far, very few studies have tackled this issue. For instance, the green microalga *Chlamydomonas reinhardtii* changes its physiology when exposed to elevated carbon dioxide over multiple generations, showing reduced CO₂ uptake using carbon-concentrating mechanisms (Collins *et al.*, 2006) and a marine coccolithophore has the potential to adapt to future CO₂ concentrations (Lohbeck *et al.*, 2012). Unpublished work at volcanic seeps off Ischia (Italy)

indicates that the genome of the brown macroalga *Dictyota* sp. changes at high pCO₂, resulting in the dominance of a stress-resistant form (Porzio, 2010).

Although there is scant information regarding macroalgal acclimatisation to elevated CO₂, their response to other changing abiotic conditions is widely studied. For example, there are species-specific differences in the tolerance of macroalgae to changes in salinity (Ryan *et al.*, 2004), temperature (Collén and Davison, 2001) and light (Bischof *et al.*, 2006) depending on the natural variability of their habitat. In some cases, intraspecific differences in responses to environmental stressors have been detected (Pearson *et al.*, 2009). These differences can have a hereditary component (Nielsen *et al.*, 2003) and environmental isolation can lead to rapid speciation, such as for *Fucus* spp. in the Baltic Sea (Bergström *et al.*, 2005).

Epifaunal communities are affected by increased CO₂ as well, with decreased abundance of molluscs and an increase of some crustacean taxa (Kroeker *et al.*, 2011). The above responses mostly conform to predictions based on laboratory experiments (Kroeker *et al.*, 2013a), but communities studies have also found unexpected community changes due to altered inter-specific interactions (Hale *et al.*, 2011). Invertebrates can also exhibit enhanced sensitivity to ocean acidification if they are concurrently exposed to another stressor, such as increased temperature or low food availability (Rodolfo-Metalpa *et al.*, 2011; Kroeker *et al.*, 2013a; Thomsen *et al.*, 2013).

Since ocean acidification is only one of the changes humans are causing in the marine realm, we have to consider that several abiotic factors are acting interdependently, with interactive and sometimes unexpected results (Shears and Ross, 2010; Gaylord *et al.*, 2014). Even if calcifying macroalgae have the

potential to acclimatise or adapt to high CO₂, they could be more sensitive to any additional stressors due to the increased energetic cost of calcification (Bradassi *et al.*, 2013). On the other hand, non-calcifying algae could be more resistant to additional stressors as they have more energy available after reducing their use of carbon concentrating mechanisms (CCMs; Cornwall *et al.*, 2012), leading to more drastic community changes compared to the effects of CO₂ alone.

In coastal waters, copper is a common pollutant as it is mined in many regions (Figure 7.1); however, copper can also derive from urban runoff (Pitt, 1995), industrial waste (Apte and Day, 1998) or antifouling paints (Paulson *et al.*, 1989). Copper is extremely toxic at high concentrations, especially before binding to organic material (Hall *et al.*, 1998). As a consequence, copper pulses are common in coastal waters near human settlements and industries. Copper accumulates in macroalgal tissues and can strongly inhibit photosynthesis by damaging photosystem II (Schröder *et al.*, 1994). Many invertebrate taxa are negatively affected by copper as well (Johnston *et al.*, 2002), and seaweed epifauna is more strongly affected because they are exposed to copper through the macroalgae they live in and feed upon (Roberts *et al.*, 2006). Other effects of elevated copper concentrations on marine flora and fauna include reduced growth and calcification, altered osmoregulatory processes and oxidative damage (Thurberg *et al.*, 1973; Kangwe *et al.*, 2001; Collén *et al.*, 2003), although there is large among-taxa variability in copper sensitivity (Mayer-Pinto *et al.*, 2010). In addition, some organisms can be more sensitive to copper exposure at elevated CO₂ levels because of the higher energetic cost of maintaining physiological processes (Roberts *et al.*, 2013).

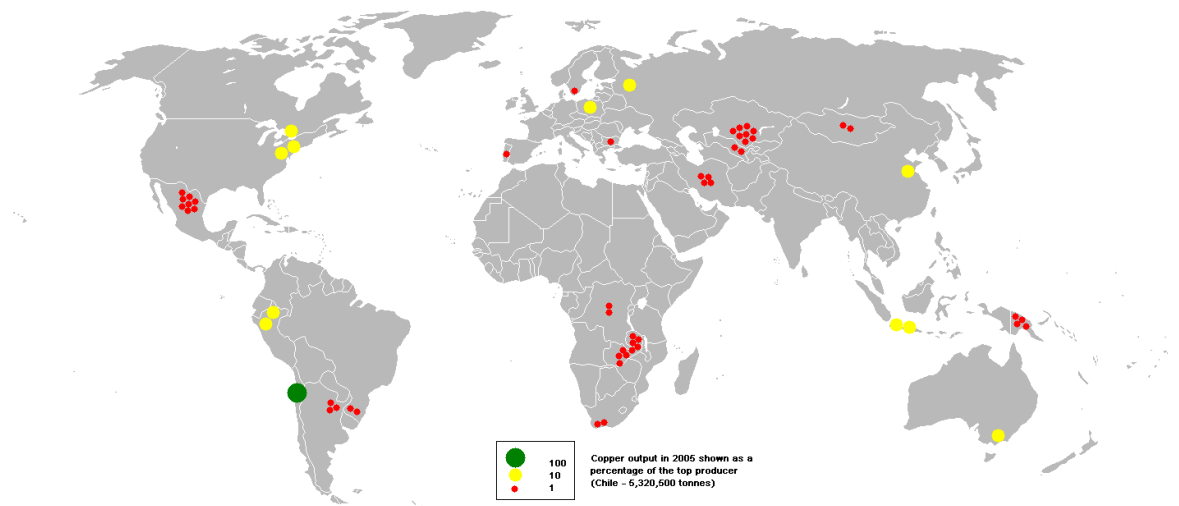


Figure 7.1. Copper production in 2005 shown as a percentage of the top producer (Chile, 5320500 tonnes). Data from British Geological Survey.

This study investigated how populations of a calcifying and a non-calcifying alga from high or reference pCO₂ areas responded to a short-term copper pulse *in situ*, and assesses how re-colonisation by seaweed epifauna was affected by copper exposure at different pCO₂ levels. The hypotheses tested were:

- 1) A non-calcifying alga (*Cystoseira corniculata*) is more resistant to short-term copper stress in high CO₂ conditions;
- 2) A calcifying alga (*Jania rubens*) is less resistant to short-term copper stress in high pCO₂ conditions, but this effect is reduced for algae acclimatised to high CO₂;
- 3) *Cystoseira corniculata* epifaunal colonisation is negatively affected by copper exposure, and the effect of copper is stronger at high CO₂.

7.2 Methods

7.2.1 Study area

Experiments were carried out in June and September 2013 at two sites (see Chapter 2, Figure 2.1), one characterised by high pCO₂ due to hydrothermal activity (SEEP) and a reference site (REF A); detailed sampling dates and sample sizes are reported in Table 1.1F. Macroalgae were also collected from another reference site (REF B). A geochemical survey of the area revealed that none of the study sites was contaminated with respect to copper, making the area suitable for testing the effects of copper pollution on non-adapted organisms (Chapter 2).

7.2.2 Experimental design

Two common macroalgal species were chosen to test the combined effects of elevated carbon dioxide and copper, the brown alga *Cystoseira corniculata* in June 2013 and the articulated coralline *Jania rubens* in September 2013. Similarly sized thalli were collected from three sites, one characterised by high pCO₂ (SEEP) and two reference sites (REF A and REF B). The algae were kept in coolers and transported from their site of origin to the sites REF A and SEEP, and attached with cable ties on plastic attached to concrete blocks and deployed at the same depth the thalli were collected from (<0.5 m). Individuals from REF A and SEEP were transplanted both in their site of origin and in the other site, while individuals from REF B were transplanted to REF A and SEEP. Ten individuals per species per treatment were attached to nets, left 48 h to acclimatise to the new conditions and then half of them were exposed for three days to increased copper levels via plaster blocks containing copper attached to

their nets. A scheme of the experimental design is shown in Figure 7.2, and transplanted *J. rubens* is shown in Figure 7.3.

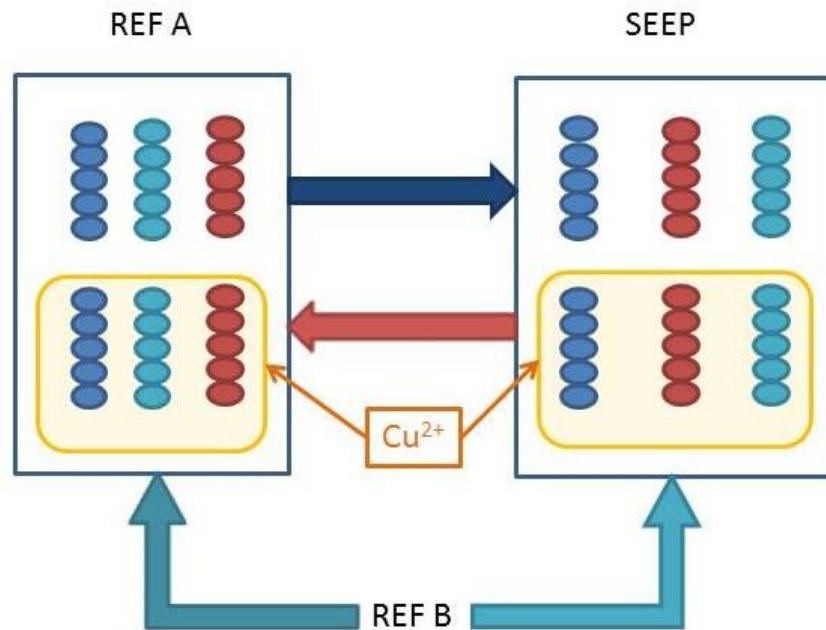


Figure 7.2. Off Methana (Greece), ten individuals from SEEP (red circles), REF A (blue circles) and REF B (light blue circles) were transplanted to SEEP and REF A (blue rectangles) in June (*C. corniculata*) and September 2013 (*J. rubens*). After 48 h, half were exposed to 36 h copper pulses (shaded).



Figure 7.3. *Jania rubens* transplanted near seeps off Methana (Greece) in September 2013 before being exposed to copper; the individual thalli were attached to plastic nets using

cable ties, and the net was attached to a concrete block deployed on the rocky shore at depth < 0.5 m.

For these experiments, CuSO₄ (copper II sulfate anhydrous) was used as a reference toxicant following methods described by Johnston and Webb (2000). 3.2 g of CuSO₄ were dissolved in 13 g of deionized water and refrigerated at 4°C for 60 min. Fifteen grams of dental plaster were refrigerated for 60 min, then mixed with the cool copper solution. The plaster was poured into 4 cm diameter plastic cups and left to dry for seven days. The same process was used to make control blocks except for the CuSO₄ addition. Plaster was changed daily and the removed blocks were air dried and weighed to check that all macroalgae were exposed to a comparable amount of copper.

In June 2013, an additional experiment was performed to test how *C. corniculata* re-colonisation by invertebrates was influenced by copper at different pCO₂ levels. Ten similarly sized *C. corniculata* thalli per site were detached from the rocky substratum using hammer and chisel, briefly rinsed with fresh water to remove all mobile invertebrates and attached to the nets used for the macroalgal physiology experiment, resulting in five copper-exposed and five control thalli per site.

7.2.3 Environmental parameters monitoring

Environmental parameters were measured daily for the duration of the experiments. Temperature, salinity and pH were monitored in both sites with a multiprobe (YSI Professional Series, Professional Plus) and total alkalinity was sampled twice per site on the first and the last day of the experiment using borosilicate bottles. Total alkalinity samples were treated and analysed according to the procedures detailed in Chapter 2. The other carbonate

chemistry parameters were calculated from pH and total alkalinity using CO2Sys software (Lewis and Wallace, 1998).

7.2.4 Sampling and laboratory analyses

Physiological responses of transplanted thalli of both species were assessed by measuring *in vivo* chlorophyll *a* fluorescence associated with Photosystem II by using a portable pulse amplitude modulated fluorometer Diving-PAM (Diving PAM, Walz, Effeltrich, Germany). The maximum quantum yield (F_v/F_m) of apical shoots was measured after 10 minutes of dark acclimation before transplanting the seaweeds, after the acclimation period and after copper exposure. Appropriate duration of dark acclimation was determined by measuring F_v/F_m of ten thalli per species after 5, 10, 15 and 20 minutes in the dark. Maximum quantum yield (F_v/F_m) relates the capacity for photochemical quenching ($F_v = F_m - F_0$, where F_0 is the basal fluorescence of dark-adapted thalli and F_m is the maximal fluorescence after a saturation light pulse of $> 4000 \mu\text{mol m}^{-2} \text{s}^{-1}$) to the total fluorescence emission of closed PSII reaction centres (F_m). F_v/F_m is then directly proportional to the quantum efficiency of PSII photochemistry (Butler 1978), and its reduction from maximal values is an indicator of stress responses, and specifically of metal stress (Mallick and Mohn, 2003).

After 36 h of copper exposure, *C. corniculata* thalli were collected and transported to the field laboratory in coolers. There their apical parts were gently scrubbed of epiphytes, rinsed with distilled water and immediately frozen in liquid nitrogen. The samples were subsequently stored at -80°C until they were analysed for copper content and pigment composition. In June 2013, *C. corniculata* thalli for the invertebrate re-colonisation experiment were covered with plastic zip-lock bags, taken from the site and transported to the field

laboratory, where they were sieved (200 µm mesh) and stored in 70% Industrial Methylated Spirit (IMS). Samples were later sorted and mobile invertebrates identified to the lowest possible taxonomic level. Macroalgal thalli were dried in an oven at 50 °C for 72h and weighed (± 1 mg accuracy) to determine dry mass (DW).

Samples for copper concentration were freeze-dried for 24h and ground with pestle and mortar; approximately 0.1 g of each sample was weighed in acid-washed Teflon tubes with a high precision digital scale (0.1 mg accuracy). Two ml of concentrated nitric acid were then added; the tube containing the digestant was then placed in a high-Throughput Microwave Reaction System Run (MARSXpress, CEM Corporation, Matthews, USA) and gently heated to boiling for at least 1 h to ensure full digestion. Samples were allowed to cool, quantitatively transferred into pre-cleaned 10 ml volumetric flasks and diluted to volume with Milli-Q water. Blanks were prepared following the same procedure, but omitting the sample; the digested samples were then analysed using inductively coupled plasma optical emission spectrometry (ICP-OES).

Samples for pigment analysis were freeze-dried in the dark for 24h, after which they were grinded in pure acetone using mortar and pestle. Extraction occurred at 4°C for 24 h in the dark. After extraction samples were centrifuged at 4000 rpm for 15 min at 4°C. Pigment content was then analysed using the Gauss-Peak Spectra method (Küpper *et al.*, 2007). Samples were scanned in a dual-beam spectrophotometer from 350 nm to 750 nm at 1 nm steps. The absorbance spectra were introduced in the GPS fitting library using SigmaPlot. The employment of this library allowed to identify and quantify Chlorophyll a, Chlorophyll c1 and c2, Pheophytin a, Fucoxanthin, Antheraxanthin, β -carotene, Violaxanthin and Zeaxanthin for *C. corniculata* and Chlorophyll a, Pheophytin a,

β -cryptoxanthin, Antheraxanthin, β -carotene, Violaxanthin and Zeaxanthin for *J. rubens*. For phycobiliproteins approximately 0.5 g of tissue was homogenised in 10 mL 0.1 M phosphate buffer (pH 6.8). After being left at 4°C in the dark overnight, extracts were centrifuged for 10 minutes at 1000g and read in the spectrophotometer at the wavelengths determined by Beer and Eshel (1985).

7.2.5 Statistical analyses

All data were tested for normality and homogeneity of variances by visual evaluation of boxplots and residuals and using Levene's test, respectively. Analysis of pH data was performed using a non-parametric analysis (Kruskal-Wallis ANOVA); the two study periods were analysed separately. Mass loss of plaster blocks containing copper was performed using a one-way ANOVA with site as fixed factor. Copper content in seaweed tissues and changes in F_v/F_m following transplant and copper exposure were analysed using three-way ANOVAs with three fixed factors (site of origin, site of transplant, copper exposure). The analysis of hydrophilic pigments and phycobilins (only for September 2013) was performed through three-way MANOVAs with the same factors of previous analyses. When the data did not meet Mauchly's test of sphericity, the degrees of freedom were corrected using Greenhouse-Geisser estimates of sphericity. All of the analyses above were performed using SPSS v. 19 (IBM, USA).

Mobile invertebrates community composition and abundance was tested using a two-factor PERMANOVA with "site" and "copper" as fixed factors and "biomass" as a covariate. A square-root transformation was used to reduce the influence of abundant taxa in the community, and Type I sums of squares with 9,999 permutation of residuals under a reduced model was used. Variance

derived from significant interactions was then decomposed to determine which factor determined the significant interaction, and pairwise tests were performed when necessary. A nMDS plot was also used to visually inspect the similarities among samples. A SIMPER analysis was then used to determine the contribution of each taxon to the average Bray-Curtis dissimilarity between levels of a factor if the PERMANOVA analysis was significant. The SIMPER analysis was performed on broad taxonomic categories for ease of interpretation. All analyses above were performed using PRIMER 6 with PERMANOVA+ extension (Plymouth Routines In Multivariate Ecological Research, version 6).

7.3 Results

7.3.1 Environmental parameters

Data for environmental parameters monitored during the experiments are shown in Table 7.1. Statistical analyses of pH data revealed significant differences among sites in both seasons, and pH was lower at the SEEP site compared to the controls. On the other hand, average total alkalinity was similar among all sites and seasons. Temperature and salinity varied seasonally, but only showed small variability among sites.

Table 7.1. Mean (\pm SD) pH, total alkalinity (TA), temperature (T) and salinity (S) measured during the experiments, as well as parameters calculated with CO2SYS ($p\text{CO}_2$, bicarbonate (HCO_3^-) and carbonate (CO_3^{2-}) ions concentrations and saturation state of aragonite (Ω_{Ar}) and calcite (Ω_{Ca}); n=3-13.

June 2013									
	pH_{NBS}	TA (mmol kg^{-1})	T ($^{\circ}\text{C}$)	S (ppt)	$p\text{CO}_2$ (μatm)	HCO_3^- (mmol kg^{-1})	CO_3^{2-} (mmol kg^{-1})	Ω_{Ar}	Ω_{Ca}
SEEP	7.59 \pm 0.06	2.785	24.77 \pm 0.69	37.93 \pm 0.11	2205.9 \pm 312.4	2578.2 \pm 25.6	86.6 \pm 10.7	2.03 \pm 0.25	1.34 \pm 0.17
REF A	8.10 \pm 0.08	2.701	24.12 \pm 0.43	38.20 \pm 0.42	575.1 \pm 134.0	2148.9 \pm 78.5	229.0 \pm 32.1	5.36 \pm 0.73	3.53 \pm 0.48
REF B	8.11 \pm 0.04	2.703	22.96 \pm 0.45	38.16 \pm 0.45	543.4 \pm 54.9	2156.9 \pm 24.8	226.5 \pm 10.3	5.30 \pm 0.25	3.48 \pm 0.16
September 2013									
	pH_{NBS}	TA (mmol kg^{-1})	T ($^{\circ}\text{C}$)	S (ppt)	$p\text{CO}_2$ (μatm)	HCO_3^- (mmol kg^{-1})	CO_3^{2-} (mmol kg^{-1})	Ω_{Ar}	Ω_{Ca}
SEEP	7.65 \pm 0.03	2.785	26.50 \pm 0.17	39.60 \pm 0.10	1913.9 \pm 121.1	2532.2 \pm 14.2	105.5 \pm 3.2	2.44 \pm 0.13	1.62 \pm 0.09
REF A	8.12 \pm 0.02	2.701	25.87 \pm 0.06	39.07 \pm 0.35	534.2 \pm 33.4	2097.6 \pm 16.5	249.8 \pm 0.9	5.81 \pm 0.23	3.86 \pm 0.15
REF B	8.10 \pm 0.04	2.703	25.60 \pm 0.36	38.90 \pm 0.08	572.8 \pm 68.6	2129.3 \pm 39.1	237.8 \pm 1.8	5.54 \pm 0.38	3.67 \pm 0.24

7.3.2 Copper exposure and accumulation

In June 2013, plaster blocks containing copper in the sites REF A and SEEP did not show significant differences in mass loss as they were deployed in the field ($F_{1,7}=0.016$, $p=0.903$); at both sites, plaster blocks lost approximately 68% of their initial mass, releasing comparable amounts of copper in seawater. Tissue copper content in *C. corniculata*, however, was significantly different between transplant sites, and copper had a significant effect as well (Table 7.2). Samples originating from REF B had to be removed from analysis due to high sample loss. Figure 7.4 shows that *C. corniculata* exposed to copper had much higher tissue copper concentration than control thalli, and that site of transplant had a major effect on copper accumulation, with individuals transplanted to SEEP accumulating 3-4 times more copper than those transplanted to REF A.

Table 7.2. ANOVA on log-transformed copper concentration in *C. corniculata* thalli measured at the end of the experiment of June 2013. The table shows main factors and their interactions and sum of squares (SS), degrees of freedom (df), Mean Squares (MS), F-ratios (F) and p values. Significant p values (< 0.05) are highlighted.

Source	Type III SS	df	MS	F ratio	p
Copper	89.456	1	89.456	209.475	< 0.001
Origin	0.836	1	0.836	1.958	0.172
Transplant	22.459	1	22.459	52.591	< 0.001
Copper * Transplant	0.434	1	0.434	1.017	0.321
Origin * Transplant	0.568	1	0.568	1.330	0.258
Origin * Copper	1.087	1	1.087	2.545	0.121
Origin * Transplant * Copper	0.124	1	0.124	0.290	0.594
Error	13.239	31	0.427		
Total	130.769	38			

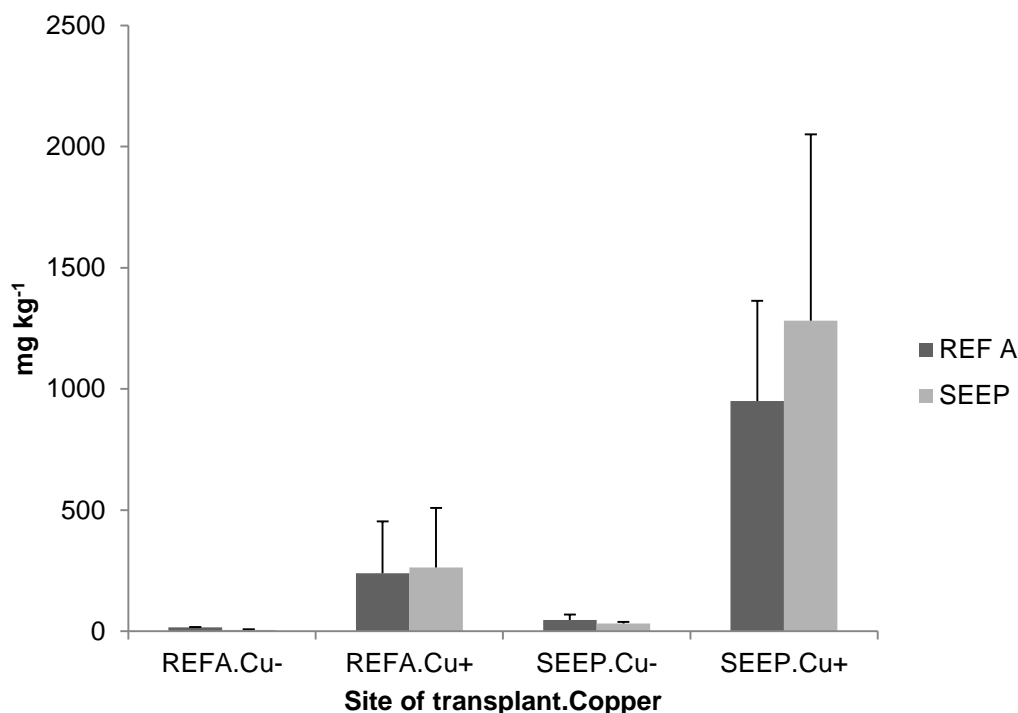


Figure 7.4. Mean (\pm SD, n=4-5) copper concentration (mg kg^{-1}) of *C. corniculata* thalli transplanted from REF A or SEEP not exposed (Cu-) or exposed (Cu+) to copper at REF A and SEEP in June 2013.

In September 2013, percent mass loss of plaster blocks containing copper significantly differed between the sites REF A and SEEP ($F_{1,7}=14.926$, $p=0.008$); plaster blocks deployed at REF A lost approximately 78% of their initial mass, releasing more copper in seawater compared to the SEEP site, where plaster blocks only decreased in mass by 55%. Statistical analysis of tissue copper content in *J. rubens* showed that copper exposure caused different effects in the two sites (site of transplant * copper interaction significant) and that copper concentration depended on the macroalgae origin as well (Table 7.3). Figure 7.5 shows that *J. rubens* exposed to copper had higher tissue copper concentration than control thalli, but this difference was much more evident at the SEEP site than at REF A. Furthermore, thalli originally from SEEP accumulated more copper than those originating from the reference sites.

Table 7.3. ANOVA on log-transformed copper concentration in *J. rubens* thalli measured at the end of the experiment of September 2013. The table shows main factors and their interactions and sum of squares (SS), degrees of freedom (df), Mean Squares (MS), F-ratios (F) and p values. Significant p values (< 0.05) are highlighted.

Source	Type III SS	df	MS	F ratio	p
Origin	1.896	2	0.948	6.652	0.003
Transplant	1.243	1	1.243	8.719	0.005
Copper	21.126	1	21.126	148.212	< 0.001
Origin * Transplant	0.209	2	0.105	0.734	0.485
Origin * Copper	0.458	2	0.229	1.607	0.212
Transplant * Copper	0.593	1	0.593	4.161	0.047
Origin * Transplant * Copper	0.172	2	0.086	0.604	0.551
Error	6.557	46	0.143		
Total	32.106	57			

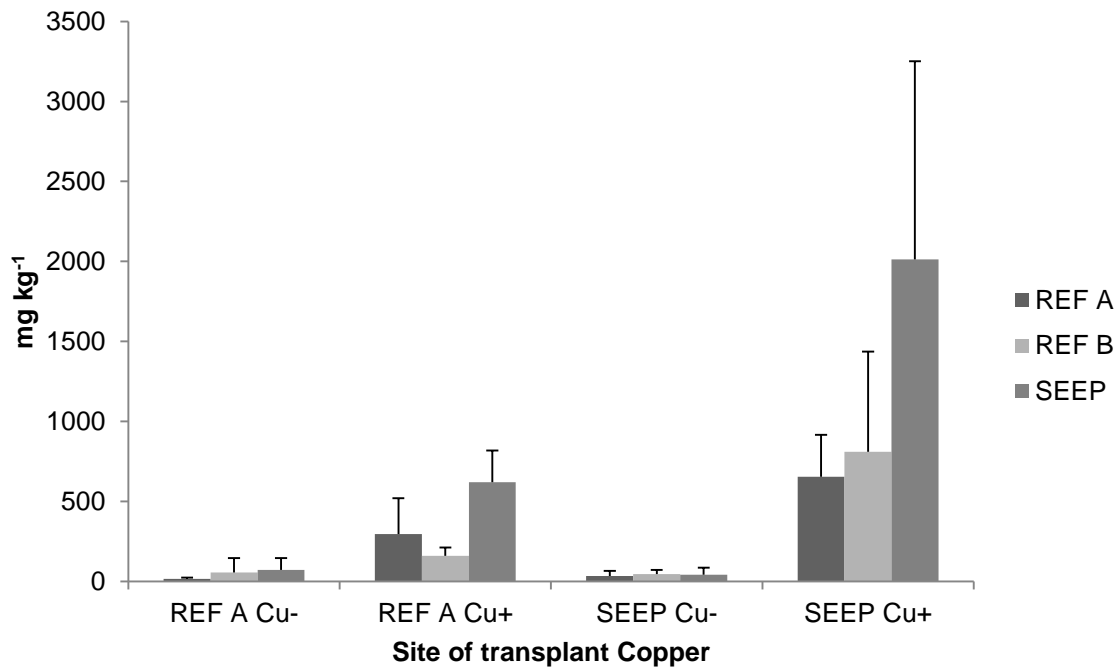


Figure 7.5. Mean (\pm SD, $n=3-5$) copper concentration (mg kg^{-1}) of *J.rubens* thalli transplanted from REF A, REF B or SEEP not exposed (Cu-) or exposed (Cu+) to copper at REF A and SEEP in September 2013.

7.3.3 Maximum quantum yield (F_v/F_m)

Change in maximum quantum yield in *C. corniculata* exposed to copper in June 2013 showed a significant interaction of origin and copper both after transplant and after copper exposure (Table 7.4). This was due to a sharp decrease in maximum quantum yield of the thalli from REF B that were to be exposed to copper; the same thalli recovered from the transplant later than the other groups, leading to a median increase in maximum quantum yield of about 0.2 after copper exposure, whereas all other groups showed no significant effects of copper (Figure 7.6).

Table 7.4. ANOVA on change in maximum quantum yield (F_v/F_m) after transplant (upper part) and after copper exposure (lower part) for *C. corniculata* thalli in June 2013. The table shows main factors and their interactions and sum of squares (SS), degrees of freedom (df), Mean Squares (MS), F-ratios (F) and p values. Significant p values (< 0.05) are highlighted.

Effect of transplant:					
Source	Type III SS	df	MS	F ratio	p
Origin	0.194	2	0.097	7.054	0.002
Transplant	0.065	1	0.065	4.731	0.035
Copper	0.048	1	0.048	3.488	0.069
Origin * Transplant	0.051	2	0.025	1.842	0.171
Origin * Copper	0.163	2	0.082	5.941	0.005
Transplant * Copper	<0.001	1	<0.001	0.022	0.882
Origin * Transplant * Copper	0.002	2	0.001	0.072	0.931
Error	0.578	42	0.014		
Total	1.046	53			

Effect of copper:					
Source	Type III SS	df	MS	F ratio	p
Origin	0.126	2	0.063	8.867	0.001
Transplant	0.005	1	0.005	0.658	0.422
Copper	0.020	1	0.020	2.782	0.103
Origin * Transplant	0.016	2	0.008	1.091	0.345
Origin * Copper	0.061	2	0.030	4.254	0.021
Transplant * Copper	0.002	1	0.002	0.323	0.573
Origin * Transplant * Copper	0.002	2	0.001	0.158	0.854
Error	0.299	42	0.007		
Total	0.519	53			

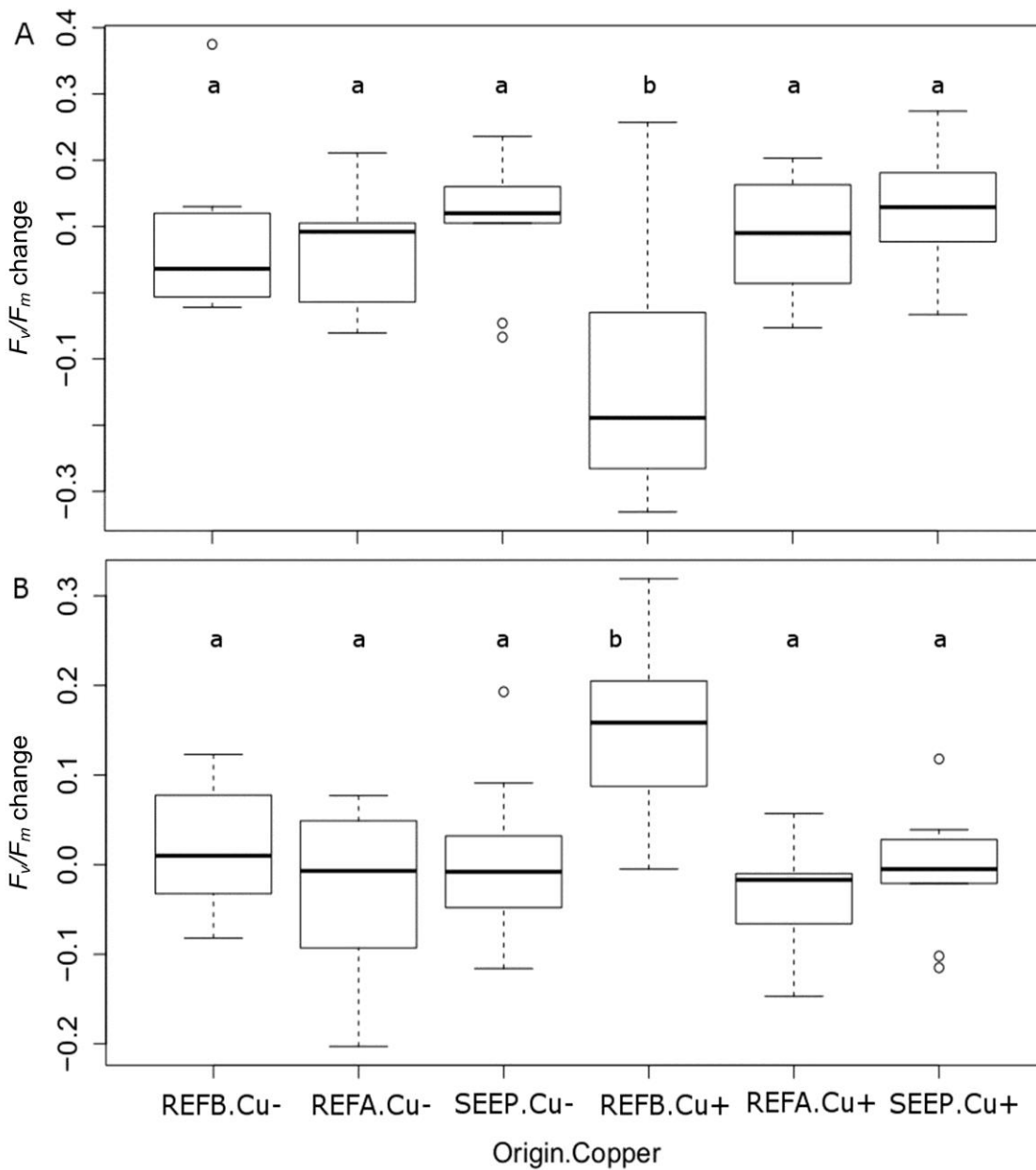


Figure 7.6. Changes in maximum quantum yield (F_v/F_m) following *C. corniculata* thalli transplant (A) and copper exposure (B) in June 2013 depending on their site of origin (REF A, REF B or SEEP) and their exposure to copper (Cu- = no; Cu+ = yes); $n = 7-10$. Horizontal line = median, vertical boxes = 25th and 75th percentiles, whiskers = min/max values if smaller than 1.5 times the inter-quartile range and dots = outliers.

Change in maximum quantum yield in *J. rubens* exposed to copper in September 2013 showed a significant interaction of site of origin and site of transplant before copper exposure, but no significant effects of copper exposure (Table 7.5). This was due to a decrease in maximum quantum yield of the thalli

from REF A transplanted at SEEP and a concurrent increase in maximum quantum yield of thalli from the other reference site transplanted at SEEP (Figure 7.7).

Table 7.5. ANOVA on change in maximum quantum yield (F_v/F_m) after transplant (upper part) and after copper exposure (lower part) for *J. rubens* thalli in September 2013. The table shows main factors and their interactions and sum of squares (SS), degrees of freedom (df), Mean Squares (MS), F-ratios (F) and p values. Significant p values (< 0.05) are highlighted.

Effect of transplant					
Source	Type III SS	df	MS	F ratio	p
Origin	0.036	2	0.018	1.162	0.323
Transplant	0.012	1	0.012	0.779	0.383
Copper	0.001	1	0.001	0.048	0.827
Origin * Transplant	0.138	2	0.069	4.417	0.018
Origin * Copper	0.010	2	0.005	0.326	0.724
Transplant * Copper	0.015	1	0.015	0.962	0.333
Origin * Transplant * Copper	0.053	2	0.026	1.681	0.199
Error	0.627	40	0.016		
Total	0.920	51			
Effect of copper					
Source	Type III SS	df	MS	F ratio	p
Origin	0.003	2	0.002	0.069	0.934
Transplant	0.004	1	0.004	0.171	0.681
Copper	0.032	1	0.032	1.275	0.266
Origin * Transplant	0.093	2	0.046	1.871	0.167
Origin * Copper	0.014	2	0.007	0.274	0.762
Transplant * Copper	0.049	1	0.049	1.997	0.165
Origin * Transplant * Copper	0.014	2	0.007	0.275	0.761
Error	0.989	40	0.025		
Total	1.208	51			

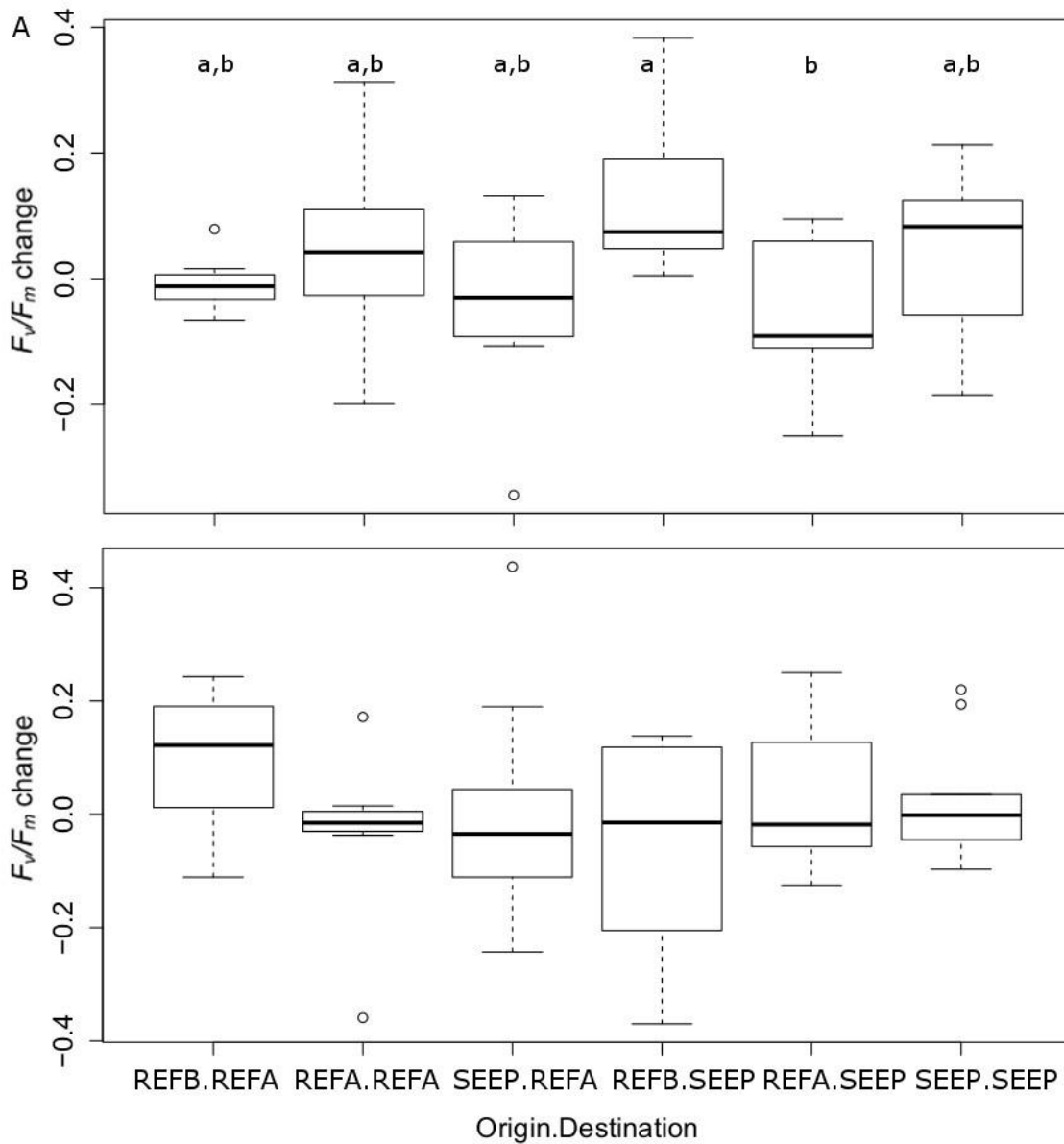


Figure 7.7. Changes in maximum quantum yield (F_v/F_m) following *J. rubens* thalli transplant (A) and copper exposure (B) in September 2013 depending on their site of origin (REF A, REF B or SEEP) and their site of transplant (REF A or SEEP); $n = 7-10$. Horizontal line = median, vertical boxes = 25th and 75th percentiles, whiskers = min/max values if smaller than 1.5 times the inter-quartile range and dots = outliers.

7.3.4 Pigment contents

In the experiment performed in June 2013 on *C. corniculata*, copper had a significant effect on pheophytin *a* and antheraxanthin, while chlorophyll *c*, pheophytin *a* and fucoxanthin were significantly affected by the site of origin (Table 7.6). Figure 7.8 shows that thalli exposed to copper had higher antheraxanthin concentration, but lower pheophytin *a*. On the other hand, thalli originally from SEEP had higher chlorophyll *c* and lower pheophytin *a* and fucoxanthin compared with samples originally from REF A. Samples originating from REF B had to be removed from analysis due to high sample loss.

Table 7.6. MANOVA on pigment concentrations in *C. corniculata* thalli measured after the end of the experiment of June 2013. The table shows main factors and their interactions and dependent variables. F-ratios (F) and p values are reported when significant ($p < 0.05$).

Response variable	Origin	Transplant	Copper	Origin * Transplant	Origin* Copper	Transplant * Copper	Origin * Transplant * Copper
Chl <i>a</i>	-	-	-	-	-	-	-
Chl <i>c</i>	F(1,29)= 5.1 p=0.032	-	-	-	-	-	-
Pheophytin <i>a</i>	F(1,29)= 25.8 p<0.001	-	F(1,29)= 6.0 p=0.021	-	-	-	-
β-carotene	-	-	-	-	-	-	-
Fucoxanthin	F(1,29)= 5.6 p=0.025	-	-	-	-	-	-
Violaxanthin	-	-	-	-	-	-	-
Antheraxanthin	-	-	F(1,29)= 7.8 p=0.009	-	-	-	-
Zeaxanthin	-	-	-	-	-	-	-

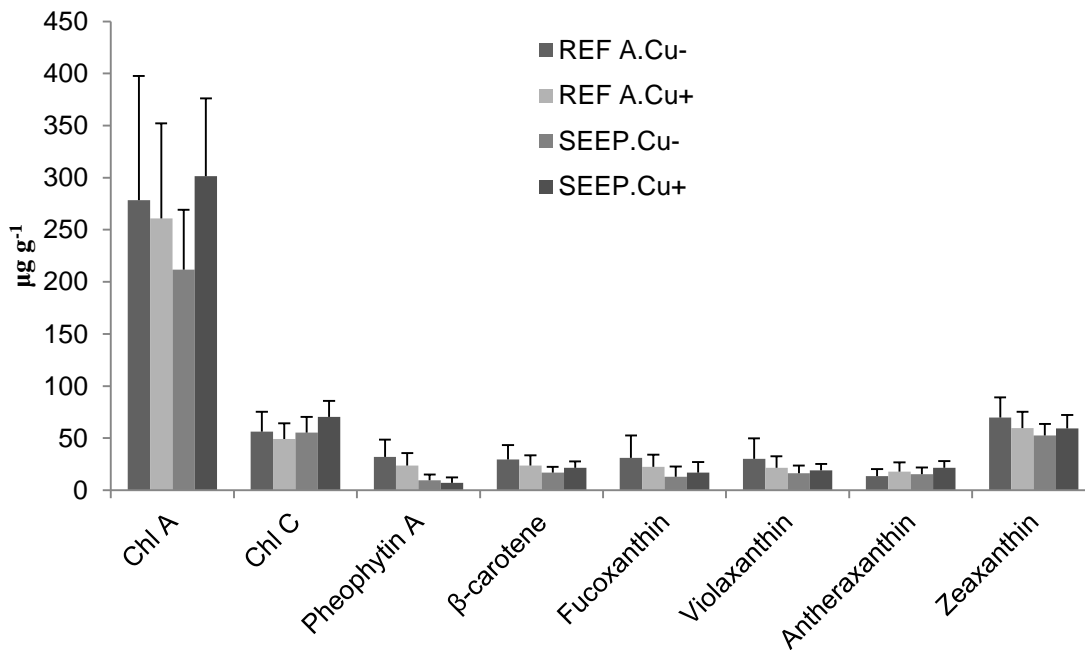


Figure 7.8. Mean (\pm SD, $n=9-10$) pigment concentrations ($\mu\text{g g}^{-1}$ dry mass) of *C. corniculata* thalli transplanted from REF A or SEEP not exposed (Cu-) or exposed (Cu+) to copper in June 2013.

In the experiment performed in September 2013 on *J. rubens*, copper had a significant effect on β -cryptoxanthin, β -carotene and zeaxanthin, while pheophytin A was significantly affected by the site of transplant and zeaxanthin was significantly affected by the interaction of site of origin and site of transplant (Table 7.7). Figure 7.9 shows that thalli exposed to copper had lower β -carotene and zeaxanthin concentration, but higher β -cryptoxanthin. On the other hand, thalli transplanted to SEEP had higher pheophytin A than those transplanted to REF A. Zeaxanthin concentration was higher in thalli transplanted from their site of origin to a different site (i.e. REF A to SEEP and vice versa) compared to concentrations in thalli that remained in their site of origin.

Table 7.7. MANOVA on pigment concentrations in *J. rubens* thalli measured after the end of the experiment of September 2013. The table shows main factors and their interactions and dependent variables. F-ratios (F) and p values are reported when significant ($p < 0.05$).

Response variable	Origin	Transplant	Copper	Origin * Transplant	Origin * Copper	Transplant * Copper	Origin * Transplant * Copper
Chl a	-	-	-	-	-	-	-
Pheophytin a	-	F(1,26)= 15.3 p=0.001	-	-	-	-	-
β cryptoxanthin	-	-	F(1,26)= 13.5 p=0.001	-	-	-	-
Antheraxanthin	-	-	-	-	-	-	-
β -carotene	-	-	F(1,26)= 7.9 p=0.009	-	-	-	-
Violaxanthin	-	-	-	-	-	-	-
Zeaxanthin	-	-	F(1,26)= 9.2 p=0.005	F(1,26)=5.0 p=0.033	-	-	-

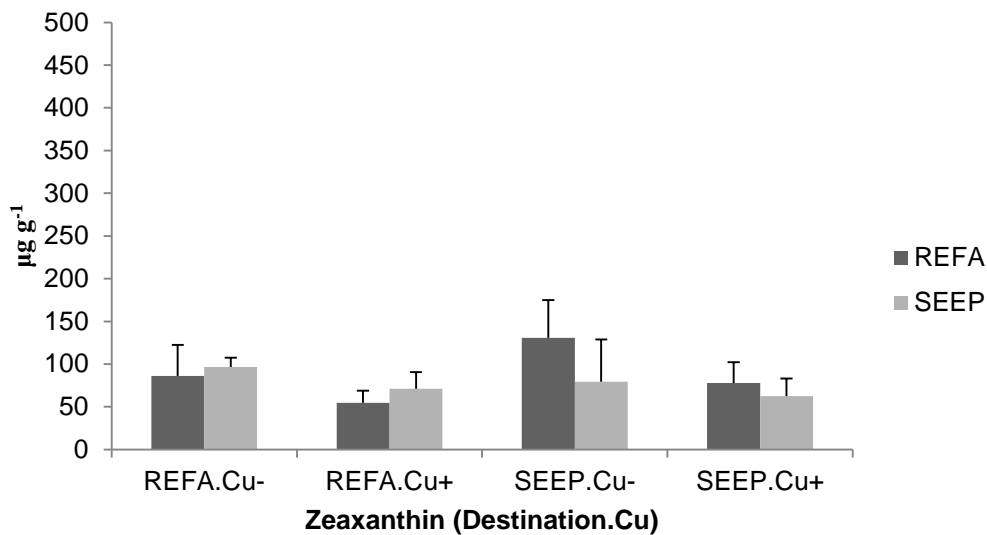
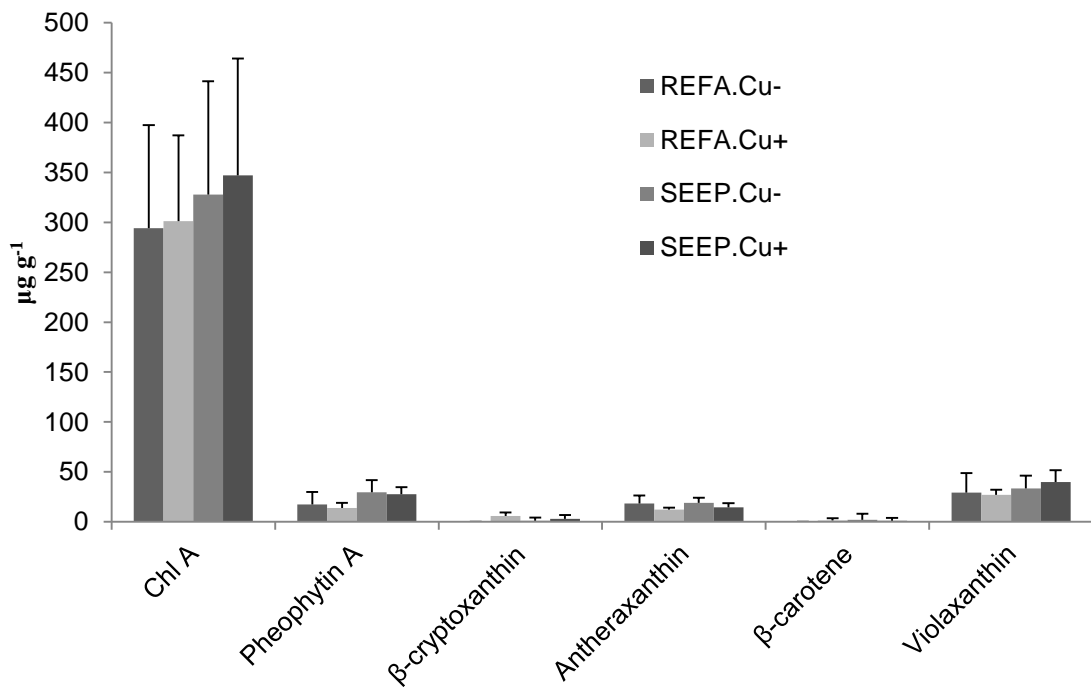


Figure 7.9. Upper part: mean (\pm SD, $n=8-9$) pigment concentrations ($\mu\text{g g}^{-1}$ dry mass) of *J. rubens* thalli transplanted to REF A or SEEP not exposed (Cu-) or exposed (Cu+) to copper in September 2013. Lower part: mean (\pm SD, $n=3-5$) zeaxanthin concentration ($\mu\text{g g}^{-1}$ dry mass) of *J. rubens* thalli transplanted to REF A or SEEP from REF A and SEEP not exposed (Cu-) or exposed (Cu+) to copper in September 2013.

With regards to phycobilins, only phycoerythrin (PE) showed any significant difference among treatments, with a significant site of transplant * copper interaction, whereas phycocyanin (PC) seemed unaffected by the experiment (Table 7.8). At REF A, phycoerythrin concentration increased in thalli exposed to copper, while the opposite was true from *J. rubens* individuals at SEEP, where thalli exposed to copper had lower phycoerythrin concentration compared with controls (Figure 7.10).

Table 7.8. MANOVA on phycoerythrin (PE) and phycocyanin (PC) concentrations in *J. rubens* thalli measured after the end of the experiment of September 2013. The table shows main factors and their interactions and dependent variable, sum of squares (SS), degrees of freedom (df), Mean Squares (MS), F-ratios (F) and p values. Significant p values (< 0.05) are highlighted.

Source	Dependent Variable	Type III SS	df	MS	F-ratio	p
Origin	PE	0.118	1	0.118	0.262	0.614
	PC	0.001	1	0.001	0.001	0.977
Transplant	PE	1.623	1	1.623	3.591	0.071
	PC	1.227	1	1.227	1.506	0.232
Copper	PE	0.005	1	0.005	0.011	0.919
	PC	1.627	1	1.627	1.997	0.171
Origin * Transplant	PE	1.361	1	1.361	3.012	0.096
	PC	0.644	1	0.644	0.790	0.383
Origin * Copper	PE	0.002	1	0.002	0.004	0.947
	PC	2.402	1	2.402	2.947	0.099
Transplant * Copper	PE	2.572	1	2.572	5.692	0.026
	PC	1.409	1	1.409	1.729	0.202
Origin * Transplant * Copper	PE	0.016	1	0.016	0.035	0.853
	PC	0.989	1	0.989	1.213	0.282
Error	PE	10.394	23	0.452		
	PC	18.742	23	0.815		
Total	PE	15.965	30			
	PC	26.690	30			

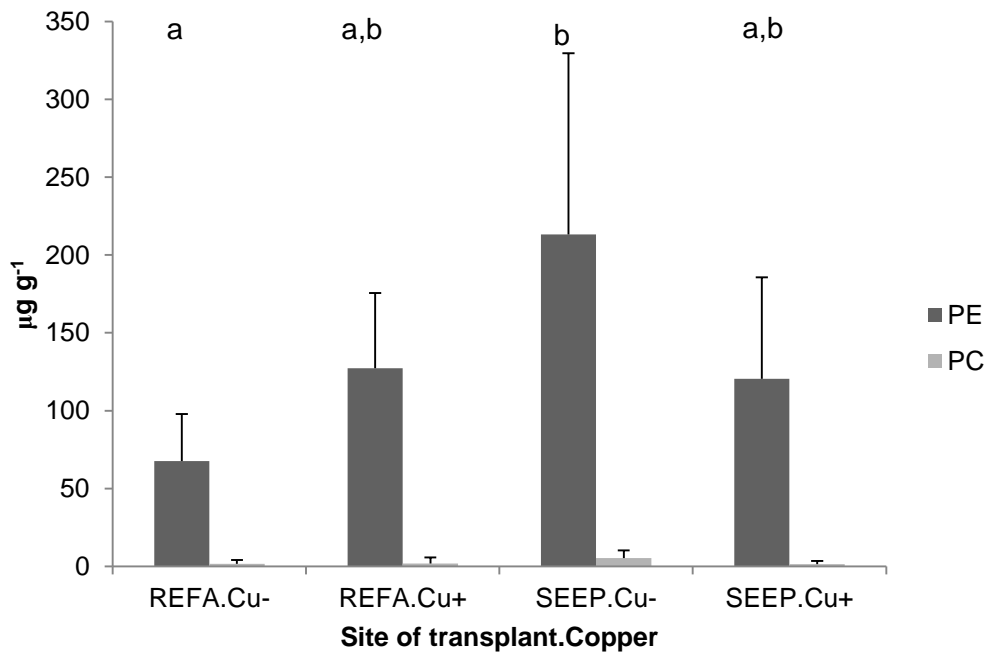


Figure 7.10. Mean (\pm SD, n=6-9) phycoerythrin (PE) and phycocyanin (PC) concentrations ($\mu\text{g/g}$) of *J. rubens* thalli transplanted to REF A or SEEP not exposed (Cu-) or exposed (Cu+) to copper in REF A and SEEP in September 2013.

7.3.5 Invertebrate re-colonisation

Invertebrate communities inhabiting *C. corniculata* thalli were significantly affected by copper, but this effect was not consistent between sites (Site x Copper interaction significant), even after considering the effect of individual thalli biomass on invertebrate community structure (Table 7.9a). Pairwise comparisons showed that copper only had a significant effect near the seeps, but not in the reference site (Table 7.9b). This was also evident from the nMDS plot, where samples from REF A exposed and not exposed to copper are all grouped together, whereas samples from SEEP are separated from REF A samples, but also clearly grouped depending on their copper exposure (Figure 7.11).

Table 7.9. PERMANOVA analyses of square-root transformed invertebrate abundances in *C. corniculata* thalli from copper exposure experiment in June 2013. The first table shows main factors and their interactions and degrees of freedom (df), sum of squares (SS), pseudo-F, permutational p and unique permutations for each of them. The second table shows pair-wise comparisons between copper treatments at both sites. Significant p values (< 0.05) are highlighted.

A)	Source	df	SS	MS	Pseudo-F	P(perm)	Unique perms
	Biomass	1	2193.4	2193.4	3.2403	0.0029	9937
	Site	1	5429.8	5429.8	8.0213	0.0001	9916
	Copper	1	1510.2	1510.2	2.2310	0.0116	9920
	Biomass x Site	1	1036.5	1036.5	1.5312	0.1236	9930
	Biomass x Copper	1	441.99	441.99	0.6529	0.7933	9926
	Site x Copper	1	1373.5	1373.5	2.0291	0.0244	9933
	Biomass x Site x Copper	1	554.56	554.56	0.8192	0.6289	9938
	Residual	11	7446.1	676.92			
	Total	18	19986				

B)	Within level 'REF A' of factor 'Site'			
	Groups	t	P(perm)	Unique perms
	Cu+, Cu-	1.2129	0.1598	9805
	Within level 'SEEP' of factor 'Site'			
	Groups	t	P(perm)	Unique perms
	Cu+, Cu-	1.6212	0.0102	9917

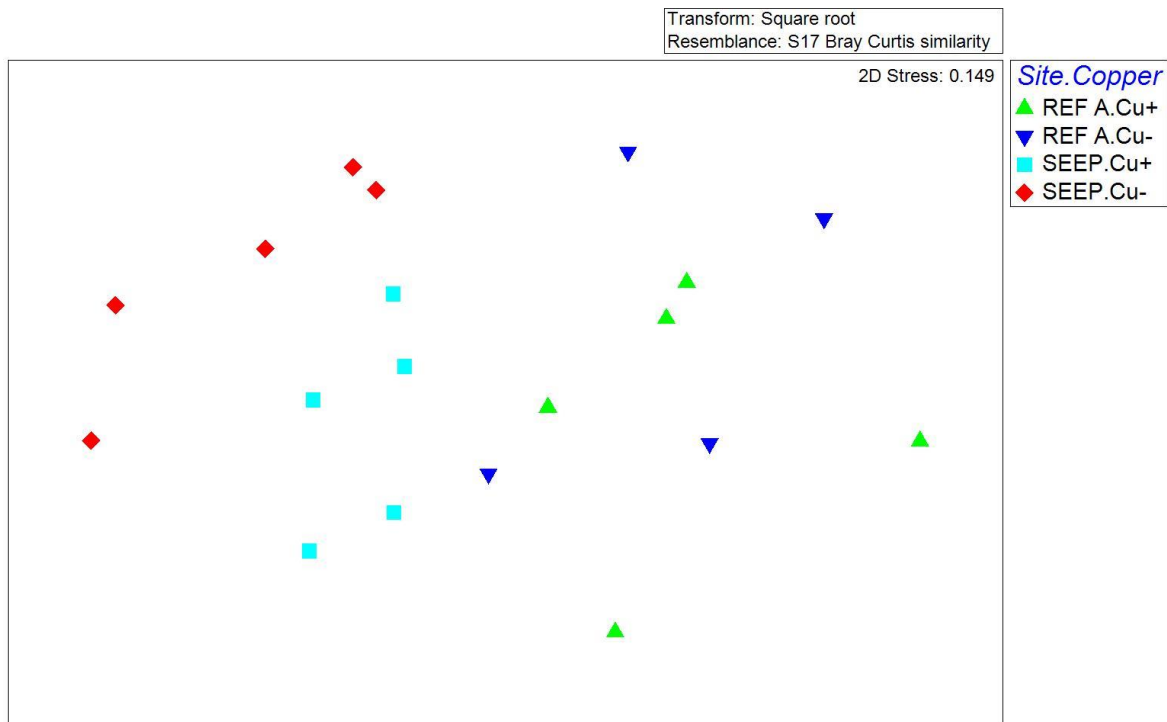


Figure 7.11: MDS plot of invertebrate assemblages on *C. corniculata* thalli placed at REF A or SEEP, and not exposed (Cu-) or exposed (Cu+) to copper in June 2013.

SIMPER analysis showed that crustaceans, molluscs and polychaetes were the main taxa driving differences between sites and copper treatments (Table 7.10). Mean abundance of these taxa is shown in Figure 7.12, showing that all crustacean groups and ophiuroids consistently increased near the seeps when seaweed thalli were not exposed to copper; copper exposure had a negligible effect on their abundance in the reference site and a dramatic negative effect at SEEP. On the other hand, polychaetes were largely unaffected by changes in pCO₂, but their abundance greatly increased in the thalli exposed to copper near the seeps. Gastropods exhibited another type of response, with their abundance decreasing near the seeps and further decreasing when exposed to copper at elevated CO₂. Bivalve and oligochaete abundances were very low and no clear pattern was detectable.

Table 7.10. SIMPER analysis showing the average dissimilarities between sites and copper treatments and which taxonomic groups contributes to the dissimilarity up to 90%. For each taxon, the average abundance in the two groups, their average dissimilarity, the dissimilarity to standard deviation ration and the taxon contribution and cumulative contribution are shown.

Groups REF A & SEEP; Average dissimilarity = 32.05						
Species	REF A	SEEP	Av.Diss	Diss/SD	Contrib%	Cum.%
	Av.Abund	Av.Abund				
Copepods	5.46	8.52	6.53	1.28	20.36	20.36
Gastropods	2.15	0.10	3.94	2.18	12.28	32.65
Amphipods	3.49	5.34	3.86	1.23	12.04	44.68
Polychaetes	3.72	4.06	3.57	1.12	11.13	55.81
Tanaids	3.19	4.55	2.93	1.32	9.14	64.95
Ostracods	1.72	2.37	2.29	1.25	7.16	72.10
Isopods	1.98	2.56	2.11	0.90	6.59	78.69
Bivalves	0.92	0.34	1.43	1.35	4.45	83.14
Ophiuroids	0.16	0.72	1.34	0.79	4.19	87.33
Oligochaetes	0.73	0.20	1.28	0.96	4.00	91.34

Groups Cu+ & Cu-; Average dissimilarity = 27.61						
Species	Cu+	Cu-	Av.Diss	Diss/SD	Contrib%	Cum.%
	Av.Abund	Av.Abund				
Copepods	6.19	8.05	5.42	1.26	19.64	19.64
Polychaetes	4.50	3.24	3.85	1.08	13.94	33.58
Amphipods	4.10	4.87	3.14	1.38	11.38	44.97
Isopods	1.70	2.93	3.10	1.78	11.21	56.18
Ostracods	2.34	1.75	2.54	1.28	9.21	65.39
Decapods	3.61	4.24	1.98	1.31	7.18	72.57
Gastropods	1.11	1.03	1.39	0.70	5.02	77.59
Ophiuroids	0.24	0.69	1.35	0.80	4.89	82.47
Oligochaetes	0.31	0.60	1.16	0.86	4.21	86.68
Bivalves	0.54	0.69	1.00	0.92	3.63	90.31

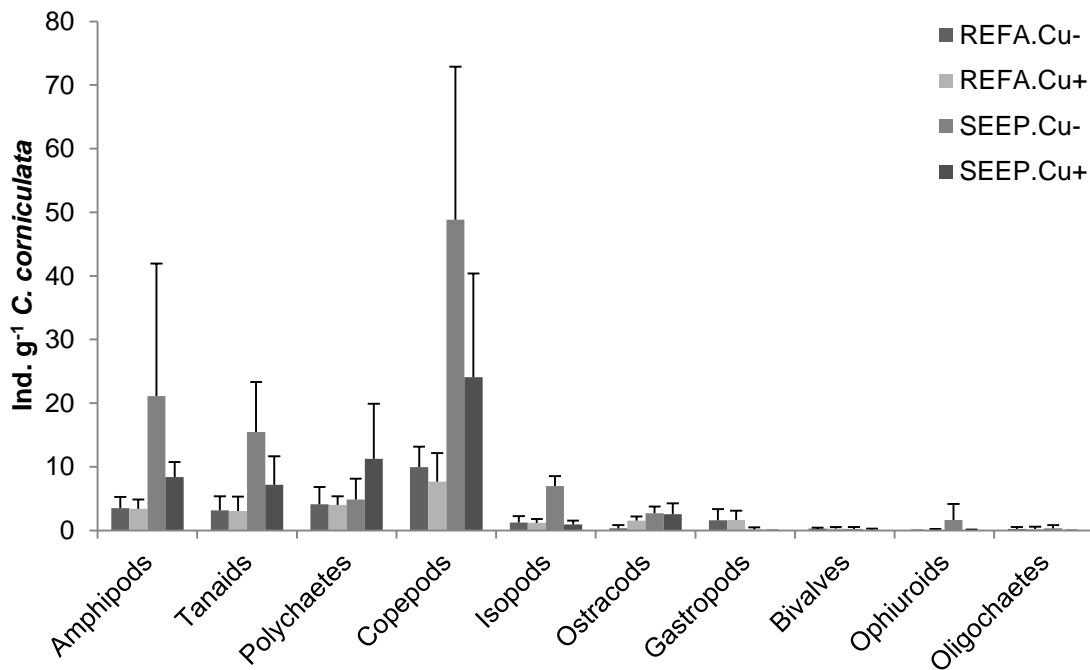


Figure 7.12. Mean (\pm SD, n=4-5) number of individuals for each of the main taxonomic groups. Abundances were normalised by *C. corniculata* dry mass; *C. corniculata* thalli were placed in REF A or SEEP and exposed (Cu+) or not exposed (Cu-) to copper for 36h in June 2013.

7.4 Discussion

This is the first investigation of the combined effect of elevated carbon dioxide and metal toxicity on macroalgal physiology and invertebrate communities. Copper accumulation in both *C. corniculata* and *J. rubens* increased at elevated pCO₂ levels, even though copper released from plaster blocks was the same (June 2013) or less (September 2013) near the seeps than at the reference site. Long-term acclimatisation effects on copper accumulation were evident for the coralline alga *J. rubens*, as thalli grown near the seeps accumulated significantly more copper than those transplanted from reference sites.

Copper bioavailability is expected to increase with decreased seawater pH (Richards *et al.*, 2011) and might explain increased copper accumulation at high

CO₂. However, seaweeds accumulate copper for over 24 h after its addition to seawater (Connan and Stengel, 2011a). As Cu²⁺ ions were not complexed immediately while plaster block continuously released them, copper was equally bioavailable at both sites. Copper uptake, however, is regulated by metabolic activity (Connan and Stengel, 2011a), so it is possible that macroalgae had more energy available after down-regulating carbon concentrating mechanisms (CCMs). Reduced use of CCMs following increased CO₂ availability has already been proven for some macroalgae (Olischläger and Wiencke, 2013), and this might explain the copper accumulation pattern observed in *C. corniculata*.

As elevated CO₂ increases the energetic cost of calcification (Bradassi *et al.*, 2013), *J. rubens* thalli just transplanted from reference sites probably used most of the surplus energy derived from increased CO₂ levels to maintain calcification rates. They thus showed a relatively small increase in copper accumulation. On the other hand, thalli grown at high CO₂ may have mechanisms in place to make calcification at high pCO₂ energetically sustainable in the long term. They are therefore likely to have higher metabolic activity and accumulate more copper than thalli not acclimatised to elevated CO₂ levels. Coralline algal calcification is controlled by alginic acid and sulfated polysaccharides (Koch *et al.*, 2013), which are also known to have a high affinity for metals (Raize *et al.*, 2004). Increased production of calcification-inducing compounds in *J. rubens* acclimatised to high CO₂ could enhance copper accumulation, potentially increasing its vulnerability to metal toxicity.

Physiological responses to copper examined in both macroalgal species were not influenced by acclimatisation to increased carbon dioxide (i.e. no significant site of origin * copper interactions). In fact, maximum quantum yield (F_v/F_m) was only affected by transplant, while some pigments showed effects of site of origin

and copper in *C. corniculata* and of site of transplant, copper and site of origin in *J. rubens*. Copper is known to decrease F_v/F_m in some species of red algae (Küpper *et al.*, 2002; Brown and Newman, 2003; Baumann *et al.*, 2009), whereas maximum quantum yield of brown algae is mostly unaffected at moderate copper levels (Nielsen *et al.*, 2003; Nielsen and Nielsen, 2005; Baumann *et al.*, 2009; Nielsen and Nielsen, 2010).

Copper exposure only caused a small decrease of pheophytin A and a small increase of antheraxanthin in *C. corniculata*. Since the latter was not associated with an increase in the xanthophyll cycle pool size, these pigments are unlikely to play a role in copper defence for this species. This is in accord with previous studies on *Fucus serratus*, where no change in xanthophyll pool size was found in light-adapted thalli after copper exposure (Nielsen *et al.*, 2003; Nielsen and Nielsen, 2010). On the other hand, *J. rubens* thalli exposed to copper showed a small increase in β -cryptoxanthin, but a bigger decrease in β -carotene and zeaxanthin, resulting in a decrease in total carotenoids. Decreased carotenoids concentrations were previously found in a red alga exposed to high copper concentrations (5-10 ppm; Gouveia *et al.*, 2013), whereas red algae exposed to Cu^{2+} concentrations of 0.2-0.5 ppm often increase their carotenoids content to counter copper toxicity (Brown and Newman, 2003; Collén *et al.*, 2003; Pinto *et al.*, 2011). *J. rubens*, however, did not show the reduction in chlorophyll *a* found in another red alga at high Cu^{2+} concentrations (Gouveia *et al.*, 2013). This suggests the experimental copper pulse exposed *J. rubens* to relatively high Cu^{2+} concentrations. There was a reduction in phycoerithrin content when *J. rubens* was exposed to copper at SEEP, but not at REF A. Decreased phycobilins concentration is considered a sensitive indicator of copper stress (Küpper *et al.*, 2002; Brown and Newman, 2003; Xia *et al.*, 2004). *J. rubens*

transplanted near the seeps might be more sensitive to copper exposure because of the increased energetic cost of maintaining calcification rates at elevated CO₂ (Bradassi *et al.*, 2013) or because of increased copper accumulation.

Macroalgae counter negative effects of copper exposure by synthesizing metal-binding compounds such as metallothioneins and phytochelatins (Lobban and Harrison, 1994) and by increasing the activity of antioxidant enzymes (Collén *et al.*, 2003). Synthesis of complex molecules is energy expensive, so growth is reduced in many macroalgal species even at low copper levels (Collén *et al.*, 2003; Brown and Newman, 2003; Nielsen *et al.*, 2003; Xia *et al.*, 2004). Fucoid and articulate coralline algae, however, are relatively slow-growing species whose growth rates are unlikely to be measurable after 36 hours. In brown algae, phlorotannins movement to the cell wall and exudation in the surrounding seawater provides additional defence against copper damage (Connan and Stengel, 2011b). Phlorotannins are polyphenols characteristic of phaeophytes that bind metal ions reducing their toxicity; their increased proportion in the cell walls of algae exposed to copper and increased release in the environment could have contributed to the lack of observed effects of copper in *C. corniculata*. However, it is possible that some effects of copper exposure have not been detected in this study. Lipid peroxidation, antioxidant enzymes activity and antioxidant compounds all increase following copper exposure of 48 to 96 hours (Collén *et al.*, 2003; Contreras *et al.*, 2005). In red algae, mycosporine-like amino-acids (MAAs) are important antioxidant compounds that are up-regulated after short exposure to oxidative stress (Karsten *et al.*, 1998). Further research is therefore needed before concluding that *C. corniculata* is not negatively affected by copper pulses at high CO₂ levels.

Although acclimatisation to elevated CO₂ had no effects on macroalgal responses to copper, *C. corniculata* thalli collected at SEEP had higher chlorophyll *c* content and slightly lower pheophytin A and fucoxanthin contents compared to those collected at reference sites. On the other hand, pheophytin a content increased in *J. rubens* transplanted near the seeps, possibly a short-term response to increased CO₂. *J. rubens* pigments also showed some transplant effect, with zeaxanthin content being higher in thalli transplanted to a different site (i.e. SEEP. REFA and REFA.SEED) compared to those transplanted to their site of origin (i.e. SEEP.SEED and REFA.REFA). Short-term and long-term effects of CO₂ on macroalgal physiology will be compared in the next Chapter.

Invertebrate colonisation was significantly affected by copper exposure, but only at the high CO₂ site. This is probably due to very high copper accumulation by *C. corniculata* at elevated CO₂, as copper release rates in seawater were similar between sites in June 2013. Some crustaceans are more sensitive to copper at elevated CO₂ levels (Roberts *et al.*, 2013), which could contribute to their observed decrease when exposed to copper near the seeps. The specific responses of invertebrate taxa are consistent with previous studies: many crustaceans increase in abundance with increased CO₂ (Kroeker *et al.*, 2011), but are negatively affected by copper (Roberts *et al.*, 2006). Gastropods abundance is negatively affected by both carbon dioxide (Hale *et al.*, 2011; Kroeker *et al.*, 2011) and copper (Roberts *et al.*, 2006), while many polychaete species are largely unaffected by both factors (Roberts *et al.*, 2006; Cigliano *et al.*, 2010). The increase in polychaete abundances in *C. corniculata* thalli exposed to copper at the high CO₂ site was therefore unexpected, but it is possible they had more space and resources available following the marked

decrease in crustaceans. A similar pattern has already been detected by Hale *et al.* (2011), who found increased nematode abundance following a decrease in the abundance of sensitive taxa as CO₂ increased. Copper exposure combined with ocean acidification could however affect polychete larval stages (Lewis *et al.*, 2012; Campbell *et al.*, 2014).

Overall, *J. rubens* appeared more sensitive to copper than *C. corniculata*, especially at elevated CO₂, as well as showing changes in copper accumulation patterns following long-term exposure to high CO₂. These species are currently the two main space occupiers on shallow rocky shores off Methana, but *J. rubens* is at competitive disadvantage with *C. corniculata* when CO₂ levels are high (see Chapter 3). This study shows that *J. rubens* is likely to be negatively affected by the interaction of ocean acidification and copper pollution, and therefore at risk of local extinction. Since only two species (a calcifying red alga and a non-calcifying brown alga) were examined in the present study, the results are not applicable to all competitive interaction between calcifying and non-calcifying algae, as red and brown algae have very different physiologies, which could also influence *J. rubens* and *C. corniculata* interactions (Lobban and Harrison, 1994).

Ocean acidification increased seaweed copper bioaccumulation, and had significant effects on their epifauna. This adds to a growing body of research showing that indirect effects of ocean acidification are at least as important as its direct effects (Kroeker *et al.*, 2013c). Decreased growth rates of coralline algae with increased CO₂ can make them less competitive and cause communities to become dominated by fleshy algae (Kroeker *et al.*, 2013c), or cause changes in herbivore performance through decreased food quality (Rossoll *et al.*, 2012; Poore *et al.*, 2013). Interactive negative effects of ocean

acidification and copper pollution on competitive ability of *J. rubens* and abundance of many epifaunal taxa, especially heavily calcified ones, suggest that benthic communities will dramatically change in copper-polluted areas. These areas are relatively common worldwide and include the copper mining regions illustrated in Figure 7.2; here, it is essential that local managers reduce copper pollution to reduce the negative effects of ocean acidification on macroalgal communities and the services they provide.

Chapter 8

General discussion

8.1 Main findings and implications for marine systems

Macroalgal beds are an extremely important habitat in temperate coastal environments, as they provide vital ecosystem services such as oxygen production, nutrient cycling, water depuration, fisheries production and shore protection from waves (Rönnbäck *et al.*, 2007). Information on macroalgal beds responses to ocean acidification at the community level that take into account biological interactions and adaptation potential are therefore needed to reliably forecast future ecosystem state and take appropriate measures to adapt to or mitigate the possible reduction of ecosystem services provided by those habitats. This thesis contributes to achieving this objective, and its main findings are illustrated in Figure 8.1. All this thesis' objectives were achieved; specifically:

- Geochemical surveys at seeps off Methana showed that this site is suitable to study the effects of high CO₂ on benthic communities, as no confounding gradients in temperature, salinity, total alkalinity, nutrients, hydrogen sulphide or heavy metals were found (Chapter 2).
- At Mediterranean CO₂ seeps off Italy and Greece, macroalgal communities greatly changed, with fucoid algal abundance increasing and coralline algal abundance decreasing as pCO₂ increased (Chapter 3). Epifaunal communities changed as well: at high CO₂ sites, abundance of heavily calcified taxa (e.g. gastropods, bivalves) decreased, while more resistant taxa (mainly polychaetes) abundances increased at high CO₂ (Chapter 4).
- Strength of herbivore top-down control did not appear to change at different pCO₂ levels, even though densities of calcifying intertidal and

subtidal herbivores (i.e. limpets and sea urchins) decreased at elevated $p\text{CO}_2$ (Chapter 5).

- Non-reversible acclimatisation did not seem to play a role in benthic community changes with increased $p\text{CO}_2$, as the responses of transplanted calcified and non-calcified macroalgae to elevated CO_2 did not depend on their history of $p\text{CO}_2$ exposure (Chapter 6).
- Exposure to an additional stressor (i.e. copper pollution) had no additional negative effects on the physiology of a calcifying alga, but there were strong interactive effects on seaweed epifauna, reducing abundances of some taxa that were weakly affected or advantaged by exposure to elevated $p\text{CO}_2$ alone (e.g. amphipods; Chapter 7).

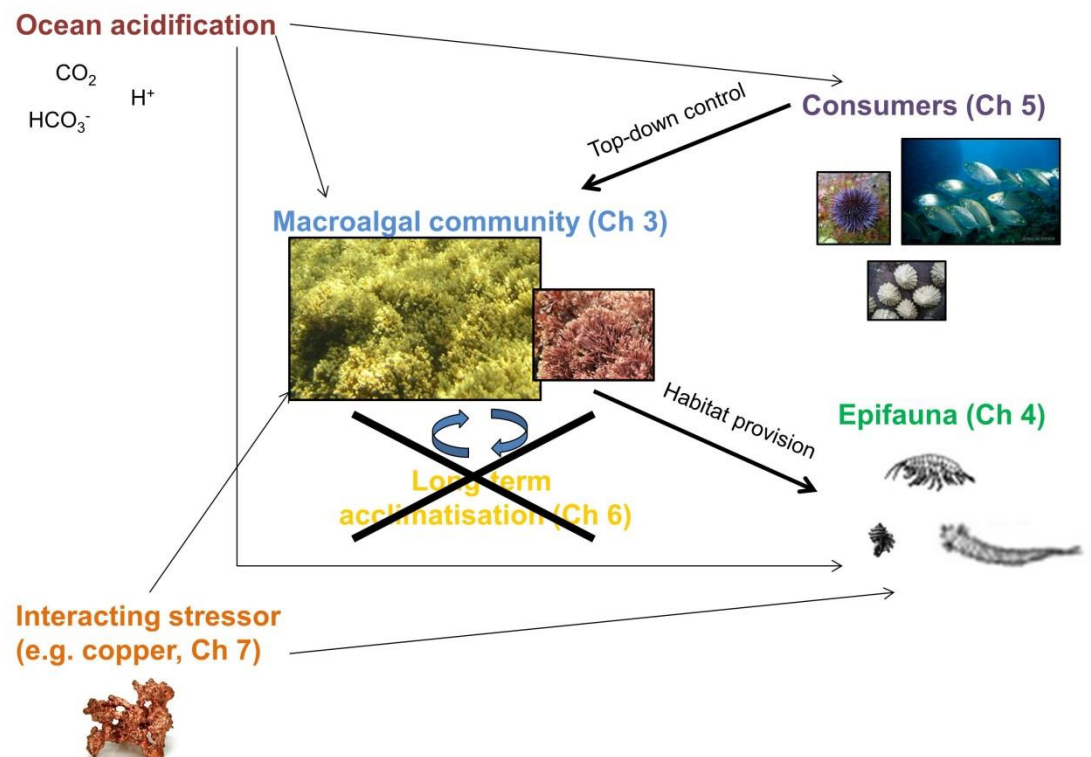


Figure 8.1. Visual abstract of thesis results; macroalgal communities (Chapter 3) and their epifauna (Chapter 4) change with increasing $p\text{CO}_2$ levels, with heavily calcified macroalgae and invertebrates decreasing in abundance at elevated CO_2 . Long-term acclimatisation to

elevated pCO₂ did not seem to have permanent effects on dominant macroalgal species, as no significant effects of origin site on macroalgal physiology were found (Chapter 6). I also found that decreased calcifying herbivores densities do not significantly affect the strength of top-down control on macroalgal communities (Chapter 5), and that ocean acidification and short-term copper pollution interact and produce larger negative effect on a dominant calcifying macroalga, but especially on seaweed epifauna (Chapter 7).

8.1.1 Benthic community responses to ocean acidification

General patterns of benthic community changes with increasing pCO₂ levels at volcanic seeps off Italy and Greece were consistent with results from laboratory experiments and other ocean acidification analogues in that diversity and abundance of calcifying organisms decreased as CO₂ levels increased (Kroeker *et al.*, 2013a). Macroalgal communities responded in very similar ways at all Mediterranean seep sites studied so far, with a decrease in calcifying macroalgae and an increase in *Sargassum vulgare* abundance (Porzio *et al.*, 2011; Chapter 3). Epifaunal communities showed different patterns depending on the study area and the habitat studied (Chapter 4). While epifaunal communities of fucoid algae show a decrease of most invertebrate taxa at elevated pCO₂ at Methana, polychaete abundance increased at high CO₂ at Vulcano (Chapter 4). On the other hand, turf epifauna at seeps off Ischia showed an increase in crustaceans at elevated CO₂ (Kroeker *et al.*, 2011), seagrass-dwelling amphipods and polychaetes increase in abundance at elevated CO₂ levels off Ischia (Garrard *et al.*, 2014), and nematode abundance increased in Atlantic turf epifaunal communities exposed to ocean acidification conditions (Hale *et al.*, 2011). In addition, epiphyte communities of *Cystoseira corniculata* at Methana did not change significantly with CO₂ (Chapter 4), possibly because *C. corniculata* photosynthesis raised local pH and protected

epiphytes from the negative effects of increased CO₂ (Cornwall *et al.*, 2014). This clearly shows that site- and habitat-specific interactions among species result in different communities at high CO₂.

Studies in nutrient-rich areas have shown that calcifiers can remain abundant in areas with naturally high pCO₂ if food is not limiting. For instance, barnacles and mussels are dominant in upwelling water off Kiel fjord, where pCO₂ reaches concentrations over 1000 µatm but nutrient levels are high (Thomsen *et al.*, 2010), while spirorbid worms from an upwelling area in the Baltic Sea are negatively affected by CO₂ only at levels over 3000 µatm (Saderne and Wahl, 2013). However, climate change is expected to reduce nutrient availability in surface waters due to increased water stratification (Sarmiento *et al.*, 2004), meaning that results from upwelling areas might underestimate the negative impacts of ocean acidification. Seeps off Methana and Vulcano are oligotrophic, and have similar nutrient concentrations (Chapter 2; Johnson, 2012). Although the Eastern Mediterranean is usually more oligotrophic than the Western basin (Siokou-Frangou *et al.*, 2010), the Saronikos Gulf has relatively high nutrient concentrations due to riverine inputs and urbanisation (Tsiamis *et al.*, 2013). In contrast, south-eastern Mediterranean coastal waters are ultra-oligotrophic ([Chl a] < 0.06 mg*m⁻³; Shushkina *et al.*, 1997) during the warmest part of the year (Siokou-Frangou *et al.*, 2010); comparable chlorophyll concentrations are only found in the Northern Red Sea (Labiosa *et al.*, 2003) and in subtropical gyres (Kletou and Hall-Spencer, 2012). As low food availability impairs organisms' ability to cope with increased CO₂ (Thomsen *et al.*, 2013), these nutrient-poor ecosystems are probably highly vulnerable to ocean acidification. However, community responses to elevated CO₂ in ultra-oligotrophic coastal areas are virtually unstudied.

This thesis contributes to revealing general patterns of community responses to high CO₂. However, general limitations of using volcanic seeps as ocean acidification laboratories, described in detail in Chapter 2, should be taken into account. In addition, more controlled studies (e.g. using mesocosms or field pCO₂ manipulations) would determine the exact CO₂ concentrations that trigger the observed community changes (Gattuso *et al.*, 2014). Insights could also be gained from the study of a wider range of habitats (e.g. soft substrata).

8.1.2 Changes in biological interactions at elevated pCO₂

Changes in biological interactions with increasing CO₂ are poorly known, although there is evidence that calcifying macroalgae become less competitive at elevated CO₂ (Kroeker *et al.*, 2013c; Short *et al.*, 2014) and reduced sea urchin grazing appears to favour increased macroalgal biomass (Johnson *et al.*, 2012). In this thesis, experiments on intertidal and subtidal rocky shores demonstrated that reduced abundances of calcifying herbivores at elevated CO₂ do not necessarily have a significant effect on sessile community composition (Chapter 5). At Vulcano, limpets had little effect on macroalgal communities in reference conditions, and their reduced densities with increasing CO₂ did not affect macroalgal communities, whereas carbon dioxide changed the specific composition and structure of intertidal communities. On the other hand, sea urchins strongly controlled macroalgal biomass on subtidal rocky reefs off Methana, but grazing control on macroalgal biomass was maintained at high CO₂ thanks to a marked increase in the abundance of herbivorous fish.

These results show that while ocean acidification can profoundly affect marine ecosystems, functional redundancy within trophic groups such as herbivores can reduce its effect. Since coastal environments have low functional redundancy, even when diversity is relatively high (Micheli *et al.*, 2014),

preserving diversity in marine ecosystems is essential for maintaining ecosystem function in the face of future environmental changes. In the Mediterranean Sea, overfishing of apex predators has led to higher abundances of sea urchins and herbivorous fish, as they are usually not targeted by commercial fisheries (Guidetti and Dulčić, 2007; Guidetti and Sala, 2007). High herbivore densities can often lead to impoverished macroalgal communities with much lower diversity biomass than unexploited Mediterranean coastal ecosystems (Sala *et al.*, 2012).

Thus, unvaried grazing pressure at different CO₂ levels may maintain suboptimal community structure. Figure 8.2A shows typical subtidal communities found at Methana at elevated pCO₂, with high fish biomass and a *Cystoseira* belt reaching depths of up to 12 meters (author's personal observation). This suggests that in the long term, non-calcifying macroalgae benefit from increased CO₂ levels and overall primary productivity is likely higher near the seeps than at reference sites, where the biomass of macroalgae and fish is lower (Figure 8.2B).

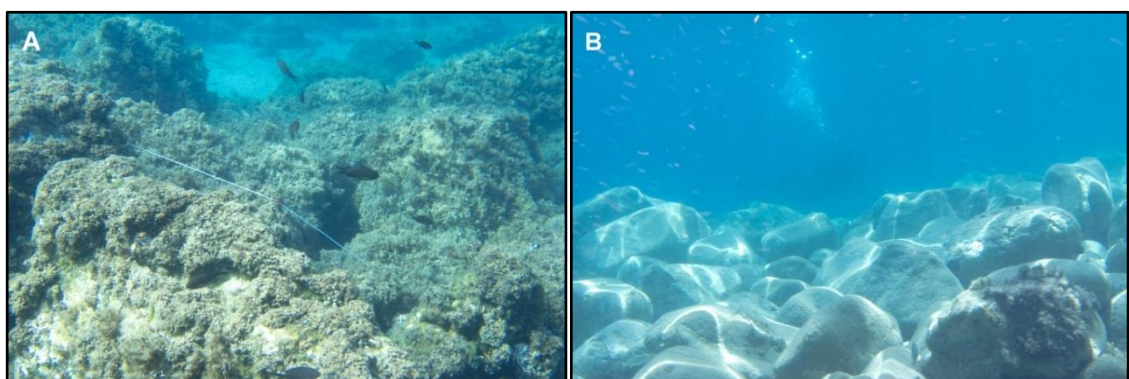


Figure 8.2. Typical seascape near seeps off Methana (A) and at reference sites (B) at ~ 3 m depth; areas near the seeps had higher macroalgal cover and higher fish biomass than reference sites, which were dominated by crustose coralline algae and sea urchins (photos by Maria Salomidi, September 2013).

Findings of this thesis have improved our knowledge on how herbivory will be affected by elevated CO₂. There is still very little research on how other biological interactions, especially predator-prey interactions, will be influenced by ocean acidification in temperate systems, but Amaral *et al.* (2012) found that mussels grown at low pH are more vulnerable to crab predation. In tropical environments, recent studies show that changes in vulnerability to predators are size- and species-specific for fish, as some predators will be negatively affected by elevated pCO₂ as well (Ferrari *et al.*, 2011; Allan *et al.*, 2013). In addition, this thesis shows that changes in herbivory due to ocean acidification vary depending on the habitat studied, meaning that more research would be needed to predict responses of marine communities in a variety of habitats.

Both herbivore exclusion experiments reported in this thesis were performed at one reference and one high CO₂ site only. At Vulcano and Methana, pCO₂ is considered the main driver of change, with other environmental factors (e.g. temperature, salinity, heavy metals, hydrogen sulphide, wave exposure) not varying significantly between study sites (Boatta *et al.*, 2013; Chapter 2). Between-sites differences reported in Chapter 5 are therefore likely to be caused by changes in pCO₂ levels, but repeating these experiments in more than one reference site would improve their power and give more reliable results.

8.1.3 Adaptation potential to ocean acidification

In this thesis, two dominant macroalgal species (the fucoid alga *Cystoseira corniculata* and the coralline alga *Jania rubens*) were transplanted between reference and high CO₂ sites for several months in order to assess whether they had permanently acclimatised to elevated pCO₂, which might give an indication of their adaptation potential (Chapter 6). In addition, short-term effects

of elevated CO₂ were assessed on some physiological parameters in the same two species (Chapter 7). Comparison of short- and long-term effects of carbon dioxide on *C. corniculata* and *J. rubens* (Table 8.1) shows that there were very small effects on *C. corniculata* physiology in the short term, while in the long term it was evident that some pigments (chlorophyll *c* and antheraxanthin) concentration increase in thalli exposed to elevated CO₂ for several months. In addition, in the long term elevated carbon dioxide increased *C. corniculata* maximum electron transport rates (rETR_{max}), C:N ratio and phlorotannin content, as well as decreasing epiphyte cover. *J. rubens* showed increases in some pigments concentration when transplanted to elevated CO₂; in the short term, pheophytin *a* and phycoerithryin increased in thalli exposed to high CO₂, whereas in the long term there was an increase in chlorophyll *a*, violaxanthin, zeaxanthin and phycocyanin. On the other hand, all other parameters measured in *J. rubens* did not change significantly after the thalli were transplanted near the seeps.

Table 8.1. Summary of the effect of elevated CO₂ on physiological parameters measured in thalli of *Cystoseira corniculata* and *Jania rubens* transplanted for 3 days (short term; Chapter 7) or 4-9 months (long term; Chapter 6). +: increase in parameter value; -: decrease in parameter value; n.s.: no significant effect; n.m.: parameter not measured.

Response variable	<i>Cystoseira corniculata</i>		<i>Jania rubens</i>	
	Short-term	Long-term	Short-term	Long-term
Photochemistry				
F_v/F_m	n.s.	n.s.	n.s.	n.s.
rETR _{max}	n.m.	+	n.m.	n.s.
I _k	n.m.	n.s.	n.m.	n.s.
α _{ETR}	n.m.	n.s.	n.m.	n.s.
NPQ	n.m.	n.s.	n.m.	n.s.
Pigments				
Chlorophyll a	n.s.	n.s.	n.s.	+
Chlorophyll c	n.s.	+	n.m.	n.m.
Pheophytin a	n.s.	n.s.	+	n.s.
β-carotene	n.s.	n.s.	n.s.	n.s.
Fucoxanthin	n.s.	n.s.	n.m.	n.m.
Violaxanthin	n.s.	n.s.	n.s.	+
Antheraxanthin	n.s.	+	n.s.	n.s.
Zeaxanthin	n.s.	n.s.	n.s.	+
β-cryptoxanthin	n.m.	n.m.	n.s.	n.s.
Phycoerythrin	n.m.	n.m.	+	n.s.
Phycocyanin	n.m.	n.m.	n.s.	+
Growth	n.m	n.s.	n.m	n.s.
Epiphyte cover	n.m	-	n.m	n.m
C:N	n.m	+	n.m	n.s.
C_{inorg}	n.m	n.m	n.m	n.s.
Phenol content	n.m.	+	n.m.	n.m.

Overall, both species seemed to change their physiology relatively quickly (more than three days, but less than four or nine months for *J. rubens* and *C. corniculata*, respectively), as the site of origin had very little effect on the physiology of long-term transplants. Macroalgae commonly show high phenotypic plasticity (Demes *et al.*, 2009), which could help calcifying species such as *J. rubens* to physiologically buffer negative effects of ocean acidification. However, phenotypic plasticity is known to slow down genetic adaptation by reducing selection gradients (Sunday *et al.*, 2014), meaning that if CO₂ will increase over *J. rubens*' current tolerance, this species may disappear.

Some physiological parameters were significantly different depending on the site of transplant in both species. While *C. corniculata* seemed to be favoured at high CO₂ levels (decreased epiphyte cover, higher phlorotannin content and maximum electron transport rates), *J. rubens* only showed increased concentration of some pigments. This probably leads to increased competitiveness of *C. corniculata*, as proven by the increase in its cover and the concurrent decrease of *J. rubens* cover as CO₂ increases (Chapter 3).

This highlights the importance of studying ocean acidification responses at the community level, as even calcifying algae that seem to cope relatively well with increased carbon dioxide, such as *J. rubens*, can be outcompeted by non-calcifying macroalgae that benefit from increased CO₂ levels, such as *C. corniculata*. This is in accord with a previous study showing that some calcifying algae can survive a moderate increase in pCO₂ levels, but their slower growth rates at high CO₂ reduce their competitive abilities (James *et al.*, 2014). Reduced growth rates at increased CO₂ have commonly been reported for coralline algae (Kroeker *et al.*, 2013a), although articulated coralline algae are less sensitive to ocean acidification than crustose forms (Johnson *et al.*, 2014).

J. rubens did not show significant differences in linear growth rates between sites, but it is possible that other life stages of this species are negatively affected by elevated CO₂. Increased chemical defences or altered morphology of *C. corniculata* could have deterred *J. rubens* settlement at elevated CO₂ levels. Changes in macroalgal morphology or chemical defences influence the cover of their epiphytes, such as *J. rubens* (Jennings and Steinberg, 1997; Jones and Thornber, 2010). It is also possible that an episode of extremely high CO₂ drastically decreased *J. rubens* abundance. Recovery of *J. rubens*

population might be extremely difficult at elevated CO₂, especially considering the limited distance its gametes travel (Jones and Moorjani, 1973). This hypothesis is supported by the fact that thalli of *J. rubens* transplanted to the seeps created areas of high *J. rubens* cover (Figure 8.3), suggesting that recruitment of this species is not impaired by moderate CO₂ enrichment, but recovery after extreme events is difficult because of the small distance its gametes travel.



Figure 8.3. *J. rubens* thalli transplanted near seeps off Methana are indicated by white plastic labels, and the high cover of *J. rubens* around them suggests this species' recruitment is not impaired by moderate pCO₂ enrichment.

Not all the physiological responses of these two macroalgal species may have been detected: many replicates were lost due to high wave action, leaving one treatment of *C. corniculata* with only three replicates and leaving only one usable reference site for *J. rubens* transplants. Low sample sizes reduce our

ability to detect small differences among treatments (Quinn and Keough, 2002), and reciprocal transplants to test for local adaptation should be performed using multiple reference sites (Sanford and Kelly, 2011). The species studied in this thesis should ideally be repeated in laboratory conditions (i.e. common garden experiment) to better assess the mechanisms of macroalgal responses to elevated CO₂.

8.1.4 Interaction with other stressors

Studying the interaction of ocean acidification with other anthropogenic stressors is essential to reliably predict future conditions of marine ecosystems, as multiple stressors often interact synergistically; it is therefore very difficult to understand their combined effect from single-stressor experiments (Crain *et al.*, 2008). In this thesis, copper levels were manipulated *in situ* at different pCO₂ levels near volcanic seeps (Chapter 7). Results from these copper manipulation experiments showed that the combined effects of ocean acidification and copper pollution interact to increase copper accumulation in two macroalgal species (*Cystoseira corniculata* and *Jania rubens*), and this amplified the effects of ocean acidification on epifaunal communities. Interactive effects of ocean acidification and copper pollution have been largely overlooked by researchers so far, although it has been proven that these factors have synergistic negative effect on amphipods and polychaetes (Lewis *et al.*, 2012; Roberts *et al.*, 2013; Campbell *et al.*, 2014). The experiments in this thesis showed for the first time that tackling a local stressor such as copper pollution can help managing the impacts of a global stressor such as ocean acidification, similarly to what has already been demonstrated for other local stressors (e.g. eutrophication, sediment runoff; Ghedini *et al.*, 2013).

Many others anthropogenic stressors interact with ocean acidification to influence marine ecosystems. For instance, climate change is also causing an increase of temperature and UV radiation as well as decreased oxygen in marine systems (IPCC, 2014); further pressures on marine ecosystems include eutrophication, overfishing, invasive species and metal pollution (Halpern *et al.*, 2007). While ocean acidification and increased temperature are increasingly studied together (Kroeker *et al.*, 2013a), combinations of more than two stressors are rarely studied because of logistical constraints (Crain *et al.*, 2008). This thesis concentrated on one stressor only (ocean acidification) due to the difficulties in manipulating the environment *in situ*, but its only experiment concurrently investigating two factors highlighted that synergistic effects of anthropogenic stressors are likely and that future research needs to address the cumulative impacts of multiple variables.

8.2 Summary and direction for future research

Ocean acidification has the potential to influence a wide range of physical, chemical and biological processes in the marine environment (Doney *et al.*, 2009). This thesis contributes to a growing body of research assessing the effects of ocean acidification on marine temperate rocky reefs. It is clear from these findings that temperate macroalgal communities and their epifauna change significantly with increasing CO₂, and subtidal herbivore communities drastically shift from sea urchins to fish with increasing CO₂. Experiments performed as part of this thesis have also shown that dominant macroalgal species at Methana have very high phenotypic plasticity, and change their physiology in a few months to acclimatise to pCO₂ levels up to 1700 µatm. Interactive effects of ocean acidification and copper pollution have also been proven to increase copper accumulation in macroalgae and indirectly affect their

epifauna. These findings have implications for the modelling of impacts of elevated CO₂ on marine ecosystems.

The findings from this thesis have highlighted that some marine taxa can tolerate, and sometimes thrive at, CO₂ levels up to 1700 µatm. Furoid algae were the main group to benefit from increased carbon dioxide, and at Methana *Cystoseira corniculata* could be found much deeper near the seeps than at the reference sites (~ 12 m vs ~ 2 m; author's personal observation). Since overall macroalgal biomass was higher at elevated CO₂, it is very likely that primary productivity increases when CO₂ levels are high at Mediterranean rocky reefs. On the other hand, decreased diversity at elevated CO₂ has implications for ecosystem functioning of communities exposed to ocean acidification, especially if key species are lost. For instance, decreased coralline algal abundance and diversity near the studied seeps has the potential to influence carbon cycling in temperate systems. Coralline algae are one of the most important taxa for long-term carbon storage in the marine environment (Andersson *et al.*, 2008). Their decreasing abundance could therefore reduce the ability of temperate macroalgal beds to act as carbon sinks, even though an increase in furoid algal biomass might counter that effect (Chung *et al.*, 2011).

Our knowledge of ecosystem effects of ocean acidification is, however, still in its infancy. Using volcanic CO₂ seeps is a powerful approach to test hypotheses formulated following laboratory and mesocosm experiments, and can produce hypotheses to be verified in controlled conditions. Results from this thesis have revealed how temperate communities may change and how some organisms may change their physiology when exposed to ocean acidification. Patterns of rocky reef community changes are becoming clear after consistent results from mesocosm and field observations (Kroeker *et al.*, 2011; Porzio *et al.*, 2011;

Kroeker *et al.*, 2013a). Changes in ecosystem functions with increasing CO₂, however, have rarely been tested in complex marine ecosystems. Ocean acidification is known to increase seagrass productivity at seeps off Vulcano (Apostolaki *et al.*, 2014), but macroalgal productivity responses are not as clear and have not been measured *in situ* so far (Hofmann *et al.*, 2011; Noisette *et al.*, 2013b; Olabarria *et al.*, 2013). Macroalgal communities not only contribute to coastal primary productivity, but offer other valuable ecosystem services, such as nutrient cycling, water depuration, fisheries production and shore protection from waves (Rönnbäck *et al.*, 2007). Responses of these processes to ocean acidification have scarcely been studied, and are a priority for future research.

Populations of *Cystoseira corniculata* and *Jania rubens* exposed for centuries to high and variable pCO₂ do not seem to have permanently acclimatised to ocean acidification, as their physiology was not influenced by their site of origin after a few months of acclimatisation to different pCO₂ levels. Very high phenotypic plasticity may slow down genetic adaptation, meaning that pCO₂ values above those physiological mechanisms can buffer could be detrimental to the two species studied in this thesis (Sunday *et al.*, 2014). However, it is possible that these species have in fact adapted to elevated pCO₂, but their high phenotypic plasticity might have masked inter-population differences. Genetic studies are therefore needed to confirm that only phenotypic plasticity is at play in this instance. Furthermore, adaptation potential to ocean acidification is known for very few species and more studies are urgently needed to understand how marine organisms may adapt to ocean acidification (Reusch, 2014).

Predictions of community responses to ocean acidification are extremely important, but anthropogenic CO₂ emissions are causing other environmental changes, such as increased temperatures (IPCC, 2014). Moreover, human

pressures such as pollution and overfishing are contributing to degradation of marine ecosystems, and managing them is essential to improve the resilience of marine ecosystems to climate change (Ghedini *et al.*, 2013). Although laboratory experiments have been conducted to examine interactions between anthropogenic stressors, chiefly temperature (Kroeker *et al.*, 2013a), *in situ* studies are extremely rare because of the logistical difficulties in manipulating stressors in the field. Although complex, field experiments involving more than one stressor will be essential to understand how marine ecosystems will respond to future environmental changes, as interactive effects of stressors are often not predictable from single-stressor experiments (Gobler *et al.*, 2014).

References:

Abdallah A.M.A., Abdallah M.A. and Beltagy A.I. (2005). Contents of heavy metals in marine seaweeds from the Egyptian coast of the Red Sea. *Chemistry and Ecology*, 21: 399-411.

Airoldi L. and Beck M. (2007). Loss, status and trends for coastal marine habitats of Europe. *Oceanography and Marine Biology: An Annual Review*, 45: 347-407.

Al-Horani F.A., Al-Moghrabi S.M. and de Beer D. (2003). Microsensor study of photosynthesis and calcification in the scleractinian coral, *Galaxea fascicularis*: active internal carbon cycle. *Journal of Experimental Marine Biology and Ecology*, 288: 1-15.

Allan B.J.M., Domenici P., McCormick M.I., Watson S.-A. and Munday P.L. (2013). Elevated CO₂ affects predator-prey interactions through altered performance. *PLoS ONE*, 8: e58520.

Allison G. (2004). The influence of species diversity and stress intensity on community resistance and resilience. *Ecological Monographs*, 74: 117-134.

Alsterberg C., Eklöf J.S., Gamfeldt L., Havenhand J.N. and Sundbäck K. (2013). Consumers mediate the effects of experimental ocean acidification and warming on primary producers. *Proceedings of the National Academy of Sciences*, 110: doi: 10.1073/pnas.1303797110.

Amaral V., Cabral H.N. and Bishop M.J. (2011). Resistance among wild invertebrate populations to recurrent estuarine acidification. *Estuarine, Coastal and Shelf Science*, 93: 460-467.

- Amaral V., Cabral H.N. and Bishop M.J. (2012). Effects of estuarine acidification on predator-prey interactions. *Marine Ecology Progress Series*, 445: 117-127.
- Anderson M.J. and Ter Braak C.J.F. (2003). Permutation tests for multi-factorial analysis of variance. *Journal of Statistical Computational Simulation*, 73: 85-113.
- Andersson A.J., Mackenzie F.T. and Lerman A. (2005). Coastal ocean and carbonate systems in the high CO₂ world of the Anthropocene. *American Journal of Science*, 305: 875-918.
- Andersson A.J., Mackenzie F.T. and Bates N.R. (2008). Life on the margin: implications of ocean acidification on Mg-calcite, high latitude and cold-water marine calcifiers. *Marine Ecology Progress Series*, 373: 265-273.
- Andersson A.J., Kuffner I.B., Mackenzie F.T., Jokiel P.L., Rodgers K.S. and Tan A. (2009). Net loss of CaCO₃ from a subtropical calcifying community due to seawater acidification: mesocosm-scale experimental evidence. *Biogeosciences*, 6: 1811-1823.
- Angilletta M.J. (2009) Thermal adaptation: a theoretical and empirical synthesis. Oxford University Press, 289 pp.
- Anthony K.R.N., Kline D.I., Diaz-Pulido G., Dove S. and Hoegh-Guldberg O. (2008). Ocean acidification causes bleaching and productivity loss in coral reef builders. *Proceedings of the National Academy of Sciences*, 105: 17442-17446.
- Anthony K.R.N., Kleypas J.A. and Gattuso J.-P. (2011a). Coral reefs modify their seawater carbon chemistry - implications for impacts of ocean acidification. *Global Change Biology*, 17: 3655-3666.
- Anthony K.R.N., Maynard J.A., Diaz-Pulido G., Mumby P.J., Marshall P.A., Cao L. and Hoegh-Guldberg O.V.E. (2011b). Ocean acidification and warming will lower coral reef resilience. *Global Change Biology*, 17: 1798-1808.

- Apostolaki E.T., Vizzini S., Hendriks I.E. and Olsen Y.S. (2014). Seagrass ecosystem response to long-term high CO₂ in a Mediterranean volcanic vent. *Marine Environmental Research*, 99: 9-15.
- Apte S.C. and Day G.M. (1998). Dissolved metal concentrations in the Torres Strait and Gulf of Papua. *Marine Pollution Bulletin*, 36:298-304.
- Arnold T., Mealey C., Leahey H., Miller A.W., Hall-Spencer J.M., Milazzo M. and Maers K. (2012). Ocean acidification and the loss of phenolic substances in marine plants. *PLoS ONE*, 7: e35107.
- Austin J., Butchart N. and Shine K.P. (1992). Possibility of an Arctic ozone hole in a doubled-CO₂ climate. *Nature*, 360: 221-225.
- Baggini C., Salomidi M., Voutsinas E., Bray L., Krasakopoulou E. and Hall-Spencer J.M. (2014). Seasonality affects macroalgal community response to increases in pCO₂. *PLoS ONE*, 9: e106520.
- Ballesteros, E. (1984). Els vegetals i la zonació litoral: espècies, comunitats i factors que influenixen en la seva distribució. PhD thesis, Universitat de Barcelona, Spain.
- Ballesteros E. (1986). Mé todos de análisis estructural en comunidades naturales, en particular del fitobentos. *Oecologia Aquatica*, 8: 117-131.
- Ballesteros E., Torras X., Pinedo S., García M., Mangialajo L. and de Torres M. (2007). A new methodology based on littoral community cartography dominated by macroalgae for the implementation of the European Water Framework Directive. *Marine Pollution Bulletin*, 55: 172-180.
- Barton A., Hales B., Waldbusser G.G., Langdon C. and Feely R.A. (2012). The Pacific oyster, *Crassostrea gigas*, shows negative correlation to naturally

elevated carbon dioxide levels: implications for near-term ocean acidification effects. *Limnology Oceanography*, 57: 698 - 710.

Bates C.R. and DeWreede R.E. (2007). Do changes in seaweed biodiversity influence associated invertebrate epifauna? *Journal of Experimental Marine Biology and Ecology*, 344: 206-214.

Bates C.R. (2009). Host taxonomic relatedness and functional-group affiliation as predictors of seaweed-invertebrate epifaunal associations. *Marine Ecology Progress Series*, 387: 125-136.

Baumann H.A., Morrison L. and Stengel D.B. (2009). Metal accumulation and toxicity measured by PAM-Chlorophyll fluorescence in seven species of marine macroalgae. *Ecotoxicology and Environmental Safety*, 72: 1063-1075.

Bazterrica M.C., Silliman B.R., Hidalgo F.J., Crain C.M. and Bertness M.D. (2007). Limpet grazing on a physically stressful Patagonian rocky shore. *Journal of Experimental Marine Biology and Ecology*, 353: 22-34.

Beardall J., Stojkovic S. and Larsen S. (2009). Living in a high CO₂ world: Impacts of global climate change on marine phytoplankton. *Plant Ecology and Diversity*, 2: 191-205.

Beer S. and Eshel A. (1985). Determining phycoerithrin and phycocyanin concentrations in aqueous crude extract of red algae. *Australian Journal of Marine and Freshwater Research*, 36: 785-792.

Belegreatis M.R., Bitis I., Economou-Amilli A. and Ott J.A. (1999). Epiphytic patterns of macroalgal assemblages on *Cystoseira* species (Fucales, Phaeophyta) in the east coast of Attica (Aegean Sea, Greece). *Hydrobiologia*, 412: 67-80.

Bellan-Santini D., Karaman G., Krapp-Schickel G., Ledoyer M., Myers A., Ruffo S. and Schiecke U. (1982). The Amphipoda of the Mediterranean. Part 1: Gammaridae (Acanthonotozomatidae to Gammaridae). *Mémoires de l'Institut océanographique, Monaco*, 13. Institut Océanographique: Monaco. ISBN 2-7260-0133-5. 364 pp.

Bellan-Santini D., Diviacco G., Krapp-Schickel G. and Ruffo S. (1989). The Amphipoda of the Mediterranean. Part 2. Gammaridea (Haustoriidae to Lysianassidae). *Mémoires de l'Institut océanographique, Monaco*, 13. Institut Océanographique: Monaco. ISBN 2-7260-0140-8. 576 pp.

Bellan-Santini D., Karaman G., Krapp-Schickel G., Ledoyer M. and Ruffo S. (1993). The Amphipoda of the Mediterranean. Part 3: Gammaridea (Melphidippidae to Talitridae), Ingolfiellidea, Caprellidea. *Mémoires de l'Institut océanographique, Monaco*, 13. Institut Océanographique: Monaco. ISBN 2-7260-0160-2. 813 pp.

Bellan-Santini D., Karaman G., Ledoyer M., Myers A., Ruffo S. and Vader W. (1998). The Amphipoda of the Mediterranean. Part 4: Localities and Map, Addenda to Parts 1-3, Key to Families, Ecology, Faunistics and Zoogeography, Bibliography, Index. *Mémoires de l'Institut océanographique, Monaco*, 13. Institut Océanographique: Monaco. ISBN 2-7260-0201-3. 959 pp.

Bender D., Diaz-Pulido G. and Dove S. (2014). The impact of CO₂ emission scenarios and nutrient enrichment on a common coral reef macroalga is modified by temporal effects. *Journal of Phycology*, 50: 203-215.

Bendscheider K. and Robinson R.J. (1952). A new spectrometric method for the determination of nitrite in seawater. *Journal of Marine Research*, 11: 87-96.

Benedetti-Cecchi L., Nuti S. and Cinelli F. (1996). Analysis of spatial and temporal variability in interactions among algae, limpets and mussels in low-shore habitats on the west coast of Italy. *Marine Ecology Progress Series*, 144:87-96.

Benedetti-Cecchi L., Bulleri F. And Cinelli F. (2000). The interplay of physical and biological factors in maintaining mid-shore and low-shore assemblages on rocky coasts in the north-west Mediterranean. *Oecologia*, 123: 406-417.

Benedetti-Cecchi L., Bulleri F., Acunto S. and Cinelli F. (2001). Scales of variation in the effects of limpets on rocky shores in the northwest Mediterranean. *Marine Ecology Progress Series*, 209: 131-141.

Benner I., Diner R.E., Lefebvre S.C., Li D., Komada T., Carpenter E.J. and Stillman J.H. (2013). *Emiliania huxleyi* increases calcification but not expression of calcification-related genes in long-term exposure to elevated temperature and pCO₂. *Philosophical Transactions of the Royal Society B: Biological Sciences*, 368: 20130049.

Bergström L., Tatarenkov A., Johannesson K., Jönsson R.B. and Kautsky L. (2005). Genetic and morphological identification of *Fucus radicans* sp. nov. (Fucales, Phaeophyceae) in the brackish Baltic Sea. *Journal of Phycology*, 41:1025-1038.

Bianchi C.N., Dando P.R. and Morri C. (2011). Increased diversity of sessile epibenthos at subtidal hydrothermal vents: seven hypotheses based on observations at Milos Island, Aegean Sea. *Advances in Oceanography and Limnology*, 2: 1-31.

Bibby R., Cleall-Harding P., Rundle S., Widdicombe S. and Spicer J. (2007). Ocean acidification disrupts induced defences in the intertidal gastropod *Littorina littorea*. *Biology Letters*, 3: 699-701.

Bischof K., Gómez I., Molis M., Hanelt D., Karsten U., Lüder U., Roleda M.Y., Zacher K., Wiencke C., Amils R., Ellis-Evans C. and Hinghofer-Szalkay H. (2006). Ultraviolet radiation shapes seaweed communities. *Review of Environmental Sciences and Biotechnology*, 5:141–166.

Blackford J.C. (2010). Predicting the impacts of ocean acidification: challenges from an ecosystem perspective. *Journal of Marine Systems*, 81: 12-18.

Blake R.E. and Duffy J.E. (2010). Grazer diversity affects resistance to multiple stressors in an experimental seagrass ecosystem. *Oikos*, 119: 1625-1635.

Boatta F., D'Alessandro W., Gagliano A.L., Liotta M., Milazzo M., Rodolfo-Metalpa R., Hall-Spencer J.M. and Parello F. (2013). Geochemical survey of Levante Bay, Vulcano Island (Italy), a natural laboratory for the study of ocean acidification. *Marine Pollution Bulletin*, 73: 485-494.

Borowitzka M.A. (1987). Calcification in algae - mechanisms and the role of metabolism. *Critical Reviews in Plant Sciences*, 6: 1-45.

Bradassi F., Cumani F., Bressan G. and Dupont S. (2013). Early reproductive stages in the crustose coralline alga *Phymatolithon lenormandii* are strongly affected by mild ocean acidification. *Marine Biology*, 160: 2261-2269.

Bray L., Pancucci-Papadopoulou M.A. and Hall-Spencer J.M. (2014). Sea urchin response to rising $p\text{CO}_2$ shows ocean acidification may fundamentally alter the chemistry of marine skeletons. *Mediterranean Marine Science*. DOI: 10.12681/mms.579.

Breitbarth E., Bellerby, R.J., Neill, C.C., Ardelan M.V., Meyerhöfer M., Zöllner E., Croot P.L. and Riebesell U. (2010). Ocean acidification affects iron speciation during a coastal seawater mesocosm experiment. *Biogeosciences*, 7: 1065-1073.

Brewer P.O., Goyet C. and Friederich G. (1997). Direct observation of the oceanic CO₂ increase revisited. *Proceedings of the National Academy of Sciences USA*, 94: 8308-8313.

Brewer P. G. and Hester K. C. (2009). Ocean acidification and the increasing transparency of the ocean to low-frequency sound. *Oceanography*, 22: 86-93.

Briffa M., de la Haye K. and Munday P.L. (2012). High CO₂ and marine animal behaviour: Potential mechanisms and ecological consequences. *Marine Pollution Bulletin*, 64: 1519-1528.

Brock E., Åberg P. and Pavia H. (2008). Phlorotannins as chemical defense against macroalgal epiphytes on *Ascophyllum nodosum*. *Journal of Phycology*, 37: 8.

Brodie J., Williamson C.J., Smale D.A., Kamenos N.A., Mieszkowska N., Santos R., Cunliffe M., Steinke M., Yesson C., Anderson K.M., Asnaghi V., Brownlee C., Burdett H.L., Burrows M.T., Collins S., Donohue P.J., Harvey B., Foggo A., Noisette F., Nunes J., Ragazzola F., Raven J.A., Schmidt D.N., Suggett D., Teichberg M. and Hall-Spencer J.M. (2014). The future of the northeast Atlantic benthic flora in a high CO₂ world. *Ecology and Evolution*, 4: 2787-2798.

Brown M.T. and Newman J.E. (2003). Physiological responses of *Gracilariopsis longissima* (S.G. Gmelin) Steentoft, L.M. Irvine and Farnham (Rhodophyceae) to sub-lethal copper concentrations. *Aquatic Toxicology*, 64: 201-213.

Bubel A. (1975). An ultrastructural study of the mantle of the barnacle, *Elminius modestus* (Darwin) in relation to shell formation. *Journal of Experimental Marine Biology and Ecology*, 20: 287-324.

Büdenbender J., Riebesell U. and Form A. (2011). Calcification of the Arctic coralline red alga *Lithothamnion glaciale* in response to elevated CO₂. *Marine Ecology Progress Series*, 441: 79-87.

Bulleri F., Benedetti-Cecchi L. and Cinelli F. (1999). Grazing by the sea urchins *Arbacia lixula* L. and *Paracentrotus lividus* Lam. in the Northwest Mediterranean. *Journal of Experimental Marine Biology and Ecology*, 241: 81-95.

Bulleri F., Menconi M., Cinelli F. and Benedetti-Cecchi L. (2000). Grazing by two species of limpets on artificial reefs in the northwest Mediterranean. *Journal of Experimental Marine Biology and Ecology*, 255: 1-19.

Burkepile D.E. and Hay M.E. (2006). Herbivore vs nutrient control of marine primary producers: context-dependent effects. *Ecology*, 87: 3128-3139.

Burnell O.W., Russell B.D., Irving A.D. and Connell S.D. (2013). Eutrophication offsets increased sea urchin grazing on seagrass caused by ocean warming and acidification. *Marine Ecology Progress Series*, 485: 37-46.

Butler W.L. (1978). Energy distribution in the photochemical apparatus of photosynthesis. *Annual Review of Plant Physiology*, 29: 345-378.

Cahill A.E., Aiello-Lammens M.E., Fisher-Reid M.C., Hua X., Karanewsky C.J., Ryu H.Y., Sbeglia G.C., Spagnolo F., Waldron J.B., Warsi O. and Wiens J.J. (2013). How does climate change cause extinction? *Proceedings of the Royal Society B: Biological Sciences*, 280: 20121890.

Caldeira K. and Wickett M.E. (2003). Oceanography: Anthropogenic carbon and ocean pH. *Nature*, 425: 365-365.

Caldeira K. and Wickett M.E. (2005). Ocean model predictions of chemistry changes from carbon dioxide emissions to the atmosphere and ocean. *Journal of Geophysical Research*, 110: C09S04.

Calosi P., Rastrick S.P.S., Graziano M., Thomas S.C., Baggini C., Carter H.A., Hall-Spencer J.M., Milazzo M. and Spicer J.I. (2013a). Distribution of sea urchins living near shallow water CO₂ vents is dependent upon species acid-base and ion-regulatory abilities. *Marine Pollution Bulletin*, 73: 470-484.

Calosi P., Turner L.M., Hawkins M., Bertolini C., Nightingale G., Truebano M. and Spicer J.I. (2013b). Multiple physiological responses to multiple environmental challenges: an individual approach. *Integrative and Comparative Biology*, 53: 660-670.

Calosi P., Rastrick S.P.S., Lombardi C., de Guzman H.J., Davidson L., Jahnke M., Giangrande A., Hardege J.D., Schulze A., Spicer J.I. and Gambi M.-C. (2013c). Adaptation and acclimatization to ocean acidification in marine ectotherms: an *in situ* transplant experiment with polychaetes at a shallow CO₂ vent system. *Philosophical Transactions of the Royal Society B: Biological Sciences*, 368: 20120444.

Cameron J.N. (1985). Post-moult calcification in the blue crab (*Callinectes sapidus*): relationship between apparent net H⁺ excretion, calcium and bicarbonate. *Journal of Experimental Biology*, 119: 275-285.

Campbell J.E. and Fourqurean J.W. (2011). Novel methodology for *in situ* carbon dioxide enrichment of benthic ecosystems. *Limnology and Oceanography Methods*, 9: 97-109.

Campbell J.E. and Fourqurean J.W. (2013). Effects of in situ CO₂ enrichment on the structural and chemical characteristics of the seagrass *Thalassia testudinum*. *Marine Biology*, 160: 1465-1475.

Campbell J.E. and Fourqurean J.W. (2014). Ocean acidification outweighs nutrient effects in structuring seagrass epiphyte communities. *Journal of Ecology*, 102: 730-737.

Campbell A.L., Mangan S., Ellis R.P. and Lewis C. (2014). Ocean acidification increases copper toxicity to the early life-history stages of the polychaete *Arenicola marina* in artificial seawater. *Environmental Science & Technology*, DOI 10.1021/es502739m.

Capaccioni B., Tassi F. and Vaselli O. (2001). Organic and inorganic geochemistry of low temperature gas discharges at the Baia di Levante beach, Vulcano Island, Italy. *Journal of Volcanological and Geothermal Research*, 108: 173-185.

Caramanna G., Voltattorni N. and Maroto-Valer M.M. (2011). Is Panarea Island (Italy) a valid and cost-effective natural laboratory for the development of detection and monitoring techniques for submarine CO₂ seepage? *Greenhouse Gases: Science and Technology*, 1: 200-210.

Cardellini C., Chiodini G. and Frondini F., 2003. Application of stochastic simulation to CO₂ flux from soil: mapping and quantification of gas release. *Journal of Geophysical Research*, 108 (B9): 2425.

Chauvin A., Denis V. and Cuet P. (2011). Is the response of coral calcification to seawater acidification related to nutrient loading? *Coral Reefs*, 30: 1-13.

Chapman P. M. and Wang F. (2001). Assessing sediment contamination in estuaries. *Environmental Toxicology and Chemistry*, 20: 3-22.

- Chemello R. and Milazzo M. (2002). Effect of algal architecture on associated fauna: some evidence from phytal molluscs. *Marine Biology*, 140: 981-990.
- Chiantore M., Vielmini I., Privitera D., Mangialajo L. and Cattaneo-Vietti R. (2008). Habitat effects on the population structure of *Paracentrotus lividus* and *Arbacia lixula*. *Chemistry and Ecology*, 24: 145–157.
- Chiodini G., Cioni R., Guidi M., Raco B. and Marini L. (1998). Soil CO₂ flux measurements in volcanic and geothermal areas. *Applied Geochemistry*, 13: 543-552.
- Christen N., Calosi P., McNeill C.L. and Widdicombe S. (2013). Structural and functional vulnerability to elevated pCO₂ in marine benthic communities. *Marine Biology*, 160: 2113-2128.
- Christie H., Norderhaug K.M. and Fredriksen S. (2009). Macrophytes as habitat for fauna. *Marine Ecology Progress Series*, 396: 221-233.
- Chung I., Beardall J., Mehta S., Sahoo D. and Stojkovic S. (2011). Using marine macroalgae for carbon sequestration: a critical appraisal. *Journal of Applied Phycology*, 23: 877-886.
- Cigliano M., Gambi M.C., Rodolfo-Metalpa R., Patti F.P. and Hall-Spencer J.M. (2010). Effects of ocean acidification on invertebrate settlement at volcanic CO₂ vents. *Marine Biology*, 157: 2489-2502.
- Clarke K.R. and Ainsworth M. (1993). A method of linking multivariate community structure to environmental variables *Marine Ecology Progress Series*, 92: 205-219.
- Clarke K.R. and Gorley R.N. (2006). PRIMER v6: User Manual/Tutorial. PRIMER-E, Plymouth.

Cline J.D. (1989). Spectrophotometric determination of hydrogen sulphide in natural waters. *Limnology and Oceanography*, 14: 454-458.

Cohen A.L. and Holcomb M. (2009). Why corals care about ocean acidification: Uncovering the mechanism. *Oceanography*, 22: 118-127.

Coleman R., Underwood A., Benedetti-Cecchi L., Åberg P., Arenas F., Arrontes J., Castro J., Hartnoll R., Jenkins S., Paula J., Santana P. and Hawkins S. (2006). A continental scale evaluation of the role of limpet grazing on rocky shores. *Oecologia*, 147: 556-564.

Collén J. and Davison I.R. (2001). Seasonality and thermal acclimation of reactive oxygen metabolism in *Fucus vesiculosus* (Phaeophyceae). *Journal of Phycology*, 37: 474-481.

Collén J., Pinto E., Pedersen M. and Colepicolo P. (2003). Induction of oxidative stress in the red macroalga *Gracilaria tenuistipitata* by pollutant metals. *Archives of Environmental Contamination and Toxicology*, 45:337-342.

Collins S., Rost B. and Ryneerson T.A. (2014). Evolutionary potential of marine phytoplankton under ocean acidification. *Evolutionary Applications*, 7: 140-155.

Coma R., Ribes M., Gili J.-M. and Zabala M. (2000). Seasonality in coastal benthic ecosystems. *Trends in Ecology & Evolution*, 15: 448-453.

Connan S. and Stengel D.B. (2011a). Impacts of ambient salinity and copper on brown algae: 1. Interactive effects on photosynthesis, growth, and copper accumulation. *Aquatic Toxicology*, 104: 94-107.

Connan S. and Stengel D.B. (2011b). Impacts of ambient salinity and copper on brown algae: 2. Interactive effects on phenolic pool and assessment of metal binding capacity of phlorotannin. *Aquatic Toxicology*, 104: 1-13.

Connell S.D., Russell B.C., Turner D.J., Shepherd S.A., Kildae T., Miller D.J., Airoidi L. and Cheshire, A. (2008). Recovering a lost baseline: Missing kelp forests from a metropolitan coast. *Marine Ecology Progress Series*, 360: 63-72.

Connell S.D. and Russell B.D. (2010). The direct effects of increasing CO₂ and temperature on non-calcifying organisms: Increasing the potential for phase shifts in kelp forests. *Proceedings of the Royal Society B: Biological Sciences*, 277: 1409-1415.

Connell S.D., Kroeker K.J., Fabricius K.E., Kline D.I. and Russell B.D. (2013). The other ocean acidification problem: CO₂ as a resource among competitors for ecosystem dominance. *Philosophical Transactions of the Royal Society B: Biological Sciences*, 368: 20120442.

Contreras L., Moenne A. and Correa J.A. (2005). Antioxidant responses in *Scytosiphon lomentaria* (Phaeophyceae) inhabiting copper-enriched coastal environments. *Journal of Phycology*, 41: 1184-1195.

Cornwall C.E., Hepburn C.D., Pritchard D., Currie K.I., McGraw C.M., Hunter K.A. and Hurd C.L. (2012). Carbon-use strategies in macroalgae: Differential responses to lowered pH and implications for ocean acidification. *Journal of Phycology*, 48:137-144.

Cornwall C.E., Hepburn C.D., McGraw C.M., Currie K.I., Pilditch C.A., Hunter K.A., Boyd P.W. and Hurd C.L. (2013). Diurnal fluctuations in seawater pH influence the response of a calcifying macroalga to ocean acidification. *Proceedings of the Royal Society B: Biological Sciences*, 280: 20132201.

Cornwall C.E., Boyd P.W., McGraw C.M., Hepburn C.D., Pilditch C.A., Morris J.N., Smith A.M. and Hurd C.L. (2014). Diffusion boundary layers ameliorate the

negative effects of ocean acidification on the temperate coralline macroalga *Arthrocardia corymbosa*. *PLoS ONE*, 9: e97235.

Couto R.P., Neto A.I. and Rodrigues A.S. (2010). Metal concentration and structural changes in *Corallina elongata* (Corallinales, Rhodophyta) from hydrothermal vents. *Marine Pollution Bulletin*, 60: 509-514.

Crain C.M., Kroeker K. and Halpern B.S. (2008). Interactive and cumulative effects of multiple human stressors in marine systems. *Ecology Letters*, 11: 1304-1315.

Crawford K.J., Raven J.A., Wheeler G.L., Baxter E.J. and Joint I. (2011). The Response of *Thalassiosira pseudonana* to Long-Term Exposure to Increased CO₂ and Decreased pH. *PLoS ONE*, 6: e26695.

Crook E., Potts D., Rebolledo-Vieyra M., Hernandez L. and Paytan A. (2012). Calcifying coral abundance near low-pH springs: implications for future ocean acidification. *Coral Reefs*, 31: 239-245.

D'Alessandro W., Brusca L., Kyriakopoulos K., Rotolo S., Michas G., Minio M. and Papadakis G. (2006). Diffuse and focused carbon dioxide and methane emissions from the Sousaki geothermal system, Greece. *Geophysical Research Letters*, 33: L05307.

D'Alessandro W., Brusca L., Kyriakopoulos K., Michas G. and Papadakis G. (2008). Methana, the westernmost active volcanic system of the South Aegean Arc (Greece): Insight from fluids geochemistry. *Journal of Volcanology and Geothermal Research*, 178: 818-828.

Dando P.R., Stüben D. and Varnavas S.P. (1999). Hydrothermalism in the Mediterranean Sea. *Progress In Oceanography*, 44: 333-367.

Dando P.R., Aliani S., Arab H., Bianchi C.N., Brehmer M., Cocito S., Fowlers S.W., Gundersen J., Hooper L.E., Kölbh R., Kuevere J., Linke P., Makropoulos K.C., Meloni R., Miquel J.C., Morri C., Müller S., Robinson C., Schlesner H., Sieverts S., Störr R., Stüben D., Thormm M., Varnavas S.P. and Ziebiss W. (2000). Hydrothermal studies in the Aegean Sea. *Physics and Chemistry of the Earth, Part B: Hydrology, Oceans and Atmosphere*, 25: 1-8.

De Biasi A.M. and Aliani S. (2003). Shallow-water hydrothermal vents in the Mediterranean Sea: Stepping stones for Lessepsian migration? *Hydrobiologia*, 503: 37-44.

De Bodt C., Van Oostende N., Harlay J., Sabbe K. and Chou L. (2010). Individual and interacting effects of pCO₂ and temperature on *Emiliania huxleyi* calcification: Study of the calcite production, the coccolith morphology and the coccosphere size. *Biogeosciences*, 7: 1401-1412.

Dean R.L. and Connell J.H., 1987. Marine invertebrates in an algal succession. III. Mechanisms linking habitat complexity with diversity. *Journal of Experimental Marine Biology and Ecology*, 109: 249-273.

Decker G.L. and Lennarz W.J. (1988). Skeletogenesis in the sea urchin embryo. *Development*, 103: 231-247.

Demes K.W., Graham M.H. and Suskiewicz T.S. (2009). Phenotypic plasticity reconciles incongruous molecular and morphological taxonomies: the giant kelp, *Macrocystis* (Laminariales, Phaeophyceae), is a monospecific genus. *Journal of Phycology*, 45: 1266-1269.

Dethier M.N., Graham E.S., Cohen S. and Tear L.M. (1993). Visual versus random-point percent cover estimation: 'objective' is not always better. *Marine Ecology Progress Series*, 96: 93-100.

Dias B.B., Hart M.B., Smart C.W. and Hall-Spencer J.M. (2010). Modern seawater acidification: The response of foraminifera to high-CO₂ conditions in the Mediterranean Sea. *Journal of the Geological Society*, 167: 843-846.

Diaz-Pulido G., Gouezo M., Tilbrook B., Dove S. and Anthony K.R.N. (2011). High CO₂ enhances the competitive strength of seaweeds over corals. *Ecology Letters*, 14: 156-162.

Diaz R.J. and Rosenberg R. (2008). Spreading dead zones and consequences for marine ecosystems. *Science*, 321: 926-929.

Doneddu M. and Trainito E. (2005). Conchiglie del Mediterraneo. Guida al riconoscimento dei molluschi conchigliati, 2nd edition. Il Castello Editore; 256 pp.

Doney S.C., Fabry V.J., Feely R.A. and Kleypas J.A. (2009). Ocean acidification: the Other CO₂ problem. *Annual Review of Marine Science*, 1: 169-192.

Dupont S., Dorey N. and Thorndyke M. (2010). What meta-analysis can tell us about vulnerability of marine biodiversity to ocean acidification? *Estuarine Coastal and Shelf Science*, 89: 182-185.

Edgar G.J. (1992). Patterns of colonization of mobile epifauna in a Western Australian seagrass bed. *Journal of Experimental Marine Biology and Ecology*, 157: 225-246.

Egilsdottir H., Noisette F., Noël L.L.J., Olafsson J. and Martin S. (2013). Effects of pCO₂ on physiology and skeletal mineralogy in a tidal pool coralline alga *Corallina elongata*. *Marine Biology*, 160: 2103-2112.

Eilers P.H.C. and Peeters J.C.H. (1988). A model for the relationship between light intensity and the rate of photosynthesis in phytoplankton. *Ecological Modelling*, 42: 199-215.

Ellis R.P., Bersey J., Rundle S.D., Hall-Spencer J.M. and Spicer J.I. (2009). Subtle but significant effects of CO₂ acidified seawater on embryos of the intertidal snail, *Littorina obtusata*. *Aquatic Biology*, 5: 41-48.

Endler J.A. (1977). Geographic variation, speciation, and clines. Princeton University Press, Princeton, NJ. 262 pp.

Engelen A.H., Espirito-Santo C., Simões T., Monteiro C., Serrão E.A., Pearson G.A. and Santos R.O.P. (2008). Periodicity of propagule expulsion and settlement in the competing native and invasive brown seaweeds, *Cystoseira humilis* and *Sargassum muticum* (Phaeophyta). *European Journal of Phycology*, 43: 275-282.

Eriksson B.K., van Sluis C., Sieben K., Kautsky L. and Raberg S. (2011). Omnivory and grazer functional composition moderate cascading trophic effects in experimental *Fucus vesiculosus* habitats. *Marine Biology*, 158: 747-756.

Evans T.G., Chan F., Menge B.A. and Hofmann G.E. (2013). Transcriptomic responses to ocean acidification in larval sea urchins from a naturally variable pH environment. *Molecular Ecology*, 22: 1609-25.

Fabricius K.E., Langdon C., Uthicke S., Humphrey C., Noonan S., De'ath G., Okazaki R., Muehllehner N., Glas M.S. and Lough J.M. (2011). Losers and winners in coral reefs acclimatized to elevated carbon dioxide concentrations. *Nature Climate Change*, 1: 165-169.

Fabricius K.E., De'ath G., Noonan S. and Uthicke S. (2014). Ecological effects of ocean acidification and habitat complexity on reef-associated macroinvertebrate communities. *Proceedings of the Royal Society B: Biological Sciences*, 281: 20132479.

Fabry V.J., Seibel B.A., Feely R.A. and Orr J.C. (2008). Impacts of ocean acidification on marine fauna and ecosystem processes. *Ices Journal of Marine Science*, 65: 414-432.

Falkenberg L.J., Russell B.D. and Connell S.D. (2012). Stability of strong species interactions resist the synergistic effects of local and global pollution in kelp forests. *PLoS ONE*, 7: e33841.

Falkenberg L., Russell B. and Connell S. (2013a). Contrasting resource limitations of marine primary producers: implications for competitive interactions under enriched CO₂ and nutrient regimes. *Oecologia*, 172: 575-583.

Falkenberg L.J., Russell B.D. and Connell S.D. (2013b). Future herbivory: the indirect effects of enriched CO₂ may rival its direct effects. *Marine Ecology Progress Series*, 492: 85-95.

Falkenberg L.J., Connell S.D. and Russell B.D. (2014). Herbivory mediates the expansion of an algal habitat under nutrient and CO₂ enrichment. *Marine Ecology Progress Series*, 497: 87-92.

Feely R.A., Sabine C.L., Hernandez-Ayon J.M., Ianson D. and Hales B. (2008). Evidence for upwelling of corrosive "acidified" water onto the continental shelf. *Science*, 320: 1490-1492.

Feely R.A., Alin S.R., Newton J., Sabine C.L., Warner M., Devol A., Krembs C. and Maloy C. (2010). The combined effects of ocean acidification, mixing, and respiration on pH and carbonate saturation in an urbanized estuary. *Estuarine Coastal and Shelf Science*, 88: 442-449.

Ferrari M.C.O., McCormick M.I., Munday P.L., Meekan M.G., Dixon D.L., Lonnstedt Ö. and Chivers D.P. (2011). Putting prey and predator into the CO₂

equation - qualitative and quantitative effects of ocean acidification on predator-prey interactions. *Ecology Letters*, 14: 1143-1148.

Filbee-Dexter K. and Scheibling R.E. (2014). Sea urchin barrens as alternative stable states of collapsed kelp ecosystems. *Marine Ecology Progress Series*, 495, 1-25.

Findlay H.S., Kendall M.A., Spicer J.I. and Widdicombe S. (2010). Relative influences of ocean acidification and temperature on intertidal barnacle post-larvae at the northern edge of their geographic distribution. *Estuarine Coastal and Shelf Science*, 86: 675-682.

Findlay H.S., Wood H.L., Kendall M.A., Spicer J.I., Twitchett R.J. and Widdicombe S. (2011). Comparing the impact of high CO₂ on calcium carbonate structures in different marine organisms. *Marine Biology Research*, 7: 565-575.

Fisher K. and Martone P.T. (2014). Field study of growth and calcification rates of three species of articulated coralline algae in British Columbia, Canada. *The Biological Bulletin*, 226: 121-130.

Floeter S.R., Behrens M.D., Ferreira C.E.L., Paddack M.J. and Horn M.H. (2005). Geographical gradients of marine herbivorous fishes: patterns and processes. *Marine Biology*, 147: 1435-1447.

Folin O. and Ciocalteu V. (1927). On tyrosine and tryptophane determinations in proteins. *Journal of Biological Chemistry*, 73, 627-650.

Fong C.W., Lee S.Y. and Wu R.S.S. (2000). The effects of epiphytic algae and their grazers on the intertidal seagrass *Zostera japonica*. *Aquatic Botany*, 67: 251-261.

Form A.U. and Riebesell U. (2011). Acclimation to ocean acidification during long-term CO₂ exposure in the cold-water coral *Lophelia pertusa*. *Global Change Biology*. DOI: 10.1111/j.1365-2486.2011.02583.x

Fraschetti S., Terlizzi A. and Benedetti-Cecchi L. (2005). Patterns of distribution of marine assemblages from rocky shores: evidence of relevant scales of variation. *Marine Ecology Progress Series*, 296: 13-29.

Friligos N. (1991). Eutrophication assessment in Greek coastal waters. *Water and the Environment*, edited by J. Rose. Gordon and Breach Science Publishers.

Frommel A.Y., Maneja R., Lowe D., Malzahn A.M., Geffen A.J., Folkvord A., Piatkowski U., Reusch T.B.H. and Clemmesen C. (2012). Severe tissue damage in Atlantic cod larvae under increasing ocean acidification. *Nature Climate Change*, 2: 42-46.

Gao K., Aruga Y., Asada K., Ishihara T., Akano T. and Kiyohara M. (1993). Calcification in the articulated coralline alga *Corallina pilulifera*, with special reference to the effect of elevated CO₂ concentration. *Marine Biology*, 117: 129-132.

Gao K.S., Ruan Z.X., Villafane V.E., Gattuso J.P. and Helbling E.W. (2009). Ocean acidification exacerbates the effect of UV radiation on the calcifying phytoplankter *Emiliana huxleyi*. *Limnology and Oceanography*, 54: 1855-1862.

Gao K.S. and Zheng Y.Q. (2010). Combined effects of ocean acidification and solar UV radiation on photosynthesis, growth, pigmentation and calcification of the coralline alga *Corallina sessilis* (Rhodophyta). *Global Change Biology*, 16: 2388-2398.

Garrard S., Hunter R.C., Frommel A.Y., Lane A.C., Phillips J.C., Cooper R., Dineshram R., Cardini U., McCoy S.J., Arnberg M., Rodrigues Alves B.G., Annane S., Orte M.R., Kumar A., Aguirre-Martínez G.V., Maneja R.H., Basallote M.D., Ape F., Torstensson A. and Bjoerk M.M. (2013). Biological impacts of ocean acidification: a postgraduate perspective on research priorities. *Marine Biology*, 160: 1789-1805.

Garrard S.L., Gambi M.C., Scipione M.B., Patti F.P., Lorenti M., Zupo V., Paterson D.M. and Buia M.C. (2014). Indirect effects may buffer negative responses of seagrass invertebrate communities to ocean acidification. *Journal of Experimental Marine Biology and Ecology*, 461: 31-38.

Gattuso J.-P., Bijma J., Gehlen M., Riebesell U. and Turley C. (2011). Ocean acidification: knowns, unknowns, and perspectives. In Gattuso J.-P. and Hansson L. (eds.) *Ocean Acidification*. 352 pp. Oxford University Press, UK.

Gattuso J.P., Kirkwood W., Barry J.P., Cox E., Gazeau F., Hansson L., Hendriks I., Kline D.I., Mahacek P., Martin S., McElhany P., Peltzer E.T., Reeve J., Roberts D., Saderne V., Tait K., Widdicombe S. and Brewer P.G. (2014). Free Ocean CO₂ Enrichment (FOCE) systems: present status and future developments. *Biogeosciences Discussion*, 11: 4001-4046.

Gaylord B., Kroeker K.J., Sunday J.M., Anderson K.M., Barry J.P., Brown N.E., Connell S.D., Dupont S., Fabricius K.E., Hall-Spencer J.M., Klinger T., Milazzo M., Munday P.L., Russell B.D., Sanford E., Schreiber S.J., Thiyagarajan V., Vaughan M.L.H., Widdicombe S. and Harley C.D.G. (2014). Ocean acidification through the lens of ecological theory. *Ecology*, 140902120430003.

Geider R. and La Roche J. (1994). The role of iron in phytoplankton photosynthesis, and the potential for iron-limitation of primary productivity in the sea. *Photosynthesis Research*, 39: 275-301.

Ghedini G., Russell B. and Connell S. (2013). Managing local coastal stressors to reduce the ecological effects of ocean acidification and warming. *Water*, 5: 1653-1661.

Giakoumi S., Cebrian E., Kokkoris G.D., Ballesteros E. and Sala E. (2012). Relationships between fish, sea urchins and macroalgae: The structure of shallow sublittoral communities in the Cyclades, Eastern Mediterranean. *Estuarine, Coastal and Shelf Science*, 109: 1-10.

Gibbs S.J., Bown P.R., Sessa J.A., Bralower T., and Wilson P. (2006). Nannoplankton extinction and origination across the Paleocene - Eocene Thermal Maximum. *Science*, 314: 1770-1773.

Gilpin L.C., Davidson K. and Roberts E. (2004). The influence of changes in nitrogen: silicon ratios on diatom growth dynamics. *Journal of Sea Research*, 51:21-35.

Gobler C.J., DePasquale E.L., Griffith A.W. and Baumann H. (2014). Hypoxia and acidification have additive and synergistic negative effects on the growth, survival, and metamorphosis of early life stage bivalves. *PLoS ONE*, 9: e83648.

Godbold J.A. and Solan M. (2013). Long-term effects of warming and ocean acidification are modified by seasonal variation in species responses and environmental conditions. *Philosophical Transactions of the Royal Society of London. Series B, Biological sciences*, 368: 20130186.

Gooding R.A., Harley C.D.G. and Tang E. (2009). Elevated water temperature and carbon dioxide concentration increase the growth of a keystone

echinoderm. *Proceedings of the National Academy of Sciences of the United States of America*, 106: 9316-9321.

Goss R. and Jakob T. (2010). Regulation and function of xanthophyll cycle-dependent photoprotection in algae. *Photosynthesis Research*, 106: 103-122.

Gouveia C., Kreusch M., Schmidt É.C., Felix M.R.d.L., Osorio L.K.P., Pereira D.T., dos Santos R., Ouriques L.C., Martins R.d.P., Latini A., Ramlov F., Carvalho T.J.G., Chow F., Maraschin M. and Bouzon Z.L. (2013). The Effects of Lead and Copper on the Cellular Architecture and Metabolism of the Red Alga *Gracilaria domingensis*. *Microscopy and Microanalysis*, 19: 513-524.

Graham M.H. (2004). Effects of local deforestation on the diversity and structure of Southern California giant kelp forest food webs. *Ecosystems*, 7: 341-357.

Griffith G.P., Fulton E.A. and Richardson A.J. (2011). Effects of fishing and acidification-related benthic mortality on the southeast Australian marine ecosystem. *Global Change Biology*, 17: 3058-3074.

Guidetti P. and Dulčić J. (2007). Relationships among predatory fish, sea urchins and barrrens in Mediterranean rocky reefs across a latitudinal gradient. *Marine Environmental Research*, 63: 168-184.

Guidetti P. and Sala E. (2007). Community-wide effects of marine reserves in the Mediterranean Sea. *Marine Ecology Progress Series*, 335: 43-56.

Gutow L., Rahman M.M., Bartl K., Saborowski R., Bartsch I. and Wiencke C. (2014). Ocean acidification affects growth but not nutritional quality of the seaweed *Fucus vesiculosus* (Phaeophyceae, Fucales). *Journal of Experimental Marine Biology and Ecology*, 453: 84-90.

Gutowska M.A., Melzner F., Portner H.O. and Meier S. (2010). Cuttlebone calcification increases during exposure to elevated seawater pCO₂ in the cephalopod *Sepia officinalis*. *Marine Biology*, 157: 1653-1663.

Häder D.-P., Lebert M., Mercado J., Aguilera J., Salles S., Flores-Moya A., Jiménez C. and Figueroa F.L. (1996). Photosynthetic oxygen production and PAM fluorescence in the brown alga *Padina pavonica* measured in the field under solar radiation. *Marine Biology*, 127: 61-66.

Hale R., Calosi P., McNeill L., Mieszkowska N. and Widdicombe S. (2011). Predicted levels of future ocean acidification and temperature rise could alter community structure and biodiversity in marine benthic communities. *Oikos*, 120: 661-674.

Hall L.W.J., Scott M.C. and Killen W.D. (1998). Ecological risk assessment of copper and cadmium in surface waters of Chesapeake Bay Watershed. *Environmental Toxicology and Chemistry*, 17:1172-1189.

Hall-Spencer J.M., Rodolfo-Metalpa R., Martin S., Ransome E., Fine M., Turner S.M., Rowley S.J., Tedesco D. and Buia M.-C. (2008). Volcanic carbon dioxide vents show ecosystem effects of ocean acidification. *Nature*, 454: 96-99.

Halm H., Lüder U.H. and Wiencke C. (2010). Induction of phlorotannins through mechanical wounding and radiation conditions in the brown macroalga *Laminaria hyperborea*. *European Journal of Phycology*, 46: 16-26.

Halpern B.S., Selkoe K.A., Micheli F. and Kappel C.V. (2007). Evaluating and ranking the vulnerability of global marine ecosystems to anthropogenic threats. *Conservation Biology*, 21: 1301-1315.

Haritonidis S., Nikolaidis G. and Tsekos I. (1986). Seasonal variation in the biomass of marine macrophyta from Greek coasts. *Marine Ecology*, 7: 359-370.

Harley C.D.G. (2002). Light availability indirectly limits herbivore growth and abundance in a high rocky intertidal community during the winter. *Limnology and Oceanography*, 47: 1217–1222.

Harley C.D.G., Anderson K.M., Demes K.W., Jorve J.P., Kordas R.L., Coyle T.A. and Graham M.H. (2012). Effect of climate change on global seaweeds communities. *Journal of Phycology*, 48: 1064-1078.

Hay M.E., Duffy J.E., Pfister C.A. and Fenical W. (1987). Chemical defense against different marine herbivores: are amphipods insect equivalents? *Ecology*, 68: 1567-1580.

Hendriks I.E., Olsen Y.S., Ramajo L., Basso L., Steckbauer A., Moore T.S., Howard J. AND Duarte C.M. (2014). Photosynthetic activity buffers ocean acidification in seagrass meadows. *Biogeosciences*, 11: 333-346.

Hereu B., Zabala M. and Sala E. (2008). Multiple controls of community structure and dynamics in a sublittoral marine environment. *Ecology*, 89: 3423-3435.

Hester K.C., Peltzer E.T., Kirkwood W.J. and Brewer, P.G. (2008). Unanticipated consequences of ocean acidification: A noisier ocean at lower pH. *Geophysical Research Letters*, 35: doi: 10.1029/2008GL034913.

Hilmi N., Allemand D., Dupont S., Safa A., Haraldsson G., Nunes P.L.D., Moore C., Hattam C., Reynaud S., Hall-Spencer J., Fine M., Turley C., Jeffree R., Orr J., Munday P. and Cooley S. (2012). Towards improved socio-economic assessments of ocean acidification's impacts. *Marine Biology*, doi: 10.1007/s00227-012-2031-5.

Hofmann G.E., Barry J.P., Edmunds P.J., Gates R.D., Hutchins D.A., Klinger T. and Sewell M.A. (2010). The effect of ocean acidification on calcifying

organisms in marine ecosystems: an organism-to-ecosystem perspective. *Annual Review of Ecology, Evolution and Systematics*, 41:127-147.

Hofmann G.E., Smith J.E., Johnson K.S., Send U., Levin L.A., Micheli F., Paytan A., Price N.N., Peterson B., Takeshita Y., Matson P.G., Crook E.D., Kroeker K.J., Gambi M.C., Rivest E.B., Frieder C.A., Yu P.C. and Martz T.R. (2011). High-frequency dynamics of ocean pH: a multi-ecosystem comparison. *PLoS ONE*, 6: e28983.

Hofmann L.C., Yildiz G., Hanelt D. and Bischof K. (2011). Physiological responses of the calcifying rhodophyte, *Corallina officinalis* (L.), to future CO₂ levels. *Marine Biology*, 159: 783-792.

Hofmann L.C., Straub S. and Bischof K. (2012). Competition between calcifying and noncalcifying temperate marine macroalgae under elevated CO₂ levels. *Marine Ecology Progress Series*, 464: 89-105.

Holcomb M., McCorkle D.C. and Cohen A.L. (2010). Long-term effects of nutrient and CO₂ enrichment on the temperate coral *Astrangia poculata* (Ellis and Solander, 1786). *Journal of Experimental Marine Biology and Ecology*, 386: 27-33.

Holcomb M., Cohen A.L. and McCorkle D.C. (2011). A gender bias in the calcification response to ocean acidification. *Biogeosciences Discussion*, 8: 8485-8513.

Hönisch B., Hemming N.G., Archer D., Siddall M., and McManus J.F. (2009). Atmospheric carbon dioxide concentration across the mid-Pleistocene transition. *Science*, 324: 1551-4.

Hoppe C.J.M., Langer G. and Rost B. (2011). *Emiliania huxleyi* shows identical responses to elevated pCO₂ in TA and DIC manipulations. *Journal of Experimental Marine Biology and Ecology*, 406: 54-62.

Howes D.E., Harper J.R. and Owens E.H. (1994). British Columbia physical shore-zone mapping system. Resources Inventory Committee (RIC) report by the Coastal Task Force, RIC Secretariat, Victoria, B.C., 71 pp.

Hübner A., Rahders E., Rahner S., Halbach P. and Varnavas S.P. (2004). Geochemistry of hydrothermally influenced sediments off Methana (Western Hellenic Volcanic Arc). *Chemie der Erde - Geochemistry*, 64: 75-94.

Hughes T.P. (1994). Catastrophes, phase shifts, and large-scale degradation of a Caribbean coral reef. *Science*, 265: 1547-1551.

Hughes T.P., Rodrigues M.J., Bellwood D.R., Ceccarelli D., Hoegh-Guldberg O., McCook L., Moltschaniwskyj N., Pratchett M.S., Steneck R.S. and Willis B. (2007). Phase shifts, herbivory, and the resilience of coral reefs to climate change. *Current Biology*, 17: 360-365.

Hurd C.L. (2000). Water motion, marine macroalgal physiology, and production. *Journal of Phycology*, 36: 453-472.

Hutchins D.A., Mulholland M.R. and Fu F.X. (2009). Nutrient cycles and marine microbes in a CO₂-enriched ocean. *Oceanography*, 22: 128-145.

Iglesias-Rodriguez M.D., Halloran P.R., Rickaby R.E.M., Hall I.R., Colmenero-Hidalgo E., Gittins J.R., Green D.R.H., Tyrrell T., Gibbs S.J., von Dassow P., Rehm E., Armbrust E.V. and Boessenkool K.P. (2008). Phytoplankton calcification in a high-CO₂ world. *Science*, 320: 336-340.

Inguaggiato S., Mazot A., Diliberto I.S., Inguaggiato C., Madonia P., Rouwet D. and Vita F. (2012). Total CO₂ output from Vulcano island (Aeolian Islands, Italy).

Geochemistry Geophysics Geosystems, 13: Q02012,
doi:10.1029/2011GC003920.

Inoue S., Kayanne H., Yamamoto S. and Kurihara H. (2013). Spatial community shift from hard to soft corals in acidified water. *Nature Climate Change*, 3: 683-687.

Intergovernmental Panel on Climate Change (2014). Climate change 2014: the physical science basis. Contribution of working group I to the fourth assessment report of the Intergovernmental Panel on Climate Change. Cambridge University Press, Cambridge, UK.

Italiano F., Nuccio P.M. and Sommaruga C. (1984). Gas/steam and thermal energy release measured at the gaseous emissions of the Baia di Levante of Vulcano Island, Italy. *Acta Vulcanologica*, 5: 89-94.

James R.K., Hepburn C.D., Cornwall C.E., McGraw C.M. and Hurd C.L. (2014). Growth response of an early successional assemblage of coralline algae and benthic diatoms to ocean acidification. *Marine Biology*, 161: 1687-1696.

Jennings J.G. and Steinberg P.D. (1997). Phlorotannins versus other factors affecting epiphyte abundance on the kelp *Ecklonia radiata*. *Oecologia*, 109: 461-473.

Johnson V.R. (2012). A study of marine benthic algae along a natural carbon dioxide gradient. PhD thesis, Plymouth University, UK, 274 pp.

Johnson V.R., Russell B.D., Fabricius K.E., Brownlee C. and Hall-Spencer J.M. (2012). Temperate and tropical brown macroalgae thrive, despite decalcification, along natural CO₂ gradients. *Global Change Biology*, 18: 2792-2803.

Johnson V., Brownlee C., Rickaby R., Graziano M., Milazzo M. and Hall-Spencer J. (2013). Responses of marine benthic microalgae to elevated CO₂. *Marine Biology*, 160: 1813-1824.

Johnson M.D., Price N.N. and Smith J.E. (2014). Contrasting effects of ocean acidification on tropical fleshy and calcareous algae. *PeerJ*, 2: e411.

Johnston E.L. and Webb J.A. (2000). Novel techniques for field assessment of copper toxicity on fouling assemblages. *Biofouling* 15:165-173.

Johnston E.L. and Keough M.J. (2002). Direct and indirect effects of repeated pollution events on marine hard-substrate assemblages. *Ecological Applications*, 12:1212-1228.

Johnston E.L. and Roberts D.A. (2009). Contaminants reduce the richness and evenness of marine communities: A review and meta-analysis. *Environmental Pollution*, 157: 1745-1752.

Jokiel P.L., Rodgers K.S., Kuffner I.B., Andersson A.J., Cox E.F. and Mackenzie F.T. (2008). Ocean acidification and calcifying reef organisms: A mesocosm investigation. *Coral Reefs*, 27: 473-483.

Jones W.E. and Moorjani S.A. (1973). The attachment and early development of the tetraspores of some coralline red algae. *Special Publications of the Marine Biological Associations of India*, 1973: 293-304.

Jones E. and Thornber C.S. (2010). Effects of habitat-modifying invasive macroalgae on epiphytic algal communities. *Marine Ecology Progress Series*, 400: 87-100.

Jormalainen V., Honkanen T. and Heikkilä N. (2001). Feeding preferences and performance of a marine isopod on seaweed hosts: cost of habitat specialization. *Marine Ecology Progress Series*, 220: 219-230.

Kalogirou S., Wennhage H. and Pihl L. (2012). Non-indigenous species in Mediterranean fish assemblages: Contrasting feeding guilds of *Posidonia oceanica* meadows and sandy habitats. *Estuarine, Coastal and Shelf Science*, 96: 209-218.

Kamal J. (2011). Quantification of alkaloids, phenols and flavonoids in sunflower (*Helianthus annuus* L.). *African Journal of Biotechnology*, 10: 3149-3151.

Kamenos N.A., Burdett H.L., Aloisio E., Findlay H.S., Martin S., Longbone C., Dunn J., Widdicombe S. and Calosi P. (2013). Coralline algal structure is more sensitive to rate, rather than the magnitude, of ocean acidification. *Global Change Biology*, 19: 3621-3628.

Kangwe J.W., Hellblom F., Semesi A.K., Mtolera M.S.P. and Bjork M. (2001). Heavy metal inhibition of calcification and photosynthetic rates of the geniculate calcareous alga *Amphiroa tribulus*. *Marine Science Development in Tanzania and Eastern Africa*, 1:147-157.

Karageorgis A.P., Anagnostou C.L. and Kaberi H. (2005). Geochemistry and mineralogy of the NW Aegean Sea surface sediments: implications for river runoff and anthropogenic impact. *Applied Geochemistry*, 20:69-88.

Karlen D.J., Price R.E., Pichler T. and Garey J.R. (2010). Changes in benthic macrofauna associated with a shallow-water hydrothermal vent gradient in Papua New Guinea. *Pacific Science*, 64: 391-404.

Karsten U., Franklin L.A., Lüning K. and Wiencke C. (1998). Natural ultraviolet radiation and photosynthetically active radiation induce formation of mycosporine-like amino acids in the marine macroalga *Chondrus crispus* (Rhodophyta). *Planta*, 205: 257-262.

Kelly M.W. and Hofmann G.E. (2012). Adaptation and the physiology of ocean acidification. *Functional Ecology*, 27: 980-990.

Kelly M.W., Padilla-Gamiño J.L. and Hofmann G.E. (2013). Natural variation and the capacity to adapt to ocean acidification in the keystone sea urchin *Strongylocentrotus purpuratus*. *Global Change Biology*, 19: 2536-2546.

Kerrison P., Hall-Spencer J.M., Suggett D.J., Hepburn L.J. and Steinke M. (2011). Assessment of pH variability at a coastal CO₂ vent for ocean acidification studies. *Estuarine, Coastal and Shelf Science*, 94: 129-137.

Key R.M., Kozyr A., Sabine C.L., Lee K., Wanninkhof R., Bullister J.L., Feely R.A., Millero F.J., Mordy C. and Peng T.H. (2004). A global ocean carbon climatology: Results from Global Data Analysis Project (GLODAP). *Global Biogeochemical Cycles*, 18: GB4031.

Khan N., Ryu K.Y., Choi J.Y., Nho E.Y., Habte G., Choi H., Kim M.H., Park K.S. and Kim K.S. (2015). Determination of toxic heavy metals and speciation of arsenic in seaweeds from South Korea. *Food Chemistry*, 169: 464-470.

Kletou D. and Hall-Spencer J.M. (2012) Threats to ultraoligotrophic marine ecosystems. In Cruzado A. (ed.) *Marine Ecosystems*. InTech - Open Access Publisher. ISBN 979-953-307-4305.

Kline D.I., Teneva L., Schneider K., Miard T., Chai A., Marker M., Headley K., Opdyke B., Nash M., Valetich M., Caves J.K., Russell B.D., Connell S.D., Kirkwood B.J., Brewer P., Peltzer E., Silverman J., Caldeira K., Dunbar R.B., Koseff J.R., Monismith S.G., Mitchell B.G., Dove S. and Hoegh-Guldberg O. (2012). A short-term *in situ* CO₂ enrichment experiment on Heron Island (GBR). *Scientific Reports*, 2: doi:10.1038/srep00413.

Koch M., Bowes G., Ross C. and Zhang X.-H. (2013). Climate change and ocean acidification effects on seagrasses and marine macroalgae. *Global Change Biology*, 19: 103-132.

Koroleff, F. (1970). Direct determination of ammonia in natural waters as indophenol blue. In: *Information on Techniques and Methods for Seawater Analysis*. Charlottenlund, International Council for the Exploration of the Sea. Interlab. Report, 3: 19-22.

Korpinen S., Jormalainen V. and Ikonen J. (2008). Selective consumption and facilitation by mesograzers in adult and colonizing macroalgal assemblages. *Marine Biology*, 154: 787-794.

Kroeker K.J., Kordas R.L., Crim R.N. and Singh G.G. (2010). Meta-analysis reveals negative yet variable effects of ocean acidification on marine organisms. *Ecology Letters*, 13: 1419-1434.

Kroeker K.J., Micheli F., Gambi M.C. and Martz T.R. (2011). Divergent ecosystem responses within a benthic marine community to ocean acidification. *Proceedings of the National Academy of Sciences*, 108: 14515-14520.

Kroeker K.J., Kordas R.L., Crim R., Hendriks I.E., Ramajo L., Singh G.S., Duarte C.M. and Gattuso J.-P. (2013a). Impacts of ocean acidification on marine organisms: quantifying sensitivities and interaction with warming. *Global Change Biology*, 19: 1884-1896.

Kroeker K.J., Gambi M.C. and Micheli F. (2013b). Community dynamics and ecosystem simplification in a high-CO₂ ocean. *Proceedings of the National Academy of Sciences USA*, 110: 12721-6.

Kroecker K.J., Micheli F. and Gambi M.C. (2013c). Ocean acidification causes ecosystem shifts via altered competitive interactions. *Nature Climate Change*, 3: 156-159.

Kübler J.E., Johnston A.M. and Raven J.A. (1999). The effects of reduced and elevated CO₂ and O₂ on the seaweed *Lomentaria articulata*. *Plant, Cell & Environment*, 22: 1303-1310.

Küffner I.B., Andersson A.J., Jokiel P.L., Rodgers K.S. and Mackenzie F.T. (2008). Decreased abundance of crustose coralline algae due to ocean acidification. *Nature Geoscience*, 1: 114-117.

Küpper H., Šetlík I., Spiller M., Küpper F.C. and Prášil O. (2002). Heavy metal-induced inhibition of photosynthesis: targets of in vivo heavy metal chlorophyll formation. *Journal of Phycology*, 38: 429-441.

Küpper H., Seibert S. and Aravind P. (2007). A fast, sensitive and inexpensive alternative to analytical pigment HPLC: quantification of chlorophylls and carotenoids in crude extracts by fitting with Gauss-peak-spectra. *Analytical Chemistry*, 79: 7611-7627.

La Mesa G. and Vacchi M. (1999). An analysis of the coastal fish assemblage of the Ustica island marine reserve (Mediterranean Sea). *Marine Ecology*, 20: 147-165.

Labiosa R.G., Arrigo K.R., Genin A., Monismith S.G. and van Dijken G. (2003). The interplay between upwelling and deep convective mixing in determining the seasonal phytoplankton dynamics in the Gulf of Aqaba: Evidence from SeaWiFS and MODIS. *Limnology and Oceanography*, 48: 2355-2368.

Landes A. and Zimmer M. (2012). Acidification and warming affect both a calcifying predator and prey, but not their interaction. *Marine Ecology Progress Series*, 450: 1-10.

Langer G., Nehrke G., Probert I., Ly J. and Ziveri P. (2009). Strain-specific responses of *Emiliana huxleyi* to changing seawater carbonate chemistry, *Biogeosciences*, 6: 2637-2646.

Langer G., Nehrke G., Baggini C., Rodolfo-Metalpa R., Hall-Spencer J. and Bijma J. (2014). Limpets counteract ocean acidification induced shell corrosion by thickening of aragonitic shell layers. *Biogeosciences Discussion*, 11: 12571-12590.

Lawrence J.M. (2013). Edible sea urchins: biology and ecology. 3rd edition. Elsevier, Boston, 380 pp.

Le Quéré C., Raupach M.R., Canadell J.G., Marland G. *et al.* (2009). Trends in the sources and sinks of carbon dioxide. *Nature Geoscience*, 2: 831-836.

Leimu R. and Fischer M. (2008). A meta-analysis of local adaptation in plants. *PLoS ONE*, 3: e4010.

Lewis J.R. (1964). The ecology of rocky shores. English University Press, London, 323 pp.

Lewis E. and Wallace W.R. (1998) Program developed for CO₂ system calculations. Carbon dioxide information analysis center, Oak Ridge National Laboratory. US Department of Energy, Oak Ridge.

Lewis C., Clemow K. and Holt W. (2012). Metal contamination increases the sensitivity of larvae but not gametes to ocean acidification in the polychaete *Pomatoceros lamarckii* (Quatrefages). *Marine Biology*, 160: 2089-2101.

- Lischka S., Büdenbender J., Boxhammer T. and Riebesell U. (2010). Impact of ocean acidification and elevated temperatures on early juveniles of the polar shelled pteropod *Limacina helicina*: Mortality, shell degradation, and shell growth. *Biogeosciences Discussion*, 7: 8177-8214.
- Lobban C.S. and Harrison P.J. (1994). Seaweed ecology and physiology. Cambridge University Press.
- Locke A. and Sprules W.G. (2000). Effects of acidic pH and phytoplankton on survival and condition of *Bosmina longirostris* and *Daphnia pulex*. *Hydrobiologia*, 437: 187-196.
- Lohbeck K.T., Riebesell U. and Reusch T.B.H. (2012). Adaptive evolution of a key phytoplankton species to ocean acidification. *Nature Geosciences*, 5: 346-351.
- Lombardi C., Cocito S., Gambi M., Cisterna B., Flach F., Taylor P., Keltie K., Freer A. and Cusack M. (2011). Effects of ocean acidification on growth, organic tissue and protein profile of the Mediterranean bryozoan *Myriapora truncata*. *Aquatic Biology*, 13: 251-262.
- Long E. R. and MacDonald D. D. (1998). Recommended uses of empirically derived, sediment quality guidelines for marine and estuarine ecosystems. *Human and Ecological Risk Assessment*. 4: 1019-1039.
- Lüthi D., Le Floch M., Bereiter B., Blunier T., Barnola J.M., Siegenthaler U., Raynaud D., Jouzel J., Fischer H., Kawamura K. and Stocker T.F. (2008). High-resolution carbon dioxide concentration record 650,000-800,000 years before present. *Nature*, 453: 379-382.

Maas A.E., Wishner K.F. and Seibel B.A. (2012). The metabolic response of pteropods to acidification reflects natural CO₂-exposure in oxygen minimum zones. *Biogeosciences*, 9: 747-757.

Maher W.A. and Clarke S.M. (1984). The occurrence of arsenic in selected marine macroalgae from two coastal areas of South Australia. *Marine Pollution Bulletin*, 15: 111-112.

Mallick N. and Mohn F.H. (2003). Use of chlorophyll fluorescence in metal-stress research: a case study with the green microalga *Scenedesmus*. *Ecotoxicology and Environmental Safety*, 55: 64-69.

Manzello D.P. (2010). Coral growth with thermal stress and ocean acidification: lessons from the eastern tropical Pacific. *Coral Reefs*, 29: 749-758.

Manzello D.P., Enochs I.C., Melo N., Gledhill D.K. and Johns E.M. (2012). Ocean Acidification Refugia of the Florida Reef Tract. *PLoS ONE*, 7: e41715.

Marshall D.J., Santos J.H., Leung K.M.Y. and Chak W.H. (2008). Correlations between gastropod shell dissolution and water chemical properties in a tropical estuary. *Marine Environmental Research*, 66: 422-429.

Martin J.H., Gordon R.M. and Fitzwater S.E. (1990). Iron in Antarctic waters. *Nature*, 345: 156-158.

Martin S., Rodolfo-Metalpa R., Ransome E., Rowley S., Buia M.C., Gattuso J.P. and Hall-Spencer J. (2008). Effects of naturally acidified seawater on seagrass calcareous epibionts. *Biology Letters*, 4: 689-692.

Martin S. and Gattuso J.P. (2009). Response of Mediterranean coralline algae to ocean acidification and elevated temperature. *Global Change Biology*, 15: 2089-2100.

- Martin S., Cohu S., Vignot C., Zimmerman G. and Gattuso J.-P. (2013). One-year experiment on the physiological response of the Mediterranean crustose coralline alga, *Lithophyllum cabiochae*, to elevated pCO₂ and temperature. *Ecology and Evolution*, 3: 676-693.
- Mayol E., Ruiz-Halpern S., Duarte C.M., Castilla J.C. and Pelegrí J.L. (2012). Coupled CO₂ and O₂-driven compromises to marine life in summer along the Chilean sector of the Humboldt Current System. *Biogeosciences*, 9: 1183-1194.
- McConnaughey T.A. and Whelan J.F. (1997). Calcification generates protons for nutrient and bicarbonate uptake. *Earth Science Reviews*, 42: 95-117.
- McCormick M.I., Watson S.-A. and Munday P.L. (2013). Ocean acidification reverses competition for space as habitats degrade. *Scientific Reports*, 3, doi:10.1038/srep03280.
- McDermid K. and Stuercke B. (2003). Nutritional composition of edible Hawaiian seaweeds. *Journal of Applied Phycology*, 15: 513-524.
- McDonald M.R., McClintock J.B., Amsler C.D., Rittschof D., Angus R.A., Orihuela B. and Lutostanski K. (2009). Effects of ocean acidification over the life history of the barnacle *Amphibalanus amphitrite*. *Marine Ecology Progress Series*, 385: 179-187.
- Melwani A.R. and Kim S.L. (2008). Benthic infaunal distributions in shallow hydrothermal vent sediments. *Acta Oecologica*, 33: 162-175.
- Melzner F., Gutowska M.A., Langenbuch M., Dupont S., Lucassen M., Thorndyke M.C., Bleich M. and Portner H.O. (2009). Physiological basis for high CO₂ tolerance in marine ectothermic animals: Pre-adaptation through lifestyle and ontogeny? *Biogeosciences*, 6: 2313-2331.

Melzner F., Stange P., Trübenbach K., Thomsen J., Casties I., Panknin U., Gorb S.N. and Gutowska M.A. (2011). Food supply and seawater pCO₂ impact calcification and internal shell dissolution in the blue mussel *Mytilus edulis*. *PLoS ONE*, 6: e24223.

Melzner F., Thomsen J., Koeve W., Oschlies A., Gutowska M., Bange H., Hansen H. and Körtzinger A. (2013). Future ocean acidification will be amplified by hypoxia in coastal habitats. *Marine Biology*, 160: 1875-1888.

Mendes L., Zambotti-Villela L., Colepicolo P., Marinho-Soriano E., Stevani C. and Yokoya N. (2013). Metal cation toxicity in the alga *Gracilaria domingensis* as evaluated by the daily growth rates in synthetic seawater. *Journal of Applied Phycology*, 25: 1939-1947.

Menge B.A., Foley M.M., Pamplin J., Murphy G. and Pennington C. (2010). Supply-side ecology, barnacle recruitment, and rocky intertidal community dynamics: Do settlement surface and limpet disturbance matter? *Journal of Experimental Marine Biology and Ecology*, 392: 160-175.

Mercado J.M., Santos C.B., Perez-Llorens J.L. and Vergara J.J. (2009). Carbon isotopic fractionation in macroalgae from Cadiz Bay (Southern Spain): Comparison with other bio-geographic regions. *Estuarine Coastal and Shelf Science*, 85: 449-458.

Mayer-Pinto M., Underwood A.J., Tolhurst T. and Coleman R.A. (2010). Effects of metals on aquatic assemblages: What do we really know? *Journal of Experimental Marine Biology and Ecology*, 391: 1-9.

Micheli, F., Cottingham K.L., Bascompte J., Bjørnstad O.N., Eckert G.L., Fischer J.M., Keitt T.H., Kendall B.E., Klug J.L. and Rusak J.A. (1999). The dual nature of community variability. *Oikos*, 85: 161-169.

Micheli F. and Halpern B.S. (2005). Low functional redundancy in coastal marine assemblages. *Ecology Letters*, 8: 391-400.

Micheli F., Mumby P.J., Brumbaugh D.R., Broad K., Dahlgren C.P., Harborne A.R., Holmes K.E., Kappel C.V., Litvin S.Y. and Sanchirico J.N. (2014). High vulnerability of ecosystem function and services to diversity loss in Caribbean coral reefs. *Biological Conservation*, 171: 186-194.

Miller A.W., Reynolds A.C., Sobrino C. and Riedel G.F. (2009). Shellfish face uncertain future in high CO₂ world: Influence of acidification on oyster larvae calcification and growth in estuaries. *PLoS ONE*, 4(5): e5661.

Millero F.J., Woosley R., Ditrolio B. and Waters J. (2009). Effect of ocean acidification on the speciation of metals in seawater. *Oceanography*, 22: 72-85.

Monro K. and Poore A.G.B. (2005). Light quantity and quality induce shade-avoiding plasticity in a marine macroalga. *Journal of Evolutionary Biology*, 18: 426-435.

Morey G., Moranta J., Massutí E., Grau A., Linde M., Riera F. and Morales-Nin B. (2003). Weight-length relationships of littoral to lower slope fishes from the Western Mediterranean. *Fisheries Research*, 62: 89-96.

Morri C., Bianchi C.N., Cocito S., Peirano A., Biase A.M.D., Aliani S., Pansini M., Boyer M., Ferdeghini F., Pestarino M. and Dando P. (1999). Biodiversity of marine sessile epifauna at an Aegean island subject to hydrothermal activity: Milos, eastern Mediterranean Sea. *Marine Biology*, 135: 729-739.

Moulin L., Catarino A.I., Claessens T. and Dubois P. (2011). Effects of seawater acidification on early development of the intertidal sea urchin *Paracentrotus lividus* (Lamarck 1816). *Marine Pollution Bulletin*, 62: 48-54.

Moutin T. and Raimbault P. (2002). Primary production, carbon export and nutrients availability in western and eastern Mediterranean Sea in early summer 1996 (MINOS cruise). *Journal of Marine Systems*, 33: 273-288.

Mucci A., Starr M., Gilbert D. and Sundby B. (2011). Acidification of Lower St. Lawrence estuary bottom waters. *Atmosphere-Ocean*, 49: 206-218.

Mullin J.B. and Riley J.P. (1955). The colorimetric determination of silicate with special reference to sea and natural waters. *Analytica Chimica Acta*, 12: 162-176.

Munday P.L., Cheal A.J., Dixon D.L., Rummer J.L. and Fabricius K.E. (2014). Behavioural impairment in reef fishes caused by ocean acidification at CO₂ seeps. *Nature Climate Change*, doi:10.1038/nclimate2195.

Murphy J. and Riley J.P. (1962). A modified solution method for determination of phosphate in natural waters. *Analytica Chimica Acta*, 27: 31-36.

Nash M.C., Opdyke B.N., Troitzsch U., Russell B.D., Adey W.H., Kato A., Diaz-Pulido G., Brent C., Gardner M., Prichard J. and Kline D.I. (2012). Dolomite-rich coralline algae in reefs resist dissolution in acidified conditions. *Nature Climate Change*, doi:10.1038/nclimate1760.

Nielsen H.D., Brownlee C., Coelho S.M. and Brown M.T. (2003). Inter-population differences in inherited copper tolerance involve photosynthetic adaptation and exclusion mechanisms in *Fucus serratus*. *New Phytologist*, 160:157-165.

Nielsen H.D. and Nielsen S.L. (2005). Photosynthetic responses to Cu²⁺ exposure are independent of light acclimation and uncoupled from growth inhibition in *Fucus serratus* (Phaeophyceae). *Marine Pollution Bulletin*, 51: 715-721.

Nielsen H.D. and Nielsen S.L. (2010). Adaptation to high light irradiances enhances the photosynthetic Cu²⁺ resistance in Cu²⁺ tolerant and non-tolerant populations of the brown macroalgae *Fucus serratus*. *Marine Pollution Bulletin*, 60: 710-717.

Nienhuis S., Palmer A.R. and Harley C.D.G. (2010). Elevated CO₂ affects shell dissolution rate but not calcification rate in a marine snail. *Proceedings of the Royal Society B-Biological Sciences*, 277: 2553-2558.

Noisette F., Duong G., Six C., Davoult D. and Martin S. (2013a). Effects of elevated pCO₂ on the metabolism of a temperate rhodolith *Lithothamnion corallioides* grown under different temperatures. *Journal of Phycology*, 49: 746-757.

Noisette F., Egilisdottir H., Davoult D. and Martin S. (2013b). Physiological responses of three temperate coralline algae from contrasting habitats to near-future ocean acidification. *Journal of Experimental Marine Biology and Ecology*, 448: 179-187.

Norderhaug K.N., Christie H., Fossa J.H. and Fredriksen S. (2005). Fish-macrofauna interactions in a kelp (*Laminaria hyperborea*) forest. *Journal of the Marine Biological Association of the U.K.*, 85: 1279-1286.

Ockendon N., Baker D.J., Carr J.A., White E.C., Almond R.E.A., Amano T., Bertram E., Bradbury R.B., Bradley C., Butchart S.H.M., Doswald N., Foden W., Gill D.J.C., Green R.E., Sutherland W.J., Tanner E.V.J. and Pearce-Higgins J.W. (2014). Mechanisms underpinning climatic impacts on natural populations: altered species interactions are more important than direct effects. *Global Change Biology*, 20: 2221-2229.

Olabarria C., Arenas F., Viejo R.M., Gestoso I., Vaz-Pinto F., Incera M., Rubal M., Cacabelos E., Veiga P. and Sobrino C. (2013). Response of macroalgal assemblages from rockpools to climate change: effects of persistent increase in temperature and CO₂. *Oikos*, 122: 1065-1079.

Olischläger M. and Wiencke C. (2013). Ocean acidification alleviates low-temperature effects on growth and photosynthesis of the red alga *Neosiphonia harveyi* (Rhodophyta). *Journal of Experimental Botany*, 64: 5587-5597.

Orr J.C., Fabry V.J., Aumont O., Bopp L., Doney S.C., Feely R.A., Gnanadesikan A., Gruber N., Ishida A., Joos F., Key R.M., Lindsay K., Maier-Reimer E., Matear R., Monfray P., Mouchet A., Najjar R.G., Plattner G.-K., Rodgers K.B., Sabine C.L., Sarmiento J.L., Schlitzer R., Slater R.D., Totterdell I.J., Weirig M.-F., Yamanaka Y. and Yool A. (2005). Anthropogenic ocean acidification over the twenty-first century and its impact on calcifying organisms. *Nature*, 437: 681-686.

Orr J.C. (2011). Recent and future changes in ocean carbonate chemistry. In Gattuso J.-P. and Hansson L. (eds.) *Ocean Acidification*. 352 pp. Oxford University Press, UK.

Palumbi S.R. (1994). Genetic divergence, reproductive isolation, and marine speciation. *Annual Review of Ecology and Systematics*, 25: 547-572.

Pansch C., Schaub I., Havenhand J. and Wahl M. (2014). Habitat traits and food availability determine the response of marine invertebrates to ocean acidification. *Global Change Biology*, 20: 765-777.

Pansini M., Morri C. and Bianchi C.N. (2000). The sponge community of a subtidal area with hydrothermal vents: Milos island, Aegean Sea. *Estuarine, Coastal and Shelf Science*, 51: 627-635.

- Papworth D. (2012). Relationship between high pCO₂ levels and calcareous epibiota of the seaweed *Sargassum vulgare*. Undergraduate dissertation, Plymouth University, 12 pp.
- Parker L.M., Ross P.M., O'Connor W.A., Borysko L., Raftos D.A. and Pörtner H.-O. (2012). Adult exposure influences offspring response to ocean acidification in oysters. *Global Change Biology*, 18: 82-92.
- Paulson A.J., Curl H.C.J. and Feely R.A. (1989). Estimates of trace metal inputs from non-point sources discharged into estuaries. *Marine Pollution Bulletin*, 20:549-555.
- Pearson G.A., Lago-Leston A. and Mota C. (2009). Frayed at the edges: selective pressure and adaptive response to abiotic stressors are mismatched in low diversity edge populations. *Journal of Ecology*, 97:450-462.
- Pecoraino G., Brusca L., D'Alessandro W., Giammanco S., Inguaggiato S. and Longo M. (2005). Total CO₂ output from Ischia Island volcano (Italy). *Geochemistry Journal*, 39: 451-458.
- Pérès J.M. and Picard J. (1964). Nouveau manuel de bionomie benthique de la Méditerranée. *Rec. Trav. Stat. mar. Endoume*, 31: 1-37.
- Phillips D.J.H. (1990). Use of macroalgae and invertebrates as monitors of metal levels in estuarine and coastal waters. In R. W. Furness & P. S. Rainbow (Eds.), *Heavy metals in the marine environment* (pp. 81-100). CRC, Boca Raton, Florida.
- Piazzi L., Balata D., Pertusati M. and Cinelli F. (2004). Spatial and temporal variability of Mediterranean macroalgal coralligenous assemblages in relation to habitat and substratum inclination. *Botanica Marina*, 47: 105-115.

Pielou E.C. (1966). The measurement of diversity in different types of biological collections. *Journal of Theoretical Biology*, 13: 131-144.

Pingree R.D., Holligan P.M., Mardell G.T. and Head R.N. (1976). The influence of physical stability on spring, summer and autumn phytoplankton blooms in the Celtic Sea. *Journal of the Marine Biological Association of the United Kingdom*, 56: 845-873.

Pinto E., Carvalho A.P., Cardozo K.H.M., Malcata F.X., Anjos F.M.d. and Colepicolo P. (2011). Effects of heavy metals and light levels on the biosynthesis of carotenoids and fatty acids in the macroalgae *Gracilaria tenuistipitata* (var. liui Zhang & Xia). *Revista Brasileira de Farmacognosia*, 21: 349-354.

Pistevos J.C.A., Calosi P., Widdicombe S. and Bishop J.D.D. (2011). Will variation among genetic individuals influence species responses to global climate change? *Oikos*, 120: 675-689.

Pitt R.E. (1995). Effects of urban runoff on aquatic biota. In Hoffman D.J., Rattner B.A., Burton G.A.J. and Cairns J.J., Eds. *Handbook of ecotoxicology*. Lewis Publishers, Boca Raton, Florida, USA, pp. 609-630.

Poore A.G.B., Campbell A.H. and Steinberg P.D. (2009). Natural densities of mesograzers fail to limit growth of macroalgae or their epiphytes in a temperate algal bed. *Journal of Ecology*: 97, 164-175.

Poore A.G.B., Campbell A.H., Coleman R.A., Edgar G.J., Jormalainen V., Reynolds P.L., Sotka E.E., Stachowicz J.J., Taylor R.B., Vanderklift M.A. and Emmett Duffy J. (2012). Global patterns in the impact of marine herbivores on benthic primary producers. *Ecology Letters*, 15: 912-922.

Poore A.B., Graba-Landry A., Favret M., Sheppard Brennan H., Byrne M. and Dworjanyn S. (2013). Direct and indirect effects of ocean acidification and warming on a marine plant-herbivore interaction. *Oecologia*, 173: 1113-1124.

Pörtner H.O., Langenbuch M. and Reipschlag A. (2004). Biological impact of elevated ocean CO₂ concentrations: Lessons from animal physiology and earth history. *Journal of Oceanography*, 60: 705-718.

Porzio, L. (2010). Water acidification: effects on the macroalgal community. PhD Thesis, University of Naples Federico II (Italy), 214 pp.

Porzio L., Buia M.C. and Hall-Spencer J.M. (2011). Effects of ocean acidification on macroalgal communities. *Journal of Experimental Marine Biology and Ecology*, 400: 278-287.

Porzio L., Garrard S.L. and Buia M.C. (2013). The effect of ocean acidification on early algal colonization stages at natural CO₂ vents. *Marine Biology*, 160: 2247-2259.

Post E. and Pedersen C. (2008). Opposing plant community responses to warming with and without herbivores. *Proceedings of the National Academy of Sciences*, 105: 12353-12358.

Price N.N., Hamilton S.L., Tootell J.S. and Smith J.E. (2011). Species-specific consequences of ocean acidification for the calcareous tropical green algae *Halimeda*. *Marine Ecology Progress Series*, 440: 67-78.

Privitera D., Chiantore M., Mangialajo L., Glavic N., Kozul W. and Cattaneo-Vietti R. (2008). Inter- and intra-specific competition between *Paracentrotus lividus* and *Arbacia lixula* in resource-limited barren areas. *Journal of Sea Research*, 60: 184-192.

Quinn G.P. and Keough M.J. (2002). Experimental design and data analysis for biologists. *Cambridge University Press*, Cambridge, UK.

Raize O., Argaman Y. and Yannai S. (2004). Mechanisms of biosorption of different heavy metals by brown marine macroalgae. *Biotechnology and Bioengineering*, 87: 451-458.

Raman D., Venkateshwarlu Reddy P., Vijay Kumar B. and Murthy U.S.N. (2013). Atomic Absorption Spectroscopic determination and comparison of trace elements in the seaweeds. *International Journal of Modern Chemistry and Applied Science*, 1: 12-24.

Raven J.A., Johnston A.M., Kübler J.E., Korb R.E., McInroy S.G., Handley L.L., Scrimgeour C.M., Walker D.I., Beardall J., Vanderklift M., Fredriksen S. and Dunton K.M. (2002). Mechanistic interpretation of carbon isotope discrimination by marine macroalgae and seagrasses. *Functional Plant Biology*, 29: 355-78.

Raven J., Caldeira K., Elderfield H., Hoegh-Guldberg O., Liss P., Riebesell U., Shepherd J., Turley C. and Watson A. (2005). Ocean acidification due to increasing atmospheric carbon dioxide. *Royal Society Special Report*. Policy document 12/05. London.

Raven J.A., Giordano M., Beardall J. and Maberly S.C. (2012). Algal and aquatic plant carbon concentrating mechanisms in relation to environmental change. *Photosynthesis Research*, 109: 281-96.

Reusch T.B.H. (2014). Climate change in the oceans: evolutionary versus phenotypically plastic responses of marine animals and plants. *Evolutionary Applications*, 7: 104-122.

- Richards R., Chaloupka M., Sanò M. and Tomlinson R. (2011). Modelling the effects of "coastal" acidification on copper speciation. *Ecological Modelling*, 222: 3559-3567.
- Ridgwell A. and Schmidt D. (2010). Past constraints on the vulnerability of marine calcifiers to massive carbon dioxide release. *Nature Geoscience*, 3: 196-200.
- Riebesell U., Zondervan I., Rost B., Tortell P.D., Zeebe R.E. and Morel F.M.M. (2000). Reduced calcification of marine plankton in response to increased atmospheric CO₂. *Nature*, 407: 364-367.
- Riebesell U. (2008). Climate change: Acid test for marine biodiversity. *Nature*, 454: 46-47.
- Riebesell U., Fabry V.J., Hansson L. and Gattuso J.-P. (Eds.) (2010). Guide to best practices for ocean acidification research and data reporting: Luxembourg: Publications Office of the European Union.
- Riedl R. (1991). Fauna e flora del Mediterraneo; dalle alghe ai mammiferi una guida sistematica alle specie che vivono nel Mar Mediterraneo. Franco Muzzio Editore, Roma. 777 pp.
- Ries J.B., Cohen A.L. and McCorkle D.C. (2009). Marine calcifiers exhibit mixed responses to CO₂-induced ocean acidification. *Geology*, 37: 1131-1134.
- Rink S., Kuhl M., Bijima J. and Spero H.J. (1998). Microsensor studies of photosynthesis and respiration in the symbiotic foraminifer, *Orbulina universa*. *Marine Biology*, 131: 583-595.
- Roberts D.A., Poore A.G.B. and Johnston E.L. (2006). Ecological consequences of copper contamination in macroalgae: Effects on epifauna and

associated herbivores. *Environmental Toxicology and Chemistry*, 25: 2470-2479.

Roberts D.A., Johnston E.L. and Poore A.G.B. (2008). Contamination of marine biogenic habitats and effects upon associated epifauna. *Marine Pollution Bulletin*, 56:1057-1065.

Roberts D.A., Birchenough S.N.R., Lewis C., Sanders M.B., Bolam T. and Sheahan D. (2013). Ocean acidification increases the toxicity of contaminated sediments. *Global Change Biology*, 19: 340-351.

Rodolfo-Metalpa R., Houlbreque F., Tambutte E., Boisson F., Baggini C., Patti F.P., Jeffree R., Fine M., Foggo A., Gattuso J.P. and Hall-Spencer J.M. (2011). Coral and mollusc resistance to ocean acidification adversely affected by warming. *Nature Climate Change*, 1: 308-312.

Rodriguez-Tovar F.J., Uchman A., Alegret L. and Molina E. (2011). Impact of the Paleocene-Eocene Thermal Maximum on the macrobenthic community: Ichnological record from the Zumaia section, northern Spain. *Marine Geology*, 282: 178-187.

Rönnbäck P., Kautsky N., Pihl L., Troell M., Söderqvist T. and Wennhage H. (2007). Ecosystem goods and services from Swedish coastal habitats: Identification, valuation, and implications of ecosystem shifts. *Ambio*, 36: 534-544.

Rosa R. and Seibel B.A. (2008). Synergistic effects of climate-related variables suggest future physiological impairment in a top oceanic predator. *Proceedings of the National Academy of Sciences of the United States of America*, 105: 20776-20780.

Rossoll D., Bermúdez R., Hauss H., Schulz K.G., Riebesell U., Sommer U. and Winder M. (2012). Ocean acidification-induced food quality deterioration constrains trophic transfer. *PLoS ONE*, 7: e34737.

Russell B.D., Thompson J.A.I., Falkenberg L.J. and Connell S.D. (2009). Synergistic effects of climate change and local stressors: CO₂ and nutrient-driven change in subtidal rocky habitats. *Global Change Biology*, 15: 2153-2162.

Russell B.D., Passarelli C.A. and Connell S.D. (2011). Forecasted CO₂ modifies the influence of light in shaping subtidal habitat. *Journal of Phycology*, 47: 744-752.

Russell B.D., Connell S.D., Findlay H.S., Tait K., Widdicombe S. and Mieszkowska N. (2013). Ocean acidification and rising temperatures may increase biofilm primary productivity but decrease grazer consumption. *Philosophical Transactions of the Royal Society B: Biological Sciences*, 368: 20120438.

Ryan K.G., Ralph P. and McMinn A. (2004). Acclimation of Antarctic bottom-ice algal communities to lowered salinities during melting. *Polar Biology*, 27:679-686.

Saderne V. and Wahl M. (2013). Differential responses of calcifying and non-calcifying epibionts of a brown macroalga to present-day and future upwelling pCO₂. *PLoS ONE*, 8: e70455.

Sala E. and Boudouresque C.F. (1997). The role of fishes in the organization of a Mediterranean sublittoral community.: I: Algal communities. *Journal of Experimental Marine Biology and Ecology*, 212: 25-44.

Sala E., Boudouresque C.F. and Harmelin-Vivien M.L. (1998). Fishing, trophic cascades, and the structure of algal assemblages: evaluation of an old but untested paradigm. *Oikos*, 82: 425-439.

Sala E., Kizilkaya Z., Yildirim D. and Ballesteros E. (2011). Alien marine fishes deplete algal biomass in the Eastern Mediterranean. *PLoS ONE*, 6: e17356.

Sala E., Ballesteros E., Dendrinou P., Di Franco A., Ferretti F., Foley D., Fraschetti S., Friedlander A., Garrabou J., Güçlüsoy H., Guidetti P., Halpern B.S., Hereu B., Karamanlidis A.A., Kizilkaya Z., Macpherson E., Mangialajo L., Mariani S., Micheli F., Pais A., Riser K., Rosenberg A.A., Sales M., Selkoe K.A., Starr R., Tomas F. and Zabala M. (2012). The structure of Mediterranean rocky reef ecosystems across environmental and human gradients, and conservation implications. *PLoS ONE*, 7: e32742.

Sales M., Cebrian E., Tomas F. and Ballesteros E. (2011). Pollution impacts and recovery potential in three species of the genus *Cystoseira* (Fucales, Heterokontophyta). *Estuarine, Coastal and Shelf Science*, 92: 347-357.

Sánchez-Moyano J.E., García-Adiego E.M., Estacio F.J. and García-Gómez J.C. (2000). Effect of environmental factors on the spatial distribution of the epifauna of the alga *Stypocaulon scoparia* in Algeciras Bay, Southern Spain. *Aquatic Ecology*, 34:355-367.

Sanford E. and Kelly M.W. (2011). Local adaptation in marine invertebrates. *Annual Review of Marine Science*, 3, 509-535.

Sarmiento J.L., Slater R., Barber R., Bopp L., Doney S.C., Hirst A.C., Kleypas J., Matear R., Mikolajewicz U., Monfray P., Soldatov V., Spall S.A. and Stouffer R. (2004). Response of ocean ecosystems to climate warming. *Global Biogeochemical Cycles*, 18: GB3003.

Sarthou G. and Jeandel C. (2001). Seasonal variations of iron concentrations in the Ligurian Sea and iron budget in the Western Mediterranean Sea. *Marine Chemistry*, 74: 115-129.

Schreiber U., Endo T., Mi H. and Asada K. (1995). Quenching analysis of chlorophyll fluorescence by the saturation pulse method: particular aspects relating to the study of eukaryotic algae and cyanobacteria. *Plant and Cell Physiology*, 36: 873-882.

Schröder W.P., Arellano J.B., Bitter T., Barón M., Eckert H.J. and Regner G. (1994). Flash-induced absorption spectroscopy studies of copper interaction with photosystem II in higher plants. *Journal of Biological Chemistry*, 269:32865-32870.

Schubert N., García-Mendoza E. and Pacheco-Ruiz I. (2006). Carotenoid composition of marine red algae. *Journal of Phycology*, 42: 1208-1216.

Schulz K.G., Ramos J.B.E., Zeebe R.E. and Riebesell U. (2009). CO₂ perturbation experiments: Similarities and differences between dissolved inorganic carbon and total alkalinity manipulations. *Biogeosciences*, 6: 2145-2153.

Seely G.R., Duncan M.J. and Vidaver W.E. (1972). Preparative and analytical extraction of pigments from brown algae with dimethyl sulfoxide. *Marine Biology*, 12:184-188.

Semesi I.S., Beer S. and Bjork M. (2009). Seagrass photosynthesis controls rates of calcification and photosynthesis of calcareous macroalgae in a tropical seagrass meadow. *Marine Ecology Progress Series*, 382: 41-47.

Shannon C.E. and Weaver W. (1949). A mathematical theory of communication. University of Illinois Press. ISBN 0-252-72548-4.

Shaw E.C., Munday P.L. and McNeil B.I. (2013). The role of CO₂ variability and exposure time for biological impacts of ocean acidification. *Geophysical Research Letters*, 40: 4685-4688.

Shears N.T. and Ross P.M. (2010). Toxic cascades: multiple anthropogenic stressors have complex and unanticipated interactive effects on temperate reefs. *Ecology Letters*, 13:1149-1159.

Shi D.L., Xu Y., Hopkinson B.M. and Morel F.M.M. (2010). Effect of ocean acidification on iron availability to marine phytoplankton. *Science*, 327: 676-679.

Shin P.K.S. and Lam W.K.C. (2001). Development of a marine sediment pollution index. *Environmental Pollution*, 113: 281-291.

Short J., Kendrick G.A., Falter J. and McCulloch M.T. (2014). Interactions between filamentous turf algae and coralline algae are modified under ocean acidification. *Journal of Experimental Marine Biology and Ecology*, 456, 70-77.

Shushkina E.A., Vinogradov M.E., Lebedeva L.P., and Anokhina L.L. (1997). Productivity characteristics of epipelagic communities of the world's oceans. *Oceanology*, 37: 346-353.

Siokou-Frangou I., Christaki U., Mazzocchi M.G., Montresor M., Ribera d'Alcalá M., Vaqué D. and Zingone A. (2010). Plankton in the open Mediterranean Sea: a review. *Biogeosciences*, 7: 1543-1586.

Small D., Calosi P., White D., Spicer J.I. and Widdicombe S. (2010). Impact of medium-term exposure to CO₂ enriched seawater on the physiological functions of the velvet swimming crab *Necora puber*. *Aquatic Biology*, 10: 11-21.

Spatharis S., Orfanidis S., Panayotidis P. and Tsirtsis G. (2011). Assembly processes in upper subtidal macroalgae: the effect of wave exposure. *Estuarine, Coastal and Shelf Science*, 91: 298-305.

Spicer J.I. (2014). What can an ecophysiological approach tell us about the physiological responses of marine invertebrates to hypoxia? *The Journal of Experimental Biology*, 217: 46-56.

Steinacher M., Joos F., Frolicher T.L., Plattner G.-K. and Doney S.C. (2009). Imminent ocean acidification projected with the NCAR global coupled carbon cycle-climate model. *Biogeosciences*, 6: 515-33.

Steneck R.S. and Dethier M.N. (1994). A functional group approach to the structure of algal-dominated communities. *Oikos*, 69: 476-498.

Steneck R.S., Graham M.H., Bourque B.J., Corbett D., Erlandson J.M., Estes J.A. and Tegner M.J. (2002). Kelp forest ecosystems: biodiversity, stability, resilience and future. *Environmental Conservation*, 29: 436-459.

Sunday J.M., Crim R.N., Harley C.D.G. and Hart M.W. (2011). Quantifying rates of evolutionary adaptation in response to ocean acidification. *PLoS ONE*, 6: e22881.

Sunday J.M., Calosi P., Dupont S., Munday P.L., Stillman J.H. and Reusch T.B.H. (2014). Evolution in an acidifying ocean. *Trends in Ecology & Evolution*, 29: 117-125.

Susini M.-L., Thibaut T., Meinesz A. and Forcioli D. (2007). A preliminary study of genetic diversity in *Cystoseira amentacea* (C. Agardh) Bory var. *stricta* Montagne (Fucales, Phaeophyceae) using random amplified polymorphic DNA. *Phycologia*, 46: 605-611.

Swanson A.K. and Fox C.H. (2007). Altered kelp (Laminariales) phlorotannins and growth under elevated carbon dioxide and ultraviolet-B treatments can influence associated intertidal food webs. *Global Change Biology*, 13: 1696-1709.

Tarasov V.G., Gebruk A.V., Mironov A.N. and Moskalev L.I. (2005). Deep-sea and shallow-water hydrothermal vent communities: Two different phenomena? *Chemical Geology*, 224: 5-39.

Taskin E., Jahn R., Öztürk M., Furnari G. and Cormaci M. (2012). The Mediterranean *Cystoseira* (with photographs). Manisa, Turkey: Celar Bayar University, pp. 1-75.

Taylor R.B. (1998). Density, biomass and productivity of animals in four subtidal rocky reef habitats: the importance of small mobile invertebrates. *Marine Ecology Progress Series*, 172: 37-51.

Taylor J.D., Ellis R., Milazzo M., Hall-Spencer J.M. and Cunliffe M. (2014). Intertidal epilithic bacteria diversity changes along a naturally occurring carbon dioxide and pH gradient. *FEMS Microbiology Ecology*, 89: 670-678.

Tellier F., Tapia J., Faugeron S., Destombe C. and Valero M. (2011). The *Lessonia nigrescens* species complex (Laminariales, Phaeophyceae) shows strict parapatry and complete reproductive isolation in a secondary contact zone. *Journal of Phycology*, 47: 894-903.

Thiermann F., Akoumianaki I., Hughes J.A. and Giere O. (1997). Benthic fauna of a shallow-water gaseohydrothermal vent area in the Aegean Sea (Milos, Greece). *Marine Biology*, 128: 149-159.

Thomas E. (2007). Cenozoic mass extinctions in the deep sea: what disturbs the largest habitat on Earth? *Geological Society of America Special Papers*, 424: 1-23.

Thomsen J., Gutowska M.A., Saphorster J., Heinemann A., Trubenbach K., Fietzke J., Hiebenthal C., Eisenhauer A., Kortzinger A., Wahl M. and Melzner F. (2010). Calcifying invertebrates succeed in a naturally CO₂-rich coastal habitat

but are threatened by high levels of future acidification. *Biogeosciences*, 7: 3879-3891.

Thomsen J. and Melzner F. (2010). Moderate seawater acidification does not elicit long-term metabolic depression in the blue mussel *Mytilus edulis*. *Marine Biology*, 157: 2667-2676.

Thomsen J., Casties I., Pansch C., Körtzinger A. and Melzner F. (2013). Food availability outweighs ocean acidification effects in juvenile *Mytilus edulis*: laboratory and field experiments. *Global Change Biology*, 19: 1017-1027.

Thurberg F.P., Dawson M.A. and Collier R.S. (1973). Effects of copper and cadmium on osmoregulation and oxygen consumption in two species of estuarine crabs. *Marine Biology*, 23: 171-175.

Tilman D. (1999). The ecological consequences of changes in biodiversity: a search for general principles. *Ecology*, 80: 1455-1474.

Tittensor D.P., Baco A.R., Hall-Spencer J.M., Orr J.C. and Rogers A.D. (2010). Seamounts as refugia from ocean acidification for cold-water stony corals. *Marine Ecology - Evolutionary Perspective*, 31: 212-225.

Tsiamis K., Panayotidis P., Salomidi M., Pavlidou A., Kleinteich J., Balanika K. and Küpper F.C. (2013). Macroalgal community response to re-oligotrophication in Saronikos Gulf. *Marine Ecology Progress Series*, 472: 73-85.

Tyrrell T. (2008). Calcium carbonate cycling in future oceans and its influence on future climates. *Journal of Plankton Research*, 30: 141-156.

Venn A., Tambutté E., Holcomb M., Allemand D. and Tambutté S. (2011). Live tissue imaging shows reef corals elevate pH under their calcifying tissue relative to seawater. *PLoS ONE*, 6: e20013.

Vergés A., Alcoverro T. and Ballesteros E. (2009). Role of fish herbivory in structuring the vertical distribution of canopy algae *Cystoseira* spp. in the Mediterranean Sea. *Marine Ecology Progress Series*, 375: 1-11.

Verges A., Steinberg P.D., Hay M.E., Poore A.G., Campbell A.H., Ballesteros E., Heck K.L., Jr., Booth D.J., Coleman M.A., Feary D.A., Figueira W., Langlois T., Marzinelli E.M., Mizerek T., Mumby P.J., Nakamura Y., Roughan M., van Sebille E., Gupta A.S., Smale D.A., Tomas F., Wernberg T. and Wilson S.K. (2014). The tropicalization of temperate marine ecosystems: climate-mediated changes in herbivory and community phase shifts. *Proceedings of the Royal Society B: Biological Sciences*, 281: 20140846.

Vizzini S., Di Leonardo R., Costa V., Tramati C.D., Luzzu F. and Mazzola A. (2013). Trace element bias in the use of CO₂-vents as analogues for low-pH environments: Implications for contamination levels in acidified oceans. *Estuarine, Coastal and Shelf Science*, 134: 19-30.

Waz P.M., Kirkwood W.J., Peltzer E.T., Hester K.C. and Brewer P.G. (2008). Creating controlled CO₂ perturbation experiments on the seafloor - development of FOCE techniques. In: *Oceans 2008 - Mts/leea Kobe techno-ocean, vols 1-3*, pp. 750-753.

Whalen M.A., Duffy J.E. and Grace J.B. (2012). Temporal shifts in top-down vs. bottom-up control of epiphytic algae in a seagrass ecosystem. *Ecology*, 94: 510-520.

Whiteley N.M. (2011). Physiological and ecological responses of crustaceans to ocean acidification. *Marine Ecology Progress Series*, 430: 257-271.

Wernberg T. and Vanderklift M.A. (2010). Contribution of temporal and spatial components to morphological variation in the kelp *Ecklonia* (Laminariales). *Journal of Phycology*, 46: 153-161.

Widdicombe, S., Dupont, S. and Thorndyke, M. (2010). Laboratory experiments and benthic mesocosm studies. In *Guide to best practices for ocean acidification research and data reporting*, edited by Riebesell U., Fabry V.J., Hansson L. and Gattuso J.-P. Luxembourg: Publications Office of the European Union. p. 53-66.

Wilbur K.M. (1964). Shell formation and regeneration, in: *Physiology of the Mollusca 1*, edited by: Wilbur K.M. and Yonge C.M., Academic Press, New York, 243-282.

Williamson C.J., Najorka J., Perkins R., Yallop M.L. and Brodie J. (2014). Skeletal mineralogy of geniculate corallines: providing context for climate change and ocean acidification research. *Marine Ecology Progress Series*, 513: 71-84.

Wood H.L., Spicer J.I. and Widdicombe S. (2008). Ocean acidification may increase calcification rates, but at a cost. *Proceedings of the Royal Society B-Biological Sciences*, 275: 1767-1773.

Wood H.L., Spicer J.I., Lowe D.M. and Widdicombe S. (2010). Interaction of ocean acidification and temperature; the high cost of survival in the brittlestar *Ophiura ophiura*. *Marine Biology*: 157, 2001-2013.

Wootton J.T., Pfister C.A. and Forester J.D. (2008). Dynamic patterns and ecological impacts of declining ocean pH in a high-resolution multi-year dataset. *Proceedings of the National Academy of Sciences*, 105: 18848-18853.

Xia J.R., Li Y.J., Lu J. and Chen B. (2004). Effects of copper and cadmium on growth, photosynthesis, and pigment content in *Gracilaria lemaneiformis*. *Bulletin of Environmental Contamination and Toxicology*, 73: 979-986.

Yamada K., Hori M., Tanaka Y., Hasegawa N. and Nakaoka M. (2010). Contribution of different functional groups to the diet of major predatory fishes at a seagrass meadow in northeastern Japan. *Estuarine, Coastal and Shelf Science*, 86: 71-82.

Yildiz G., Hofmann Laurie C., Bischof K. and Dere Ş. (2013). Ultraviolet radiation modulates the physiological responses of the calcified rhodophyte *Corallina officinalis* to elevated CO₂. *Botanica Marina*, 56: 161-168.

Zachos J.C., Rähl U., Schellenberg S.A., Sluijs A., Hodell D.A., Kelly D.C., Thomas E., Nicolo M., Raffi I., Lourens L.J., McCarren H. and Kroon D. (2005). Rapid acidification of the ocean during the Paleocene-Eocene Thermal Maximum. *Science*, 308: 1611-1615.

Zeebe R.E. and Westbroek P. (2003). A simple model for the CaCO₃ saturation state of the ocean: the 'Strangelove', the 'Neritan', and the 'Cretan' Ocean. *Geochemistry Geophysics Geosystems*, 4: 1104, doi:10.1029/2003GC000538.

Zeebe R.E. and Ridgwell A. (2011). Past Changes of Ocean Carbonate Chemistry. In *Ocean acidification* edited by Gattuso J.-P. and Hansson L. Oxford University Press, UK.

Zohary T. and Robarts R.D. (1998). Experimental study of microbial P limitation in the eastern Mediterranean. *Limnology and Oceanography*, 43(3): 387-395.

Appendix A:

Benthic percent cover at Methana and biomass at Vulcano (Chapter 3)

Appendix A1: mean (\pm SE, n=3) percent cover of benthic organisms at Methana in May and September 2012.

May 2012 Taxon	Site				
	REF A	REF B	200 E	200 W	SEEP
<i>Cystoseira corniculata</i>	51.43 \pm 14.00	47.71 \pm 15.47	62.57 \pm 13.36	61.43 \pm 12.57	31.57 \pm 15.29
<i>Cystoseira amentacea</i>	7.86 \pm 4.98	0	0	0	0
<i>Dictyota</i> sp.	21.14 \pm 8.78	14.29 \pm 5.71	10.71 \pm 4.94	11.43 \pm 4.59	14.43 \pm 9.44
<i>Cladostephus spongiosus</i>	0	0	0	7.71 \pm 3.96	3.14 \pm 3.14
<i>Padina pavonica</i> (non-calcified)	0	0	1.71 \pm 1.71	1.57 \pm 1.57	15.29 \pm 10.18
<i>Padina pavonica</i> (calcified)	5.29 \pm 3.21	5.00 \pm 1.89	0	0	0
<i>Sargassum vulgare</i>	2.86 \pm 2.86	8.57 \pm 8.57	4.00 \pm 1.65	2.86 \pm 1.49	36.29 \pm 16.25
<i>Cladophora</i> sp.	0	0	0	0	0.57 \pm 0.57
<i>Halimeda tuna</i>	0	0.14 \pm 0.14	0	0.14 \pm 0.14	0.14 \pm 0.14
<i>Halopteris scoparia</i>	1.43 \pm 1.43	11.43 \pm 7.69	0.57 \pm 0.57	0	0
CCA	0.86 \pm 0.70	3.43 \pm 1.41	19.29 \pm 12.56	9.86 \pm 9.21	0
Porifera (black)	0	0	1.14 \pm 1.14	0	0
Bare substratum	7.71 \pm 3.27	2.14 \pm 1.49	0	0	0
<i>Jania rubens</i>	2.14 \pm 1.49	0.86 \pm 0.70	0	0	0
<i>Sargassum</i> sp.	0	5.71 \pm 4.14	0	0	0
<i>Caulerpa racemosa</i>	0	0.71 \pm 0.71	0	0	0
<i>Falkenbergia</i> sp.	0	0	0	0	0
Porifera (orange)	0	0	0	0	0
<i>Amphiroa</i> sp.	0	0	0	0	0
<i>Corallina caespitosa</i>	0	0	0	0	0
Turf algae	0	0	0	0	0
Hydrozoa	0	0	0	0	0

Taxon	Site				
	REF A	REF B	200 E	200 W	SEEP
<i>Cystoseira corniculata</i>	18.33 ± 7.15	24.17 ± 12.41	47.50 ± 11.74	39.67 ± 14.02	57.67 ± 17.98
<i>Cystoseira amentacea</i>	0	0	0	0	0
<i>Dictyota</i> sp.	0	0	0	0	0
<i>Cladostephus spongiosus</i>	0	0	0	10.83 ± 7.24	0
<i>Padina pavonica</i> (non-calcified)	0	0	0	0	0
<i>Padina pavonica</i> (calcified)	0	1.17 ± 0.83	0	0	0
<i>Sargassum vulgare</i>	0	0	0	0	0.17 ± 0.17
<i>Cladophora</i> sp.	0	0	0	0	3.33 ± 3.33
<i>Halimeda tuna</i>	0	0	0.17 ± 0.17	0	0.33 ± 0.33
<i>Halopteris scoparia</i>	5.00 ± 5.00	0	0	5.00 ± 5.00	0
CCA	15.00 ± 4.83	17.83 ± 8.11	13.67 ± 4.01	7.50 ± 5.59	0.33 ± 0.33
Porifera (black)	0	0	0	0	0
Bare substratum	4.17 ± 3.27	11.67 ± 6.67	0	5.83 ± 3.75	8.67 ± 3.38
<i>Jania rubens</i>	55.83 ± 10.83	21.67 ± 8.43	35.67 ± 10.02	23.33 ± 8.91	1.67 ± 1.05
<i>Sargassum</i> sp.	0	16.17 ± 12.99	0	3.00 ± 1.63	25.83 ± 15.78
<i>Caulerpa racemosa</i>	0	0	0	0	0
<i>Falkenbergia</i> sp.	0	0	0	0	2.00 ± 0.93
Porifera (orange)	0.83 ± 0.83	0	1.67 ± 1.67	0	1.67 ± 1.67
<i>Amphiroa</i> sp.	0	0.67 ± 0.49	0.50 ± 0.50	0	0
<i>Corallina caespitosa</i>	0	0	0.83 ± 0.83	0	0
Turf algae	0	3.00 ± 3.00	0	5.00 ± 5.00	0
Hydrozoa	0.83 ± 0.83	0.83 ± 0.83	0	0	0

Appendix A2: mean (\pm SE, n=4) macroalgal biomass (grams of dry weight) at Vulcano in May 2010.

Taxon	Site		
	REF A	Mid pCO ₂	High pCO ₂
<i>Cystoseira</i> sp.	26.724 \pm 10.946	4.373 \pm 1.460	27.083 \pm 29.746
<i>Flabellia petiolata</i>	0.192 \pm 0.083	0.770 \pm 0.557	7.192 \pm 5.994
<i>Caulerpa prolifera</i>	0	0.358 \pm 0.265	2.061 \pm 0.880
Turf algae	0.912 \pm 0.415	2.648 \pm 0.391	4.651 \pm 3.093
<i>Sargassum</i> sp.	0.629 \pm 0.627	0	3.353 \pm 3.915
<i>Caulerpa racemosa</i>	0	0.454 \pm 0.343	0.022 \pm 0.045
<i>Nitophyllum punctatum</i>	0	0	0.005 \pm 0.010
<i>Chylocladia pelagosae</i>	0	0	0
CCA	0.919 \pm 0.634	1.531 \pm 0.633	0.372 \pm 0.665
<i>Rytiphloea tinctoria</i>	0.016 \pm 0.016	0.028 \pm 0.028	0.008 \pm 0.015
<i>Peyssonnelia</i> sp.	0	1.491 \pm 1.385	0.015 \pm 0.030
<i>Halopteris scoparia</i>	1.121 \pm 0.753	0.374 \pm 0.374	0
Gigartinales	0	0.010 \pm 0.010	0
Cladophorales	0	0.006 \pm 0.006	0
<i>Dictyopteris membranacea</i>	2.760 \pm 1.676	0.403 \pm 0.140	0
<i>Ulothrix</i> sp.	0	0.002 \pm 0.002	0
<i>Ceramium</i> sp.	0	0.002 \pm 0.002	0
<i>Acetabularia acetabulum</i>	0.110 \pm 0.110	0	0
<i>Dictyota</i> sp.	0.821 \pm 0.300	1.032 \pm 0.541	0.669 \pm 0.309
Articulated coralline	0.363 \pm 0.166	0	0
<i>Cladophora</i> sp.	0	0.044 \pm 0.041	0.043 \pm 0.055
Ceramiales	0.002 \pm 0.002	0	0.044 \pm 0.088
<i>Rhodymenia ligulata</i>	0	0	0.042 \pm 0.024
<i>Stilophora tenella</i>	0	0.031 \pm 0.031	0.005 \pm 0.009
<i>Halopteris</i> sp.	0.006 \pm 0.005	0.056 \pm 0.032	0
<i>Anadyomene stellata</i>	0	0.005 \pm 0.005	0.026 \pm 0.052
<i>Pterocladia</i> sp.	0	0.033 \pm 0.021	0
<i>Taonia atomaria</i>	0.133 \pm 0.082	0.054 \pm 0.043	0.463 \pm 0.926
<i>Osmundea truncata</i>	0	0.002 \pm 0.001	0
<i>Padina pavonica</i>	0.001 \pm 0.001	0.087 \pm 0.025	0
<i>Dictyota fasciola</i>	0.332 \pm 0.295	0	0

Appendix B:

Epifaunal abundance at Methana and Vulcano (Chapter 4)

Appendix B1: mean (\pm SE, n=3) abundance of epifaunal invertebrates at Methana in May 2012.

OTU	REF A	REF B	200 E	200 W	SEEP
Foraminifera					
<i>Amphistegina lobifera</i>	220.00 \pm 95.55	173.33 \pm 25.18	5.67 \pm 3.28	7.33 \pm 5.04	0.67 \pm 0.21
Agglutinated	119.00 \pm 83.92	28.33 \pm 10.73	0	0	0
Calcified sp. 1	2.67 \pm 0.33	3.33 \pm 1.76	0	0	0
Calcified sp. 2	0	0	2.00 \pm 1.00	0	0
Sipuncula					
	7.00 \pm 1.53	15.33 \pm 6.17	1.67 \pm 0.67	8.67 \pm 3.84	15.00 \pm 0.32
Platyhelminthes					
	0	0	2.00 \pm 1.53	1.33 \pm 0.88	2.00 \pm 0.37
Bryozoa					
	0.01 \pm 0.01	0.02 \pm 0.01	0.16 \pm 0.08	0.01 \pm 0.01	0
Mollusca					
Bivalvia					
<i>Arca noeae</i>	0.67 \pm 0.67	0	0	0.67 \pm 0.67	0
Arcidae sp. 1	1.33 \pm 0.33	0.33 \pm 0.33	0	0.33 \pm 0.33	0
Arcidae sp. 2	0.33 \pm 0.33	0	0	0	0
Arcidae sp. 3	0.33 \pm 0.33	0	0	0	0
Bivalvia sp. 1	35.33 \pm 15.34	41.67 \pm 12.55	11.67 \pm 4.33	5.00 \pm 1.53	0
Bivalvia sp. 2	0	0.67 \pm 0.67	0.33 \pm 0.33	0.33 \pm 0.33	0
<i>Cardita</i> sp.	0	0.67 \pm 0.33	0	0	0
Ostreoidea sp.	0	0	0.33 \pm 0.33	0	0
Gastropoda					
<i>Alvania cimex</i>	0	0.33 \pm 0.33	0	0	0
<i>Alvania geryonia</i>	0.33 \pm 0.33	0	0	0	0
<i>Alvania lactea</i>	0	0.33 \pm 0.33	0	0	0

<i>Cerithiopsis</i> sp. 1	0.33 ± 0.33	0.67 ± 0.33	0	0	0
<i>Cerithiopsis</i> sp. 2	0	1.00 ± 1.00	0	0	0
<i>Cerithiopsis tubercularis</i>	0	0.33 ± 0.33	0	0	0
<i>Cerithium vulgatum</i>	0	0.33 ± 0.33	0	0	0
<i>Columbella rustica</i> var. 1	0.33 ± 0.33	1.00 ± 0.58	1.67 ± 0.88	0.33 ± 0.33	0
<i>Columbella rustica</i> var. 2	0	0.33 ± 0.33	0	0	0
<i>Columbella rustica</i> var. 3	0	0	0	0.33 ± 0.33	0
<i>Columbella rustica</i> var. 4	0	0	1.00 ± 1.00	0	0
<i>Columbella</i> sp.	0	0.33 ± 0.33	0	0.33 ± 0.33	0
<i>Diodora graeca</i>	0.33 ± 0.33	0	0	0	0
Gasteropoda sp. 1	0.33 ± 0.33	1.33 ± 0.88	0	0	0
Gasteropoda sp. 2	0	0.33 ± 0.33	0	0	0
Gasteropoda sp. 3	0	0.33 ± 0.33	0	0	0
Gasteropoda sp. 4	0.67 ± 0.33	0	0	0	0
Gasteropoda sp. 5	0.67 ± 0.67	0	0	0	0
Gasteropoda sp. 6	0.33 ± 0.33	0	0	0	0
Gasteropoda sp. 7	0	0.33 ± 0.33	0	0	0
<i>Hinia costulata</i>	1.00 ± 0.58	0	0	0.67 ± 0.67	0
<i>Jujubinus</i> sp.	0	0.33 ± 0.33	0	0	0
<i>Jujubinus striatus</i>	0	0.33 ± 0.33	0	0	0
Muricidae sp.	0	0	0.33 ± 0.33	0	0
Omalogyridae sp.	0.33 ± 0.33	4.33 ± 2.19	0	0	0
<i>Patella</i> sp.	0.33 ± 0.33	0.33 ± 0.33	0	0	0
<i>Pusillina</i> sp.	1.00 ± 1.00	1.00 ± 0.58	0	0	0
<i>Rissoina</i> sp.	0	0.33 ± 0.33	0	0	0

<i>Setia maculata</i>	0	2.00 ± 1.53	0	0	0
<i>Triphora perversa</i>	0	0.33 ± 0.33	0	0	0
Polychaeta					
Polychaeta	107.67 ± 1.67	85.00 ± 19.52	217.00 ± 37.27	490.00 ± 149.29	176.33 ± 4.49
Serpulidae	1.33 ± 0.33	1.67 ± 0.33	3.00 ± 1.00	0.67 ± 0.67	0
Crustacea					
Amphipoda					
<i>Amphilocus</i> sp.	1.67 ± 0.33	2.00 ± 0.58	2.00 ± 1.53	1.67 ± 1.20	2.00 ± 0.37
<i>Ampithoe</i> sp.	22.33 ± 2.19	9.33 ± 4.37	351.00 ± 28.02	159.00 ± 59.18	150.67 ± 14.63
Aoridae sp.	16.67 ± 11.20	41.33 ± 17.25	32.00 ± 20.13	14.00 ± 2.52	22.33 ± 5.15
<i>Apherusa</i> sp.	10.67 ± 4.10	10.33 ± 6.84	0	0.67 ± 0.67	0.67 ± 0.21
<i>Peltocoxa</i> sp.	0	1.00 ± 0.58	0	0	0
<i>Dexamine spiniventris</i>	0	1.00 ± 1.00	0	0.33 ± 0.33	0
<i>Hyale</i> sp.	204.00 ± 55.77	68.33 ± 26.57	681.33 ± 357.19	837.33 ± 211.58	367.67 ± 13.45
<i>Gammaropsis</i> sp.	80.00 ± 20.53	34.33 ± 8.29	574.00 ± 158.35	70.00 ± 35.34	245.33 ± 12.72
<i>Microprotopus</i> sp.	0	0.33 ± 0.33	0	0	0
<i>Ericthonius</i> sp.	8.33 ± 2.67	1.67 ± 1.20	325.67 ± 77.62	323.33 ± 170.95	180.00 ± 22.10
<i>Ischyrocerus</i> sp.	0.67 ± 0.67	1.67 ± 1.20	13.00 ± 8.14	1.33 ± 0.88	10.00 ± 2.21
<i>Jassa</i> sp.	74.00 ± 18.03	9.00 ± 5.51	145.00 ± 93.74	29.00 ± 14.01	39.00 ± 5.48
<i>Leucothoe</i> sp.	1.00 ± 1.00	0	9.67 ± 5.93	0	1.00 ± 0.18
<i>Elasmopus</i> sp.	39.00 ± 11.68	38.67 ± 0.67	54.33 ± 9.84	37.00 ± 3.61	73.33 ± 10.88
<i>Maera</i> sp.	21.33 ± 16.34	36.00 ± 5.86	17.00 ± 9.29	5.67 ± 4.18	31.33 ± 5.56
<i>Pereionotus</i> sp.	0	20.33 ± 5.24	4.33 ± 1.20	62.3 3 ± 48.84	33.33 ± 4.42
<i>Podocerus</i> sp.	57.00 ± 8.50	124.33 ± 27.94	180.33 ± 12.84	7.33 ± 3.18	84.33 ± 4.96
<i>Stenothoe</i> spp.	142.67 ± 83.79	340.33 ± 61.50	80.00 ± 26.95	4.33 ± 1.86	6.00 ± 0.63

<i>Caprella</i> sp.	11.33 ± 5.24	35.33 ± 2.96	12.33 ± 4.91	2.33 ± 1.33	0
Ostracoda	1.00 ± 0.58	19.00 ± 13.05	2.67 ± 1.45	4.33 ± 2.33	0.33 ± 0.11
Copepoda					
Harpacticoida	4.00 ± 2.52	93.67 ± 51.27	14.00 ± 6.11	17.00 ± 7.77	6.33 ± 1.19
Cirripedia	0.67 ± 0.67	0	4.00 ± 2.08	0	0
Tanaidacea					
<i>Leptochelia savignyi</i>	30.67 ± 3.84	14.33 ± 4.98	175.33 ± 38.89	215.00 ± 52.74	126.00 ± 7.77
<i>Tanais dulongii</i>	2.33 ± 0.33	72.00 ± 8.02	5.00 ± 1.15	5.33 ± 4.33	0
<i>Araphura brevimanus</i>	0	1.33 ± 0.33	0	0	0
Isopoda					
Asellota	61.00 ± 32.73	81.00 ± 60.18	160.67 ± 35.93	25.67 ± 2.31	84.67 ± 7.98
Sphaeromatidea	5.33 ± 3.38	12.00 ± 5.29	1.67 ± 0.88	0.67 ± 0.67	4.00 ± 0.63
Decapoda	2.66 ± 1.33	8.00 ± 2.60	0.66 ±	0	0
Pycnogonida	1.67 ± 0.88	0.67 ± 0.33	10.00 ± 5.20	1.33 ± 0.33	1.33 ± 0.28
Echinodermata					
<i>Asterina gibbosa</i>	0	0	0	0	0.33 ± 0.11
Ophiuroidea	2.67 ± 2.19	2.67 ± 1.76	37.00 ± 17.58	44.33 ± 16.29	3.33 ± 0.64

Appendix B2: mean (± SE) abundance of epifaunal invertebrates at Vulcano in June 2013.

Macroalgal host	<i>Sargassum vulgare</i>		<i>Cystoseira</i> spp.	
	600 ppm (n=9)	1200 ppm (n=10)	600 ppm (n=15)	1200 ppm (n=14)
Polychaeta				
Filter feeder	4.56 ± 2.43	159.00 ± 36.96	1.07 ± 0.27	4.64 ± 1.28
Non filter feeder	13.33 ± 3.15	145.30 ± 25.53	7.13 ± 1.55	43.71 ± 8.07
Mollusca				
Polyplacophora				
<i>Acanthochitona fascicularis</i>	0	0	0.07 ± 0.07	0
Bivalvia				
<i>Cardita calyculata</i>	0	0	0.07 ± 0.07	0

<i>Musculus discors</i>	0	0.10 ± 0.10	0.40 ± 0.19	0
<i>Musculus</i> sp. juv.	0	0	0	0.07 ± 0.07
<i>Mytilaster minimus</i>	0	0	0.53 ± 0.47	0
Gasteropoda				
<i>Alvania</i> cfr <i>hirta</i>	0	0	0	0.07 ± 0.07
<i>Ammonicera</i> <i>fischeriana</i>	0	0	0.40 ± 0.29	0.43 ± 0.20
<i>Barleeia rubra</i>	0	0	0.13 ± 0.13	0
<i>Barleeia rubra</i> juv.	0	0	0.07 ± 0.07	0
<i>Cerithium lividulum</i>	0.22 ± 0.15	0	0.07 ± 0.07	0
<i>Cerithium</i> cfr <i>scabridum</i>	0	0	0.07 ± 0.07	0
<i>Columbella rustica</i> juv	0	0.10 ± 0.10	1.07 ± 1.07	0.14 ± 0.14
<i>Columbella rustica</i>	0.11 ± 0.11	0	0.20 ± 0.14	0
<i>Eatonina cossurae</i>	2.00 ± 0.88	0	3.07 ± 0.88	0.07 ± 0.07
<i>Eatonina cossurae</i> juv	1.33 ± 0.90	0	0.13 ± 0.13	0
Gastropoda indet. juv.	0.22 ± 0.22	0	0.07 ± 0.07	0.43 ± 0.29
<i>Gibbula racketti</i>	0	0	0.07 ± 0.07	0
<i>Gibbula varia</i>	0	0	0.07 ± 0.07	0
<i>Gibbula</i> sp. juv.	0	0	0.60 ± 0.40	0.07 ± 0.07
<i>Jujubinus</i> sp. juv	0.11 ± 0.11	0	0.07 ± 0.07	0
<i>Omalogyra simplex</i>	0.11 ± 0.11	0	0.20 ± 0.11	0
<i>Pollia</i> cfr <i>dorbignyi</i> juv	0	0.10 ± 0.10	0	0
<i>Rissoa auriscalpium</i>	0	0	0	0.07 ± 0.07
<i>Rissoa guerinii</i>	0.11 ± 0.11	0	0	0
<i>Rissoa variabilis</i> juv.	0	0	1.13 ± 0.61	0.14 ± 0.10
<i>Rissoa</i> sp juv	0.11 ± 0.11	0.10 ± 0.10	0.13 ± 0.09	0.29 ± 0.22
Rissoidea indet.	0	0	0	0.07 ± 0.07
<i>Setia</i> cfr <i>maculata</i>	0.22 ± 0.22	0	0	0
<i>Setia</i> cfr <i>amabilis</i>	1.11 ± 0.75	0	0.07 ± 0.07	0
<i>Setia</i> sp. juv.	1.00 ± 0.78	0	0.07 ± 0.07	0.07 ± 0.07
Crustacea				
Copepoda (Harpacticoida)	0	0	0	0.21 ± 0.15
Amphipoda				
<i>Amphilocheus</i> <i>neapolitanus</i>	0.33 ± 0.17	0	0.07 ± 0.07	0
<i>Ampithoe</i> sp.	0	0	0	0.07 ± 0.07
<i>Ampithoe ferox</i>	0.11 ± 0.11	0.20 ± 0.20	0.13 ± 0.09	0
<i>Ampithoe helleri</i>	0	0	0.07 ± 0.07	0.21 ± 0.11
<i>Ampithoe ramondi</i>	1.89 ± 0.59	33.20 ± 8.53	2.40 ± 0.58	5.57 ± 3.03
<i>Ampithoe riedli</i>	0	0	0	0.07 ± 0.07
<i>Ampithoe spuria</i>	8.89 ± 2.47	49.80 ± 5.44	49.73 ± 8.30	73.36 ± 19.57
<i>Cymadusa</i> <i>crassicornis</i>	3.89 ± 0.90	0	5.07 ± 1.02	1.14 ± 0.54
Aoridae sp.	0.33 ± 0.24	6.40 ± 2.48	0	0.14 ± 0.14
<i>Apherusa</i> sp.	7.78 ± 1.79	0.50 ± 0.27	0.67 ± 0.35	0.29 ± 0.22

<i>Dexamine spiniventris</i>	0.33 ± 0.24	0	0.40 ± 0.24	0.07 ± 0.07
<i>Dexamine spinosa</i>	0.11 ± 0.11	0	0	0
<i>Hyale</i> sp.	5.89 ± 1.88	35.00 ± 18.63	8.40 ± 3.85	1.86 ± 0.61
<i>Hyale camptonyx</i>	0.11 ± 0.11	1.90 ± 1.28	1.00 ± 0.59	1.43 ± 0.54
<i>Hyale crassipes</i>	0	0	0	0.36 ± 0.25
<i>Hyale perieri</i>	0	0.10 ± 0.10	0.20 ± 0.14	0
<i>Hyale schmidti</i>	4.33 ± 1.35	12.30 ± 3.33	4.33 ± 1.94	4.86 ± 1.73
<i>Erichthonius</i> sp.	102.00 ± 31.51	98.10 ± 17.22	16.07 ± 5.89	20.21 ± 3.17
<i>Ischyrocerus</i> sp.	0	0	0	0.07 ± 0.07
<i>Jassa marmorata</i>	0	0.10 ± 0.10	0.13 ± 0.13	0
<i>Lysianassa costae</i>	0.11 ± 0.11	0.20 ± 0.13	0	0.07 ± 0.07
<i>Elasmopus</i> sp.	0	0	0.07 ± 0.07	0
<i>Maera inaequipes</i>	0	0	0.07 ± 0.07	0
<i>Pereionotus testudo</i>	1.89 ± 0.98	0.20 ± 0.13	0.60 ± 0.35	0.21 ± 0.11
<i>Podocerus variegatus</i>	0.89 ± 0.39	0	0.47 ± 0.27	0
<i>Stenothoe</i> sp.	15.44 ± 5.86	0.50 ± 0.22	7.20 ± 4.62	0.29 ± 0.16
<i>Urothoe elegans</i>	0.11 ± 0.11	0	0	0
<i>Caprella</i> sp.	6.56 ± 2.75	15.00 ± 5.70	1.93 ± 0.96	0.36 ± 0.17
Amphipod asp.	10.00 ± 2.19	35.20 ± 6.11	14.87 ± 2.82	15.29 ± 3.37
Tanaidacea				
<i>Araphura brevimanus</i>	2.22 ± 0.85	0.10 ± 0.10	0	0.07 ± 0.07
<i>Leptochelia savignyi</i>	41.22 ± 12.59	14.20 ± 6.36	2.47 ± 0.56	2.29 ± 1.33
<i>Tanais dulongii</i>	0.11 ± 0.11	0.30 ± 0.15	0.80 ± 0.38	0.14 ± 0.14
Isopoda				
Sphaeromatidea	0.11 ± 0.11	1.70 ± 0.67	0.27 ± 0.15	0.36 ± 0.36
Asellota	0	0	0.13 ± 0.13	0
Decapoda	0	0	0.07 ± 0.07	0
<i>Pagurus</i> sp.	0.11 ± 0.11	0	0	0
Pycnogonida	0.11 ± 0.11	0	0	0
Acarina	0.22 ± 0.15	0	0	0
Echinodermata (Ophiuroidea)	0	0	0.13 ± 0.13	0

Appendix C:

Benthic functional groups cover at Vulcano and Methana (Chapter 5)

Appendix C1: mean (\pm SE, n=3-6) percent cover of benthic functional groups at Vulcano in 2012; C=control, P=procedural control, E=exclusion.

May 2012						
Taxon	600 C	600 P	600 E	1200 C	1200 P	1200 E
<i>Padina pavonica</i>	4.17 \pm 3.00	25.00 \pm 12.58	8.33 \pm 2.71	1.67 \pm 1.67	4.17 \pm 3.00	1.67 \pm 0.83
Brown turf algae	25.00 \pm 21.26	23.33 \pm 23.33	20.42 \pm 7.08	28.33 \pm 8.33	36.67 \pm 6.67	42.08 \pm 10.42
Bare substratum	57.50 \pm 28.98	39.17 \pm 22.38	53.33 \pm 6.31	73.33 \pm 4.41	43.33 \pm 21.86	40.83 \pm 11.65
Filamentous brown algae	0	0	0	0	0	3.33 \pm 3.33
Dictyotales	8.33 \pm 6.01	5.00 \pm 2.89	4.58 \pm 1.87	1.67 \pm 1.67	0	0
<i>Chtamalus stellatus</i>	0	0	1.25 \pm 0.85	1.67 \pm 1.67	0	0
Green turf algae	0	1.67 \pm 1.67	0.42 \pm 0.42	0	15.83 \pm 15.83	9.58 \pm 7.76
Filamentous green algae	0	0	0	0	0	1.67 \pm 1.67
<i>Acetabularia acetabulum</i>	0	1.67 \pm 0.83	0.42 \pm 0.42	0	0	0.42 \pm 0.42
CCA	0.83 \pm 0.83	0.83 \pm 0.83	3.33 \pm 1.67	0	0	0
<i>Laurencia</i> sp.	0	0	0.42 \pm 0.42	0	0	0
<i>Anadyomene stellata</i>	0	0	0.42 \pm 0.42	0	0	0
Encrusting brown algae	0.83 \pm 0.83	0.83 \pm 0.83	0	0	0	0
<i>Dasycladus</i> sp.	0	0.83 \pm 0.83	0.42 \pm 0.42	0	0	0
<i>Cystoseira</i> sp.	3.33 \pm 3.33	1.67 \pm 1.67	1.67 \pm 1.67	0	0	0
Serpulidae	0	0	0.83 \pm 0.83	0	0	0
<i>Cladophora</i> sp.	0	0	0	0	0	0
<i>Valonia utricularis</i>	0	0	0	0	0	0
<i>Actinia equina</i>	0	0	0	0	0	0
<i>Anemonia viridis</i>	0	0	0	0	0	0
Articulated coralline algae	0	0	0	0	0	0

<i>Verrucaria</i> sp.	0	0	0	0	0	0
<i>Peyssonnelia</i> sp.	0	0	0	0	0	0
<i>Ralfsia verrucosa</i>	0	0	0	0	0	0
<i>Caulerpa racemosa</i>	0	0	0	0	0	0

July 2012

Taxon	600 C	600 P	600 E	1200 C	1200 P	1200 E
<i>Padina pavonica</i>	15.67 ± 6.98	34.67 ± 25.33	16.00 ± 4.68	1.00 ± 1.00	3.00 ± 2.08	4.50 ± 2.43
Brown turf algae	18.67 ± 15.30	11.00 ± 9.54	17.17 ± 8.83	45.00 ± 17.79	22.00 ± 4.36	39.33 ± 13.79
Bare substratum	36.67 ± 18.66	35.67 ± 19.06	36.50 ± 6.15	42.33 ± 15.59	65.67 ± 4.33	51.33 ± 12.66
Filamentous brown algae	1.00 ± 1.00	0	0	1.00 ± 1.00	2.33 ± 2.33	0
Dictyotales	0.67 ± 0.67	1.00 ± 1.00	1.67 ± 1.67	3.33 ± 3.33	0	0.33 ± 0.33
<i>Chtamalus stellatus</i>	0.67 ± 0.67	0.67 ± 0.67	6.17 ± 3.29	0.67 ± 0.67	1.33 ± 0.67	0.67 ± 0.42
Green turf algae	0	0	0	0	0	0
Filamentous green algae	0	0	0	0	0	0
<i>Acetabularia acetabulum</i>	0.67 ± 0.67	0.67 ± 0.67	1.67 ± 0.33	0	0	0.50 ± 0.50
CCA	18.33 ± 6.01	6.00 ± 4.58	11.00 ± 2.21	0.67 ± 0.67	1.67 ± 0.88	0.33 ± 0.33
<i>Laurencia</i> sp.	0	0	2.17 ± 0.79	0	0	0.50 ± 0.50
<i>Anadyomene stellata</i>	1.67 ± 0.88	1.00 ± 1.00	0.83 ± 0.54	4.00 ± 2.08	0.67 ± 0.67	1.17 ± 0.83
Encrusting brown algae	0	0	0	0	0	0
<i>Dasycladus</i> sp.	2.33 ± 2.33	3.33 ± 3.33	3.17 ± 1.30	0	0	0
<i>Cystoseira</i> sp.	0.67 ± 0.67	1.67 ± 0.88	1.50 ± 0.50	0	0	0
Serpulidae	1.67 ± 0.88	0	1.50 ± 1.15	0.67 ± 0.67	0	0.67 ± 0.42
<i>Cladophora</i> sp.	0	0	0.33 ± 0.33	0	1.67 ± 1.67	0
<i>Valonia utricularis</i>	0	0	0	0	0	0.67 ± 0.67
<i>Actinia equina</i>	0	0	0	0	1.00 ± 1.00	0
<i>Anemonia viridis</i>	0	1.00 ± 1.00	0	0	0	0
Articulated coralline algae	0	0.67 ± 0.67	0	0	0	0
<i>Verrucaria</i> sp.	0	0.67 ± 0.67	0	0	0	0

<i>Peyssonnelia</i> sp.	0	1.00 ± 1.00	0.33 ± 0.33	0	0	0
<i>Ralfsia verrucosa</i>	0	0	0	0	0	0
<i>Caulerpa racemosa</i>	0	0	0	0	0	0

September 2012

Taxon	600 C	600 P	600 E	1200 C	1200 P	1200 E
<i>Padina pavonica</i>	0.67 ± 0.67	18.33 ± 9.53	12.00 ± 4.31	0	1.67 ± 0.88	2.00 ± 0.77
Brown turf algae	48.33 ± 13.64	49.00 ± 11.79	52.00 ± 3.60	40.67 ± 21.30	80.33 ± 5.24	71.83 ± 14.50
Bare substratum	20.67 ± 11.10	8.33 ± 4.41	8.67 ± 5.24	25.00 ± 9.07	8.33 ± 4.41	10.50 ± 9.91
Filamentous brown algae	0	0	0	0	0	0
Dictyotales	5.67 ± 2.96	4.00 ± 1.00	2.17 ± 0.79	0	0	0.33 ± 0.33
<i>Chtamalus stellatus</i>	2.33 ± 1.45	1.00 ± 1.00	6.83 ± 2.93	1.33 ± 0.67	0.67 ± 0.67	4.17 ± 3.39
Green turf algae	0	0	0	0	1.00 ± 1.00	0.33 ± 0.33
Filamentous green algae	0	0	0	0	0	0
<i>Acetabularia acetabulum</i>	0	0.67 ± 0.67	0.33 ± 0.33	0.67 ± 0.67	0	0.33 ± 0.33
CCA	15.00 ± 5.00	8.33 ± 7.36	11.33 ± 4.14	3.33 ± 0.88	3.33 ± 0.88	1.83 ± 0.87
<i>Laurencia</i> sp.	0	0	0.83 ± 0.83	0	0	0.83 ± 0.83
<i>Anadyomene stellata</i>	1.67 ± 0.88	3.00 ± 1.73	2.83 ± 0.65	3.33 ± 2.03	1.00 ± 1.00	1.67 ± 1.17
Encrusting brown algae	0	0	0	0	0.67 ± 0.67	0
<i>Dasycladus</i> sp.	3.33 ± 3.33	3.33 ± 3.33	1.33 ± 0.88	0	0.67 ± 0.67	0.50 ± 0.50
<i>Cystoseira</i> sp.	0	1.00 ± 1.00	1.00 ± 0.63	8.00 ± 8.00	1.33 ± 0.67	1.17 ± 0.54
Serpulidae	0	1.00 ± 1.00	0.67 ± 0.42	0	0	0.33 ± 0.33
<i>Cladophora</i> sp.	0	0	0	10.67 ± 10.67	0	0.50 ± 0.50
<i>Valonia utricularis</i>	0	0	0	1.00 ± 1.00	0	0.33 ± 0.33
<i>Actinia equina</i>	0	0	0	0	1.00 ± 1.00	0
<i>Anemonia viridis</i>	0	0.67 ± 0.67	0	0	0	0
Articulated coralline algae	0	0.67 ± 0.67	0	0	0	0
<i>Verrucaria</i> sp.	0	0	0	0	0	0

<i>Peyssonnelia</i> sp.	0	0	0	0	0	0
<i>Ralfsia verrucosa</i>	2.33 ± 2.33	0	0	5.33 ± 1.67	0	3.33 ± 3.33
<i>Caulerpa racemosa</i>	0	0	0	0	0	0
October 2012						
Taxon	600 C	600 P	600 E	1200 C	1200 P	1200 E
<i>Padina pavonica</i>	1.67 ± 0.88	12.33 ± 11.35	7.33 ± 3.24	0	lost	1.80 ± 1.36
Brown turf algae	41.33 ± 7.69	49.67 ± 14.10	46.67 ± 6.64	45.67 ± 13.86	lost	46.80 ± 15.56
Bare substratum	20.00 ± 1.00	10.33 ± 6.06	4.17 ± 3.60	23.00 ± 5.57	lost	28.80 ± 12.76
Filamentous brown algae	0	0	0	0	lost	0
Dictyotales	17.33 ± 11.85	0	4.17 ± 2.71	0.67 ± 0.67	lost	2.00 ± 1.55
<i>Chtamalus stellatus</i>	0	1.00 ± 1.00	4.33 ± 3.37	1.33 ± 0.67	lost	1.20 ± 0.49
Green turf algae	0	0	0	0	lost	0
Filamentous green algae	0	0	0	0	lost	0
<i>Acetabularia acetabulum</i>	0	0.67 ± 0.67	0	0	lost	0.40 ± 0.40
CCA	17.67 ± 3.71	13.33 ± 8.82	14.50 ± 4.75	5.00 ± 1.15	lost	3.80 ± 2.46
<i>Laurencia</i> sp.	0	0	0.83 ± 0.83	0	lost	0
<i>Anadyomene stellata</i>	0.67 ± 0.67	3.00 ± 0.58	1.83 ± 0.75	2.67 ± 1.45	lost	2.00 ± 2.00
Encrusting brown algae	0	0	0	0	lost	0
<i>Dasycladus</i> sp.	0	8.33 ± 8.33	4.33 ± 2.76	0	lost	1.00 ± 1.00
<i>Cystoseira</i> sp.	0	1.67 ± 1.67	10.33 ± 5.58	15.33 ± 15.33	lost	7.80 ± 4.07
Serpulidae	0.67 ± 0.67	0.67 ± 0.67	0.50 ± 0.50	0	lost	0.60 ± 0.60
<i>Cladophora</i> sp.	0	0	0	2.33 ± 2.33	lost	0.40 ± 0.40
<i>Valonia utricularis</i>	0	0.67 ± 0.67	0.33 ± 0.33	0	lost	0
<i>Actinia equina</i>	0	0	0	0	lost	0
<i>Anemonia viridis</i>	0	1.00 ± 1.00	0	0	lost	0
Articulated coralline algae	0	0	0	0	lost	0
<i>Verrucaria</i> sp.	0	0	0	3.33 ± 3.33	lost	3.40 ± 3.40
<i>Peyssonnelia</i> sp.	0	0	0	0	lost	0

<i>Ralfsia verrucosa</i>	0	0	0	0	lost	0
<i>Caulerpa racemosa</i>	0	0	0.67 ± 0.42	0	lost	0

Appendix C2: mean (\pm SE, n=3-4) percent cover of benthic functional groups at Methana in June 2013; C=control, P=procedural control, E=exclusion.

Functional group	REF A_C	REF A_P	REF A_E	SEEP_C	SEEP_P	SEEP_E
Turf algae	49.50 ± 16.59	33.00 ± 6.51	29.25 ± 7.98	4.00 ± 1.83	25.33 ± 9.40	1.67 ± 1.67
Fucoid algae	0	0.33 ± 0.33	0.50 ± 0.50	9.25 ± 4.11	9.67 ± 1.45	1.33 ± 1.33
Fleshy brown algae	0	1.67 ± 1.67	0	0	0	33.33 ± 33.33
Calcifying brown algae	0	0	50.75 ± 17.72	0	0	30.00 ± 28.02
Encrusting black sponge	0.25 ± 0.25	0	0	2.00 ± 2.00	0.33 ± 0.33	0
Encrusting green algae	14.50 ± 10.27	8.33 ± 4.91	0.25 ± 0.25	27.25 ± 4.61	14.33 ± 9.77	0
Erect brown algae	0	0.33 ± 0.33	2.00 ± 2.00	2.25 ± 2.25	0	24.33 ± 19.55
Biofilm	0	0	0.25 ± 0.25	5.00 ± 2.68	1.00 ± 0.58	4.00 ± 4.00
Serpulids	0	0.33 ± 0.33	0	0	0	0
CCA	12.50 ± 2.90	8.00 ± 3.61	3.75 ± 2.25	1.25 ± 0.48	0.67 ± 0.67	0
Bare substratum	23.25 ± 4.80	48.00 ± 9.17	13.25 ± 6.17	49.00 ± 5.35	48.67 ± 11.67	5.33 ± 3.53

Appendix D:

Epifaunal abundance at Methana (Chapter 7)

Appendix D1: mean (\pm SE) abundance of epifaunal invertebrates exposed or not exposed to copper at Methana in June 2013.

Site	REF		SEEP	
Copper	no (n=4)	yes (n=5)	no (n=5)	yes (n=5)
Polychaeta				
non calcifying	14.75 \pm 3.97	14.40 \pm 3.01	10.60 \pm 5.56	31.40 \pm 11.45
Serpulidae	0.25 \pm 0.25	0.40 \pm 0.40	0	0
Oligochaeta	1.50 \pm 0.96	1.00 \pm 0.63	0.40 \pm 0.24	0
Sipuncula	0.75 \pm 0.48	0.20 \pm 0.20	0	0
Mollusca				
Gasteropoda				
<i>Bittium reticulatum</i>	0.50 \pm 0.29	0.40 \pm 0.24	0	0
<i>Columbella rustica</i>	0.50 \pm 0.29	0	0	0
Gasteropoda sp. 1	0	0.20 \pm 0.20	0	0
Gasteropoda sp. 2	0.25 \pm 0.25	0.20 \pm 0.20	0	0
Gasteropoda sp. 3	0.25 \pm 0.25	0	0	0
Gasteropoda sp. 4	0.25 \pm 0.25	0	0	0
Muricidae sp 1	0.25 \pm 0.25	0	0	0
<i>Odostomia acuta</i>	3.00 \pm 1.78	4.60 \pm 2.04	0	0
<i>Rissoa</i> sp.	0	0	0.20 \pm 0.20	0
Rissoidae sp. 1	0.75 \pm 0.75	0	0	0
Bivalvia				
<i>Arca noeae</i>	0.50 \pm 0.50	0	0.20 \pm 0.20	0
Bivalvia sp. 1	0.25 \pm 0.25	0.80 \pm 0.37	0.20 \pm 0.20	0.20 \pm 0.20
Bivalvia sp. 2	0.25 \pm 0.25	0	0.20 \pm 0.20	0
<i>Ostrea</i> sp.	0.25 \pm 0.25	0	0	0
<i>Striarca lactea</i>	0	0.20 \pm 0.20	0	0
Crustacea				
Ostracoda	2.25 \pm 1.65	5.80 \pm 1.56	6.80 \pm 3.40	6.20 \pm 1.56
Copepoda	41.00 \pm 12.21	25.40 \pm 6.36	110.40 \pm 56.21	64.20 \pm 20.12
Amphipoda				
<i>Elasmopus</i> sp.	2.25 \pm 1.03	1.60 \pm 0.68	3.60 \pm 1.83	4.00 \pm 1.14
<i>Hyale perieri</i>	0	0	0	0.20 \pm 0.20
<i>Hyale schmidtii</i>	0	0	8.00 \pm 3.79	1.20 \pm 0.49
<i>Hyale camptonyx</i>	0	0	1.40 \pm 0.75	0
<i>Hyale crassipes</i>	0.25 \pm 0.25	0.20 \pm 0.20	0.40 \pm 0.24	0
<i>Apherusa chierieghinii</i>	0.50 \pm 0.29	0.40 \pm 0.24	0	0
<i>Dexamine spiniventris</i>	0	0.20 \pm 0.20	0	0

<i>Erichtonius</i> sp.	0	0.20 ± 0.20	1.40 ± 0.98	0.80 ± 0.37
<i>Pereionotus testudo</i>	0	0.20 ± 0.20	1.40 ± 0.98	1.00 ± 0.45
<i>Peltocoxa gibbosa</i>	0	0	0.20 ± 0.20	0
<i>Podocerus variegatus</i>	1.50 ± 1.19	0.60 ± 0.40	0.60 ± 0.24	0.80 ± 0.37
<i>Stenothoe</i> sp.	5.75 ± 1.89	2.80 ± 0.80	0.80 ± 0.58	1.40 ± 0.93
<i>Gammaropsis</i> sp.	0	0	0.20 ± 0.20	2.60 ± 1.66
<i>Maera grossimana</i>	0	0	0.40 ± 0.24	0
<i>Maera inaequipes</i>	0	0.80 ± 0.80	0.20 ± 0.20	1.60 ± 1.12
<i>Maera</i> sp.	2.25 ± 0.95	3.60 ± 1.60	3.00 ± 1.58	4.60 ± 1.60
<i>Ampithoe riedlii</i>	0	0	7.40 ± 1.89	1.60 ± 0.51
<i>Ampithoe ramondi</i>	0	0	4.20 ± 2.18	1.20 ± 0.73
Aoridae sp.	1.00 ± 0.01	0	5.00 ± 2.59	2.40 ± 0.51
Tanaidacea				
<i>Caprella acanthifera</i>	0.50 ± 0.50	0.40 ± 0.24	0	0.40 ± 0.24
<i>Leptocheira savignyi</i>	11.00 ± 2.38	9.80 ± 3.40	25.00 ± 3.91	17.60 ± 2.64
<i>Tanais cavolinii</i>	0.25 ± 0.25	0.80 ± 0.37	0	0
<i>Leptognathia brevimanu</i>	0.50 ± 0.50	0	0	0
Isopoda				
Asellopoda	3.75 ± 2.39	1.00 ± 0.45	13.40 ± 4.87	2.40 ± 0.40
Flabellifera	2.50 ± 0.96	2.80 ± 0.92	0.80 ± 0.37	0
Cumacea	0.50 ± 0.29	0	0	0
Decapoda	0.50 ± 0.29	0	0	0
Pycnogonida	0.25 ± 0.25	0.20 ± 0.20	0	0.40 ± 0.24
Echinodermata				
<i>Amphiura</i> sp.	0	0.40 ± 0.40	2.80 ± 1.50	0.20 ± 0.20

Appendix E:

Publications

Appendix E1:

C. Baggini, M. Salomidi, E. Voutsinas, L. Bray, E. Krasakopoulou, J.M. Hall-Spencer (2014). Seasonality affects macroalgal community response to increases in pCO₂. *PLoS ONE*, 9: e106520.

Full text of this publication has been removed due to Copyright restrictions.

C. Baggini, M. Salomidi, E. Voutsinas, L. Bray, E. Krasakopoulou, J.M. Hall-Spencer (2014). Seasonality affects macroalgal community response to increases in pCO₂. *PLoS ONE*, 9: e106520.

Full text available at:

<http://journals.plos.org/plosone/article?id=10.1371/journal.pone.0106520>

Appendix E2:

L.C. Hofmann, K. Bischof, **C. Baggini**, A. Johnson, K. Koop-Jakobsen, M. Teichberg (2015). CO₂ and inorganic nutrient enrichment affect the performance of a calcifying green alga and its non-calcifying epiphyte. *Oecologia*, 177: 1157-1169.

Full text of this publication has been removed due to Copyright restrictions.

L.C. Hofmann, K. Bischof, C. Baggini, A. Johnson, K. Koop-Jakobsen, M. Teichberg (2015). CO₂ and inorganic nutrient enrichment affect the performance of a calcifying green alga and its non-calcifying epiphyte. *Oecologia*, 177: 1157-1169.

Full text available at: <http://link.springer.com/article/10.1007/s00442-015-3242-5>

Appendix E3:

G. Langer., G. Nehrke, **C. Baggini**, R. Rodolfo-Metalpa, J.M. Hall-Spencer, J. Bijma (2014). Limpets counteract ocean acidification induced shell corrosion by thickening of aragonitic shell layers. *Biogeosciences Discussions*, 11: 12571-12590.

Full text of this publication has been removed due to Copyright restrictions.

G. Langer., G. Nehrke, C. Baggini, R. Rodolfo-Metalpa, J.M. Hall-Spencer, J. Bijma (2014). Limpets counteract ocean acidification induced shell corrosion by thickening of aragonitic shell layers. *Biogeosciences Discussions*, 11: 12571-12590.

Full text available at:

<http://www.biogeosciences-discuss.net/11/12571/2014/bgd-11-12571-2014.html>

Appendix E4:

P. Calosi, S.P.S. Rastrick, M. Graziano, S.C. Thomas, **C. Baggini**, H.A. Carter, J. Hall-Spencer, M. Milazzo, J.I. Spicer (2013). Ecophysiology of sea urchins living near shallow water CO₂ vents: Investigations of acid-base balance and ionic regulation using *in-situ* transplantation. *Marine Pollution Bulletin*, 73: 470-484.

Full text of this publication has been removed due to Copyright restrictions.

P. Calosi, S.P.S. Rastrick, M. Graziano, S.C. Thomas, C. Baggini, H.A. Carter, J. Hall-Spencer, M. Milazzo, J.I. Spicer (2013). Ecophysiology of sea urchins living near shallow water CO₂ vents: Investigations of acid-base balance and ionic regulation using *in-situ* transplantation. *Marine Pollution Bulletin*, 73: 470-484.

Full text available at:

<http://www.sciencedirect.com/science/article/pii/S0025326X12005784>

Appendix E5:

S. Hahn, R. Rodolfo-Metalpa, E. Griesshaber, W.W. Schmahl, D. Buhl, J.M. Hall-Spencer, **C. Baggini**, K.T. Fehr, A. Immenhauser (2012). Marine bivalve shell geochemistry and ultrastructure from modern low pH environments: environmental effect versus experimental bias. *Biogeosciences*, 9: 1897-1914.

Full text of this publication has been removed due to Copyright restrictions.

S. Hahn, R. Rodolfo-Metalpa, E. Griesshaber, W.W. Schmahl, D. Buhl, J.M. Hall-Spencer, C. Baggini, K.T. Fehr, A. Immenhauser (2012). Marine bivalve shell geochemistry and ultrastructure from modern low pH environments: environmental effect versus experimental bias. *Biogeosciences*, 9: 1897-1914.

Full text available at:

<http://www.biogeosciences.net/9/1897/2012/bg-9-1897-2012.html>

Appendix E6:

C. Baggini, Y. Issaris, M. Salomidi, J.M. Hall-Spencer (2014). Herbivore diversity improves benthic community resilience to ocean acidification. *Journal of Experimental Marine Biology and Ecology* (accepted pending revisions).

Full text of this publication has been removed due to Copyright restrictions.

C. Baggini, Y. Issaris, M. Salomidi, J.M. Hall-Spencer (2014). Herbivore diversity improves benthic community resilience to ocean acidification. *Journal of Experimental Marine Biology and Ecology* (accepted pending revisions).